Distribution Categories:
Physics—Atomic and
Molecular (UC-34A)
Chemistry (UC-4)

ANL-84-28

ANL--84-28

DE84 014521

ARGONNE NATIONAL LABORATORY
9700 South Cass Avenue
Argonne, Illinois 60439

Proceedings of the

WORKSHOP ON ELECTRONIC AND IONIC COLLISION CROSS SECTIONS NEEDED IN THE MODELING OF RADIATION INTERACTIONS WITH MATTER

Held at
Argonne National Laboratory
December 6-8, 1983

DISCLAIMER

May 1984

Detailed understanding of the changes that radiation actions produce in molecular substances is crucial to such important applications as dosimetry, estimation of the health effects of radiation, medical diagnostics and therapy, and radiation processing of materials in industry. At the earliest stage, radiation actions are caused by collisions of electrons and other energetic particles with molecules and by the resulting excitation, ionization, and dissociation of molecules. In particular, electron collisions are the most basic, because any ionizing radiations lead to the production of many energetic electrons in matter. As a consequence, there emerge many new molecular species. Because most of these new species are highly reactive, chemical changes result.

Although it is true that complete understanding of radiation actions requires knowledge in a vast range of fields, such as condensed-phase physics and chemical kinetics, knowledge of elementary collision processes is the most fundamental. Any sound discussion about molecular mechanisms of radiation actions must include some elements of the physics and cross-section data of those collision processes.

For applications to analysis of radiation actions, the cross-section data must fulfill what I call the "trinity of requirements": the data must be (1) correct, (2) absolute, and (3) comprehensive. By the term "comprehensive," I mean that the data must pertain to a wide range of variables involved, e.g., the incident energy and the scattering angle. Much too often, the data we see in the literature are discordant (thus causing suspicion as to the correctness), relative (as opposed to absolute), and fragmentary (rather than comprehensive). The failure of the trinity of requirements is understandable because much of the collision study is motivated by interest in basic physics; to prove or disprove a point in physics, it is often sufficient and is indeed efficient to take data that are relative and limited to a small range of variables.) I believe that the trinity of requirements also applies to the modeling done in other areas, e.g., discharge phenomena, plasmas, and astrophysics.

The main thrust of my work and that of some of my colleagues over the past two decades has been to find methods to test the data correctness, to provide comprehensive data for cases of importance to applications, and to develop systematics of data over different molecular species.

The term "modeling" in the Workshop title refers to the mathematical analysis of the consequences of many collision processes for characterizing the physical stage of radiation actions. It requires as input some knowledge of collision cross sections. Traditionally, work on cross sections and work on the modeling are conducted by separate groups of scientists.

It was the purpose of the Workshop to bring these two groups together in a forum that would promote effective communication. Cross-section workers described the status of their work and told what data were available or trustworthy. Modeling workers told what kind of data were needed or were most important. I sincerely hope that the present Proceedings of the Workshop will be stimulating to both groups and will contribute to the intellectual health of radiation science.

In the preparation of these Proceedings, I have asked all the participants to send some written contributions. Thus, most of the speakers sent me summaries of their presentations; other speakers provided me with short abstracts only. Some of the participants who gave no oral presentation at the Workshop sent me written contributions afterwards. I thank all the contributors for their efforts. In the present volume, the contributions are classified into three sections, as seen in the Table of Contents. The classification is by no means logically clearcut, and is used only for convenience. Some of the contributions by cross-section experts are

closely connected with some of the contribtions by modeling experts. Intricate logical connections among different contributions indeed testify to the underlying unity of the Workshop theme.

I thank all the participants for their enthusiasm about the Workshop theme, their dedication to it, and their efforts, all of which made the Workshop a success. Finally, I acknowledge on behalf of all the participants the most generous support provided by the University of Chicago through the Argonne Board of Governors, as well as assistance by the Division of Educational Programs and by the Office of Conference Services (Office of Public Affairs) of Argonne National Laboratory.

Mitio Inokuti
Workshop Chairman and Editor

TABLE OF CONTENTS

Data-Center Activities

DISCUSSION OF ELECTRON CROSS SECTIONS FOR TRANSPORT CALCULATIONS*

Martin J. Berger
National Bureau of Standards
Washington, D.C. 20234

ABSTRACT

This paper deals with selected aspects of the cross sections needed as input for transport calculations and for the modeling of radiation effects in biological materials. Attention is centered mainly on the cross sections for inelastic interactions between electrons and water molecules and the use of these cross sections for the calculation of energy degradation spectra and of ionization and excitation yields.

INTRODUCTION

This workshop is concerned with the cross sections needed for the modeling of radiation effects, with emphasis on effects resulting from the interactions of electrons or ions with matter. It may be useful to indicate, by an example, the kind of modeling that has to be done. A typical problem arising in biomedical dosimetry is the following. Assume that a beam of high-energy radiation (charged particles, gamma rays, bremsstrahlung, neutrons) is incident onto an extended medium (for example, a human body or a phantom designed to mock up a human body, or some other biological test object). Inside the medium there is a target region of interest (for example an organ of the body, an anatomic structure, a tumor, a group of cells or a single cell, or a cell nucleus). The problem is to predict the initial physical effects of the irradiation of the target region, i.e., the changes on the atomic and molecular level (ionization, excitation, fragmentation of molecules) giving rise to later radiochemical and radiobiological effects.

The modeling problem can be divided into several related tasks. (a) One must estimate the penetration of the incident radiation from its point of entry into the medium to the target region, taking into account the combined effects of multiple elastic and inelastic scattering. (b) One must estimate the production, and further penetration through the medium, of various kinds of secondary radiations (for example, protons, alpha particles and recoil nuclei from neutron interactions; knock-on electrons (delta rays) from proton or electron interactions; photo-electrons, Compton electrons and electron-positron pairs from photon interactions). (c) One must estimate the physical changes in the target region due to the action of the primary and secondary radiations. Among the secondary radiations, electrons are of special importance because — regardless of the nature of the primary radiation — they are the intermediaries through which most, and in some cases almost all, of the radiation damage is produced. The energy degradation process, i.e., the redistribution of energy in small packets from the primary radiations to numerous secondary electrons, is described by the electron energy degradation spectrum whose calculation was pioneered by Spencer and Fano (1).

*This work was supported by the Department of Energy (Office of Health and Environmental Research) and by the Office of Naval Research.

In practical radiation dosimetry, for example in treatment planning or in radiation protection studies, one is often content with predicting radiation effects in terms of the absorbed dose (mean energy deposited per unit mass) in the target region, on the assumption that the single quantity "absorbed dose" is a fairly good predictor of chemical or biological radiation effects. It is of course well known that, for a given absorbed dose, the radiation effects vary depending on the manner in which the energy is delivered to the medium. There is a dependence on the rate at which energy is transferred to the medium along charged-particle tracks, and on the temporal pattern of energy deposition. Moreover, it is important to take into account not only the average value but also the statistical fluctuations of the amounts of energy deposited in small sites, such as cells or cell nuclei, which may be traversed only rarely by a radiation particle. From a fundamental point of view it is more important to focus on the primary activations (ionizations, excitations, dissociations) than on the delivery of energy to the medium, and the calculation of electron energy degradation spectra assumes a key role. In addition to the yields of primary radiations, one must also consider the spatial distribution and clustering of the primary activations which have an important influence on later chemical and biological processes.

A vast array of charged-particle, photon or neutron cross sections may be required as input for transport calculations in the modeling of radiation effects. The cross sections must be comprehensive and complete for the specified material of interest so as to include all possible modes of interactions and secondary particle production; they must cover a wide range of energies and all possible deflection angles. Experiments or theories most often provide information about one or a few cross sections for a restricted set of conditions, but for many materials. One must therefore synthesize the data base for transport calculations from many experimental and theoretical results while maintaining consistency between the input data. The cross sections must also be processed so that they are in the format required by the particular method used for solving the transport problem, for example so as to allow speedy sampling of energy losses and deflections in Monte Carlo calculations.

In the brief space alloted to this paper it will be possible to deal only with electrons, and to touch only on selected aspects of electron cross sections. At high energies, above, say, 10 keV, the available cross sections are fairly accurate, but are of course undergoing a steady process of updating and refinement. For example, improved results have recently been obtained in regard to the evaluation of the density-effect correction of the stopping power (2-4) and in regard to the emission of bremsstrahlung photons (5). These results, combined with a critical analysis of mean excitation energies for use in Bethe's stopping power theory, have been used for the production of new stopping-power and range tables (6).

CROSS SECTIONS FOR THE CALCULATION OF ELECTRON ENERGY DEGRADATION SPECTRA

There is considerable room for improvement in regard to the electron cross sections at low energies, for example those needed to calculate electron energy degradation spectra down to the thresholds for ionization or electron excitation. A typical set of energy degradation spectra in water vapor, from Ref. (7), is shown in Fig. 1, for electrons injected into an unbounded medium with kinetic energy T_0 (between 1 MeV and 100 eV). The results are presented in terms of a collision density $n_c(T,T_0)$, which represents the average number of inelastic collisions made at energy T by the primary injected electron and by all generations of secondary electrons from ionization events. The usual tracklength distribution $y(T,T_0)$ is equal to $\lambda(T)\ n_c(T,T_0)$, where $\lambda(T)$ is the mean free path between inelastic collisions. From the collision density one can derive the G-factor (number of events per 100 eV of injected energy) for primary activations, according to the equation

$$G(T_0) = \left(100/T_0(\text{eV})\right) \int_0^{T_0} n_c(T,T_0)\left[\sigma(T)/\sigma_{in}(T)\right]\, dT \quad ,$$

where $\sigma(T)/\sigma_{in}(T)$ is the ratio of the cross section for the type of activation of interest to the total inelastic scattering cross section. Estimated G-factors for various ionizations, excitations and dissociations in water vapor, derived from the energy degradation spectra, are shown in Table I. The question arises: what is the reliability of such results? In the first place, it should be noted that the spectra and yields were obtained by a rather simple, straightforward and accurate Monte Carlo calculation, and that the uncertainties of the results of such calculations must be ascribed largely to the uncertainties of the input cross sections.

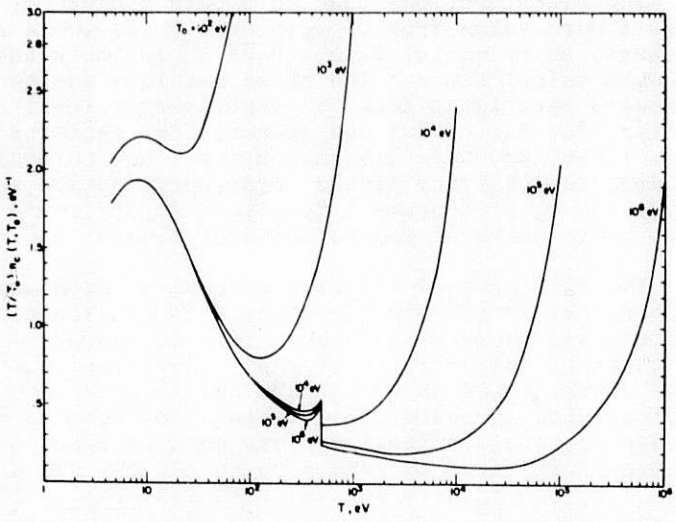

Fig. 1. Electron energy degradation spectra in water. Collision density also contains delta-function contribution $\delta(T-T_0)$ from first collision (not shown). From Ref. (7).

Table I

Yields for ionization, excitation, dissociative excitation and dissociative attachment in water vapor.

EVENT	YIELD, Number of Events per 100 eV							
T_0 =	50	100	200	500	10^3	10^4	10^5	10^6 eV
Ionization								
Orbital $1b_1$ 12.6 eV	1.156	1.241	1.305	1.339	1.346	1.340	1.338	1.335
$2a_1$ 14.7 eV	0.745	0.859	0.934	0.977	0.989	0.988	0.986	0.983
$1b_2$ 18.4 eV	0.445	0.572	0.652	0.701	0.717	0.726	0.730	0.728
$1a_2$ 32.2 eV	0.035	0.0895	0.139	0.181	0.199	0.211	0.209	0.208
O1s 539.7 eV	---	---	---	---	0.0006	0.0062	0.0095	0.0111
Excitation								
Rydberg (A+B) n=3	0.255	0.214	0.186	0.169	0.164	0.164	0.165	0.166
Rydberg (A+B) n≥4	0.102	0.0909	0.0802	0.0731	0.0713	0.0718	0.0725	0.0731
Rydberg (C+D) n=3	0.353	0.305	0.267	0.242	0.236	0.238	0.241	0.243
Rydberg (C+D) n≥4	0.270	0.243	0.215	0.196	0.191	0.193	0.196	0.198
Diff. Bands	0.764	0.723	0.653	0.601	0.589	0.601	0.611	0.617
Dissoc. Cont. 1	0.844	0.682	0.601	0.558	0.547	0.539	0.538	0.539
Dissoc. Cont. 2	0.526	0.433	0.373	0.336	0.325	0.319	0.319	0.319
Triplet 1	0.262	0.222	0.208	0.199	0.198	0.194	0.193	0.193
Triplet 2	0.0353	0.0261	0.0227	0.0213	0.0209	0.0205	0.0204	0.0204
Dissoc. Excitation								
Lyman α	0.177	0.231	0.231	0.216	0.208	0.191	0.183	0.178
Balmer α	0.0370	0.0483	0.0483	0.0452	0.0434	0.0401	0.0383	0.0372
Balmer β	0.0072	0.0093	0.0093	0.0086	0.0081	0.0074	0.0071	0.0069
Balmer γ	0.0026	0.0035	0.0034	0.0032	0.0031	0.0029	0.0029	0.0027
Balmer δ	0.0010	0.0013	0.0013	0.0012	0.0011	0.0011	0.0010	0.0010
OH 3064	0.997	0.801	0.716	0.678	0.669	0.661	0.662	0.662
OH 2800	0.0183	0.0134	0.0107	0.0091	0.0087	0.0082	0.0081	0.0081
OI 8447	0.0036	0.0044	0.0044	0.0040	0.0038	0.0033	0.0032	0.0031
OI 7774	0.0020	0.0022	0.0019	0.0015	0.0014	0.0012	0.0012	0.0012
Dissoc. Attachment								
O^-	0.188	0.158	0.147	0.141	0.140	0.138	0.137	0.137
H^-	1.345	1.145	1.079	1.037	1.023	1.010	1.005	1.004

The cross sections used to obtain yields for the excitation processes listed in Table I were taken from Olivero et al. (8) whose results are based on the combination of sparse experimental data and of approximate theoretical generalized oscillator strength calculations. The cross sections for the dissociative excitation of water molecules were taken from the experimental results of Beenakker et al. (9). Cross sections for excitation and dissociative excitation were available only for energies up to 1 keV, and were extended up to 1 MeV through the use of Fano plots, i.e., assuming the validity of the Born-approximation result that the cross section multiplied by β^2 depends linearly on $\ell n[\beta^2/(1-\beta^2)] - \beta^2$, where β is the electron velocity in units of the velocity of light.

The differential ionization cross section was assumed to be essentially inversely proportional to $(W^2 + W_0^2)$, where W is the kinetic energy of the ejected secondary electron and where W_0 = 13 eV. This dependence was suggested by Opal et al. (10) on the basis of the analysis of their electron-impact ionization measurements at 500 eV in water vapor and at 500, 1000, and 2000 eV in O_2. The differential ionization cross section, with an additional exchange correction, was normalized so as to agree with an adopted total ionization cross section based on the experimental results of Märk and Egger (11) from threshold up to 200 eV, and of Schutten et al. (12) at energies up to 20 keV, and results derived by Zeiss et al. (13) from oscillator-strength data. The ionization of a water molecule can be treated as the ejection of an electron from one of five orbitals with binding energies of 12.6, 14.7, 18.4, 32.2, and 539.7 eV (14). The relative probabilities for ejection from the various orbitals were estimated using the experimental K-shell ionization of Glupe and Mehlhorn (15), and for the other orbitals by calculations by the Weizäcker-Williams method described below. A useful check of the adopted differential ionization cross section was provided by the fact that, when combined with the excitation cross sections discussed earlier, it led to stopping-power values which at 10 keV and higher energies agreed closely with the predictions of the Bethe theory (using a mean excitation energy of 71.6 eV for water vapor). As shown in Fig. 2, below 10 keV the stopping-power derived from the combination of ionization and excitation cross sections lies below the Bethe curve, which is in accordance with one's expectations.

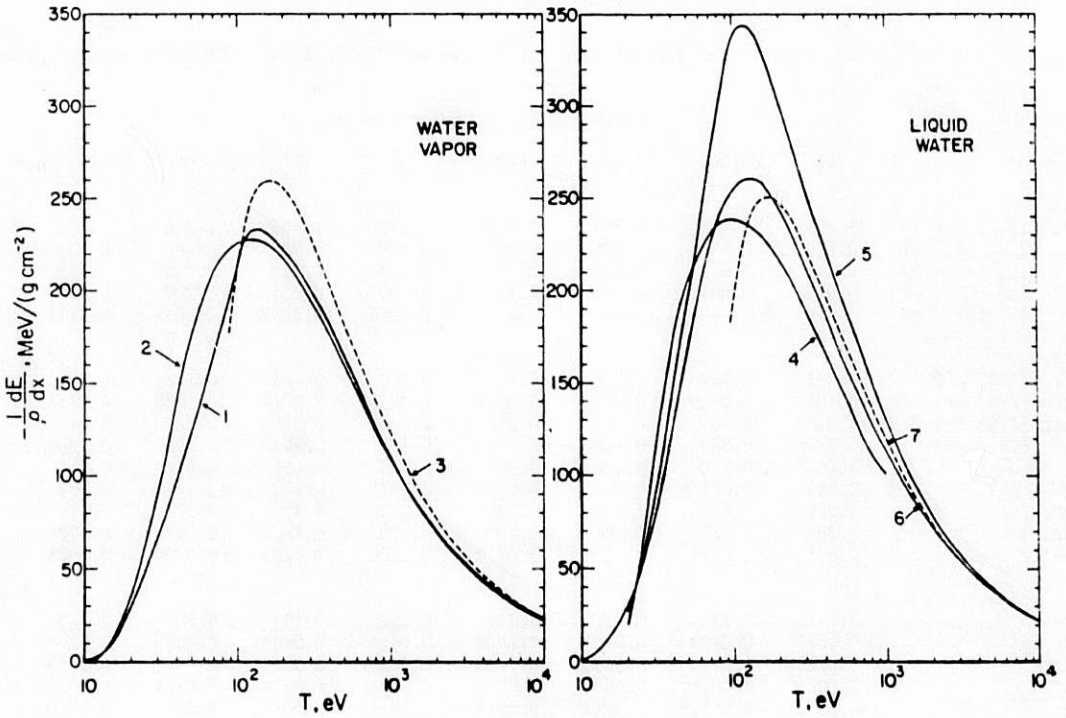

Fig. 2. Calculated electron collision stopping power. From Ref. (7).

1. Present work
2. Jackman et al. (32)
3. Bethe formula, I = 71.6 eV
4. Kutcher and Green (33)
5. Ritchie et al. (29)
6. Ashley (34)
7. Bethe formula, I = 75 eV.

As an alternative to patching together various pieces of experimental data, one can calculate the differential ionization cross section in the first Born approximation, which is straightforward in principle but difficult in practice, especially for molecules. In any case, no substantial body of Born-approximation results is as yet available for transport calculations. Another, nearly equivalent approach, which is much easier to implement, is the Weizsäcker-Williams method (16-19) in which separate treatments are applied to soft collisions (with small momentum transfers) and hard collisions. The contribution to the cross section from soft collisions (with impact parameters larger than the atomic radius) is calculated by replacing the perturbing field of the incident electron by an equivalent pulse of radiation (a virtual photon spectrum), and then treating the ionization process as the photoionization of the virtual photons. This allows the use of the rather abundant experimental data on the total photoionization cross section (20, 21) and on the partial cross sections for photoionizations from various orbitals (22). The hard collisions are treated as strictly binary interactions between the incident electron and the atomic electrons, with the use of the Mott or Møller cross sections, possibly modified by the methods of binary-encounter theory (23). Actually there are energy transfers of intermediate magnitude for which the collisions can be considered neither as soft nor as hard, and for which an accurate theory is lacking. It is therefore necessary to make semi-empirical corrections using experimental electron-impact cross sections. Kim (24) has shown how to make reliable data analyses of this kind within the framework of the Weizsäcker-Williams method.

As has been shown by Williams (16), the Weizsäcker-Williams method is applicable under conditions such that the first Born approximation is applicable. An appreciable error (leading probably to an overestimate the calculated cross section) may therefore be incurred when the Weizsäcker-Williams method is applied, as is sometimes the case, at energies below ~ 300 eV for electrons in water vapor or similar low-Z gases.

A set of cross sections for the inelastic collisions of electrons with water molecules has also been prepared by Paretzke (25), who used photoionization cross sections from many sources, including the experiment of Tan et al. (26), as input for Weizsäcker-Williams calculations of the differential ionization cross section, and who also followed Olivero et al. (8) in regard to the excitation cross sections. It has been shown (27) that the use of Paretzke's cross section set leads to stopping powers and energy degradation spectra that are rather similar to those obtained by the present author with a cross section set prepared as described above, without use of the Weizsäcker-Williams method. Unfortunately no measured energy degradation spectra are available which could be used to test the calculations. It is possible, however, to make comparisons in regard to the total ionization yield. As shown in Fig. 3, the ionization yields calculated by Paretzke and the present author are in reasonably good agreement with each other and with the experimental results of Combecher (28) for water vapor, for electron energies up to 500 eV. As shown in Ref. (27) the calculated and experimental ionization yields are also in agreement at higher energies up to 10 keV.

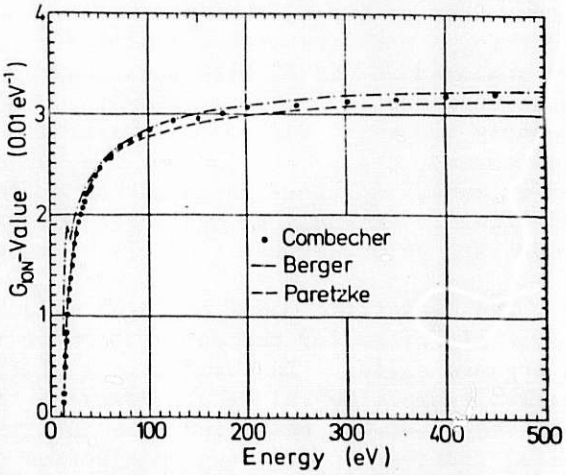

Fig. 3. Comparison of ionization yields in water vapor measured by Combecher and calculated by Paretzke and by Berger. From Ref. (27).

Instead of the yields for ionizations from various molecular orbitals, as given in Table I, one would often like to know the ionization yields associated with the production of various chemical species such as H_2O^+, OH^+, O^+, and H^+. Tan et al. (26) have measured partial oscillator-strength distributions for water vapor, at energies up to 60 eV, associated with the production of these species. These results, perhaps extrapolated to higher photon energies, could be used to predict the corresponding ionization yields from soft collisions, which constitute the majority of ionization events. It would also be possible to make use of the measurements of Schutten et al. (12) at energies up to 2 keV, which give the fragmentation pattern for water molecules resulting from electron-impact ionization. Again these results would have to be extrapolated in some manner to higher energies.

For applications in aqueous radiation chemistry and radiobiology it is important to know energy degradation spectra and activation yields in liquid water rather than in vapor. In the liquid phase the ionization thresholds are lower than in vapor, excitations are less important, and the ionization yield is perhaps 25% higher. A research effort has been underway at the Oak Ridge National Laboratory for many years to determine such liquid/vapor differences for water (29,30) and in general for all kinds of materials. In this work, the cross sections for inelastic collisions are modeled with use of a complex dielectric response function $\varepsilon(\omega,q)$ which depends on the energy transfer $\hbar\omega$ and momentum transfer $\hbar q$. In the limit of zero momentum transfer (soft collisions) the response function is derived from experimental optical data, for example, for water those of Heller et al. (31). For non-zero momentum transfers (intermediate and hard collisions) the response function is obtained through theoretical modeling. This procedure (allowing the use of experimental photon-impact data) is rather similar to the Weizsäcker-Williams method, and again the region of applicability is that of the first Born approximation. The modeling of liquid/vapor cross section differences in Refs. (29,30) is done in an intuitive manner, involving educated guesses and plausible assumptions. Unfortunately there is a scarcity of hard experimental factors which might provide quantitative checks.

Electron stopping powers in water at energies below 10 keV, derived for vapor through the combination of molecular cross sections in the present work and in (32), and through modeling with a dielectric response function for liquid water (33,34,39) are compared in Fig. 2 with each other and with the predictions of the Bethe theory. As pointed out in (33), the stopping power values around 100 eV given in (29) are probably too high, due to an unjustified empirical adjustment. Apart from this discrepancy, the predictions of the various authors, at least down to 100 eV, do not differ much, and there is no marked difference between the stopping powers for vapor and liquid. It would be desirable but presumably quite difficult to have experimental comparison values at energies near 100 eV.

The dielectric model has been used by Ashley and Williams (35) to develop a simple algorithm for the calculation of mean free paths between inelastic collisions in organic solids. The predictions of this algorithm are consistent with the available experimental data. However, the spread of the experimental data is so great that they must be considered much less reliable than the calculated mean free paths. Useful indirect information on electron cross sections at low energies can be obtained from measurements of electron energy degradation spectra in solids by Birkhoff and collaborators (36-38). These measurements, made so far only for metals and semiconductors, could perhaps be extended to organic solids. The interpretation of such measurements has not yet been fully successful. For example, difficulties arise in regard to measurements of energy degradation spectra in silicon at energies from a few eV to 30 keV (38). It has been found that the results of Monte Carlo calculations based on rather detailed solid-state cross sections are significantly lower than the measured spectra at energies from 10 eV to 1500 eV, and it is an open question whether the origin of this discrepancy is experimental, theoretical or both.

In order to be able to calculate energy degradation spectra as functions of position in the medium, one must also know the elastic scattering cross section. A conveniently parametrized set of elastic scattering cross sections for water vapor has been prepared by Zaider et al. and Brenner (39,40) through the combination of results from several experiments. If one were to convert the mean free path between elastic collisions from vapor to liquid through a simple density scaling, one would find that at energies below 10 eV the mean free path is no longer large compared to the electron wavelength. It is then no longer permissible to disregard quantum-mechanical interference in the multiple-scattering process. Either the model of successive binary collisions with individual molecules (commonly used in transport theory) must be abandoned in favor of a dynamic diffraction model, or the elastic scattering cross section must at least be modified by a suitable structure factor.

REFERENCES

1. L. V. SPENCER and U. FANO, Phys. Rev. 93, 1172 (1954).

2. M. INOKUTI and D. Y. SMITH, Phys. Rev. B, 25, 61 (1982).

3. J. C. ASHLEY, Radiat. Res. 89, 32 (1982).

4. R. M. STERNHEIMER, S. M. SELTZER, and M. J. BERGER, Phys. Rev. B26, 6067 (1982); R. M. STERNHEIMER, M. J. BERGER, and S. M. SELTZER, National Bureau of Standards Report NBSIR 83-2785 (1983).

5. R. H. PRATT, et al., Atomic and Nuclear Data Tables 20, 175 (1977); 26, 477 (1981).

6. M. J. BERGER and S. M. SELTZER, National Bureau of Standards Report NBSIR 82-2550-A (1982).

7. M. J. BERGER, Proc. 7'th Symposium on Microdosimetry, p. 521, Harwood Academic Publishers, London, 1980).

8. J. J. OLIVERO, R. W. STAGAT, and A.E.S. GREEN, J. Geophys. Res. 77, 4797 (1972).

9. C.I.M. BEENAKKER, et al., Chem. Phys. 6, 445 (1974).

10. C. B. OPAL, E. C. BEATY, and W. K. PETERSON, Atomic Data 4, 209 (1972).

11. T. D. MÄRK and F. EGGER, Int. J. Mass Spectrometry and Ion Phys. 20, 89 (1976).

12. J. J. SCHUTTEN, et al., J. Chem. Phys. 44, 3924 (1966).

13. G. D. ZEISS et al. Radiat. Res. 63, 64 (1975).

14. K. SIEGBAHN et al., ESCA Applied to Free Molecules, North-Holland, Amsterdam (1969).

15. G. GLUPE and W. MEHLHORN, J. de Phys. C4, (1971).

16. E. J. WILLIAMS, Kgl. Dansk. Videnskab. Selskab. Mat-fys. Medd. 13, No. 4 (1935).

17. W. F. MILLER, Ph.D. Thesis, Purdue University, (1955).

18. D. E. GERHART, J. Chem. Phys. 62, 821 (1975).

19. E. EGGARTER, J. Chem. Phys. 62, 833 (1975).

20. G. D. ZEISS, et al. Radiat. Res. 70, 284 (1977).

21. J. BERKOWITZ, Photoabsorption, Photoionization, and Photoelectron Spectroscopy, Academic Press, N.Y. (1979).

22. C. E. BRION and J. P. THOMSON, Compilation of Dipole Oscillator Strength, to be published.

23. L. VRIENS, Case Studies in Atomic Collision Phys. I, p. 335, North-Holland, Amsterdam (1969).

24. Y.-K. KIM, Radiat. Res. 64, 96 and 205 (1975); also Phys. Rev. A 28, 656 (1970).

25. H. PARETZKE, Paper presented at Meeting of the European Dosimetry Group, Fontenay-aux-Roses, 1977.

26. K. H. TAN, et al. Chem. Phys. 29, 299 (1978).

27. H. G. PARETZKE and M. J. BERGER, Proc. Sixth Symp. on Microdosimetry, p. 749, Harwood, New York (1978).

28. D. COMBECHER, Radiat. Res. 84, 189 (1980).

29. R. H. RITCHIE, et al. Proc. Sixth Symp. on Microdosimetry, p.345, Harwood, London (1978).

30. J. E. TURNER, et al. Radiat. Res. 92, 47 (1982).

31. M. HELLER, et al. J. Chem. Phys. 60, 3483 (1974).

32. C. E. JACKMAN, R. H. GARVEY, and A.E.S. GREEN, J. Geophys. Res. 82, 5081 (1977).

33. J. C. ASJLEY, Radiat. Res. 89, 25 (1982).

34. G. J. KUTCHER and A.E.S. GREEN, Radiat. Res. 67, 408 (1975).

35. J. C. ASHLEY and M. W. WILLIAMS, Radiat. Res. 81, 364 (1980).

36. W. J. McCONNELL, et al., Phys. Rev. 138, A1377 (1965).

37. R. D. BIRKHOFF, in Penetration of Charged Particles in Matter: A Symposium (National Academy of Sciences, Washington, D.C. 1970), pp. 1-15.

38. L. C. EMERSON, et al., Phys. Rev. B 7, 798 (1975).

39. M. ZAIDER, D. J. BRENNER, and W. W. WILSON, Radiat. Res. 96, 231 (1983).

40. J. BRENNER, to appear in Phys. in Med. and Biol.

CROSS SECTIONS NEEDED FOR INVESTIGATIONS INTO TRACK PHENOMENA AND MONTE-CARLO CALCULATIONS

Herwig G. Paretzke
GSF-Institut für Strahlenschutz
D - 8042 Neuherberg, Germany

ABSTRACT

Investigations into basic radiation action mechanisms as well as into applied radiation transport problems (e.g. electron microscopy) greatly benefit from detailed computer simulations of charged particle track structures in matter. The first and in fact most important and most difficult step in any such calculation is the derivation of reliable cross sections for the most relevant interaction processes in the material(s) unter consideration. The second step in radiation transport calculations is the testing of results or intermediate results for quantitative or qualitative consistency with other experimental or theoretical information (e.g. yields, backscatter factors). This paper discusses the types of the most important collision cross sections for studies on track phenomena by detailed Monte-Carlo calculations, the necessary accuracy of such data and various means of consistency checks of calculated results. This will be done mainly with examples taken from radiation physics as applied to dosimetric and biological problems (i.e. to gaseous and condensed targets).

INTRODUCTION

Most basic and applied investigations in the field of radiation physics can be classified into either

- research into the radiation field itself and its modifications by interaction with matter (Object Class A), or
- research into modifications in the molecular structure of the target material produced by irradiation (Object Class B).

Typical examples of Object Class A problems are radiation transport problems occurring e.g. in shielding calculations, electron microscopy, radiation therapy, ion lithography, etc. They are connected to basic questions related to the determination of stopping power, ranges, particle or energy transmission or reflection by targets. Typical results from such basic investigations are indicated quantitatively in fig. 1 for the case of 5 keV electrons impinging vertically onto the surface of a low atomic number material (here water).

For such Class A problems, Monte-Carlo transport calculations simulating the trajectories of charged or uncharged primary and/or secondary particles have increasingly proved very promising during the past 25 years. This has been mainly due to the recent availability of computers with large memories and fast processors. In the present context only charged particle transport calculations and their cross section requirements will be considered and a further restriction will be made to fast ions and to electrons. An excellent introduction into the technique of such Monte-Carlo calculations is still the well-known 1963 article by Berger[1].

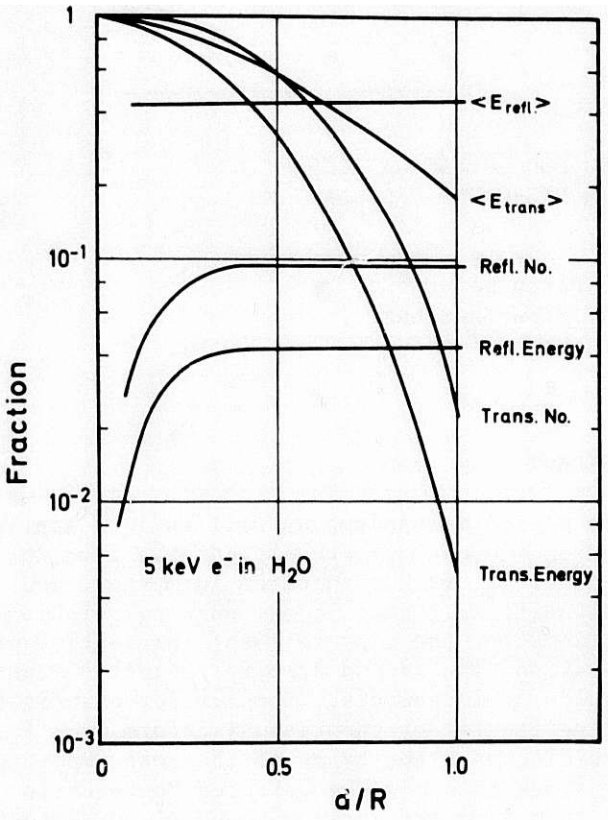

Fig. 1

Example of Object Class A problems: Energy and particle transmission and reflection for 5 keV electrons impinging vertically on water (own Monte-Carlo calculations)

Typical examples of Object Class B problems are found in radiation chemistry and biology and their present solutions are by far less satisfying than those of Class A problems. Modifications of interest in the target material can be e.g. the interim or final yields of new chemical species, the inactivation of a biological cell or even as complex as the induction of a malign tumor in an animal: years after radiation exposure. The main reasons for the unsatisfactory status of this field are the severe lack of relevant and necessary experimental and theoretical data for primary processes of radiation interaction with condensed matter, for the subsequent chemical and biochemical relaxation processes started by this disturbance, and concepts for the approximate description of the most relevant properties of and processes occurring in charged particle tracks in particular in condensed matter. For the case of gaseous targets, fortunately the status of knowledge is somewhat more advanced, and in fig. 2, as a typical example for Class B problems, yields for various new physical and chemical species produced in water vapor by slow electrons upon complete slowing down are given as calculated with detailed Monte-Carlo track structure calculations. The main types and the accuracy required of cross sections needed for such calculations of track phenomena will be discussed below.

TYPES OF COLLISION CROSS SECTIONS NEEDED

The trajectory of a charged particle and the track structure produced in a material are determined by scattering interactions of the particle with the atoms and electrons of the target. The probability of particular elastic or inelastic collisions are determined by properties of the particle as well as those of the target, and they are described by corresponding cross sections. Thus the quantitative knowledge of all relevant cross sections represents a basic pre-requisite for any detailed Monte-Carlo calculation, and the derivation and verification of these cross sections constitutes the most important part of such scientific investigations.

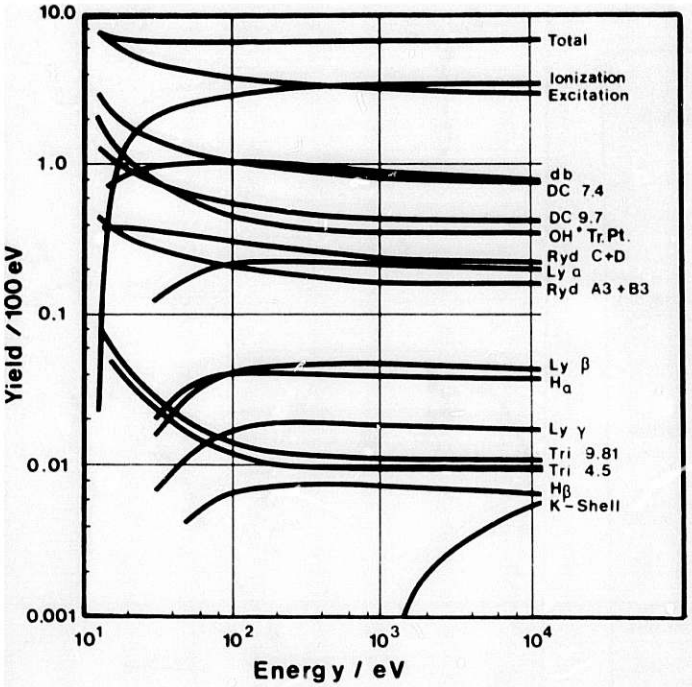

Fig. 2

Example of Object Class B problems: Yields of various new species produced in water vapor by complete slowing down of electrons as a function of their starting energy (own Monte-Carlo calculations)

For investigations into track phenomena of heavy charged particles, e.g. in pulse radiolysis radiation chemistry[2], the types of collision cross sections mainly needed in Monte-Carlo calculations are
- excitation cross sections,
- ionization cross sections differential in electronic shell, ejected electron energy, angular deflection.

For calculations e.g. of ion backscattering yields or angular distribution of ions transmitted through thin foils, however, also elastic scattering cross sections will be necessary, which otherwise play a less important role in track structure calculations. On the contrary, knowledge of differential ionization cross sections is of utmost importance since - on one hand - ionizing collisions can be responsible for up to more than 90 percent of the total energy loss of a fast ion, and - on the other hand - ionization in a target material frequently play a major role in producing serious radiation damages (e.g. in biological cells). Therefore, experiments and theoretical work on differential ionization cross sections for fast ions are of high interest in this context; such data are given e.g. by Wilson et al.[3] and by Rudd and Macek[4].

Electrons ejected in ionizing collisions of fast atoms (secondary electrons) or primary electrons also loose most of their energy by
- excitations, and
- ionizations,

and, this, the respective cross sections (as differential as for ion collisions) must be known for track phenomena investigations as well as for radiation transport problem. Also here ionizing collisions for the same reasons as given above turn out to be far more important in most questions in radiation physics than collisions leading only to excitations of target atoms. For electrons, however, because of their small mass,
- elastic collisions

and the corresponding angular deflection play a role increasing in importance with decreasing electron energy. This can clearly be seen in fig. 3 at the example of the total inelastic and elastic cross sections for electron trajectories (shown e.g. in fig. 4 for the track ends of electrons ejected in a decay of radioactive Iodine-125).

From fig. 3 the predominant role of the ionization cross sections becomes evident. For investigations into track phenomena and for radiation transport, the knowl-

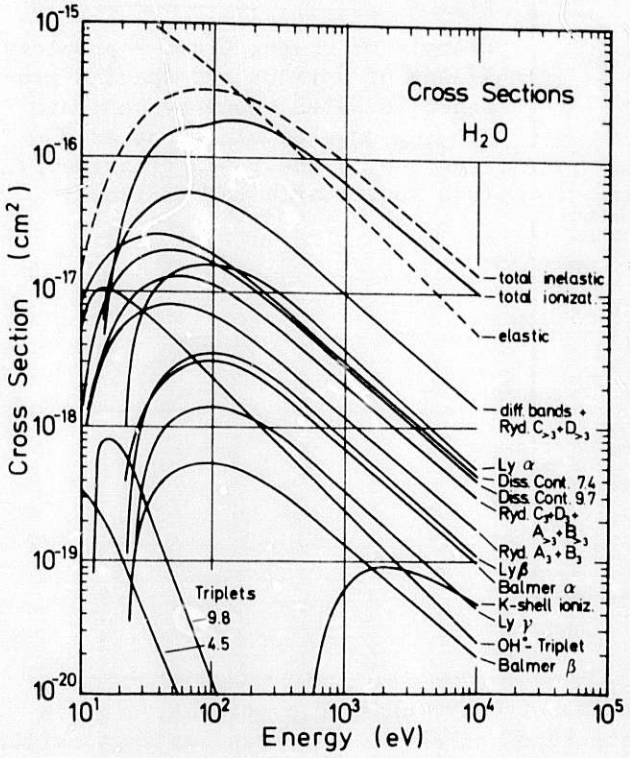

Fig. 3
Inelastic and elastic cross sections for electron impact on water vapor

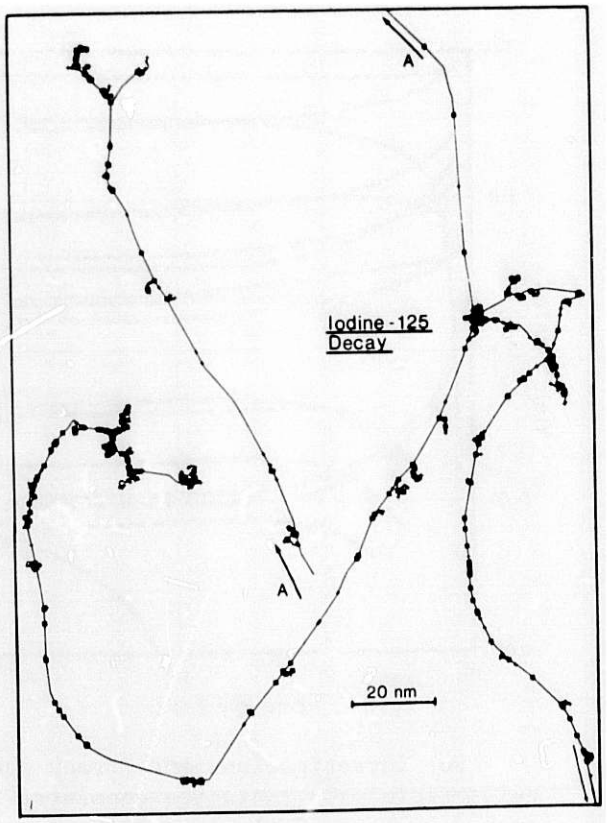

Fig. 4
Electron trajectories from the radioactive decay of I-125 (source term by courtesy of J. Booz, KfA)

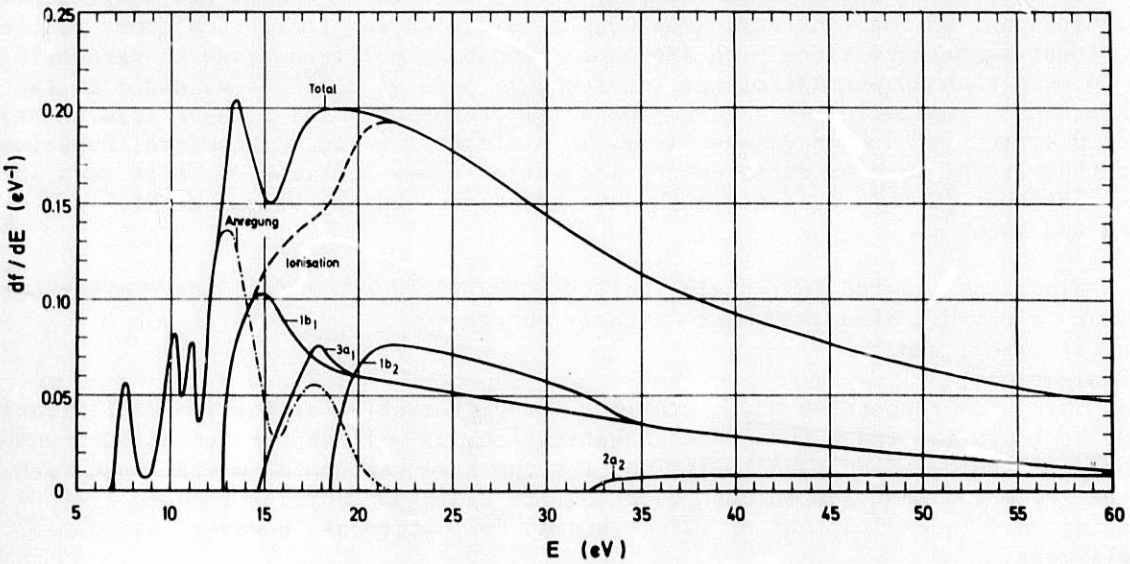

Fig. 5
Partial and total oscillator strength distribution of water vapor

edge of the energy spectra of electrons ejected in such collisions is an important necessity. If such data are not directly known or for consistency checking of such

data in particular, Kim[5] and Inokuti[6] have developed a very useful method making extensive use of photon absorption cross section which often are more readily available than electron cross sections. Using their work as guidance and deriving partial oscillator strength spectra from optical data for the target of interest (see e.g. the excellent book of Berkowitz) as has been done by us for gaseous H_2O (fig. 5), it became possible to discriminate between the reliability of sometimes contradicting data. As an example, in fig. 6 Platzman-plots of secondary electron spectra measured by various authors are plotted versus the Rydberg energy divided by the corresponding energy transfer R/E. The shapes of all three sets of data evidently disagree with each other, and only with the help of oscillator strength data and the approach of Kim and Inokuti does it become possible to identify here the data of Opal et al.[12] as the most reliable ones. Using this method then differential ionization cross sections also for other primary electron energies could be derived (fig. 6), showing clearly the high importance of photon absorption data for electron and ion transport calculations.

ACCURACY OF CROSS SECTION DATA

The accuracy needed in Monte-Carlo calculations for radiation transport problems or investigations into track phenomena evidently depends on the type of result one is interested in. For depth dose calculations, e.g. less accuracy in certain excitation cross sections is necessary than for calculations of the spatial luminousity profile of this certain optical emission line in a material. For total yield calculations no information at all is needed on the angular dependency of inelastic collissions and the elastic scattering cross section. However, for detailed track structure calculations determining the locations and types of all activations produced by the passage of a charged particle, e.g. as the boundary condition for subsequent chemical reactions, accurate knowledge also on the angular behaviour of inelastic and elastic cross sections will be needed. This makes it evident that no generally valid statement can be made as to the accuracy needed for such calculations.

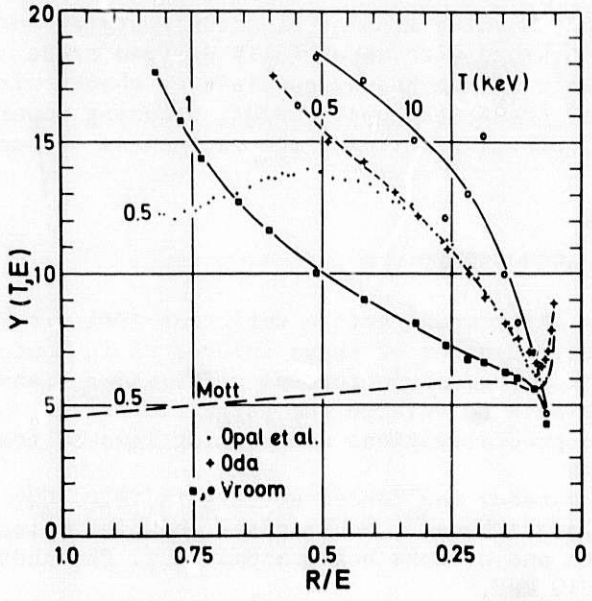

Fig. 6

Platzman-plots of measured secondary electron spectra for electron impact or water vapor

At this occasion it should be pointed out that certain experimental data, e.g. the so-called W-value, which can be measured with high accuracy, and the Fano-factor (Inokuti et al.[7]) provide very sensitive consistency checks for the accuracy of measured data well within their original error bars. From fig. 7 it is evident,

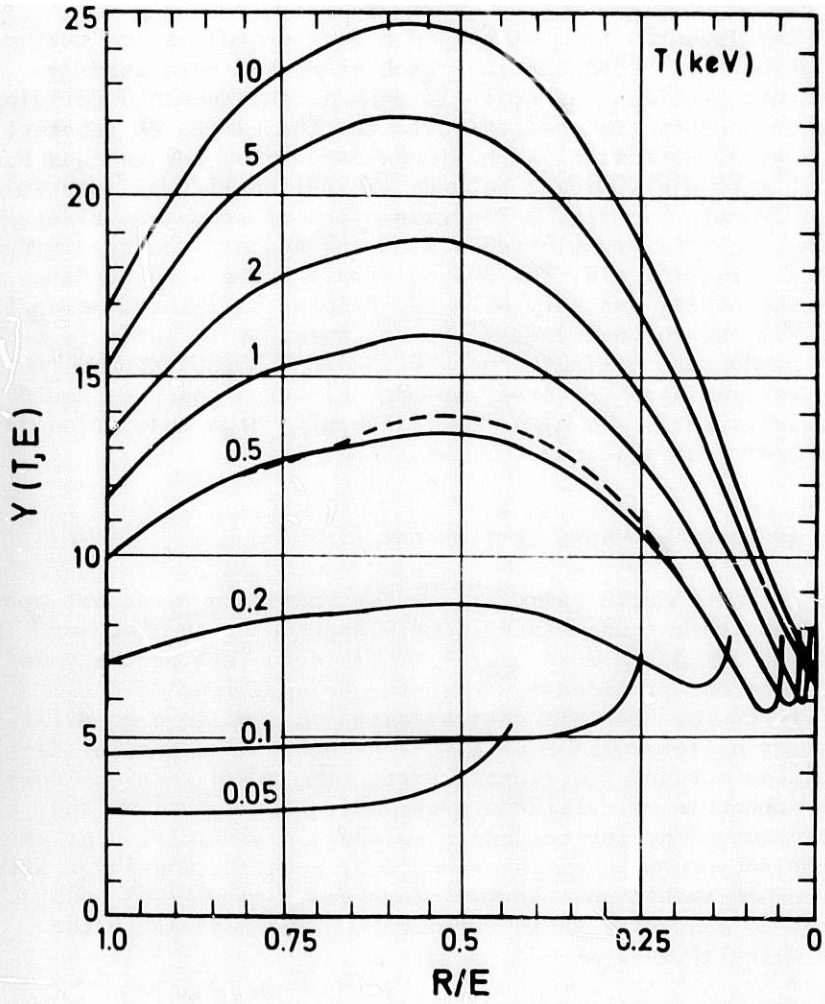

Fig. 7

Platzman-plots of theoretical secondary electron spectra for various primary electron energies as derived from oscillator strength for water vapor

that very good agreement with the constant W-value at high electron energies and the strong increase at low energies can be obtained with a carefully derived cross section data set. Such an greement can only be reached by consistency checks with all information on total and differential cross sections, yields, stopping power, foil transmission and reflection curves, etc., underlining the usefulness of such data for track structure calculations.

FUTURE RESEARCH NEEDED

Since this workshop takes place only three weeks before Christmas 1984, it might be appropriate to formulate the cross section needs of those interested in Monte-Carlo transport calculations and in track phenomena in form of a Christmas wish-list (for Christmas 198? or even 199?): To be able to enlarge the target materials covered already and to gain insight into generalisations and scaling laws of track structure **properties**, we would need more

- theoretical and experimental data for gaseous and condensed targets, e.g. CO, CO_2, O_2, Nitrogenderivatives[9], NH_3, H_2O, hydrocarbons[10], noble gases, complex molecules (e.g. DNA, amino acids), molecules with one or more heavy atoms (e.g. Phosphorous),
- for electrons from, say, 1 eV to some 10 keV,
- for protons, alphaparticles and heavier ions (say, up to Uranium) from 1 keV/n to several 100 MeV/n.

For these targets and particles the following types of data were needed:

- absolute total[11], single-, double-differential, partial cross sections for inelastic collisions (in particular for ionizations),

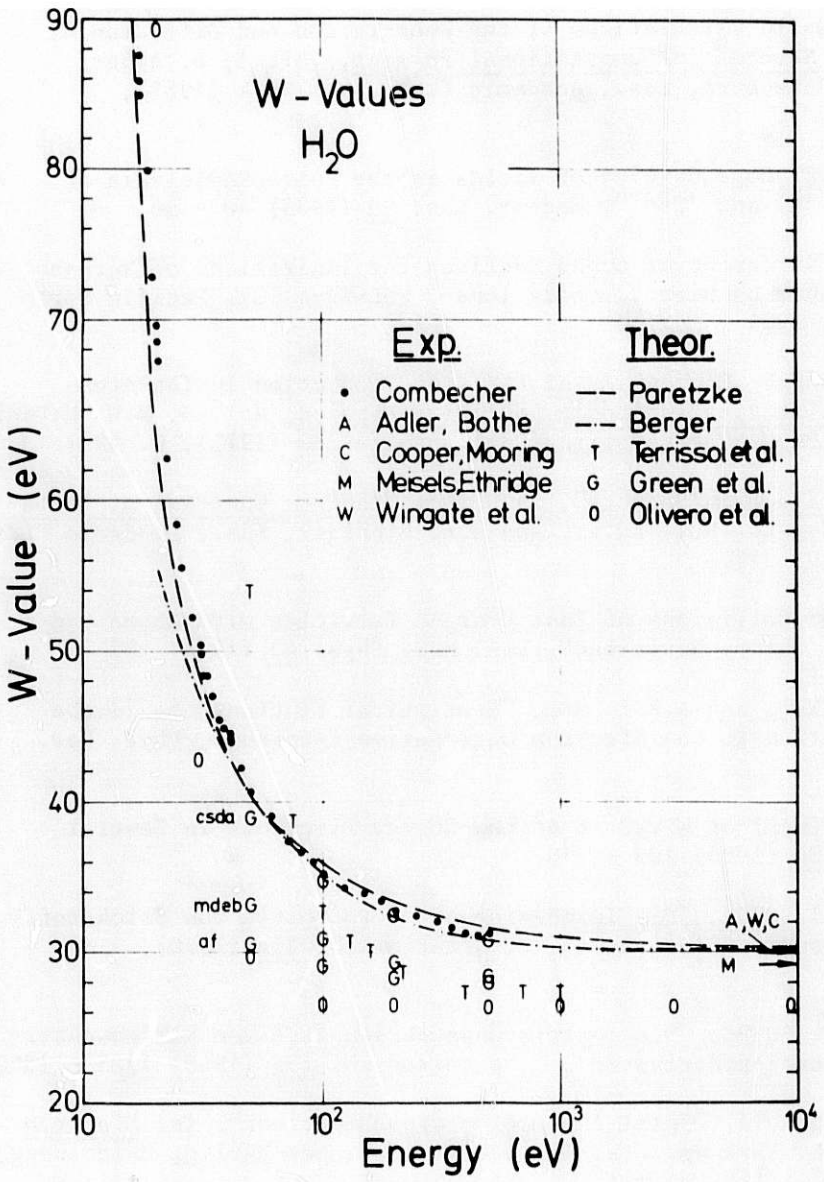

Fig. 8

Comparison of various calculated and measured data for W-values of electrons in water vapor with own calculations and experimental data of Combecher[8]

- total and differential stopping cross sections for single collisions,
- (partially) degraded electron spectra,
- yields and fluctuations of excitations, ionizations, and other new chemical products,
- spatial structure of primary activations,
- data for mixtures and heterogeneous targets.

Though all the above information is urgently needed for reliable investigations into track structure phenomena, in consideration of the difficulty involved in these topics it might be more realistic to expect the availability of most of the more difficult ones of the above data not before the end of this century.

REFERENCES

1. M.J. BERGER, "Monte Carlo Calculations of the Penetration and Diffusion of Fast Particles", in: Methods in Computational Physics, Vol. 1, B. Alder, S. Fernbach, and M. Rotenberg, Eds., Academic Press, New York (1963), p. 135 - 213

2. M.C. SAUER et al., "LET Dependencies of Yields in the Pulse Radiolysis of Aqueous Systems with $^{2}H^{+}$ and $^{4}He^{2+}$", Radiat. Res. 93 (1983) 40 - 50

3. W.E. WILSON et al., "Differential Cross Sections for Ionizations of Methane, Ammonia, and Water Vapor by High Velocity Ions", PNL-SA-11903, Pacific Northwest Laboratory, Jan. 1984

4. M.E. RUDD and J.H. MACEK, "Mechanisms of Electron Production in Ion-Atom Collisions", in: Case Studies in Atomic Collision Physics, Vol. 3, E.W. McDaniel and M.R.C. McDowell, Eds., North-Holland Publ., Amsterdam (1972), p. 49 - 136

5. Y.K. KIM, "Secondary Electron Spectra", in: Proc. 5th Int. Congress of Radiation Research, O.F. Nygard, H.I. Adler, and W.K. Sinclair, Eds., Academic Press, New York (1975) p. 219 - 226

6. M. INOKUTI, "Inelastic Collisions of Fast Charged Particles with Atoms and Molecules - The Bethe Theory Revisited", Rev. Mod. Phys. 43 (1971) 297

7. M. INOKUTI, D.A. DOUTHAT, and A.R.P. RAO, "Statistical Fluctuations in the Ionization Yield Relation to the Electron Degradation Spectrum", Phys. Rev. A22 (1980) 445 - 453

8. D. COMBECHER, "Measurement of W Values of Low-Energy Electrons in Several Gases", Radiat. Res. 84 (1980) 189 - 218

9. H.-J. GROSSE und H.-K. BOTHE, "Die Inionisierungsquerschnitte von Stickstoff- und Halogen-Kohlenwasserstoffderivaten", Z. Naturforsch. 25a (1970), 1970 - 1976

10. H.-J. GROSSE und H.-K. BOTHE, "Die Ionisierungsquerschnitte von Kohlenwasserstoffen und deren Sauerstoffderivaten", Z. Naturforsch. 23a (1968) 1583 - 1590

11. F.J. de HEER und M. INOKUTI, "Total Ionization Cross Sections", in: Electron Impact Ionization, T.D. Märk and G.H. Dunn, Eds., Springer-Verlag, Heidelberg, in preparation

12. C.B. OPAL, E.C. BEATY, W.K. PETERSON, "Tables of Secondary-Electron-Production Cross Sections", Atomic Data 4 (1972) 209 - 253

THE TRANSPORT OF LOW ENERGY ELECTRONS IN WATER AND SOME PHYSICO-CHEMICAL IMPLICATIONS

D.J. Brenner and M. Zaider

Radiological Research Laboratories
College of Physicians and Surgeons of Columbia University
New York, NY 10032

ABSTRACT

Considerable effort by numerous groups is currently being devoted to measuring or calculating cross-sections for use as input to Monte-Carlo studies of radiation effects. We address the question of how well do low-energy cross- sections need to be known in order to calculate adequately quantities of interest in the radiobiological domain.

INTRODUCTION

Transport studies of electrons in biologically relevant media (e.g. water) have usually been carried out such that the history of each electron is terminated at a few electron-volts, whereupon the remaining energy is considered to be locally deposited. Such a termination, prior to electron thermalization, has historically been motivated by two factors. First,the sparcity of experimentally determined cross-sections at very low energies and corresponding theoretical difficulties is predicting these same cross-sections - which are also strongly phase (gas/liquid) dependent. Second is the assumption that this termination would not significantly affect the resulting calculated quantities used in theoretical radiation biology.

The basis for this latter assumption is the view (prevalent till a few years ago) that the biologically radiation-sensitive regions in cells were of micrometer dimensions, i.e. significantly longer than the range of subexcitation electrons. This view, however, has been seriously challenged in recent years by the results of several experiments designed specifically to probe these sensitive sizes; these indicate that patterns of energy deposition in nanometer dimensions may be decisive in determing the biological effect. Whilst the underlying reasons for this are not fully understood it seems reasonable to attribute at least part of such "nanodosimetric" effects to so called "indirect" radiation action wherein the action is mediated through the agency of diffusing radicals created by interactions with water.

It appears timely then, to reopen the question of the importance of low energy, subexcitation electron transport and thermalization, in a quantitative manner. In this report this is done using as a criterion the time dependent-yield of radical species.

The present approach is based on some new developments in the stochastic treatment of both particle and radical-species transport. The Monte Carlo codes performing these tasks have been described in the literature [1,2]. Briefly, a first code transports electrons through water by simulating, event-by-event, their interactions. This yields, for example,the initial positions and types of the chemical species produced. A second code uses this information as input and simulates the diffusion and interaction of radicals, including formation of new species.

The calculations are exemplified here by the yields of hydrated electrons: the results, however do typify those of other species (e.g. OH, H_2O_2 etc).

LOW ENERGY CROSS-SECTIONS

Details of the Monte-Carlo code for transporting various radiations have been described elsewhere [1], therefore we mention briefly only details of the low energy electrons cross-sections used in the transport code. As the electron energy decreases below around 5 eV, vibrational interactions form the dominant mode of energy loss. These cross-sections have been experimentally determined by Seng and Linder [3].

Below about 0.5 eV rotational interactions dominate. Here less experimental data are available, although some measurements at 6 and 2 eV have been made [4]. These cross-sections were therefore calculated, using the plane-wave Born approximation, considering only point-dipole interactions. According to Takayanagi [5] such a calculation might be expected to be fairly good below about 1 eV.

The formulae used in the calculation were those described by Itikawa [6] for an asymmetric top molecule. The initial distribution of rotational states was taken from the literature [7] and the results of the calculations at 2 eV are shown in Fig. 1; the agreement with experiment is suprisingly good.

DIFFUSION AND INTERACTION OF CHEMICAL SPECIES.

The use of vibration and rotational cross-sections described in the previous section allows the transport of electrons down to thermal energies (.03 eV). Such a transport code yields the position and types of all radical species at a very early time after irradiation ($\sim 10^{-15}$ sec). A different computer code [2] is then used to simulate the diffusion and fast chemical reaction of these radical species. Such calculations have been reported previously, but have typically used an ad hoc initial distribution of radicals and have also utilized a deterministic, rather than a stochastic approach to the subsequent interactions of the species. The first of these problems is, of course, overcome here by the use of Monte-Carlo generated initial radical positions; the second problem is resolved by using a stochastic analysis technique initially suggested by Clifford et al., [8] and further developed in Ref. [2].

Full details of the stochastic transport technique may be found in Ref. [2]; basically species are assumed to diffuse and interact in a manner described by Smoluchowski's equation which gives the probability that two radicals, initially a given distance apart, will come within a specified "encounter distance" (and thus be considered to have interacted) in a given time interval. This requires knowledge of the radical-radical "encounter distance" (which may be obtained using Debye's equation and the reaction rates) and also the relative diffusion constant.

The results of a calculation for high energy electrons are shown in Fig. 2; plotted is the yield of the species eaq as a function of time after irradiation, per 100 eV of energy deposited.

SENSITIVITY OF YIELDS TO LOW ENERGY CROSS-SECTIONS

In order to judge the sensitivity of the final results to the low energy cross-sections used in the primary electron transport code a series of electron transport calculations were performed, each time multiplying either the rotational or the vibrational cross-sections by a known factor. After each transport calculation the stochastic chemistry code was run and the results compared.

The results of varying the cross-sections by different factors are shown in Figs.3 and 4. Each time, for comparison, the experimental data are shown. In general it would be expected that as the cross-sections are decreased, the radicals would initially be further apart and thus less likely to interact , making for a less marked decrease in radical yields with time; this is illustrated, for example in Fig. 3a.

Below leV the rotational cross-sections are so large (10^{-14} cm^2) that the distance an electron travels in thermalizing from this energy is typically less than the radical encounter distances, which are of the order of a few angstroms. Thus increasing the rotational cross-sections would not be expected to change the yield curve, which was found to be the case. The effects of decreasing these cross-sections are shown in Fig. 4, where again as the cross-sections are reduced, less chemical interactions occur; ultimately (see fig. 4c) the initial positions of the species are so far apart that essentially no interactions take place.

As an aside, also plotted in Fig. 2 are the experimental results of Jonah et al., [9] and Sumiyoshi and Katayama [10], which were obtained with liquid water. The reaction constants and diffusion coefficients used in the present calculation are for liquid water; however the Monte-Carlo electron transport was performed for water vapor, leading (see for example [11]) to a smaller proportion of ionizing events, and therefore smaller absolute G-values. It is not unreasonable, however, to assume that the initial point-pair distribution of radical separations will not change significanly between phases. If this is so, then a comparison of the shape, though not the absolute magnitude, of the theoretical with the experimental curve, becomes meaningful.

CONCLUSIONS

This sensitivity study is presented as an example of how the activities of the modeller and those of the producer of cross-sectional data should be correlated. For example it is apparent that large cross-sections at the end of the path of an electron leading to transport over distances less than typical chemical encounter distances (a few angstroms) need not be known that well for the calculation of chemical yields. Thus it may be that gas/liquid phase differences are not so crucial at these energies.

We plan and would encourage other groups to expand this study to include higher energies, and to observe the effects of secondary energy/angular distribution, so that the community generating cross-sections may have a better perception of the data that are necessary for such Monte-Carlo calculations.

ACKNOWLEDGEMENT

This investigation was supported in part by Contract No. DE-AC02-83ER60142 from the Department of Energy and by Grant No. CA 15307 to the Radiological Research Laboratory/Department of Radiology.

The authors gratefully acknowledge the assistance of Dr. L.A. Collins of Los Alamos National Laboratory during this work.

REFERENCES

1. M. ZAIDER, D.J. BRENNER and W. E.WILSON, "The Application of Track Calculations to Radiobiology I. Monte Carlo Simulations of Proton Tracks", Radiat. Res. 95, 231 (1983).

2. M. ZAIDER and D.J. BRENNER, "On the Stochastic Treatment of Fast Chemical Reactions," Radiat. Res. (submitted for publication).

3. G. SENG and F. LINDER, "Vibrational Excitation of Polar Molecules by Electron Impact II. Direct and Resonant Excitation in H_2O," J. Phys. B: Atom. Molec. Phys. 9, 2539 (1976).

4. K. JUNG et al., "Rotational Excitation of N_2, CO and H_2O by Low-Energy Electron Collisions," J. Phys. B: Atom. Molec. Phys. 15, 3535 (1982).

5. K. TAKAYANAGI, "Rotational and Vibrational Excitation of Polar Molecules by Slow Electrons," J. Phys. Soc. Japan 21, 507 (1966).

6. Y. ITIKAWA, "Rotational Transition in an Asymmetric - Top Molecule by Electron Collision: Application to H_2O and H_2CO," J. Phys. Soc. Japan 32, 217 (1972).

7. D.M. GATES et al., Natl. Bur. Std. Monograph 71 (1964).

8. P. CLIFFORD, N.J.B. GREEN and M.J. PILLING, "Stochastic Model Based on Pair Distribution Functions for Reactions in a Radiation-Induced Spur Containing One Type of Radical," J. Phys. Chem. 86, 1318 (1982)

9. C.D. JONAH et al., "Yield and Decay of the Hydrated Electron from 100 ps to 3ns," J. Phys. Chem. 80, 1267 (1976).

10. T. SUMIYOSHI and M. KATAYAMA, "The yield of Hydrated Electrons at 30 Picoseconds," Chem. Lett. 12, 1888 (1982).

11. J. BEDNAR, "Rydberg Enhancement of Total Ionization in Liquids Irradiated by Ionizing Radiation. II Liquid Water," Radiochem. Radioanal. Lett.45, 407 (1980).

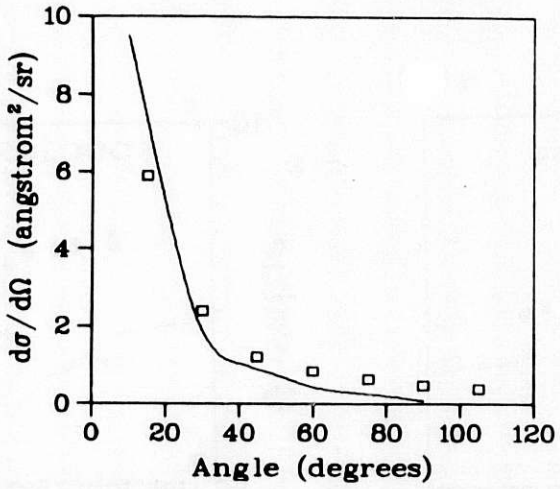

Fig. 1: Calculated (full curve) and experimental (points, Ref. [4]) rotational cross-section for 2.1 eV electrons on H_2O. Possible transitions of the rotation quantum number J and its projection τ considered in the PWBA calculation were $\Delta J = \pm 1$, $\Delta\tau = 0, \pm 2, \pm 4$..

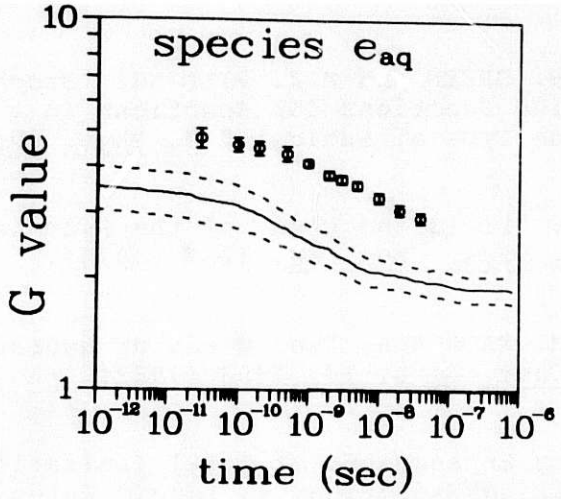

Fig. 2: Calculated (full curve) and experimental (points, Refs. [9,10]) decay of the species e_{aq} after irradiation of water by 22 MeV electrons. The broken curve are one standard deviation error bars, resulting from the finite statistics of the Monte-Carlo calculation. To facilitate comparison between the shapes of the experiment and the calculation, the data have been plotted on a logarithmic scale.

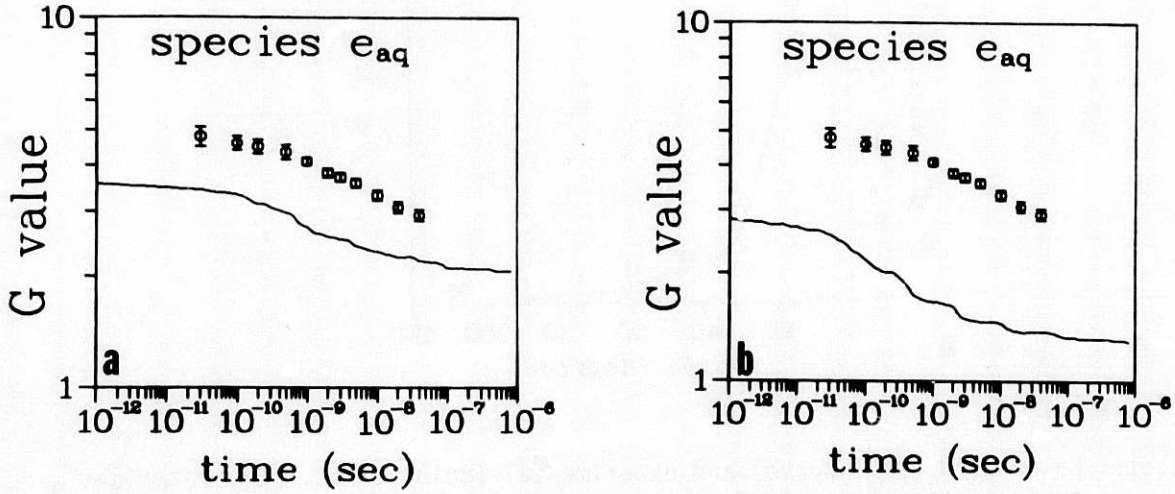

Fig. 3: Same as Fig. 2, calculated with vibrational cross-sections multiplied by 0.5 (a) and 5 (b).

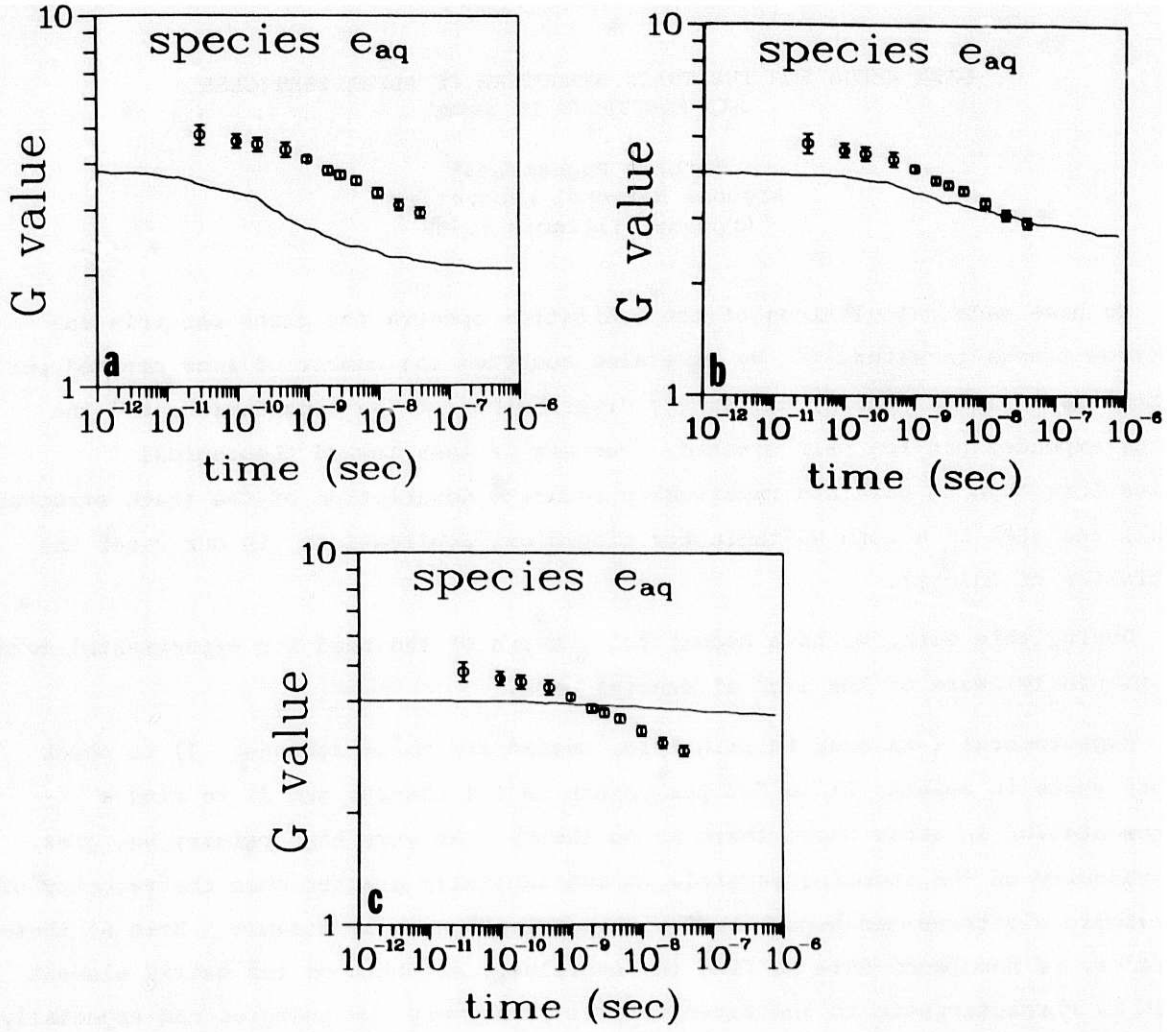

Fig.4: Same as Fig. 2, calculated with rotational cross-sections multiplied by 0.1 (a), 0.01 (b) and 0.001 (c).

DATA NEEDS FOR THE TRACK STRUCTURE OF ALPHA PARTICLES AND ELECTRONS IN WATER

Antonio Pagnamenta*
Argonne National Laboratory
Argonne, Illinois 60439

We have made calculations of the ionization spectra for alpha particle and electron tracks in water.[1,2] We have also computed the number of ions created per micrometre of track length, the energy distribution of the secondaries, and the energy expended per ion pair created. Our aim is less toward theoretical derivations than to obtain a numerically accurate description of the track structure at all energies in a form suitable for biomedical applications (in our case, the initiation of cancer).

During this work, we have become fully aware of the need for experimental data and painfully aware of the lack of crucial data.

Experimental data are, in principle, needed for three reasons: 1) to check theory where it exists, 2) to fit parameters in the theory, and 3) to find a representation in areas where there is no theory. At very high primary energies, the velocity of the incoming particle is substantially greater than the velocity of the atomic electrons and hence the Born approximation is applicable. Even at these energies, we need good data to find the oscillator strength or the matrix element which is characteristic to the water molecule. At very low energies and especially for small momentum transfers, no quantitative theory exists for these ionization processes and we have to rely almost entirely on the experimental data.

For electrons, essentially the only data available in the literature are the differential cross section measurements of Opal *et al.*[3] and the total cross section measurements of Schutten *et al.*[4] Recently, accurate determinations of the W-values for electrons on water vapor have become available through the measurements of Combecher.[5] Because of the sparseness of data, we had to use the idealization of Kim[6] who proposed to represent the glancing collision cross section as the product of a factor depending on the primary energy and essentially given by the Bethe theory and another factor dependent only on the energy of the secondaries which has

---

*Permanent address: Department of Physics, University of Illinois at Chicago, Chicago, Illinois 60680

to be taken from the data. As the data[3] are at 500 eV only, we have no test for the reliability of this factorization. A repetition of the measurements of single differential cross sections but extended to several energies above and below 500 eV would be highly desirable, as would a careful repetition of the measurements of total cross sections over a large energy range.

For the alpha particles, we were able to use the recent measurements of Toburen et al.[7], at T = 0.3 to 2 MeV, the charge-changing cross sections of Armstrong et al.,[8] the energy loss measurements of Matteson et al.,[9] and of Palmer et al.[10] The slowing down of alpha particles in water involves several processes about which only sparse information is available. Of prime interest are the charge-changing cross sections, pick-up and stripping of atomic electrons, the convoy electrons and absolute measurements of the total cross section covering a wider range of energies than the Toburen data.[7] There are several measurements of the convoy peak, but they are all in an energy range where the convoy contribution is still increasing as the energy decreases.[11] This cannot go on indefinitely and it would be most useful to have a measurement of the differential cross section at an energy below the maximum of the convoy contribution, perhaps at T = 0.1 to 0.5 MeV.

In conclusion, it should be mentioned that any good measurements on water or water vapor will receive almost instantaneous recognition as they are so relevant for many applications. Finally, Rudd[12] reports that double differential cross sections for electrons on water vapor have just been measured[12] and the convoy peak has been observed in protons on water.[13] This is an excellent start!

1. A. Pagnamenta and J. H. Marshall, ANL preprint 83-5, January 1984.
2. A. Pagnamenta and J. H. Marshall, Proc. Seventh Symp. on Microdosimetry, Oxford, England, September 8-12, 1980, J. Booz, H. G. Ebert and H. D. Hartfield, Eds., Harwood Academic Publishers Ltd., pp. 97-107 and pp. 375-385 (1981).
3. C. B. Opal, E. C. Beaty, and W. K. Peterson, Tables of secondary-electron production cross sections, Atomic Data 4, 209-253 (1972), (especially p. 243).
4. J. Schutten, F. J. DeHeer, H. R. Moustafa, A.J.H. Boerboom, and J. Kistemaker, Gross and partial ionization cross sections for electrons on water vapor in the energy range of 0.1-20 keV, J. Chem. Phys. 44, 3924-3928 (1966).
5. D. Combecher, Energy per ion-pair spectra, Radiat. Res. 84, 189-218 (1980).

6. Yong-Ki Kim, Energy distribution of secondary electrons, I. Consistency of experimental data, Radiat. Res. 61, 21-35 (1975); II. Normalization and extrapolation of experimental data, Radiat. Res. 64, 205-216 (1975).
7. L. H. Toburen, W. E. Wilson, and R. J. Popowich, Secondary electron emission from ionization of water vapor by 0.3 to 2.0 MeV He^{+} and He^{++} ions, Radiat. Res. 82, 27-44 (1980).
8. J. C. Armstrong, J. V. Mullendore, W. R. Harris and J. B. Marion, Equilibrium charge-state fractions of 0.2 to 6.5 MeV helium ions in carbon, Proc. Phys. Soc. 86, 1283 (1965).
9. S. Matteson, D. Powers, and E.K.L. Chau, Physical state effect in the stopping cross section of H_2O ice and vapor for 0.3-2.0 MeV alpha particles, Phys. Rev. A 15, 856 (1977).
10. Rita B. J. Palmer and Ahmad Akhavan-Rezayat, The stopping power of water, water-vapor and aqueous tissue, J. Phys. D: Appl. Phys. 11, 605 (1978).
11. I. A. Sellin, Electron "cusp" spectroscopy of the forward peak in continuum electron capture and loss in gases and solids, J. Physique, Colloque C1, (Suppl.), p. C1-225, (February 1979).
12. M. E. Rudd and M. A. Bolorizadeh, Contribution to this workshop.
13. M. E. Rudd, private communication.

ELECTRON COLLISION CROSS SECTIONS AND RADIATION CHEMISTRY

Y. Hatano
Department of Chemistry
Tokyo Institute of Technology
Meguro-ku, Tokyo 152, Japan

ABSTRACT

A survey is given of the cross section data needs in radiation chemistry, and of the recent progress in electron impact studies on dissociative excitation of molecules. In the former some of the important target species, processes, and collision energies are presented, while in the latter it is demonstrated that radiation chemistry is a source of new ideas and information in atomic collision research.

INTRODUCTION

Radiation chemistry needs electronic and ionic collision cross section data. The data must be correct, absolute, and comprehensive.[1] Radiation chemistry, however, has another important role in the relation between radiation research and atomic collision research. I believe that radiation chemistry is a source of new ideas and information in atomic collision research.

In the following, 1) a brief survey will be given of recent progress[2] in understanding of fundamental processes in radiolysis, and 2) an answer will be given to questions such as, "What kind of cross section data are most needed?" and "What kind of target molecules are most interesting from the point of view of radiation chemistry?" Finally, 3) from the viewpoint of radiation chemistry as a source of new ideas and information in atomic collision research, some of the following topics in our research programs will be presented.

A. Electron impact dissociative excitation of molecules (cf. Y.Hatano, *Comments on At.Mol.Phys.*, 13, 259 (1983)).
B. Electron attachment to van der Waals molecules (cf. Y.Hatano and H.Shimamori, "Electron Attachment in Dense Gases", in "Electron and Ion Swarms", ed. by L.G.Christophorou, Pergamon Press (1981)).
C. De-excitation of excited rare gas atoms and molecules (cf. Y.Hatano, 3rd Int. Symp. on Dynamics of Molecular Collisions, ICPEAC Satellite Meeting, Kaiserslautern, Aug.4-5, 1983)
D. Electron-ion recombination in dense gases, liquids and solids (cf. Y.Nakamura, K.Shinsaka and Y.Hatano, *J.Chem.Phys.*, 78, 5820 (1983)).

FUNDAMENTAL PROCESSES IN RADIOLYSIS

Radiation chemistry deals with the chemical and physico-chemical effects of the interaction of high energy ionizing radiation with matter. The succession of events that follow absorption in matter of high energy radiation is divided into three characteristic temporal stages: physical, physicochemical and chemical stages.[3] The

physical stage of radiation effects is the primary activation of molecules due to the collision of high energy incident particles, i.e., photons, electrons, heavy charged particles, neutrons, etc., with molecules to form electronically excited or ionized states of molecules and ejected electrons. Electrons thus formed have energies enough to ionize again surrounding molecules. At the steady state of radiolysis, electrons are formed in a wide range of energies via cascading electron-molecule collision processes. Consequently, electron-molecule collisions such as ionization and excitation of molecules, recombination or attachment of electrons, etc., have an important role in radiolysis. The physicochemical stage is the reaction of transient species such as excited and ionized states of molecules, free radicals, and electrons themselves. The reaction of thermalized species like thermal free radicals, which are not unique to radiation chemistry, is sometimes called the chemical stage of the radiation effects.

Let us consider and summarize briefly what happens when, for example, 1 MeV γ-rays pass through a liquid organic compound, AB.

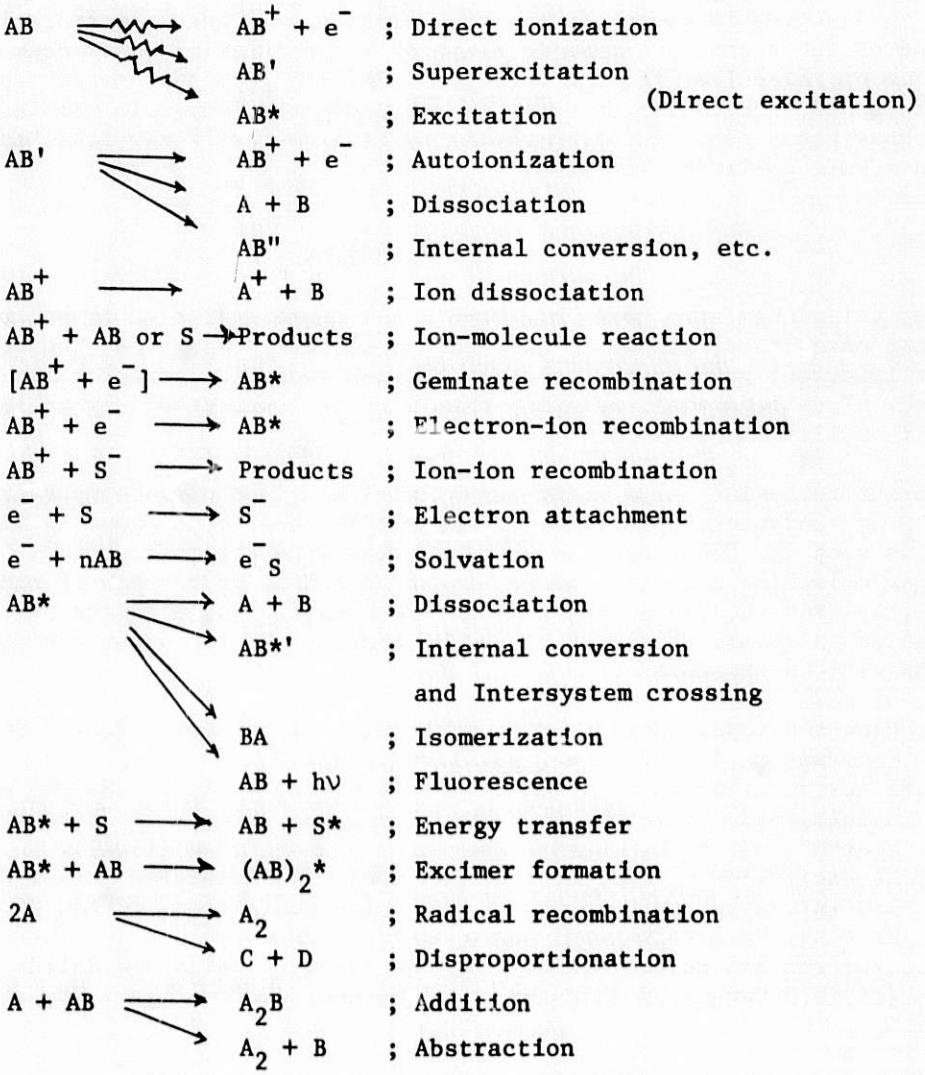

Transient species in radiolysis are thus classified as two types; firstly charged species, i.e., electrons and ions, and secondly, neutral species, i.e., excited molecules and free radicals. These species constitute the above mentioned fundamental processes in radiation chemistry.

In analyzing these processes radiation chemists must understand the present

status of the knowledge of atomic collision research and elementary reaction dynamics. The use of a matrix representation[4] is quite helpful to understand or to survey, but very briefly, diverse information on these various processes. For example, some electron collision processes are shown in Fig. 1. The present status of the knowledge of each collision process is shown, but very roughly, in Fig. 2. The results of a particular collision process at various collision energies are projected on the matrix. The matrix representation like Fig. 1 or 2 is helpful not only for analyzing a complex mechanism of radiolysis but also for finding new ideas of atomic collision research.

CROSS SECTION NEEDS IN RADIATION CHEMISTRY

Radiation chemistry needs electron collision cross section data, which must be correct, absolute, and comprehensive[1] in the collision energy range particularly from 10^2 eV down to near-thermal, or even to thermal energies. The data must include those not only on ionization and electronic-excitation processes but also on vibrational and rotational excitation processes, and also on elastic collisions. Low energy electrons including subexcitation electrons[5] have an important role in radiolysis. Electron attachment and recombination processes, and possibly also electron solvation processes are highly affected by electron energies. The data on electron impact dissociation of molecules are important particularly from the viewpoint of getting experimental evidence for the dissociation of superexcited states.

Radiation chemists are interested in various molecules not only in the gas phase but also in condensed phases, and in a variety of materials ranging from rare-gas atoms and diatomic molecules to complex molecules such as hydrocarbons, alcohols, etc., and to polymers.[2] Water is one of the most important molecules also in radiation chemistry. Followings are some of the important or popular molecules in radiation chemistry.

H_2O
cyclo-C_6H_{12}, C_6H_6
CH_4, C_2H_6, C_3H_8, n-C_4H_{10}
C_2H_4, C_3H_6, C_2H_2
n-C_6H_{14}, n-C_7H_{16}, i-C_8H_{18}
neo-C_5H_{12}, $Si(CH_3)_4$
CH_3OH, C_2H_5OH, i-C_3H_7OH
2-methyltetrahydrofuran
N_2O, CO_2, SF_6
CH_3Br, CH_3Cl, $C_6H_5CH_2Cl$
n-C_4F_{10}, C_6F_{12}, C_6F_6
H_2, D_2, N_2, CO, O_2
He, Ne, Ar, Kr, and Xe

Electron collision cross section data are also needed for toxic or corrosive molecules[6] such as

HF, HCl, HBr
F_2, Cl_2, Br_2
SiH_4, CCl_4, and
other halogen containing molecules,

and also for unstable species such as free radicals and excited atoms and molecules.

Radiation chemists are much interested in reactions in condensed phases, particularly in the behavior of electrons in liquids, glassy matrices, and dense gases. There exists therefore a large amount of experimental data in radiation chemistry concerning both dynamic and static behavior of electrons such as electron scavenging effects on product yields, electron yields per energy absorbed, electron mobilities, optical absorption spectra, electron spin resonance absorption spectra, etc. Although there exist also some theories to explain these data, the experimental results are still not fully understood. The following two kinds of experimental approach to this subject, i.e. electrons in dense and disordered media, should be made. One is the approach from the gas phase, the other is the approach from crystalline solids. Electron collisions with a completely isolated target molecule and electron scattering in crystalline solids have been relatively well understood. From the viewpoint of the former type of approach, it is highly necessary to make electron collision experiments with van der Waals molecules as targets.

It is also interesting for us in collision research to change systematically target molecules in terms of

i) Isotopes

ii) The same group of elements in the periodic table

iii) Isoelectronic series
H_2O, CH_4, NH_3, HF and Ne

iv) Isosymmetric series
H_2O and H_2S

v) Homologous series
Alkane, alkene and alkyne

vi) Isomers
- C_3H_6 and cyclo-C_3H_6
- C_4H_8-1, trans-C_4H_8-2
- cis-C_4H_8-2, i-C_4H_8,
- methylcyclopropane and cyclo-C_4H_8

RADIATION CHEMISTRY AS A SOURCE OF NEW IDEAS AND INFORMATION IN ATOMIC COLLISION RESEARCH

As described in the previous section, we could find new ideas and information in atomic collision research when we compare our present status of konwledge of each collision process with the result of fundamental processes in radiation chemistry. In this workshop one of the topics in our recent research programs is presented. A survey is given of recent experimental studies of the electron impact dissociation of simple molecules with emphasis on translational spectroscopy of dissociation fragment atoms by Doppler profile measurements of Balmer emission.[8] The principle of the experimental technique, the obtained results and discussion are summarized for H_2, D_2 and the molecules H_2O, HF, CH_4 and NH_3 in an isoelectronic sequence. Evidence has been given for the electronic structure of superexcited states and their dissociation processes.

Since about 1970 we have been making experiments on electron impact dissociative excitation of simple molecules in order to get direct evidence for dissociation of superexcited molecules. In the early 1960's Platzman indicated theoretically their important role in radiolysis based mainly on the following experimental results:[3,7,9]

i) $\eta(E) = \sigma_i(E)/\sigma_t(E) < 1$ at $E > I$, where $\eta(E)$ is photoionization efficiency at photon energy E, $\sigma_i(E)$ and $\sigma_t(E)$ are respectively ionization and total absorption cross sections, and I is the ionization potential.

ii) Hydrogen isotope effects are observed on the values of $\eta(E)$.

iii) η values obtained by photoionization experiments are almost equal to their values estimated from W-value measurements.

In the radiolysis of molecule AB, accroding to Platzman, AB is not only directly ionized or excited, but also superexcited:

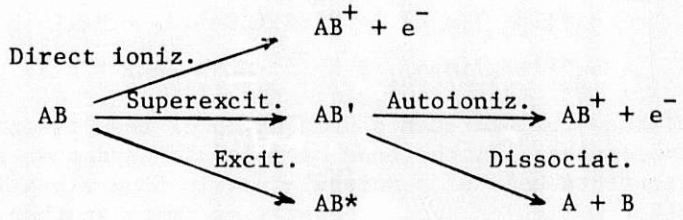

where AB' is called superexcited states whose internal energy is larger than its ionization potential. AB' is autoionized, or dissociated into neutral fragments. Because of the presence of this dissociation process, the ionization efficiency is less than unity for molecules even at energies larger than the ionization potential. de Heer et al. measured in the electron impact experiment the cross sections and their hydrogen isotope effects of Balmer and Lyman emissions formed by electron impact on H_2, D_2, H_2O, D_2O and simple hydrocarbons, and indicated the dissociation of superexcited states.[10] Ehrhardt and Linder indicated also this process experimentally on the basis of their electron-energy-loss experiments of hydrocarbons.[11]

Hatano and Shida found an experimental evidence for an important role of hot hydrogen atoms in radiolysis and ascribed their formation to the dissociation of superexcited states.[12-14] The physically essential nature of hot hydrogen atoms, i.e., how they hold the excess energy and how much energy they have, however, was not made clear. In the early 1970's Hatano, Oda, and their coworkers began to measure directly translational and/or internal energy of excited (hot) hydrogen atoms by observing the Doppler profile of Balmer emission lines in electron-molecule collision experiments.

Dissociation processes play a very important role in the decay of highly excited molecular states. For better substantiation of these states and their dissociation processes, it is indispensable to measure the kinetic energy of dissociation fragments and their angular distribution as well as to measure the threshold energy of dissociation.[15] The former measurement is called translational spectroscopy of molecular dissociation and has been successfully used by many authors,[16-23] but has been almost exclusively with charged particles and metastable or high Rydberg atoms because it has been difficult to measure directly the kinetic energy of emissive excited atoms with short lifetimes. Recently, however, some groups have independently observed anomalous Doppler profiles of Balmer emission lines produced by electron impact on simple molecules.[24-29] Similar anomalous Doppler profiles due to molecular dissociation were observed earlier in other types of experiments.[30,31] The observation of such anomalous profiles in e^--H_2 collision experiments[25-27,29,32] has made a physically clear contribution to directly understanding the dissociation potential of molecules into emissive fragments because other essential information, such as excitation spectra of Balmer emission and theories of dissociation potentials, has already been presented in detail for molecular hydrogen.

An apparatus[27] developed exclusively for measuring anomalous Doppler profiles of optical emission in electron-molecule collision experiments has shown the promising

versatility and usefulness of this method for further substantiating the dissociation potentials or processes of highly excited molecular states. This apparatus is composed of a specially devised photon counting system combined with an etalon-grating monochromator (Fig. 3) and has been applied to H_2 [27,32] and D_2,[32] the molecules such as H_2O,[33] D_2O,[33] CH_4,[34] NH_3 [34] and HF[35] isoelectronic with Ne, the molecule H_2S isosymmetric with H_2O, and other simple hydrocarbons.[32]

The experiments on H_2 and D_2 (Fig. 4) have determined the kinetic energy of $H^*(3)$[27,32] formed from doubly excited states $(2p\sigma_u)(n1\lambda)$ as well as from vibrationally excited states $(1s\sigma_g)(n1\lambda)$.

$$H_2^*(2p\sigma_u)(n1\lambda) \rightarrow H^*(3)(KE=7eV) + H(1)$$
$$H_2^*(1s\sigma_g)(n1\lambda) \rightarrow H^*(3)(KE=0.3eV) + H(1)$$

This is typical evidence for Platzman's prediction of the dissociation of superexcited states of molecules. In the case of molecular hydrogen excess energies beyond the ionization threshold of a molecule result from vibrational or double excitation. For other molecules one can easily estimate another type of excess energy resulting from inner valence excitation. This experimental technique has been applied to H_2O, HF and other more complex molecules,[33-35] giving direct evidence for the dissociation potential of inner valence excited states as well as doubly excited states. In the case of H_2O, for example, the following dissociation processes are observed.

$$H_2O^*(18eV) \rightarrow H^*(3)(KE=0.4eV) + OH(X^2\pi)$$
$$H_2O^* : (1b_2)^{-1}(nR)$$

$$H_2O^{**}(25\text{-}30eV) \rightarrow H^*(3)(KE=4eV) + O(2p^4) + H(1)$$
$$H_2O^{**} : (2a_1)^{-1}(nR) \text{ or } (3a_1)^{-1}(1b_1)^{-1}(4a_1)(nR),$$
$$(1b_1)^{-2}(2b_2)(nR)$$

$$\text{cf. } H_2O : \tilde{X}^1A_1(1a_1)^2(2a_1)^2(1b_2)^2(3a_1)^2(1b_1)^2$$

In the series of these investigations the internal energies of these highly excited states have been found to be in good agreement with the energies of corresponding molecular ions obtained from photoelectron or ESCA spectra and (e,2e) experiments.[34] This agreement implies these highly excited or superexcited states being molecular high-Rydberg states, and supports the core-ion model[23] proposed for high-Rydberg atomic dissociation fragments. Almost the same conclusion has been very recently obtained by other authors[36] using an apparatus similar to that in Fig. 3. They have measured not only Balmer-α but also β, γ, δ and ε, and have used a different method for Doppler profile analysis.

Recent review papers[8,15] summarize from the viewpoint of electron-molecule collision research the experimental technique, results and discussion which are presented in the series of above mentioned investigations, and comment on some future problems to be solved for this subject.

Some future problems needing more work on dissociative excitation of molecules are the following.

i) The use of synchrotron radiation, instead of electron beams, to excite a molecule. Referring to an interesting preliminary experiment,[37] a combination of synchrotron radiation with translational spectroscopy of dissociation fragments would highly substantiate the dissociation potential of molecules.

ii) Translational spectroscopy of dissociation fragments as combined with the measurements of electron energy loss spectra.

iii) Translational spectroscopy of H(1) as a dissociation fragment as well as the measurement of its cross section

iv) Careful comparison of σ_t with σ_i as a function of E

v) New theoretical approaches to dynamics of highly excited molecular states

vi) Measurements of the partial cross section of both dissociation and ionization of a molecule at a particular excitation energy.

Some of these problems are under study in our current research programs.

REFERENCES

1. M. Inokuti, This Workshop.
2. See, for example, a) *Proc. 7th ICRR*, Amsterdam, July 3-8, 1983, Martinus Nijhoff Publ. (1983); b) "The Study of Fast Processes and Transient Species by Electron Pulse Radiolysis", ed. by J. H. Baxendale and F. Busi, *NATO Adv. Study Ser.* Vol.86, D. Reidel Publ. Co. (1982).
3. R. L. Platzman, *Vortex*, 23, 327 (1962).
4. M. Inokuti, "Photoionization and Other Problems of Many-Electron Interactions", ed. by F. J. Wuilleumier, Plenum Publ. (1976), p.431.
5. Y. Itikawa, This Workshop.
6. These data have been compiled from the critical analysis of swarm data. See, M. Hayashi and T. Nimura, *Proc. 3rd Swarm Seminar* (1983); *J. Appl. Phys.*, 54, 4879 (1983).
7. R. L. Platzman, *Proc. 3rd ICRR*, Cortina d'Ampezzo, 1966, ed. by G. Silini, North Holland (1967), p.20.
8. Y. Hatano, *Comments on At. Mol. Phys.*, 13, 259 (1983).
9. R. L. Platzman, *Radiat. Res.*, 17, 419 (1962).
10. D. A. Vroom and F. J. de Heer, *J. Chem. Phys.*, 50, 573, 580, 1883 (1969).
11. H. Ehrhardt and F. Linder, *Z. Naturforschg.*, 22a, 444 (1966).
12. Y. Hatano, S. Shida and M. Inokuti, *J. Chem. Phys.*, 48, 940 (1968).
13. S. Shida and Y. Hatano, *Int. J. Radiat. Phys. Chem.*, 8, 171 (1976) (Review).
14. Y. Hatano, "Hot hydrogen atoms in radiation chemistry", in *"Hot Atom Chemistry"* ed. by T. Matsuura, Kodansha (1984), p.98.
15. F. J. de Heer, H. A. van Sprang and G. R. Möhlmann, *J. Chim. Phys.*, 77, 773 (1980) (Review).
16. a) N. Sasaki and T. Nakao, *Proc. Imp. Acad. Jpn.*, 11, 138 (1935); 17, 75 (1941); b) Y. Ishikawa, *ibid.*, 18, 246, 390 (1942); 19, 380 (1943).
17. A. Crowe and J. W. McConkey, *J. Phys.*, B6, 2088 (1973); *Phys. Rev. Lett.*, 31, 192 (1973).
18. G. H. Dunn and L. J. Kieffer, *Phys. Rev.*, 132, 2109 (1963).
19. R. J. van Brunt and L. J. Kieffer, *Phys. Rev.*, A2, 1293 (1970).
20. M. Misakian and J. C. Zorn, *Phys. Rev.*, A6, 2180 (1972).
21. M. Leventhal, R. T. Robiscoe and K. R. Lea, *Phys. Rev.*, 158, 49 (1967).

22. R. Clampitt and A. S. Newton, *J. Chem. Phys.*, 50, 1997 (1969).

23. J. A. Shiavone, K. C. Smyth and R. S. Freund, *J. Chem. Phys.*, 63, 1043 (1975).

24. I. Tokue, I. Nishiyama and K. Kuchitsu, *Chem. Phys. Lett.*, 35, 69 (1975).

25. R. S. Freund, J. A. Schiavone and D. F. Brader, *J. Chem. Phys.*, 64, 1122 (1976).

26. G. N. Polyakova, V. F. Erko, A. I. Ranyuk and O. S. Pavlichenko, *Sov. Phys. JETP*, 44, 921 (1976).

27. K. Ito, N. Oda, Y. Hatano and T. Tsuboi, *Chem. Phys.*, 17, 35 (1976).

28. T. Ogawa, F. Matsumoto and N. Ishibashi, *Chem. Lett.*, 207 (1976).

29. M. Glass-Maujean, *J. Phys.*, B11, 431 (1978).

30. P. M. S. Blackett and J. Franck, *Z. Phys.*, 34, 389 (1925).

31. L. Frommhold and M. A. Biondi, *Phys. Rev.*, 185, 244 (1969).

32. K. Ito, N. Oda, Y. Hatano and T. Tsuboi, *Chem. Phys.*, 21, 203 (1977).

33. N. Kouchi, K. Ito, Y. Hatano, N. Oda and T. Tsuboi, *Chem. Phys.*, 36, 239 (1979).

34. N. Kouchi, M. Ohno, K. Ito, N. Oda and Y. Hatano, *Chem. Phys.*, 67, 287 (1982).

35. M. Ohno, N. Kouchi, K. Ito, N. Oda and Y. Hatano, *Chem. Phys.*, 58 45 (1981).

36. a) T. Ogawa and M. Higo, *Chem. Phys. Lett.*, 65, 610 (1979); b) M. Higo and T. Ogawa, *Chem. Phys.*, 44, 279 (1979); c) T. Ogawa and M. Higo, *Chem. Phys.*, 52, 55 (1980); 56, 15 (1981); 66, 243 (1982); d) T. Ogawa, J. Kurawaki and M. Higo, *Chem. Phys.*, 61, 181 (1981); e) T. Ogawa, F. Miyoshi and M. Higo, *Bull. Chem. Soc. Jpn.*, 55, 1790 (1981); f) M. Higo, S. Kamata and T. Ogawa, *Chem. Phys.*, 66, 243 (1982).

37. M. Glass-Maujean, K. Köllman and K. Ito, *J. Phys.*, B12, L453 (1979).

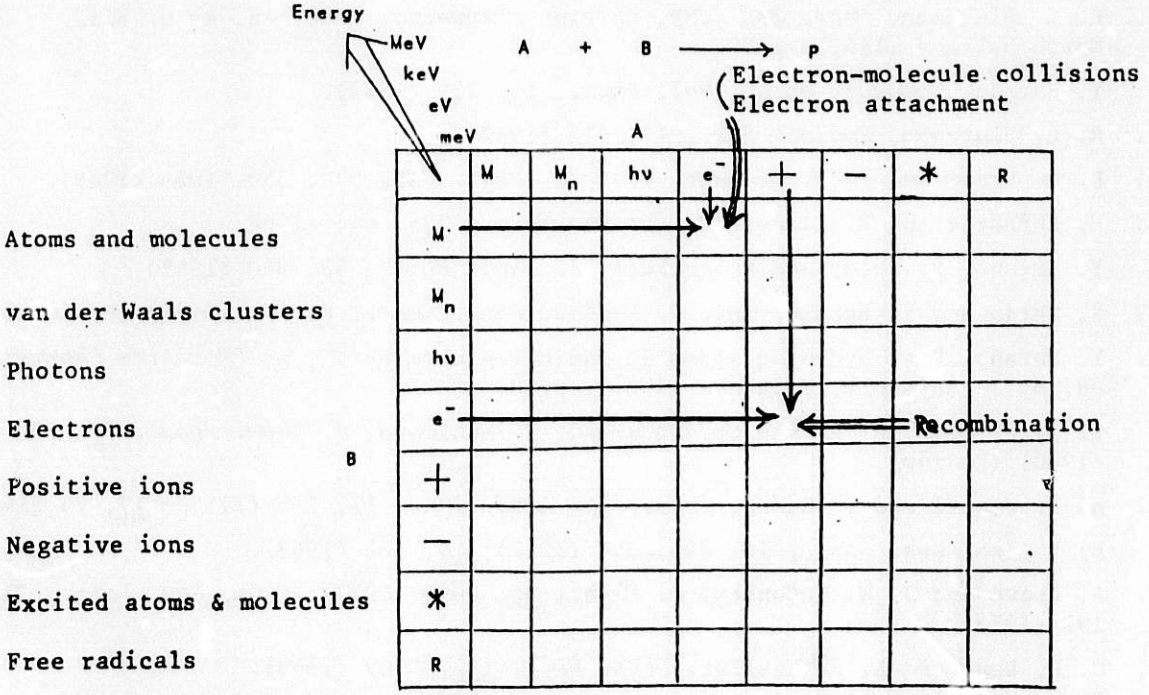

Fig. 1 The matrix representation of various collision and reaction processes between A and B to form products P at collision energies as expressed by the vertical scale. In the case of photons, photon energies are presented on the vertical scale. Electron-molecule collisions, etc., for example, are shown on the matrix.

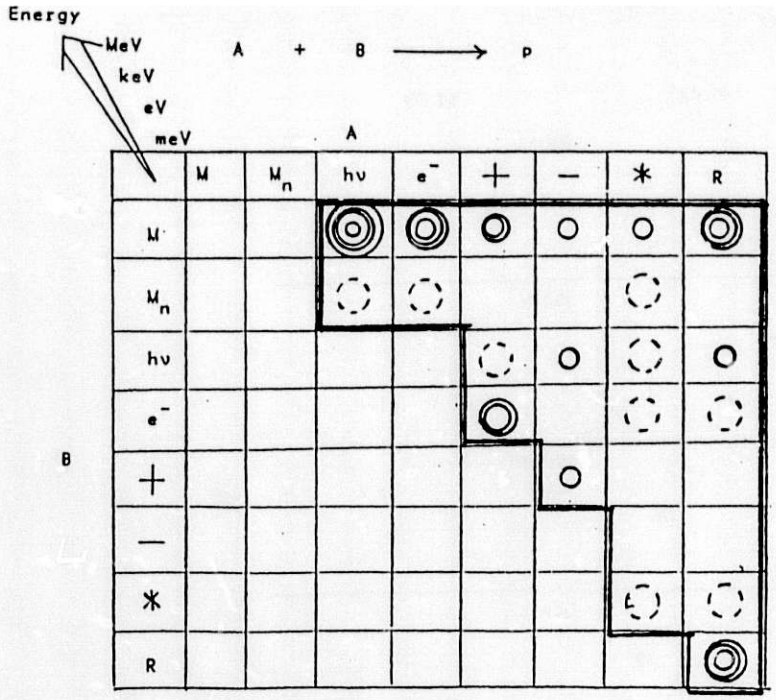

Fig. 2 A brief matrix-representation of the present status of the knowledge of each collision process. The data on a particular collision process at various collision energies are projected on the matrix. The degree of the data accumulation is expressed in the frame by the symbols; from rich to poor (blank).

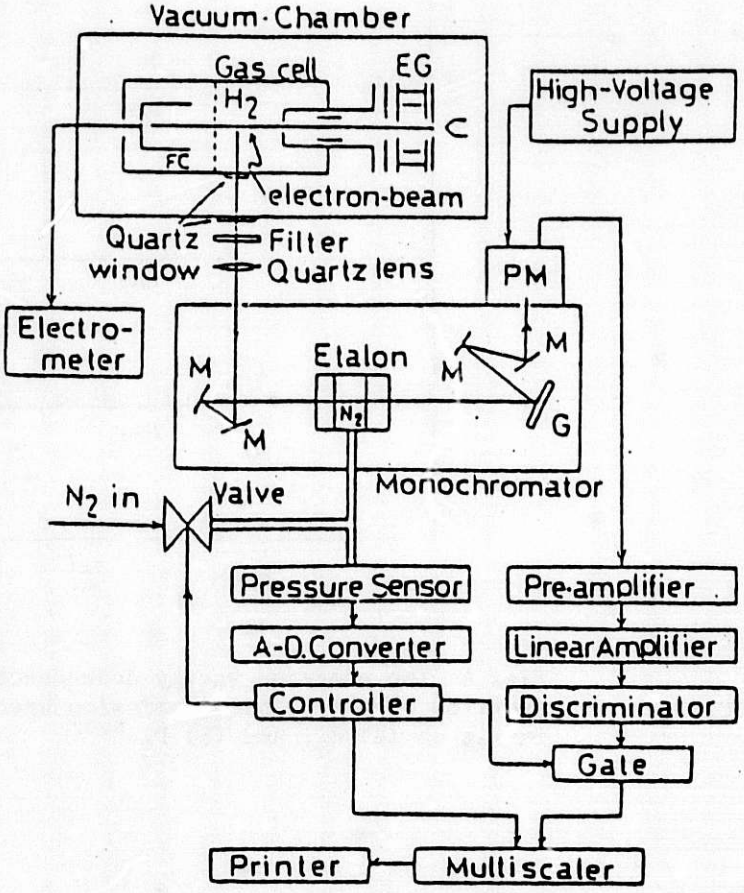

Fig. 3 Block diagram for the measurement of Balmer-α emission. EG: electron gun, FC: Faraday cup, G: Grating, M: mirrors, PM: photomultiplier. [8,27]

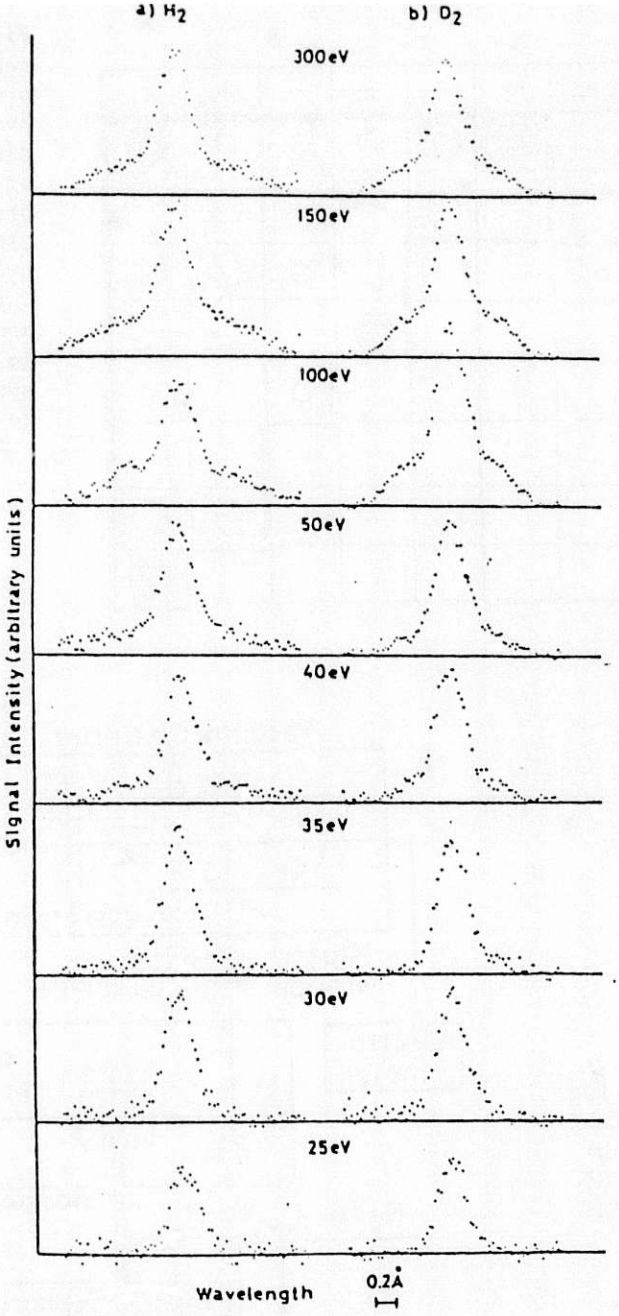

Fig. 4 The electron energy dependence of the Doppler profiles of the Balmer-α emission spectra by electron impact on (a) H_2, and (b) D_2.[8,32]

CROSS SECTION NEEDS IN THE STUDY OF GAS DISCHARGES

J. N. Bardsley

Physics Department, University of Pittsburgh
Pittsburgh, PA 15260

In studies of the motion of electrons through gases under the influence of an external electric field, the most important collision parameters are the momentum transfer cross section, the energy loss rate and the rates of various reactions such as attachment, ionization or electronic excitation. For pure gases in uniform DC fields, it is perhaps most useful to measure the relevant properties directly as a function of E/N (field strength divided by the number density of the neutral molecules). However, there is much current interest in tailoring gas mixtures to meet special goals, and it is clearly difficult to repeat each measurement for every candidate mixture. Thus, atomic collision physicists can play an important role by supplying absolute cross sections for the most important processes. For most applications, very high energy resolution is not needed; 50-100 meV would be excellent for all but the lowest incident energies. Measurements with an accuracy of 10-25% would be fine, but in many cases estimates correct to within a factor of 2 would represent a major advance.

Beginning with elastic scattering, the momentum transfer cross section is important since it controls the rates of loss of energy and directed motion for the electrons. The most reliable data come from measurements of drift velocities, which have been carried out for most, but not all, molecules of current interest. For energy loss rates through inelastic collisions, the situation is very different. Rotational excitation presents a special challenge, because of the small energy defects and the large number of initial rotational levels that are populated in many molecular gases. However, one does not need to measure each individual cross section. Instead, one wishes to know the rate at which electrons of a given energy lose energy to a gas of molecules at a known temperature. Theoretical work has been very valuable in this regard. With vibrational excitation, the experimentalist is in a much stronger position. It would be very helpful if there were a deliberate effort by the community to obtain absolute cross sections at energies between threshold and, say, 5 eV for most of the common small molecules. A similar situation is found with respect to attachment, electronic excitation, and dissociation.

Many of the most interesting discharges involve high energy densities. There is a special need for information regarding collisions involving excited species. For example, the cross sections for dissociative processes are often very sensitive to vibrational excitation in the initial molecule. In the study of the lower atmosphere and of many gas lasers and other electrical devices, we need to understand the properties of gases at densities of 10^{19} cm^{-3} and above. We must then consider the simultaneous interaction of three particles, or the effects of several consecutive two-body collisions which may involve many different particles. These problems have been attacked in recent studies of electron-ion and ion-ion recombination.

CROSS SECTIONS RELEVANT TO THE SPUTTERING & DESORPTION OF CONDENSED GASES BY IONS AND ELECTRONS

R. E. Johnson

Department of Nuclear Engineering & Engineering Physics
University of Virginia, Charlottesville, VA 22901

Sputtering and desorption induced by electronic energy deposited in solids by fast ions and electrons gives a measure of the non-radiative relaxation processes occurring near the surface. The condensed-gas solids are particularly useful to study because of their small cohesive energies, hence, large sputter yields. Many of these materials also luminesce efficiently. In this paper, the processes that lead to energetic non-radiative relaxation and/or luminescence are reviewed. Cross sections for initiating these processes by incident ions and electrons are considered and some comparisons are made with measured yields for molecular ejection and luminescence. Those cross sections desired are discussed and the problem of using gas-phase cross sections when considering events initiated in the solid is also discussed.

REMARKS ON THE THEORY OF SLOW ELECTRON COLLISIONS AND OF CONDENSED MATTER EFFECTS

U. Fano

James Franck Institute, The University of Chicago
Chicago, Illinois 60637

Attention will be directed to semi-quantitative considerations that provide guidance for the discussion and assessment of cross sections. They concern the comparison of neutral ionic targets, of targets with closed and open valence shells, the connection of collision and spectral data, the effects of correlations between an incident electron and the electrons in the target's valence shell, and simplified treatments of electron-molecule collisions. A second group of remarks will concern the features that distinguish targets in condensed state from those in gaseous phase, mainly lowering of Rydberg levels by dielectric screening, raising (or lowering) of the spectrum of oscillator strength by the plasma effect and increased dissipation of excitation into vibrations by intermolecular coupling.

ENERGY LOSS IN CONDENSED MEDIA

Edwin N. Lassettre

Department of Chemistry
Carnegie-Mellon University
Pittsburgh, Pennsylvania 15213

In retirement I have been out of the collision field for several years. Therefore, I can only give my impressions of a certain phase of the workshop discussion. For what they are worth, those impressions are as follows.

During the workshop a general concensus seemed to emerge on one primary unsolved problem, the loss in energy of electrons with kinetic energies less than the first electronic excitation potential. In water vapor, for example, this means electrons with kinetic energies below about six electron volts. This is a region in which resonances are expected to affect collision cross sections by large factors. It is also a difficult region to study experimentally in gas phase scattering. Nevertheless, it is important to do such experiments and to resolve vibrational excitations. The necessary techniques, although difficult, are apparently available. In the case of rotational excitation some success has been achieved in theoretical calculation of cross sections. On the whole, in the gas phase the situation seems hopeful although some time may be required before all the data are available.

In condensed phases the situation is less favorable. At higher kinetic energies calculations of energy deposition in water have been carried out for both gas and liquid[1] the latter by utilizing optical data on water[2] to take account of collective effects. In the sub-electronic-excitation energy range the situation is less clear. It is unlikely that collision cross sections for the gas can be carried over to the liquid, even approximately, for the following reason. A resonance in the sub-excitation region for most molecules, including H_2O, has a drastic effect on differential collision cross sections. The lifetime for this temporary negative ion of a single molecule would be changed, and probably lengthened, for a cluster of molecules. In the case of water, strong hydrogen bonds form between molecules in the liquid and affect the vibrational spectrum. This condensed phase effect is surely important and must be taken into account in any theory of energy loss in liquids and would greatly change the energy loss spectrum from that in the gas. Because of resonances this is expected to be especially true in the sub-electronic-excitation range.

Experimentally, the condensation effect could be investigated (in principle at least) by examining the scattering of low energy electrons from films condensed on a conducting substrate. The films should be thick enough to minimize the effect of substrate and might have to contain a small percentage of conducting particles (e.g. graphite) to prevent charge buildup. A rapidly deposited film on a cooled substrate, coated with graphite, forming an amorphous solid layer, would be satisfactory for comparison with gas scattering. Scattering from any type of condensed film (solid or liquid) would be worthwile.

Christophorou[3] has studied attachment coefficients in dense gases,[3] and it seemed possible to obtain collision cross sections from transport coefficients under similar conditions. However, Elford's analysis[4] indicates that this can be successful

only at very low kinetic energies where very few transitions are involved. More direct measurements from condensed films would be preferable.

REFERENCES

1. J. E. Turner, H. G. Paretzke, R. N. Hamm, H. A. Wright and R. H. Ritchie, Radiation Research 92, 47 (1982)

2. J. M. Heller, R. N. Hamm, R. D. Birkhoff and L. R. Painter, J. Chem. Phys. 60, 3483 (1974).

3. L. G. Christophorou, Chem. Revs. 76, 409 (1976).

4. M. T. Elford, in "Electron and Ion Swarms," Proceedings of the Second International Swarm Seminar, Edited by L. G. Christophorou, Pergamon Press, New York (1981), p. 11.

Particle Tracks

Robert Katz
University of Nebraska

In this workshop the words particle tracks, and modeling, have been taken to imply Monte Carlo calculations of the distribution of excitations and ionizations about the path of protons of energy less than 3 MeV, in a gas. While such calculations are needed, they represent only the briefest introduction to a solution of the particle track problem.

We need models which can predict the effects observed in a wide variety of detectors, from biological matter in vivo, through cell cultures in vitro, viruses, enzymes, and a range of physical detectors including emulsions, plastics, scintillators, thermoluminescent dosimeters, crystals which display color centers, and a variety of other physical systems. Here the term particle track has a broader meaning, implying not the initial stage of the process but the final observable end-points. The detailed pathways through which these end-points evolve after irradiation are unknown to us, except in the most general terms.

Models which seek to account for end-points must therefore rely on some sort of calibration of the detectors, to produce a parametric representation which can be folded into the initial state of excitations and ionizations following the passage of a heavy ion through the detector.

A first order model which does this, and the only model of any generality, uses gamma-rays to calibrate the detector, and then requires knowledge of the radial distribution of dose about an ion's path to yield knowledge of the track.

From atomic physics we need information about the radial distribution of dose. We should like the information to be accurate, and complete. We need experimental measurement of the radial distribution of dose, through which to test calculations. We need this information for the broadest possible range of Z and β in as many media as possible, at distances from the ion's path from, say, 5Å until the greatest radial penetration of delta rays.

As an important first contribution we need to know how to scale proton data. All we have now is a formula for the effective charge which we know to be fundamentally incorrect, though remarkably useful. All contributions to knowledge of the energy spectrum of delta rays from partially clothed ions of all Z will be most welcome.

ION AND ELECTRON IMPACT IONIZATION CROSS SECTIONS

M. Eugene Rudd

Dept. of Physics and Astronomy
University of Nebraska-Lincoln
Lincoln, NE 68588-0111

ABSTRACT

Several current projects are described in which cross sections of interest to radiation physics are being measured. These include total and multiple ionization cross secttions for protons on several gases covering a wide energy range, the measurement of cross sections differential in the angle and energy of ejected electrons for several gases including water vapor, and a review of proton ionization data. The work on water vapor has also been extended to electron and neutral hydrogen impact. A brief discussion is also given of some systematics of ionization cross sections.

INTRODUCTION

It is rather surprising that ionization cross sections are not better known since a large fraction of the stopping power is due to that process. The situation is especially serious for protons below about 100 keV where published values disagree by factors of as much as 3 and 4 in some cases. Brief descriptions are given here of several current projects designed to measure differential and total ionization cross sections by proton, electron and neutral hydrogen impact in attempt to help improve the situation.

CROSS SECTION PROJECTS RECENTLY COMPLETED

1. Total ionization cross sections for protons on gases

In collaboration with R.D. DuBois, L.H. Toburen, and C.A. Ratcliffe of Battelle Pacific NW Laboratories and with T.V. Goffe of the University of Nebraska, we have recently completed and published[1] the measurement of cross sections for the production of positive and

negative charge in He, Ne, Ar, Kr, H_2, N_2, O_2, CO, CO_2, and CH_4 by four different accelerators at the two laboratories. This is the most comprehensive proton ionization measurement so far available.

Corrections were made for neutralization of the proton beam, secondary electron production at the grid, scattering of the beam particles by the target gas, the effect of fields on the transmission of the grid, thermal transpiration, and for background currents. Five sets of data, which were taken at overlapping energy ranges, were averaged by fitting the equation:

$$\sigma = A\sigma_o \sum_i N_i I_i^{-2} x_i^B \ln(1+Dx_i)/(C+x_i^{B+1}) \qquad (1)$$

where the summation is over the less tightly bound subshells, N_i is the number and I_i the binding energy of the ith subshell, $x_i=T/I_i$, $T=E_p/1836$, and A, B, C, and D are the adjustable fitting parameters. The results are presented both in a table of cross sections and as values of the parameters. Use of the equations and the parameters allows the calculation of cross sections at energies not given in the table. Extrapolation outside the 5-4000 keV range of energies for which data were taken is possible, but not recommended.

The experimental uncertainty ranges from 8% above 500 keV through 15% at 25 keV, to 25% at 5 keV. The cross sections are generally in good agreement with the average of earlier data where available except for the case of helium where our low energy data are considerably below almost all the earlier results. Since the cross sections for helium are the lowest of any target, any contamination or spurious electron production would tend to make the measured cross sections too high. Agreement of our data with electron impact data at high energies is excellent.

In addition, electron capture cross sections are presented which were determined by subtracting the cross sections for producing positive and negative charges. Data are given for the same targets from 5 to 150 keV.

2. Multiple ionization by H^+ and He^+ impact

Also in collaboration with the Battelle group, measurements have been completed[2] giving the cross sections for multiple ionization of the rare gases. This was done by modifying the parallel-plate apparatus in the project just described by the addition of a time-of-flight system to separate the various charge states of the recoil ions. While the cross sections measured were relative, they were put on an absolute basis by comparison with the total σ_+ data from the previous project.

While multiple ionization was very small for helium, it increased as the atomic number of the target increased. The multiple ionization was also appreciably greater for He^+ projectiles than for H^+. For example, for 500 keV impact the fraction of the total ionization due to multiple ionization was as follows:

Target	H^+	He^+
He	0.5%	6.7%
Ne	6.9	38
Ar	11.5	58
Kr	44	63

It was also found that H^+ produces less multiple ionization than equal velocity electrons.

PROJECTS UNDERWAY

1. Proton ionization review

While there have been several reviews of electron impact ionization, there have been no comprehensive critical reviews of proton ionization cross sections. I have undertaken to make such a review with the collaboration of Y.K. Kim, D.H. Madison, and J.W. Gallagher under the auspices of the JILA Atomic Data Center. This review includes published data for all targets and impact energies. Although partial or differential cross section data are not being included, we plan a later review of differential measurements.

A discussion of the various methods of measuring electron production cross sections will be given with special attention to possible sources of error.

Using several bibliographic references, we are attempting to make a complete survey of all published total cross section data available. Each cross section is put in a computer file along with the energy and target. Table I shows the energy ranges of the data presently available.

Table I. Proton Total Ionization Data Available

Monatomic targets	
H	7-1500 keV
He-3	3-30
He-4	0.3-5000
Ne	0.9-4000
Na	20-100
Ar	0.4-4000
K	20-100
Kr	5-4000
Xe	8-2000
Diatomic targets	
H_2	0.4-4000
D_2	1.5-30
N_2	1-4000
CO	1-4000
O_2	2-4000
Triatomic targets	
CO_2	1-4000

Other targets	
NH_3	1-25, 250-2000 keV
SF_6	300-1800
TeF_6	300-1800
CH_4	1-4000
C_2H_2	30-100
C_2H_4	40-100
C_2H_6	30-90
C_4H_{10}	40-100
CH_3NH_2	250-2000
$(CH_3)_2NH$	250-2000
CH_3OH	8-25
C_2H_5OH	8-25
C_3H_7OH	8-25
C_4H_9OH	8-25
$C_5H_{11}OH$	8-25
$C_6H_{13}OH$	8-25
$C_7H_{15}OH$	8-25
$C_8H_{17}OH$	8-25
Air	5-180

Each experimental report is being reviewed to assess the probable extent of the systematic error in the measurement. In some cases corrections are made using more recent information. Weights will be assigned to the various data and a least-squares fit will be made to the weighted data using a fitting equation.

The fits obtained will be adjusted to be consistent with electron impact data, optical data, and distorted-wave Born approximation calculations and recommended values of cross sections for the various targets will be given.

The review should be of value to workers planning to make further measurements of cross sections as well as to those using proton impact cross sections in a variety of applications.

2. Ionization cross sections by He^+ and He^{2+}.

In collaboration with R.D. DuBois and L.H. Toburen, cross sections are being measured for electron and ion production in eleven target gases for He^+ and He^{2+} impact from 5-4000 keV. Because He^{2+} has the same m/q as H_2^+ and since the latter is very difficult to eliminate from an ion source, we are using the isotope He-3 to give an unambiguous result for the He^{2+} case.

Since the neutralization cross sections needed for making corrections in the ionization experiment are not all available in the literature, we have also undertaken to measure the cross sections σ_{10} for He^+ and σ_{20} and σ_{21} for He_{2+} from 5 to 350 keV.

3. Cross sections for water vapor

Water vapor as a target poses several experimental problems. It tends to poison certain types of electron gun cathodes, reducing their emission after only a short usage. It has a similar deleterious effect on the secondary emitting surfaces of electron multipliers. It is also difficult to pump because of its condensibility. In addition, the usual method of freezing and pumping to eliminate air from the water used to supply the target has been found to be unreliable. These difficulties explain, in part, the relative paucity of cross section data for water vapor. But because of the importance of the practical applications of data on water vapor, we have, with the collaboration of the Battelle group, undertaken a comprehensive study of it involving measurements of several different kinds of cross sections. In summary these are:

A. Energy and angular distribution of the doubly differential cross sections (DDCS) for ejection of electrons from water vapor by
   a) 50-2000 eV electrons
   b) 15-150 keV protons
   c) 20-150 keV neutral hydrogen atoms

B. Total ionization cross sections for proton impact from 5-4000 keV.

C. Dissociation cross sections for proton impact from 250-2000 keV.

Comparison of the DDCS for electron, proton, and neutral impact should yield information on the systematics of the electron ejection process and the mechanisms responsible for it.

4. Differential electron ejection cross sections

While total ionization cross sections are very important, for some work more detailed information is needed such as the energy distribution of ejected electrons. It has not yet proved feasible to measure such singly differential cross sections (SDCS) directly, but a fair amount of doubly differential cross section (DDCS) data has accumulated in which the cross sections were measured as a function of energy and angle of ejection. The DDCS can be integrated over angle to obtain the SDCS. Only three groups have published such measurements for proton impact, Larry Toburen and collaborators at Battelle Pacific NW Laboratories, Nikolaus Stolterfoht and co-workers at the Hahn-Meitner Institute in Berlin, and my co-workers and I at Nebraska. Table II lists the published DDCS data for proton impact.

Table II. Proton impact doubly differential cross section data available

Helium	5-1500 keV	Nitrogen	5-1700 keV
Neon	50-1500	Oxygen	50-1500
Argon	5-5000	Water vapor	300-1500
Krypton	1000-4200	Methane	200-2000
Xenon	300-2000	Sulfur hexafluoride	300-1800
Hydrogen	5-1500	Tellurium hexafluoride	300-1800

Clearly, there are large areas of ignorance remaining. More targets should be measured and the energy ranges for some extended. Besides the water vapor data already mentioned, we plan to extend the range of DDCS measurements for oxygen, neon, and krypton to lower energies and to obtain the first data on carbon monoxide and carbon dioxide. These will be done from 5-150 keV.

SYSTEMATICS OF PROTON IONIZATION

For modelling purposes where it is necessary to involve several parameters, tables of experimental data tend to be too voluminous to be manageable. In such cases it is highly desireable to be able to express the systematics of the process in a more compact form. This may take the form of a theoretical treatment from first principles, a semi-empirical model, or even a purely empirical equation which yields cross sections of reasonable accuracy. This section contains a brief summary of some of the approaches which can be used to obtain cross sections for ejection of electrons by proton impact.

1. Total ionization cross sections

The well-known Bethe-Born treatment of ionization at high impact energies yields the $E_p^{-1} \log E_p$ dependence on projectile energy which has been well verified by experiment. At energies lower than the maximum in the cross section curve this relation is no longer valid. An equation similar to Eq. 1 which combines an empirical power law dependence at low energies with the Bethe-Born dependence at high

energies is being tried in connection with our review.

In most such equations the fitting parameters have to be chosen separately for each target gas. We have also tried another approach which utilizes the numbers of electrons N_i and binding energy I_i for each subshell of a given target to obtain an equation which gives a small enough variation of the fitting parameters among the various targets that it could be said to have predictive value. This was the approach used in Eq. 1 which yielded reasonably consistent results. Ref. 1 should be consulted for further information.

As part of the proton review, D.H. Madison and Y.K. Kim are calculating cross sections using the distorted-wave Born approximation (DWBA). The early results of this computation indicates good agreement with experiment in the high energy region but progressively poorer results at lower energies. Unfortunately, with present-day understanding of wave functions, this calculation is only possible for monatomic targets and even there the accuracy is good only for lighter atoms.

2. Singly Differential Cross Sections (SDCS)

The classical binary encounter approximation (BEA) as applied to proton impact by Vriens[3] has been used to obtain useable values of cross sections differential in the energy E of the ejected electrons. For best results, however, the cross sections must be averaged over a realistic distribution of initial electron energies in the target atom. This integration has been given by Rudd, Gregoire, and Crooks[4] in closed form which can readily be programmed on a personal computer. The results are generally in agreement with experiment within a factor of two over nearly the entire range of electron energies that has been measured.

Miller, Toburen, and Manson[5] have recently developed a technique for calculating the energy distribution of electrons from such collisions by merging the high electron energy results from the BEA with low energy cross sections obtained from photoabsorption data and the Bethe expansion of the Born approximation. This work was discussed at this meeting.

Unfortunately, neither of these approaches works well at low impact energy where the ionization probably takes place through a curve-crossing molecular promotion mechanism as proposed by Fano and Lichten[6] rather than through a knock-on type collision. Not much theoretical attention has been paid to this energy region but a partial theory was proposed by Rudd and Macek[7,8] which yielded a simple exponential dependence on electron energy. This can be written in the form

$$\sigma(E) = \sum_i NI^{-3}F(T/I)\exp[-\alpha E/(IT)^{1/2}]/\alpha \qquad (2)$$

where α is a dimensionless constant approximately equal to unity. The function F(T/I) can be chosen such that when the exponential is integrated over all electron energies, the resulting expression yields the total ionization cross section equation at that energy.

Eq (2) describes the cross sections for proton impact[8] below about 50 keV to within a factor of 2. Because of the form of Eq (2) it is a simple matter to integrate it in various ways to obtain other quantities of interest. Examples are:

Average energy of ejected electron, $E_{av} = (IT)^{1/2}/\alpha$ (3)

Total ionization cross section, $\sigma = NI^{-2} F(T/I)(T/I)^{1/2}/\alpha$ (4)

Stopping power due to ionization, $S = I[1 + (T/I)^{1/2}/\alpha]$ (5)

Fraction of electrons with E>I, $f = \exp[-\alpha(I/T)^{1/2}]$ (6)

The equation for the average energy suggests a simple scaling law. The average energy divided by the binding energy I plotted as a function of T/I should be a universal function for all gases if we set $\alpha = 1$. Furthermore a log-log plot should be a straight line with a slope of 0.5. Fig. 1 shows such a plot and one sees that the agreement with the prediction is reasonably good at low energies.

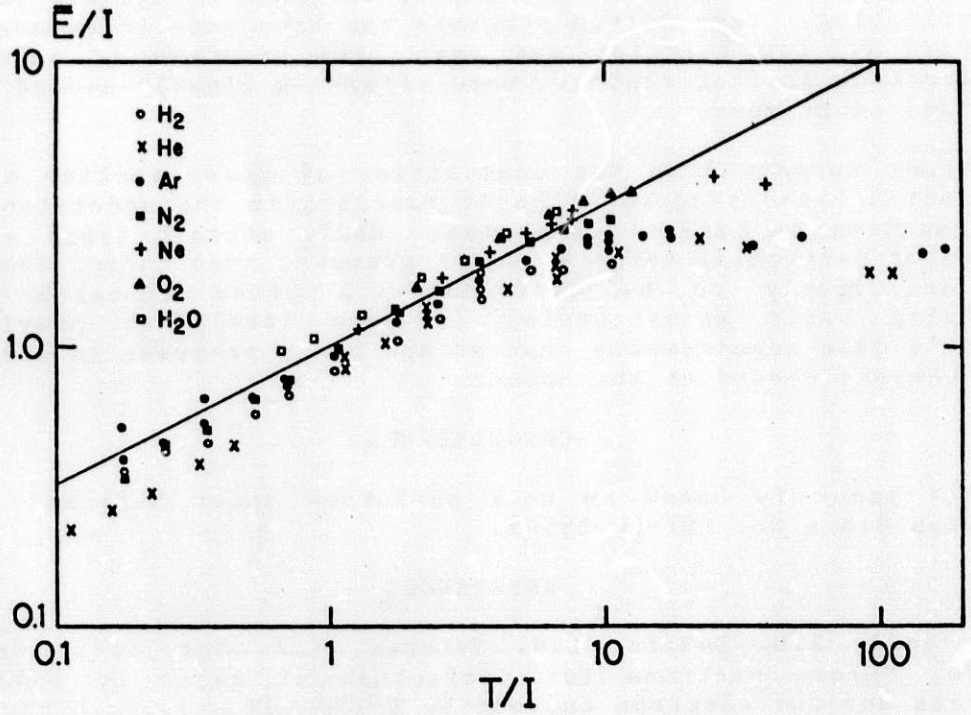

Fig. 1

Excellent results have been reported[9] for average ejected electron energy by using Eq. 3 up to 200 keV and assuming a constant value at higher proton energies.

3. Doubly Differential Cross Sections (DDCS)

Calculations of the cross section differential in both angle and energy of ejection of the electron have been made by Madison[10,11] using the DWBA method already mentioned. Again, at higher energies

this has worked reasonably well and surprisingly well even at lower impact energies. However, a complicating factor is the mechanism of electron capture to the continuum which is not described within the framework of the first Born approximation. The theoretical treatments that have been proposed for this mechanism (see, eg Macek[12]) have so far not given accurate quantitative results.

Because the DWBA requires extensive computation it would be desirable to have an empirical or semi-empirical model which gives DDCS for proton impact. Some progress along these lines has been made by W. Wilson at Battelle PNL.

CONCLUDING REMARKS

It has been only 35 years since the first proton ionization cross section measurement was reported.[13] In that relatively short time a considerble amount of data, both differential and total has been accumulated and progress has been made in understanding the systematics of the process. But this is still a young and largely unexplored field. The data, especially at low energies are scattered and conflicting. Very little progress has been made in understanding ionization at low energies and even less progress in calculating cross sections in that region. More effort is clearly needed in both theory and experiment.

Strong support from the communities of cross section users is needed for a broad program of basic research in the understanding of the mechanisms of impact ionization. While certain types of cross sections or particular targets are of greatest need today, tomorrow's needs are likely to be different. A broad research program emphasizing basic understanding is more likely to provide for tomorrow's data requirements than ad hoc crash programs to obtain the cross sections needed at the moment.

ACKNOWLEDGMENT

This paper is based on work performed under National Science Foundation Grant No. PHY-80-25599.

REFERENCES

1. M.E. Rudd, R.D. DuBois, L.H. Toburen, C.A. Ratcliffe, and T.V. Goffe, "Cross sections for ionization of gases by 5-4000 keV protons and for electron capture by 5-150 keV protons," Phys. Rev. A 28,3244 (1983).
2. R.D. DuBois, L.H. Toburen, and M.E. Rudd, "Multiple ionization of rare gases by H^+ and He^+ impact," Phys. Rev. A 29,70 (1984).
3. L. Vriens, "Binary-encounter proton-atom collision theory," Proc. Phys. Soc. 90, 935 (1967).
4. M.E. Rudd, D. Gregoire, and J.B. Crooks, "Comparison of experimental and theoretical values of cross sections for electron production by proton impact," Phys. Rev. A 3,1635 (1971).
5. J.H. Miller, L.H. Toburen, and Steven T. Manson, "Differential cross sections for ionization of helium, neon, and argon by high-velocity ions," Phys. Rev.A 27, 1337 (1983.
6. U. Fano and W. Lichten, "Interpretation of Ar^+-Ar collisions at 50

keV," Phys. Rev. Letters 14, 627 (1965).
7. M.E. Rudd and J. Macek, "Semi-empirical equation for electron ejection in proton collisions at low energies," Div. of Electron and Atomic Physics meeting, Madison, Wisc, Dec. 1978.
8. M.E. Rudd, "Energy and angular distributions of secondary electrons from 5-100 keV proton collisions with hydrogen and nitrogen molecules," Phys. Rev.A 20, 787 (1979).
9. Brian C. Edmans, private communication, 1981.
10. D.H. Madison, "Angular distribution of electrons ejected from helium by protons," Phys. Rev.A 8, 2449 (1973).
11. M.E. Rudd and D.H. Madison, "Comparison of experimental and theoretical electron ejection cross sections in helium by proton impact from 5 to 100 keV," Phys. Rev. A14, 128 (1976).
12. Joseph Macek "Theory of the forward peak in the angular distribution of electrons ejected by fast protons," Phys. Rev. A 1, 235 (1970).
13. J.P. Keene, "Ionization and charge exchange by fast ions of hydrogen and helium," Philos. Mag. 40, 369 (1949).

ABSOLUTE DOUBLY DIFFERENTIAL CROSS SECTIONS FOR THE IONIZATION OF WATER VAPOR BY ELECTRON IMPACT

Mohammad A. Bolorizadeh
and
M. Eugene Rudd

Dept. of Physics and Astronomy
University of Nebraska-Lincoln
Lincoln, NE 68588-0111

ABSTRACT

Cross sections, differential in angle and energy, were measured for the ionization of water vapor using an electron beam produced by a rotatable electron gun. Secondary electrons were energy analyzed by a parallel plate spectrometer with an energy resolution of 1%. By measuring the pressure of water vapor, the geometrical quantities involved, and the efficiency of the counting system, absolute cross sections are obtained.

Although there is much interest in the ionization of water vapor by energetic electrons, data on that process is fragmentary. The total and differential cross sections of these processes are of interest in a diversity of disciplines such as aeronomy, astrophysics, plasma physics, gaseous electronics, radiation biophysics, and track structure models. Therefore we are measuring the absolute doubly differential cross sections for the ionization of water vater vapor by electrons with 50 to 2000 eV energy. These cross sections are measured over an angular range of 15^{o} to 150^{o} with the secondary electron energies ranging from few eV to the primary energy minus the first ionization of water vapor. The experiment is performed under static gas conditions at a pressure of about 1 mTorr.

Generally the system is the one built by G.B. Crooks and M.E. Rudd[1] and used by R.D. DuBois and M.E. Rudd[2], but for this experiment several improvements were made to allow the use of water vapor as a target gas and to increase the energy of the primary electrons. A new lens system was built for the gun which enabled the use of a directly heated cathode, since poisioning of oxide coated cathodes occurs in the presence of gases like oxygen, water vapor, carbon dioxide, and air. The indirectly heated RCA oxide coated cathode was replaced by a directly heated thoria coated iridium filament purchased from Electron Technology Inc.

A new exit aperture assembly was built for the gun which included an electron suppressor after the second defining aperture. A sample of the data is presented in Figure 1. The complete set of data will be integrated over energy and/or angle to calculate total and singly differential cross sections. These data will be presented at the 15th annual DEAP meeting at Storrs, Conneticut and will also be published.

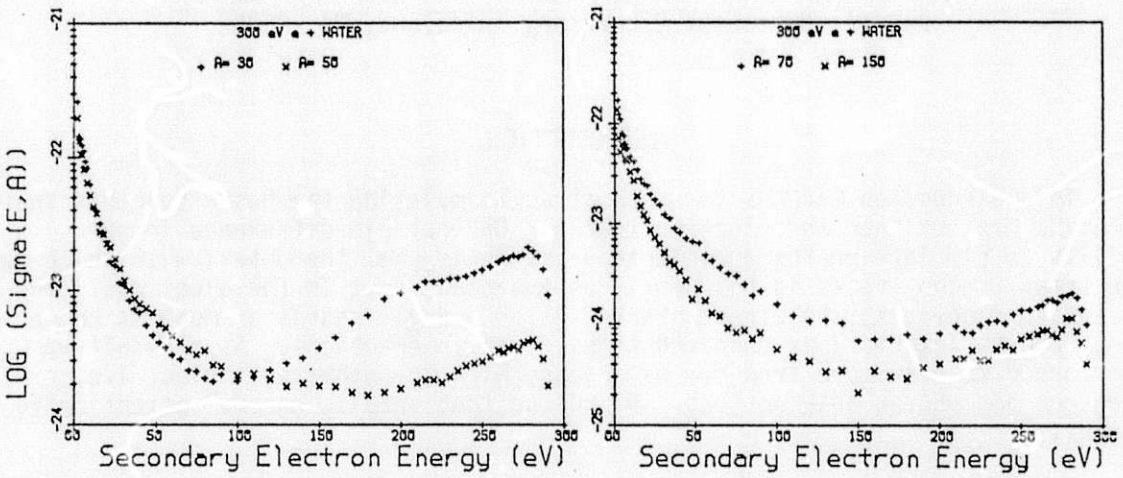

Fig. 1. Absolute doubly differential cross sections (m^2/eV*Sr) for the ionization of water vapor by 300 eV electrons. The secondary electrons were observed at 30°, 50°, 70°, and 150° angle.

ACKNOWLEDGMENT

Work is supported by the National Science Foundation under grant No. PHY-80-25599.

REFERENCES

[1]G.B. Crooks and M.E. Rudd, "Absolute elastic and inelastic differential cross sections for electron impact on helium", Bull. Am. Phys. Soc. 17,131 (1972)

[2]R.D. DuBois and M. E. Rudd, "Absolute differential cross sections for 20-800 eV electrons elastically scattered from argon", J. Phys. B8,1474 (1975)

CROSS SECTIONS USED IN PROTON-TRACK SIMULATIONS*

W.E. Wilson, L.H. Toburen, J.H. Miller and R.D. DuBois
Pacific Northwest Laboratory, Richland, WA 99352

INTRODUCTION

This discussion extends to proton track simulation the basic concepts that Paretzke has outlined for electron tracks. One notable difference in our ability to simulate proton and electron tracks is that the detail with which we can treat proton tracks is not nearly as advanced as it is for electrons. The reasons are obvious; the effort started later and not nearly as much is known about proton interactions compared to electron interactions. As a result we are forced to draw more from our experience with the other particles, i.e., electron and photon interactions. Of course that entails careful attention to theory.

In this paper we describe the present state-of-the-art of fully stripped ion (proton) track simulation up to the point where it becomes an electron track problem. From then on the basic interactions are not different from what Paretzke has described in the preceding paper. Here the practical aspects are emphasized; for the theoretical aspects the reader is referred to contributions to this workshop by Steve Manson and John Miller. Even though our remarks focus specifically on the radiological problem and in vapor phase, the basic principles which are discussed are, for the most part, equally applicable to other areas, eg. atmospheric physics, aeronomy, plasmas, sputtering, materials, etc.

Everyone is familiar with the basic facts that the primary interaction between a proton (or alpha) and matter is electronic excitation and ejection (ionization) of valence electrons via the Coulomb force and, owing to the large mass of the ion relative to that of the struck electrons, the ion's path is essentially straight. To simulate proton or alpha tracks in a realistic way, requires for each interaction

- the mean free path (obtained from the total cross section for the process), and
- spectral information about the energy and momentum transfer to the reaction products, i.e. for ionization, cross sections differential in the energy and angle of ejected electrons.

The importance of angular information is mitigated by subsequent scattering of the secondary electrons especially for low energy electrons which are also the most numerous. Therefore we will say little about this aspect, and instead concentrate on the total interaction cross sections and the energetics of the by-product emissions.

*This paper is based on work performed under U.S. Department of Energy Contract DE-AC06-76RLO-1830.

To emphasize just how important the energetics are, consider the following; for a 1 MeV proton in water vapor, about 69% of the total stopping power first appears as kinetic energy of secondary electrons originating from valence shells and another 22% is taken up in overcoming their binding i.e., in removing those electrons from their host molecule to create an electron-ion pair. An additional 7% goes into (mostly electronic) excitation, and finally about 2% goes into K-shell ionization of the oxygen in the molecule, both potential and kinetic energy of the initial secondary electron.

Single Differential Cross Sections (SDCS)

What does a typical yield of secondary electrons look like for a modest energy ion, e.g. 1 MeV proton? Figure 1 presents measured SDCS for 1 MeV protons incident on the molecular targets methane, ammonia, water vapor and neon (Lynch, et al. 1976; Toburen and Wilson, 1977). There are two regions to these data; a region at high secon[illegible]lectron energy where the four curves are very similar, except for the [illegible]aks, and a second region at low energy where the curves are dissimilar. [illegible]igh energy region the data follow very nearly a power law of slope -2 [illegible]erford predicted, illustrated by the dashed line between $10^2 < W < 10^3$ eV. Se[illegible]ondary electrons falling into this part of the spectrum are said to result from "hard collisions" and as we shall see,

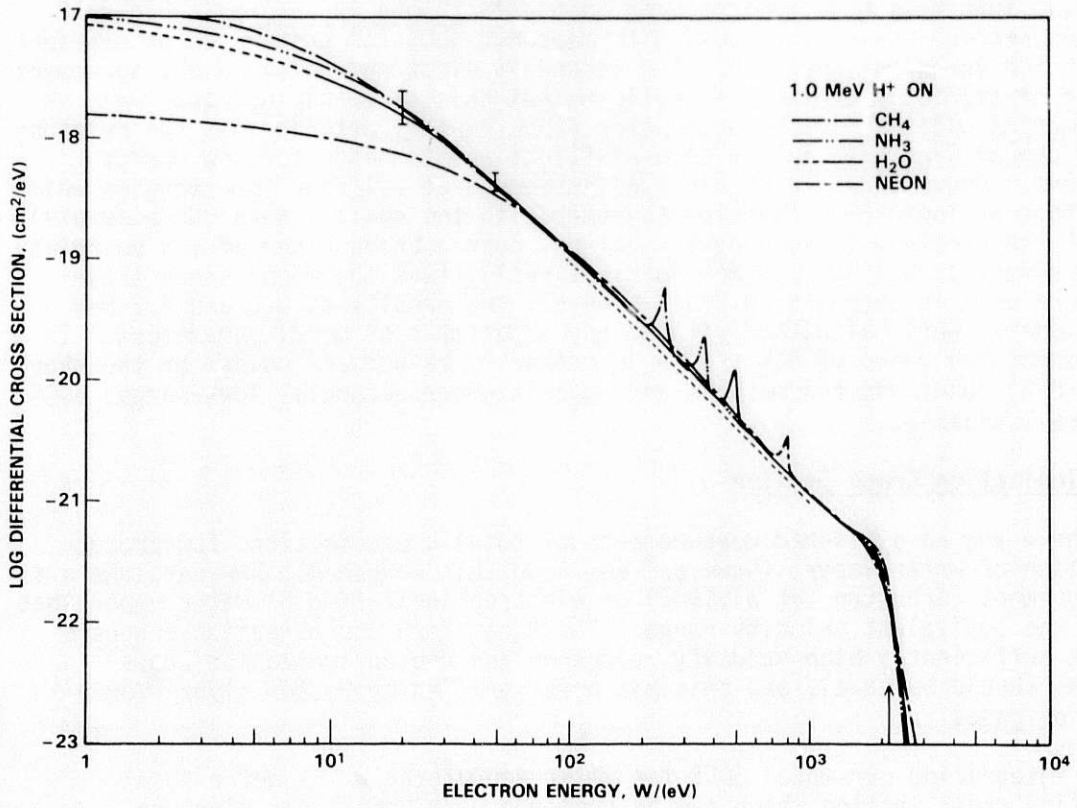

Figure 1. Single differential cross sections for electron ejection from the iso-electronic targets CH_4, NH_3, H_2O and neon by 1 MeV protons.

their yield can be adequately described by semi-classical theories, such as binary-encounter approximation (BEA) (Rudd and Macek, 1972). In the low energy (glancing collision) region, the targets exhibit differences in the yield of secondary electrons. Since the yield from glancing collisions is several orders of magnitude larger than the yield from hard collisions, the former largely determines the total ionization cross section and hence the mean free path for ionization.

For track simulations, one needs a computationally convenient analytic representation of SDCS data, such as in Figure 1, for any ion energy and eventually for any material. We have made significant progress toward this goal by developing a model for SDCS that should be applicable to any atom or molecule in the gas phase and possibly to condensed phase targets as well (Miller, et al. 1983). Since this model is described in detail in the contribution by Manson and Miller, we will restrict our attention here to the results of model calculations for water vapor.

Application of the technique requires determination of two functions of secondary electron energy, A(W) and B(W), that are properties of the electronic structure of the target and independent of projectile properties for bare ions. A(W) contains only information that is deduced from photoionization cross sections (Tan, et al., 1978; Berkowitz, 1979) and B(W) is obtained from optical data plus information determined from SDCS data at one ion energy. Figure 2 compares predictions of the model with measured SDCS for protons on water vapor at four ion energies. Note that for secondary electrons below 10 eV, agreement is poor at all ion energies. We believe that this is mainly due to experimental difficulties because water vapor rapidly deteriorates the response of the channeltron used in the time-of-flight spectrometer for low energy electrons. Above 10 eV we obtain good agreement at all four ion energies which shows that a single B(W) function together with the optical data can accurately predict the spectrum of secondary electrons over a broad range of ion energies. The agreement at 0.5 and 1.5 MeV does not really test the model since these data were used in determining B(W); however, the results at 3.0 and 4.2 MeV proton energy were calculated without any adjustment of model parameters. In determining the value of B(W) for W less than 10 eV we were guided by the shape of the B(W) functions for methane and ammonia where accurate, low-energy, SDCS data are available.

Total Ionization Cross Section

There are no published measurements of total cross sections for proton ionization of water vapor, (however, see Rudd this workshop); however, there is a measurement (Schutten, et al.1966) of electron ionization of water vapor that covers the equivalent velocity range. The first Born approximation suggests that at sufficiently high velocity, electron and proton ionization cross sections should be equal, and this has been verified by Hooper (1962) for a number of gases.

By integrating our model SDCS for water vapor over W, we get a total ionization cross section which can be compared with Schutten's electron measurement, (figure 3). Above an equivalent energy of 1 MeV, we find excellent agreement; below 1 MeV, exchange effects come into play and the electron cross section falls away as expected, whereas the ion cross section continues to increase for decreasing energy. Since the yield of low energy electrons predominates in determining the total ionization cross section, our agreement with Schutten's data gives support to the assumption made about the B(W) function for water vapor on the basis of results for CH_4 and NH_3. More data on total ionization of water by protons would clearly be valuable.

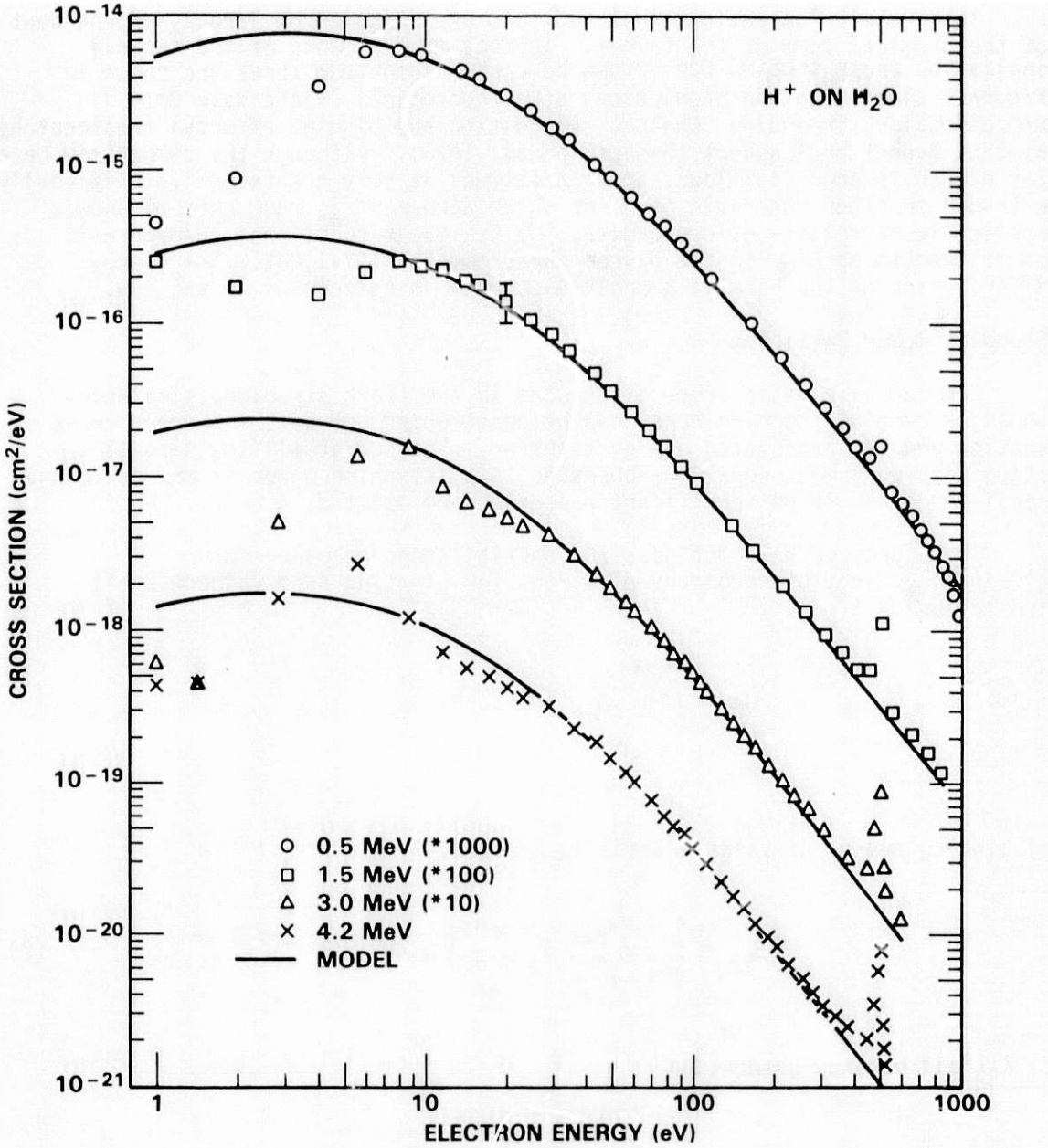

Figure 2. Differential cross section for ionization of water vapor by protons. Data at 0.5 and 1.5 MeV are from Toburen and Wilson, (1977). Data at 3.0 and 4.2 MeV are not previously published. Solid curves show model results. Upper three curves are each displaced by a decade from the curve below.

K-Shell Ionization

Inner shell ionization cross sections are found to be largely independent of the chemical form of the target. Several measurements of the K-shell ionization cross section for oxygen have been reported; three are shown in figure 4 along with the predictions of a theoretical (Plane Wave Born Approximation, including Coulomb retardation and binding effects) treatment by Basbas, Brandt and Laubert (Basbas, et al, 1973). Although the comparison here for oxygen is poor (40% low), their treatment is very tractable i.e., is easily extended to other materials (and for which agreement is much better) and is applicable at relativistic energies. We use their functional result re-normalized to agree with the oxygen measurements at 1-2 MeV. The energy distribution of the ejected K-shell electrons is calculated in the BEA.

Stopping Power Partition

For each inelastic process included in the track structure simulation model, a partial stopping power can be constructed out of the process cross section and its associated energy transfer. The sum of all the partial stopping powers must equal the observed total stopping power if one is to have consistency and if no significant processes are omitted.

Therefore, we have defined, the partial stopping power for
a) kinetic energy of secondary electrons (originating from valence shell ionization),

$$S_{KE} = \int_{o}^{W_{max}} \frac{d\sigma}{dW} \cdot dW \qquad (1)$$

b) binding energy of valence shell ionization,

$$S_{BE} = \sum_{j=1}^{4} \int_{o}^{W_{max}} I_j \cdot \frac{d\sigma_j}{dW} \cdot dW \qquad (2)$$

c) K-shell vacancy production,

$$S_{K\text{-}VAC} = [I_k + \bar{W}_k(E_I)] \cdot \sigma_k \qquad (3)$$

and finally

d) (direct) excitation

$$S_{EXC} = \sum_{n} E_n \cdot \sigma_n \qquad (4)$$

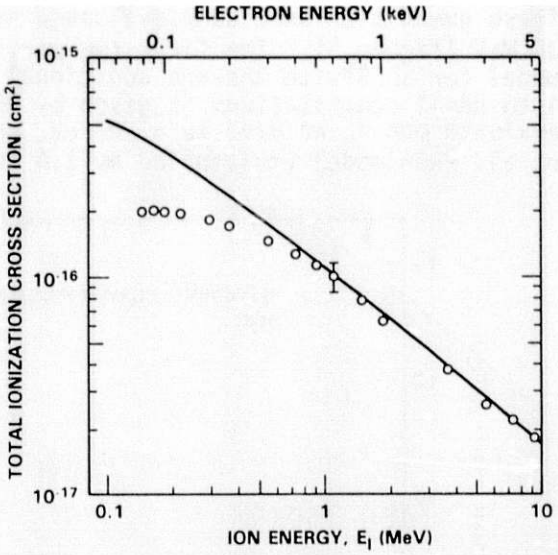

Figure 3. Total ionization cross sections for water vapor. Dashed curve was obtained by integrating our model of the SDCS over the energy of secondary electrons. Data points are for electron ionization of water and are from Schutten, et al. (1966).

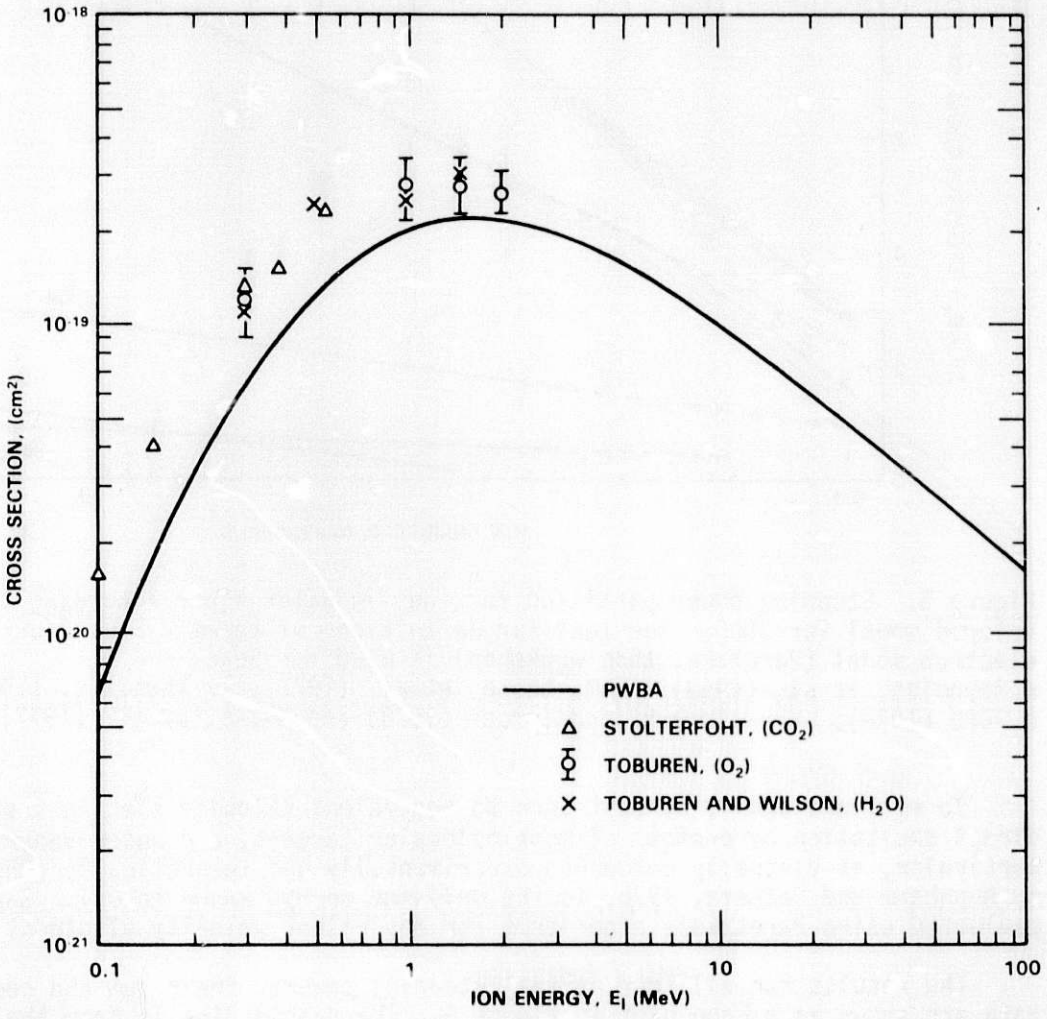

Figure 4. K-shell ionization of oxygen. Plane Wave Born Approximation (PWBA) calculation, the (Basbas, et al. 1973) includes Coulomb retardation and binding effects. Δ---Stolterfoht (1972); o---Toburen (1972); x---Toburen & Wilson (1977)

These quantities were each evaluated as a function of ion energy, from 0.3 to 30 MeV (figure 5). The first two partials, S_{KE} and S_{BE} were obtained from our model for SDCS with the one additional assumption that the partioning of B(W) into shell contributions is given by BEA (needed to evaluate eqn 2). To evaluate eqn 3, we used I_K = 540 eV, BEA for $W_K(E_I)$ and for σ_K the Basbas, et al. PWBA model (multiplied by 1.4 to agree with experiment at 2 MeV).

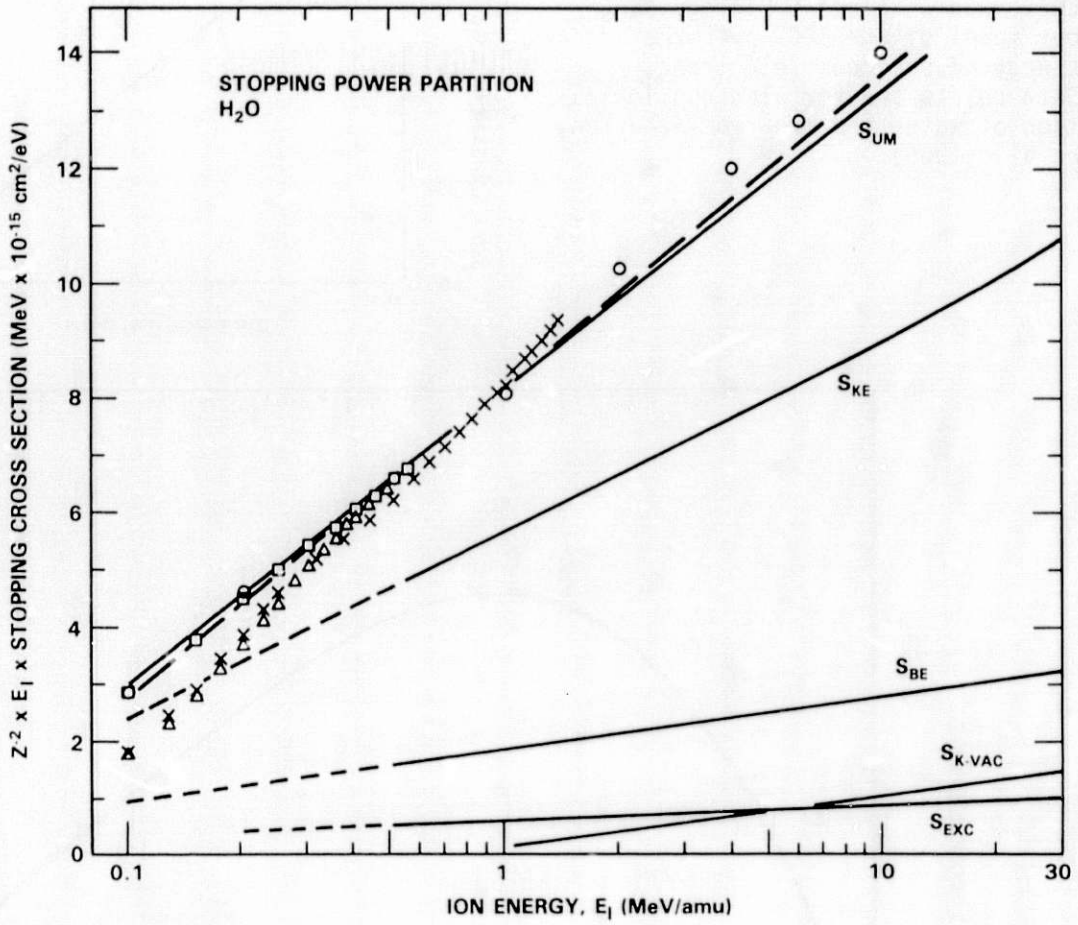

Figure 5. Stopping power partition for ions in water vapor according to the developed model for SDCS. See text for definitions of terms. Equivalent velocity electron model (Paretzke, this workshop) is used for Sexc.
+ Reynolds, et al. (1953); Δ Matteson, et al. (1977); x Thwaites, (1981); o ICRU (1970); -----Inokuti and Turner (1978) and Zeiss, et al. (1977)

To evaluate eqn 4, we must turn to equivalent velocity electrons since direct excitation by protons of most molecular targets, and water vapor in particular, is virtually untouched experimentally and theoretically (the paper by Nussbaum and Cathers, 1976, is the only one on H_2O known to us). S_{exc} was evaluated using Paretzke's algorithms for equivalent velocity electrons.

The results for all four partial stopping powers, their sum and comparison data are shown as a Fano plot in figure 5. The dashed line is from the Bethe formula (Inokuti and Turner, 1978) using a mean excitation energy, I_0, of 71.6 eV (Zeiss, 1977). Our sum of partials is about 3% lower than the dashed line at 10 MeV.

DISCUSSION AND CONCLUSIONS

It seems that the important fundamental ionization interactions for ion track simulation are reasonably well in hand, at least above 1 MeV/amu and probably above 300 keV/amu. It would be satisfying to have actual excitation data specifically for ions and not have to rely on equivalent velocity electron data. This partial stopping power apparently accounts for less than 10% of the total, so this is not a serious shortcoming. However, the problem becomes serious at lower velocities, because then we cannot assume electron and ion interactions to be equivalent. There are no published measurements of total stopping power for protons or alphas in water vapor above about 1.25 MeV/amu. Additional data above 2 MeV/amu would be useful if they can narrow the existing uncertainties; stopping power measurements accurate to 1 or 2% would be required. Certainly not an easy experiment to do. Measurements of the total ionization cross section for protons (and alphas) in water vapor are needed.

The next task in the ion track simulation problem is to go to lower ion energies; where extension of existing algorithms is not possible, we must develop new ones. Algorithms will be required for new processes, eg. charge-changing collisions to both bound and continuum states. To support this task, experimental data and theoretical treatments of ionization by "dressed" ions are needed.

Finally, the emphasis here has been on water vapor, primarily because of its radiological importance. What we have learned about extracting a hard collisions component, B(W), from a combination of particle ionization data and data on optical oscillator strengths, branching ratios, etc. (see Brion, this workshop) is equally applicable to other materials. Therefore, the accumulation and assessment of similar data for atmospheric gases, would be of considerable interest in aeronomy for example.

REFERENCES

Basbas, et al. (1973), Phys. Rev. A 7, 983. (Also see Rice, et al. (1977) Atomic Data and Nucl. Data Tables, 20. 503. and Paul, H. (1979) Atomic Data and Nucl. Data Tables, 24, 243.)

Berkowitz, N. (1979), Photoabsorption, Photoionization and Photoelectron Spectroscopy, Academic Press, New York.

Hooper, et al. (1962), Phys. Rev. 125, 2000.

ICRU (1970), International Commission on Radiation Units and Measurements, report number 16, ICRU Publications, Washington, DC 20008.

Inokuti and Turner (1978), Sixth Symposium on Microdosimetry Brussels. May 22-26, 1978, Vol. I, p. 675, ISBN 0906346029.

Lynch, et al. (1976), J. Chem. Phys. 64, 2616.

Matteson, et al. (1977), Phy. Rev. A 15, 856.

Miller, et al. (1983), Phys. Rev. A 27, 1337.

Nussbaum and Cathers (1976), J. Chem. Phys. 65, 4170.

Reynolds, et al. (1953), Phys. Rev. 92, 742.

Rudd and Macek (1972), Case Studies in Atomic Physics 3, 47.

Schutten, et al. (1966), J. Chem. Phys. 44, 3924.

Stolterfoht, N. (1972), Inner Shell Ionization Con. Atlanta. CONF720404, p.1043.

Tan, et al. (1978) J. Chem. Phys. 29, 299.

Thwaites, D.I. (1981), Phys. Med. Biol. 26, 71.

Toburen, L.H. (1972), Inner Shell Ionization Con. Atlanta CONF720404, p. 986.

Toburen and Wilson (1977), J. Chem. Phys. 66, 5202.

Zeiss, et al. (1977), Radiat. Res. 70, 284.

Rudd and Macek (1972), Case Studies in Atomic Physics 3, 47.

Electron Ejection Cross Sections in Electron and Ion Impact Ionization: Ab Initio and Semiempirical Calculations

Steven T. Manson
Department of Physics and Astronomy
Georgia State University
Atlanta, GA 30303
and
John H. Miller
Radiological Sciences Department
Pacific Northwest Laboratory
Richland, WA 99352

INTRODUCTION

Ionization cross sections for heavy ions and electrons incident on various atoms and molecules are required in the modeling of the interaction of radiation with matter. For each case, the energy distribution of secondary electrons (the single differential cross section, SDCS) is needed over a broad range of projectile and secondary electron (δ-ray) energies. In many cases the energy and angular distribution of secondary electrons (the double differential cross section, DDCS) is also necessary.

Clearly, it would be desirable to have laboratory SDCS and DDCS measurements for all of the cases required. For a variety of reasons, this is not yet possible. Thus, one must turn elsewhere to obtain the needed cross sections.

In this paper, we discuss cross sections obtained in two different ways; ab initio theory based on the first Born approximation, and a semi-empirical method based on the Bethe-Born Approximation[1-3]. In both cases, results on helium will be presented since the largest amount of data is available in this case. Applications of both methods to other target species are given in the references. The accuracy of the methods and plans for the near future are also discussed.

AB INITIO THEORY

The first Born approximation forms the framework for essentially all of the calculations of DDCS and SDCS arising from fast electron or ion impact ionization of atoms. Going into the details of either the theory of the Born approximation[1-3] or the calculation[4,5] itself, for which the reader is referred elsewhere, is beyond the scope of this paper. The crucial point of concern here is the range of validity of the first Born Approximation (FBA). Roughly speaking, FBA is good when the incident particle's momentum is not significantly altered in the collision, either in magnitude or direction, i.e., small momentum transfer compared to the projectile momentum. Since, however, the significant range of momentum transfers increases with increasing energy transfer, this means that FBA will be very good for incident electrons when the energy transferred to the target is small ($\lesssim$10%) compared to the incident electron energy. For ionic projectiles, such as protons, FBA does far

better than for electrons of equal velocity. This is due to the fact that ions are so much more massive than electrons so that their momenta are much larger, at a given velocity. Thus, as will be shown below, FBA is valid for incident protons even when the electrons ejected in the ionization process have velocities significantly larger than those of the incident protons.

In using FBA for ab initio calculations, wave functions for the target are required. Thus, even when FBA gives a good description of the collision process, the results of the calculation might still be poor if sufficiently accurate wave functions are not used for the initial (generally ground) state of the target and/or the final continuum state of the residual target ion-ejected electron system. Therefore, in assessing the results of a FBA calculation for which there is not experimental data to check against, it is necessary to scrutinize not only whether FBA is valid, but also the quality of the wave functions.

To give some idea of the accuracy of such FBA calculations, in Fig. 1 a comparison of the DDCS for 2 keV e- + He collisions at four ejected electron

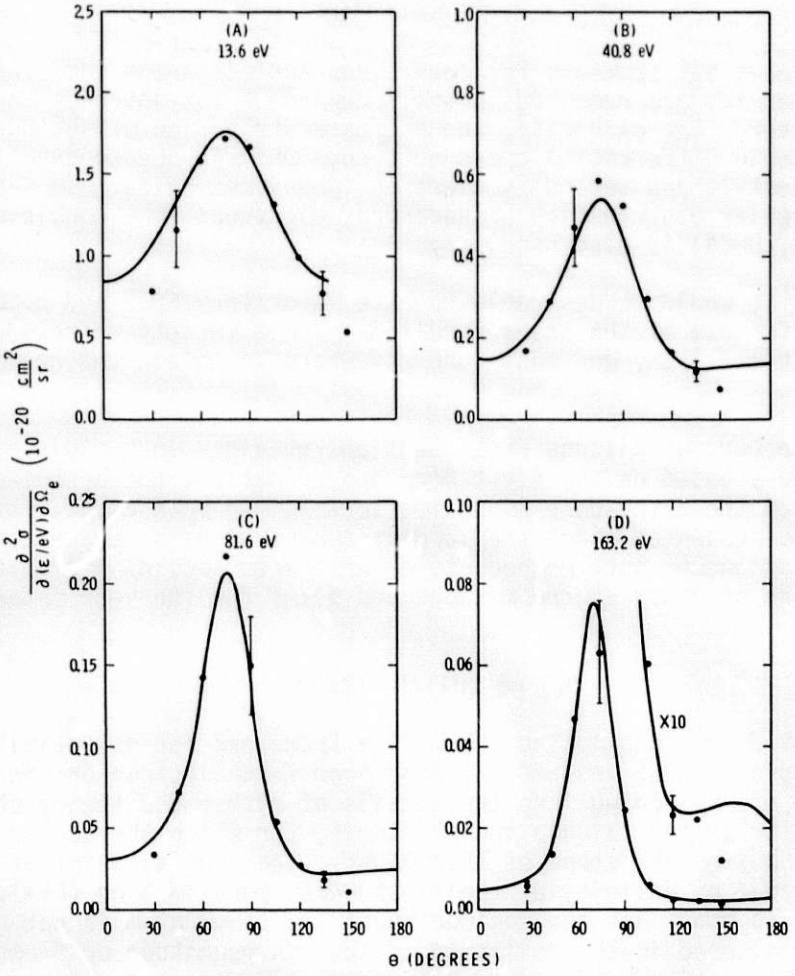

Figure 1. Angular distribution (DDCS) for electrons ejected at 13.6, 40.8, 81.6 and 163.2 eV by 2-keV electron impact on He. Solid curves are ab initio FBA calculations and data points are from Ref. 6.

energies is shown. Good agreement between the theoretical FBA results[4] and experiment[5] is seen; the disagreement at the smallest and largest angles measured are the result of an experimental difficulty[7]. Aside from those data points, however, the theoretical cross sections lie within the experimental error bars. It is clear, in addition, that if the DDCS results agree, the SDCS results, which are obtained by integrating the DDCS over ejection angle, must also agree. This is demonstrated in Fig. 2. Note, however, that there is some disagreement for electrons ejected at energies less than 10 eV. This is the result of inadequate wave functions and not FBA per se. In a calculation using more sophisticated wave functions, this discrepancy was removed[8].

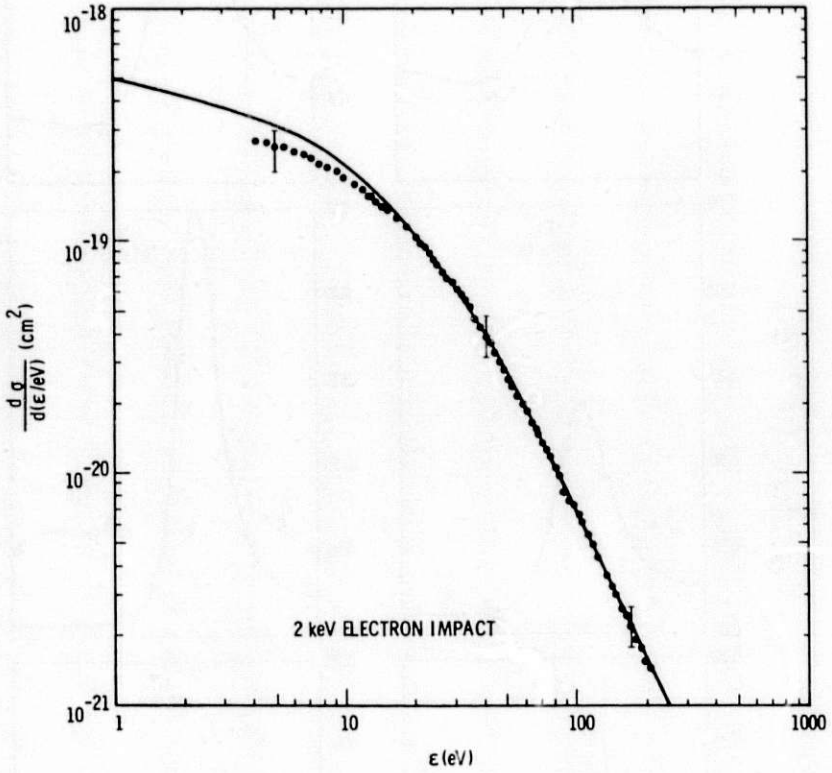

Figure 2. Single differential cross section (SDCS) for electrons ejected from He by 2-keV electron impact. Solid curve is an ab initio FBA calculation and data points are from Ref. 6.

Turning to proton impact, the DDCS comparison[4] for 1 MeV H^+ + He collisions is shown in Fig. 3. Here again we find rather good agreement except at the lowest energy which may be due to experimental difficulties. There is also a problem at small angles, less than about 45°. Here the experiment is always larger than theory. This is due to a process known as charge transfer to the continuum[9] (CTC) and is not included in FBA. Roughly speaking, it is due to the massive proton, with its positive charge, pulling electrons along with it, thus increasing the cross section at forward angles. This effect gets smaller for increasing energy[4,5] and for heavier targets[10-12]. In addition it gets nearly obliterated in the SDCS. This is shown in Fig. 4 where excellent agreement between theory and experiment is seen.

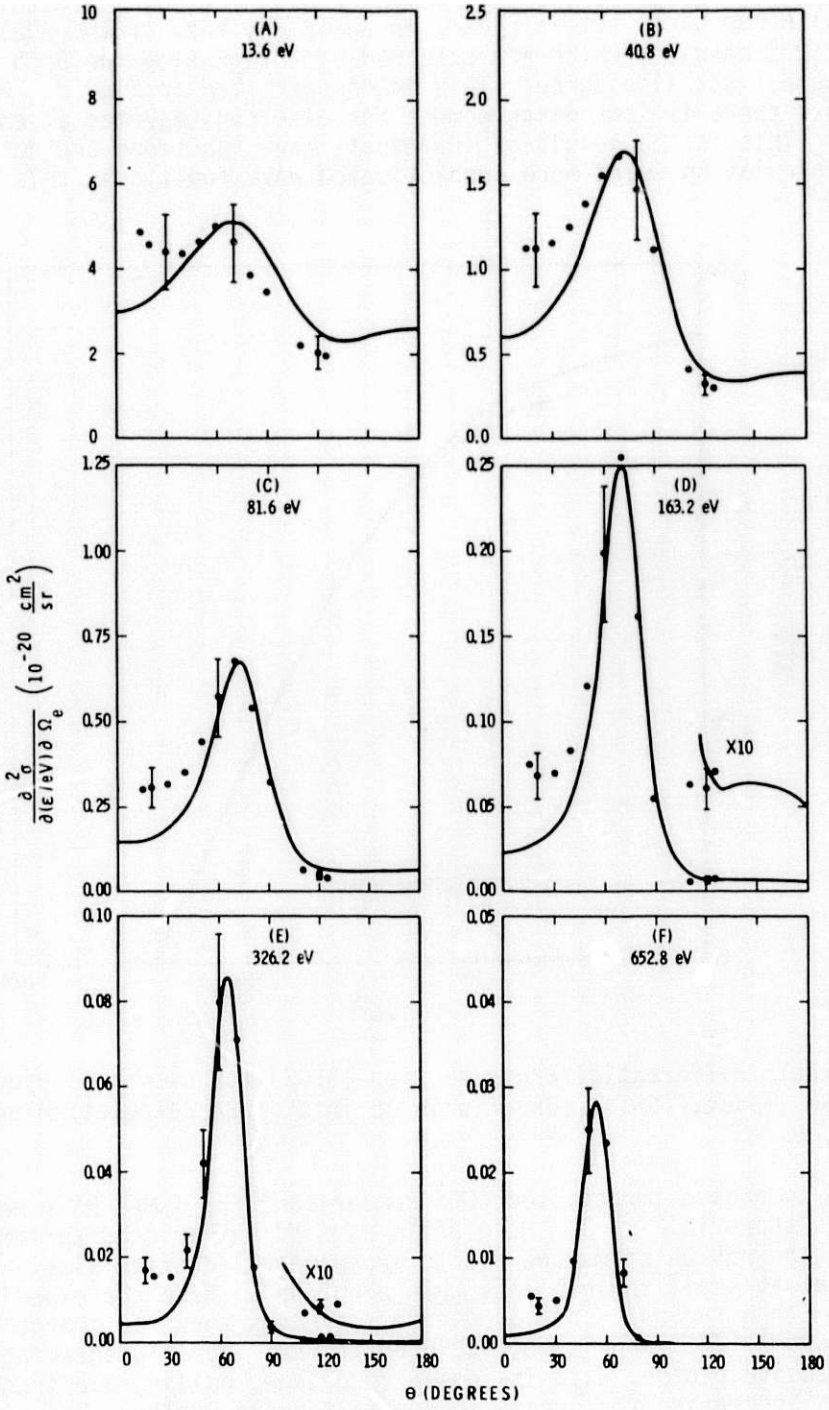

Figure 3. Angular distribution (DDCS) for electrons ejected at 13.6, 40.8, 81.6, 163.2, 326.4 and 652.8 eV by 1-MeV proton impact on He. Solid curves are ab initio FBA calculations and data points are from Ref. 19.

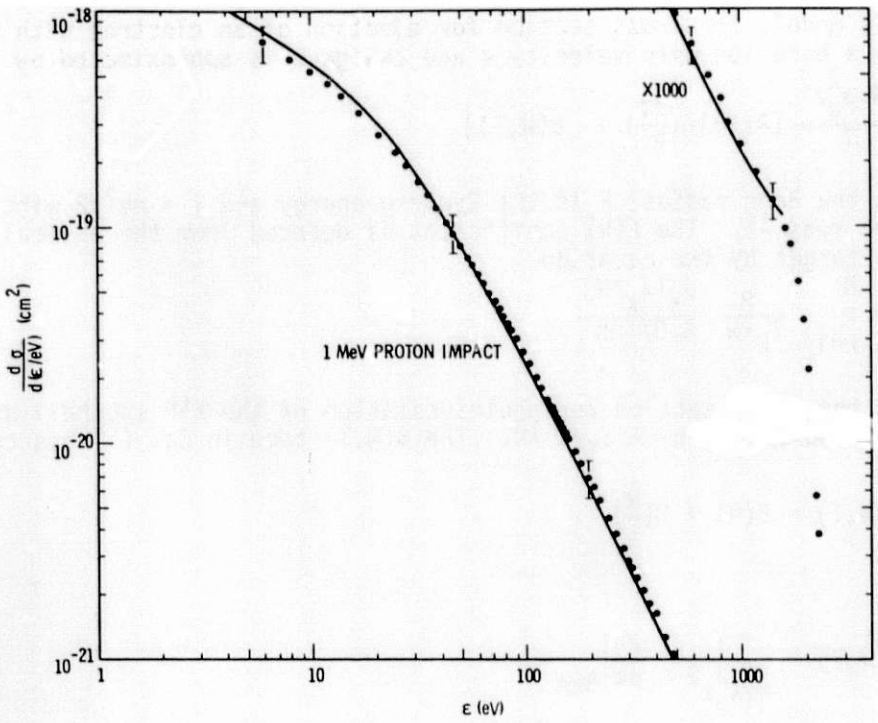

Figure 4. Single differential cross section (SDCS) for electrons ejected from He by 1-MeV protons impact. Solid curve is an ab initio FBA calculation and data points are from Ref. 19.

Although examples have been given above only for He targets, FBA calculations have been performed for other noble gases[10-12] as well. In principle, such calculations can be performed for any atomic target and, with suitable alterations, for incident ions carrying their own electrons[5,13]. These are, however, massive calculations. Furthermore, no such calculations have been carried out for molecular targets owing to the difficulties involved in treating molecular continuum wave functions. A promising method of so doing has been used for molecular photoionization[14], but has not been applied to molecular ionization by charged particles. Hopefully this will come in the near future.

SEMI-EMPIRICAL METHOD

Although the FBA provides a sound theoretical framework for calculating differential cross sections for ionization by fast, charged particles, its application in many cases is impractical due to the difficulty in obtaining accurate bound and continuum wave functions for the target as discussed above. In this section a semi-empirical method for calculating SDCS is described. This model is based on the use of experimental data to determine coefficients in Bethe's asymptotic expansion of the FBA[2,15]. These coefficients are functions of the energy transferred to the target and for bare ions are independent of projectile properties. We illustrate this point by using coefficients deduced from photoabsorption and proton impact SDCS data to predict SDCS for fast electrons.

In this model, the cross section for ejection of an electron with kinetic energy W by a bare ion with velocity v and charge z is approximated by

$$\frac{d\sigma}{dW} = \frac{4\pi a_o^2 z^2}{T} [A(W)\ln(\frac{4T}{R}) + B(W,T)] \quad (1)$$

where a_o is the Bohr radius, R is the Rydberg energy and $T = mv^2/2$ with m being the electron mass [15]. The A(W) coefficient is deduced from the optical properties of the target by the equation

$$A(W) = \sum_{k=1}^{N} \frac{R}{I_k+W} \frac{\sigma_k(I_k+W)}{8.07\ Mb} \quad (2)$$

where σ_k is the cross section for photoionization of the k^{th} subshell of the target at photon energy $h\nu = I_k+W$ [16]. The B(W,T) term in Eq. (1) has two useful limits:

$$\lim_{W\to o} B(W,T) = B(W) + O(\frac{W}{T}) \quad (3)$$

and

$$\lim_{W\to\infty} B(W,T) = \frac{T}{4\pi a_o^2 z^2} \left.\frac{d\sigma}{dW}\right|_{BEA} \quad (4)$$

where O(W/T) denotes terms of order W/T and $d\sigma/dW_{BEA}$ is the SDCS predicted by the binary-encounter approximation.[17]

Hence for small secondary electron energies, B(W,T) reduces to a function B(W) that is independent on the properties of the projectile. In a recent publication[18] this was used to experimentally determine B(W) since substitution of Eq. (3) into Eq. (1) and neglecting O(W/T) gives the result

$$B(W) = \frac{T}{4\pi a_o^2 z^2} \left.\frac{d\sigma}{dW}\right|_{exp} - A(W)\ln(\frac{4T}{R}) \quad (5)$$

Therefore, given the optical data necessary to determine A(W), accurate SDCS data at a single ion energy are sufficient determine to B(W), which is a property of the electronic structure of the target that can be used in predicting SDCS for any structureless ion at any projectile energy that is large enough to make the Bethe theory valid.

The simple BEA derived by Thomas[19] suggest that for heavy ions the right hand side of Eq. (4) is independent of T when $W \lesssim 4T$. Hence the BEA not only provides a means for calculating B(W,T) at large W but also gives a limit that is independent of ion energy to which the experimental B(W) should converge. This limit is essentially the W^{-2} dependence of the Rutherford cross section. In the region of secondary electron energy where B(W,T) is well approximated by Rutherford scattering, we make a transition between experimental B(W) values and the results obtained from the right hand side of Eq. (4). This allows a smooth transition from Bethe's quantum theory for the low energy part of the spectrum to the semi-classical BEA that is a good approximation for high energy secondary electrons. The whole spectrum can then be integrated to obtain the total ionization cross section which is an additional constraint on the model.

Figure 5 compares model calculations with data on ionization of helium by protons with energy between 0.1 and 4.2 MeV.[19] The agreement with 0.3 and 1.0 MeV proton data does not test the model since these data were used in determining B(W) for helium; however, the results at 0.1 and 4.2 MeV were obtained with no adjustable parameters. The discrepancy between model and experiment for ejection of low energy electrons by 4.2 MeV protons is probably due to experimental error since structure of the type suggested by the data is not present in the optical oscillator strength for helium.

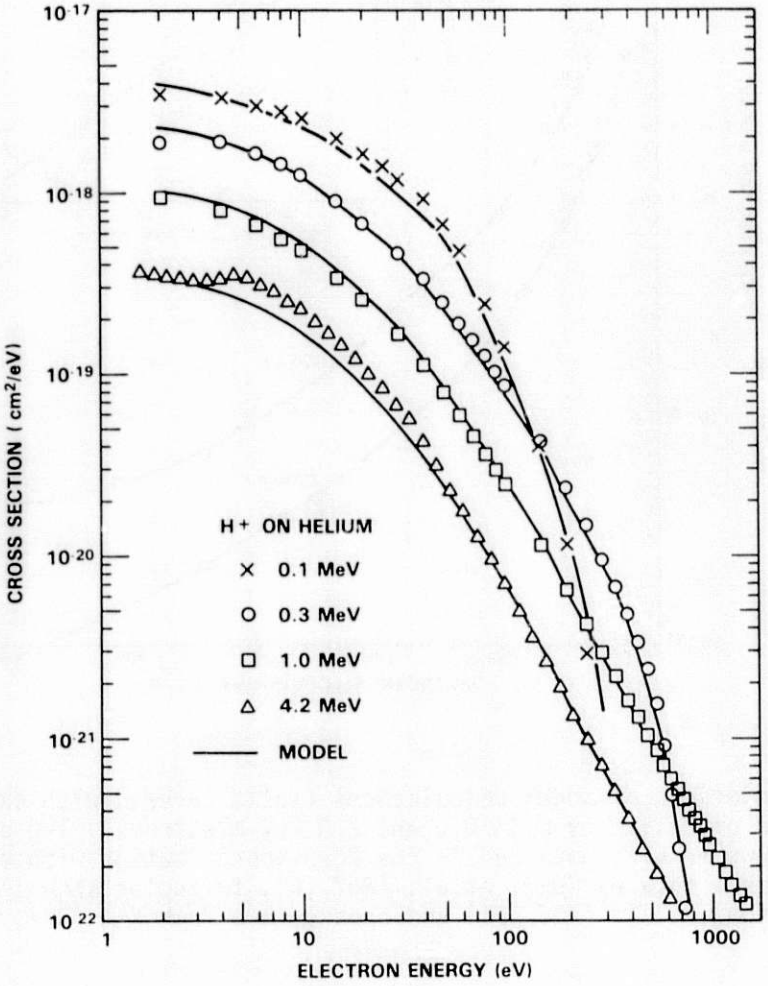

Figure 5. Semi-Empirical model calculations (solid curves) compared with the data on ionization of helium by proton impact. Experimental data tabulated in Ref. 19 are from Rudd (0.1 MeV), Toburen (0.3 and 1 MeV) and Stolterfoht (4.2 MeV).

Figure 6 compares the model with data on ionization of helium by electrons with energy between 100 and 2000 eV.[6] The crosses show values recommended by Kim[20] and the triangles show threshold results by Grissom, et al.[21] using the trapped electron technique. These results were obtained with the same experimental B(W) values used to calculate the proton impact SDCS shown in

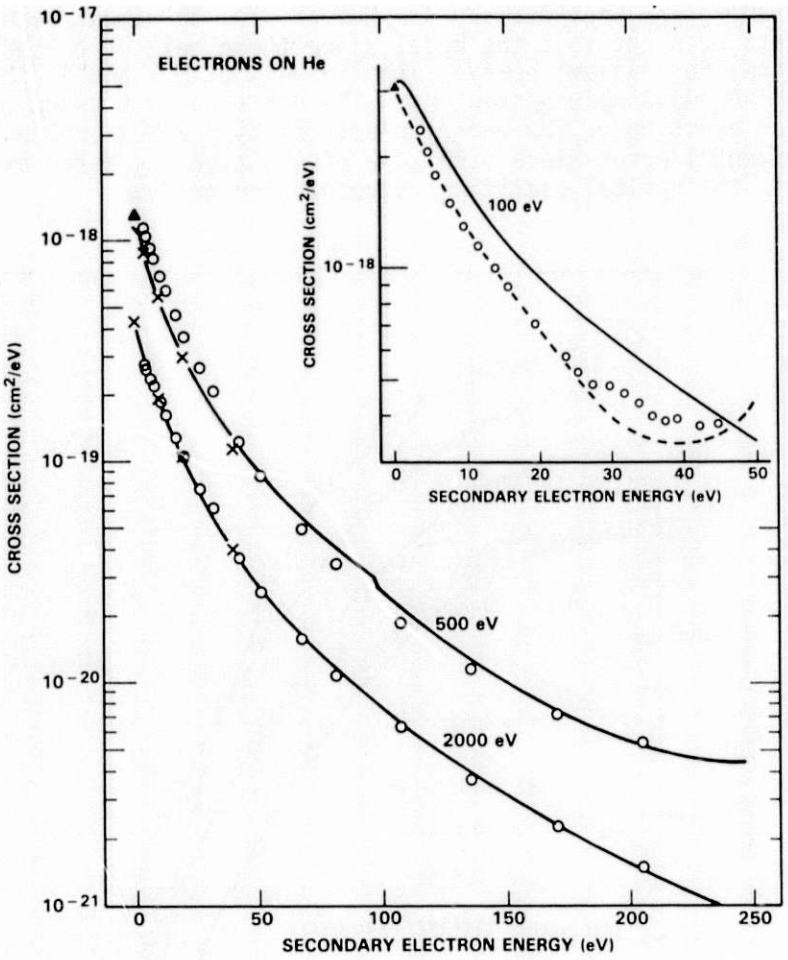

Figure 6. Comparison of model calculations (solid curves) with experimental SDCS for ionization of helium by 0.1, 0.5 and 2.0 keV electrons. The dashed curve in the insert shows results obtained in the Born approximation with exchange (Ref. 22). Open circles show data by Opal, et al. (Ref. 6), triangles show threshold measurements by Grissom, et al. (Ref. 21) and crosses are from Kim (Ref. 20).

Fig. 5 (i.e., no electron impact data were used in obtaining these results). The discontinuity in the model for ejection of 100 eV secondaries by 500 eV primaries marks the transition from the Bethe to the semi-classical theory. This transition is not continuous because for electrons the semi-classical theory (Mott cross section) includes exchange. The lack of agreement between the model and the data for 100 eV primaries is most likely due to the absence of exchange in the model results for this case. Exchange cannot be included since all secondaries have energy less than 100 eV, the secondary energy where the transition to semi-classical theory is made. The quantum calculations of Sloan[22] (dashed curve) that include exchange show good agreement with the data.

This semi-empirical method has also been used to obtain SDCS for ionization of the rare gas atoms Ne and Ar by electron and proton impact, and is being applied to the iso-electronic sequence of molecules CH_4, NH_3 and H_2O as described in the contribution by Wilson, et al. to this Workshop. Clearly the availability of partical oscillator strengths for photoionization of individual molecular electronic states[23] is a key factor in the implementation of the model to molecules. The next phase in the development of this technique will be to test its applicability to the DDCS.

ACKNOWLEDGEMENTS

This work was performed under United States Department of Energy Contract No. DE-AC06-76RLO-1830 and United States Army Research Office Contract No. DAAG-29-80-C-0027.

REFERENCES

1. N.F. Mott and H.S.W. Massey, The Theory of Atomic Collisions, Third Edition (Oxford University Press, London, 1965), pp.475-493.

2. H. Bethe, Ann. Phys 5, 325 (1930).

3. U. Fano, Phys. Rev. 95, 1198 (1954).

4. S.T. Manson, L.H. Toburen, D.H. Madison, and N. Stolterfoht, Phys. Rev. A 12, 60 (1975).

5. S.T. Manson, IEEE Trans. Nuc. Sci. NS-28, 1084 (1981).

6. C.B. Opal, E.C. Beatty, and W.K. Peterson, At. Data 4, 209 (1972).

7. R.D. DuBois and M.E. Rudd, Phys. Rev. A 17, 843 (1978).

8. T. Burnett, S.P. Roundtree, G. Doolen,and W.D. Robb, Phys Rev. A 13, 626 (1976).

9. M.E. Rudd and J.H. Macek, Case Stud. At. Coll. Phys. 3, 47 (1973 and references therein.

10. D.H. Madison and S.T. Manson, Phys. Rev. A 20, 825 (1979).

11. S.T. Manson and L.H. Toburen, VIII ICPEAC, Abstracts of Papers (Institute of Physics, Belgrade, 1973), p. 695.

12. S.T. Manson and L.H. Toburen, XICPEAC, Abstracts of Papers (Commissariat A L'Energie Atomique, Paris, 1977), p. 990.

13. S.T. Manson and L.H. Toburen, Phys. Rev. Lett. 46, 1326 (1981).

14. J.L. Dehmer and D. Dill in Electron-Molecule and Photon-Molecule Collisions, eds. T.N. Rescigno, V. McKoy, and B. Schneider (Plenum, N.Y., 1979), pp.225-265 and references therein.

15. M. Inokuti, Rev. Mod. Phys. 43, 297, (1971).

REFERENCES (contd)

16. J. Berkowitz, Photoabsorption, Photoionization and Photoelectron Spectroscopy (Academic, New York, 1979).

17. L. Vriens, Proc. Phys. Soc. London 90, 935 (1967).

18. J.H. Miller, L.H. Toburen and S.T. Manson, Phys. Rev. A 27, 1337 (1983).

19. M.E. Rudd, L.H. Toburen and N. Stolterfoht, At. Data and Nucl. Data Tables 18, 413 (1976).

20. Y.-K. Kim, Phys. Rev. A 28, 656 (1983).

21. J.T. Grissom, R.N. Compton and W.R. Garrett, Phys. Rev. A 6, 977 (1972).

22. I.H. Sloan, Proc. Roy Soc. 85, 435 (1965).

23. C.E. Brion, A. Hamnett, G.R. Wright, and M.J. Van der Wiel, J. Electron Spectrosc. 12. 323 (1977).

SCALING OF CROSS SECTIONS FOR IONIZATION BY FAST, PARTIALLY STRIPPED IONS

Yong-Ki Kim

National Bureau of Standards
Washington, DC 20234

ABSTRACT

A simple method is proposed to estimate cross sections for ionization of atoms and molecules by partially stripped ions. The method is based on the fact that slow electrons (from the target) are ejected by distant collisions and fast electrons by close collisions. Hence, slow electrons "see" fully screened projectile, while fast electrons see unscreened projectile. The proposed method is illustrated for the ionization of Ar by H^+, He^+, and He^{++} ions.

INTRODUCTION

At the Workshop, the need for a simple method to estimate ionization cross sections by partially stripped (dressed) ions was discussed. A complete description of such a process for all ions of all charge states at all velocities is impossible at present. However, it is possible to estimate the total ionization cross section of atoms and molecules (but not the projectile itself) by fast dressed ions, provided that reliable energy distribution of electrons (single differential cross section) ejected by proton impact is known. The proton speed should be the same as that of the dressed ion. This note briefly describes a method for scaling proton cross sections to estimate dressed-ion cross sections using a graphical method known as the Platzman plot.[1]

In the Platzman plot, the single differential cross section, $d\sigma/dW$, where W is the kinetic energy of an ejected electron, is expressed in units of the Rutherford cross section for a free electron and it is plotted as a function of inverse energy transfer, $E^{-1} = (W + B)^{-1}$ where B is the binding energy of the ejected electron. The Platzman plot has an advantage that the scaled cross section now represents the effective number of free electrons participating in ionization and the area under the cross section curve is directly proportional to the total ionization cross section, σ_{ion}.

Studies of $d\sigma/dW$ with the help of the Platzman plot have revealed that:[2-6] (a) Slow electrons are ejected mostly by dipole interaction, i.e., by distant collisions, and (b) Fast electrons are ejected mostly by knock-on collisions, i.e., by close collisions.

These results indicate that slow electrons are ejected by fully dressed or screened interaction, while fast electrons are ejected by bare or unscreened interaction. This change in the effective screening of the projectile has been dramatically demonstrated in an experiment by Toburen and Wilson.[7] As is shown in

Fig. 1, $d\sigma/dW$ by He^+ impact on Ar agrees well with $d\sigma/dW$ by proton impact for slow electrons ($W \lesssim 5$ eV), while the He^+ data merge into $d\sigma/dW$ by He^{++} impact for fast electrons ($W \gtrsim 100$ eV).

Additional features normally observed in $d\sigma/dW$ by fast, dressed-ion impact are: (c) Sharp peaks of Auger electrons, and (d) A broader peak at W corresponding to electrons travelling at the projectile speed.

The single peak described in (d) represents electrons stripped from the projectile by the target, and it is known as the electron-loss peak. This should be distinguished from the so-called continuum-charge-transfer peak, which also appears at the same W when the projectile energy is low (50 - 300 keV for proton). The continuum-charge-transfer peak consists of electrons ejected from the target and travelling with the projectile. The latter contributes to σ_{ion} while the former does not. The continuum-charge-transfer peak is observed in both dressed and bare but slow ions, whereas the electron-loss peak is observed only for dressed ions at any projectile speed. Experiments with fast ions will eliminate the continuum-charge-transfer peak but not the electron-loss peak.[8]

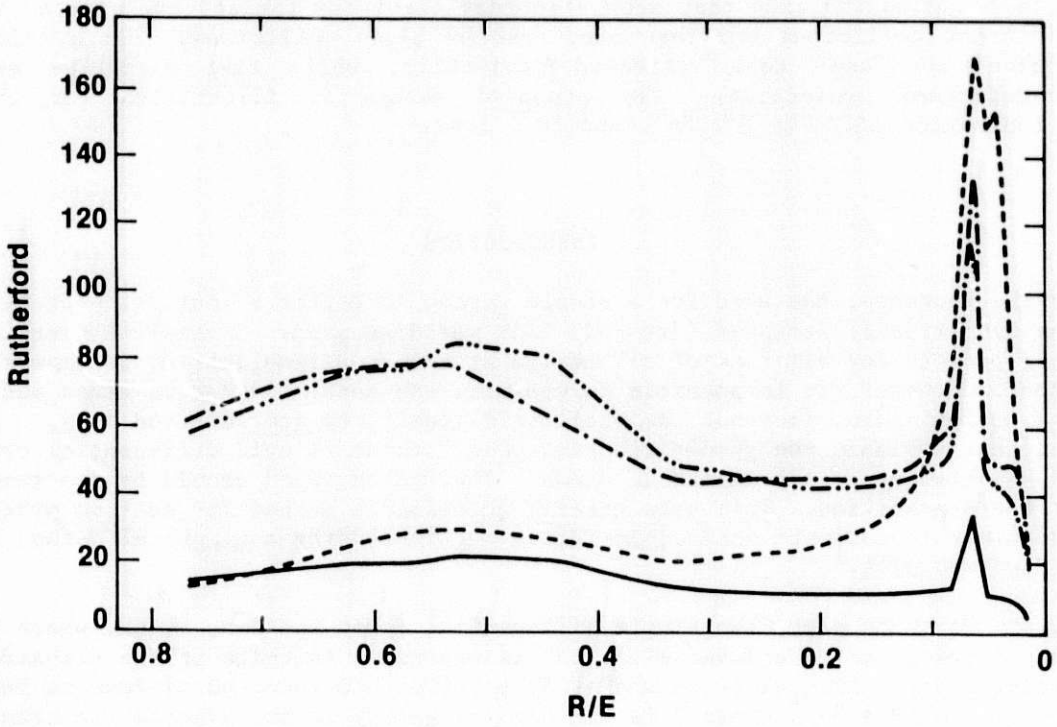

Fig. 1. Platzman plot of the single differential cross section, $d\sigma/dW$. The ordinate is $d\sigma/dW$ in units of the Rutherford cross section for a free electron. The abscissa is the inverse of energy transfer in Rydbergs. The solid curve represents $d\sigma/dW$ by 0.5-MeV proton, the dashed curve that by 2-MeV He^+, the chain-dot curve that by 2-MeV He^{++}, and the chain-dot-dot curve represents the proton-impact cross section multiplied by 4. The first three curves are based on experimental data from Ref. 7.

In Fig. 1, the peak at $R/E \approx 0.04$ for He^+ is the electron-loss peak, while the peak at $R/E \approx 0.06$ consists of several Auger peaks generated by LMM transitions. The Auger peaks are observed also in the energy distributions by proton and He^{++} impact.

Another important ingredient of our method is the fact that cross sections for fast, bare ions of nuclear charge Ze is Z^2 times corresponding cross sections for protons travelling at the same speed. This is a consequence of the first Born approximation, and has been verified in many examples.

Now we are ready to construct a "composite" $d\sigma/dW$ for dressed ions using (a), (b), and the Z^2 scaling. We start with the proton-impact $d\sigma/dW$ scaled by the Rutherford cross section at the threshold (W = 0), and connect smoothly to the $d\sigma/dW$ for bare charge, i.e., Z^2 times the proton cross section, at about W = 100 eV. If the projectile nuclear charge is not small and it is dressed with tightly bound electrons, e.g., Ne^{8+} with two K electrons, we should not use Z but subtract the number of tightly bound electrons from Z. We can use the general shape of $d\sigma/dW$ for proton impact as a guide to determine "how to connect" $d\sigma/dW$ from low W to high W.

Since the area under a curve in a Platzman plot is proportional to σ_{ion}, it is simple to estimate uncertainties arising from this somewhat arbitrary procedure. In the particular example of He^+ on Ar shown in Fig. 1, resulting σ_{ion} would not have suffered by more than 30% even if we connected $d\sigma/dW$ for proton at W = 2 eV (R/E = 0.77) and $Z^2 \times d\sigma/dW$ for proton at W = 100 eV (R/E = 0.12) by a straight line! The area under a "composite" curve thus obtained (see Fig. 2) will provide σ_{ion} for the dressed ion.

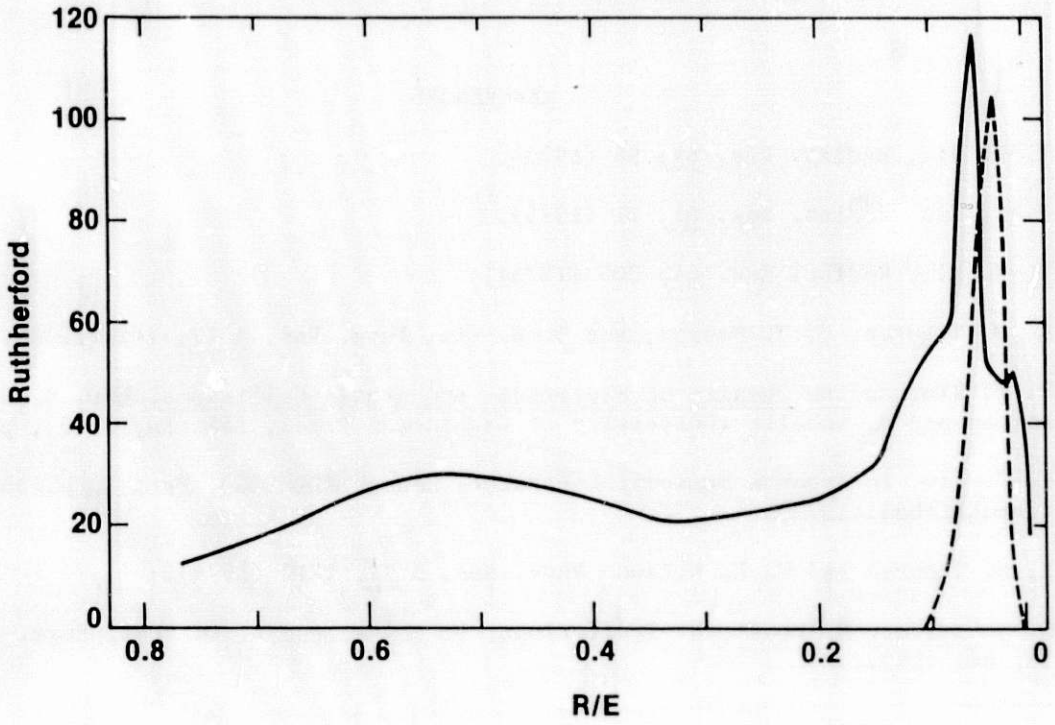

Fig. 2. Composite $d\sigma/dW$ for He^+ and the electron-loss peak. The solid curve is the "composite" cross section for He^+ constructed according to the procedure described in the text, and the dashed curve is the difference between the composite curve and the actually measured He^+ cross section. The dashed curve corresponds to the electron loss by He^+. Although the electron-loss mechanism does not affect the ionization of the target atom, it accounts for about 1/6 of the electrons produced by He^+ - Ar collision.

Obviously, this simple method depends strongly on the availability of reliable $d\sigma/dW$ by proton impact at the same speed as the dressed ion of interest. There are many powerful consistency checks that can be applied to experimental $d\sigma/dW$ by using the Platzman plot.[1-6] Since it is easier to obtain reliable experimental and theoretical cross sections for ionization by protons than by dressed ions, the proposed method will serve as a "quick but not so dirty" way to estimate σ_{ion} by dressed ion impact — hopefully within ±40% — provided that reliable proton-impact data are available.

When the projectile energy is low ($\lesssim$0.5 MeV/amu), the proposed method should not be used because the Z^2 scaling for fast ejected electrons becomes dubious and charge transfer to the projectile (electron pick-up) becomes a competing (and sometimes dominant) mechanism for the ionization of the target.

Clearly, we need more sytematic studies of $d\sigma/dW$ by dressed ions of various net charges similar to the experiment by Toburen and Wilson[7] for better understanding of ionization by partially stripped ions.

ACKNOWLEDGEMENTS

The author would like to thank Dr. L. H. Toburen for providing him with experimental data quoted in Fig. 1 as well as for stimulating discussions.

REFERENCES

1. Y.-K. Kim, Radiat. Res. 64, 96 (1975).

2. Y.-K. Kim, Radiat. Res. 61, 21 (1975).

3. Y.-K. Kim, Radiat. Res. 64, 205 (1975).

4. L. H. Toburen, S. T. Manson, and Y.-K. Kim, Phys. Rev. A 17, 148 (1978).

5. Y.-K. Kim, in The Physics of Electronic and Atomic Collisions, eds. J. S. Risley and R. Geballe (University of Washington Press, Seattle, 1975), p. 741.

6. Y.-K. Kim, in Argonne National Laboratory Report ANL-8060, Part I, p. 55 (unpublished, 1973).

7. L. H. Toburen and W. E. Wilson, Phys. Rev. A 19, 2214 (1979).

8. D. Schneider, M. Prost, N. Stolterfoht, G. Nolte, and R. Du Bois, Phys. Rev. A 28, 649 (1983).

INTERMEDIATE ENERGY ION-ATOM COLLISIONS

M. Kimura
Dept. of Physics
University of Missouri-Rolla
Rolla, MO 65401

ABSTRACT

The close-coupling method is used to study the angular scattering cross section for the process:

$$H^+ + He(1S^2) \rightarrow H^+(\theta) + He^*(1S, n^*=2)$$

A two-center atomic-orbital expansion approximation is used in conjunction with the classical trajectory formulation. Our results are in excellent agreement with recent measurements and indicate that the inclusion of charge transfer channels is important.

INTRODUCTION

Excitation, charge transfer and ionization processes in ion-atom collisions have been studied extensively from both a theoretical and an experimental standpoint. In the energy range of 15-200 keV, the interactions, which couple the various possible channels, change their character. This poses a difficult problem for understanding the dynamical aspects occurring in intermediate energy ion-atom collisions for theoretical as well as experimental investigations. From a theoretical standpoint, all of the possible channels couple strongly over the impact parameter range from small to relatively large impact parameters. This makes the simple perturbation theory, which is usually valid at high energies, invalid and hence a non-perturbative method is needed. The close-coupling technique is one which can, in principle, manage the problem of strongly coupled collision channels. However, in order to obtain fast convergence of the cross section as a function of the expansion basis set, it is extremely important to select the most important orbitals for each given set of collision conditions. In the energy range between 25 keV and 250 keV ($v > v_e$) that we are interested in, the atomic-orbital expansion method in conjunction with the classical trajectory formulation is considered to be an adequate method for application to most collision systems. This method is used to investigate the various effects found in H^+-He collisions at collision energies from 25 to 200 keV.

Method

For collisions where the orbiting velocity of the bound electron is not large compared to the velocity of the projectile a quasi-molecule is not expected to form during the collision. In this case, a two-center atomic expansion might be a better representation of the collision system. Thus one takes

$$\psi(\vec{r},t) = \sum_i a_i(t)\,\phi_i(r_T)\exp\{-i(\tfrac{1}{2}\vec{v}\cdot\vec{r} + \tfrac{1}{8}v^2 t + \varepsilon_i t)\} + \sum_j b_j(t)\,\phi_j(r_p)\exp\{-i(-\tfrac{1}{2}\vec{v}\cdot\vec{r} + \tfrac{1}{8}v^2 t + \varepsilon_j t)\} \quad (1)$$

where $\phi_i(r_T)$ and $\phi_j(r_p)$ are atomic eigenstates centered on the target and the projectile, respectively. The velocity dependent phase factors are the plane wave electron translation factors (ETF's). Substitution of Eq. (1) into the time-dependent Schrödinger equation yields a set of coupled equations. These are given by:

$$S\begin{bmatrix}\dot{a}\\ \dot{b}\end{bmatrix} = \mathcal{H}\begin{bmatrix}a\\ b\end{bmatrix} \quad (2)$$

where

$$S_{ij}^{m,n} = \langle \tilde{\phi}^m(r_i) \mid \tilde{\phi}^n(r_j)\rangle \quad (3)$$

$$\mathcal{H}_{ij}^{m,n} = \langle \tilde{\phi}^m(r_i) \mid H - i\frac{\partial}{\partial t} \mid \tilde{\phi}^n(r_j)\rangle$$

and the traveling atomic orbital $\tilde{\phi}^m$ is defined as:

$$\tilde{\phi}^m(r_i) = \phi_m(r_i)\exp\{-i(p\vec{v}\cdot\vec{r} + \tfrac{1}{8}v^2 t + \varepsilon_m t)\} \quad (4)$$

where $p = \pm \frac{1}{2}$ depending upon whether the electron is on the target or projectile.

The coupled equations, Eq. (2), are solved numerically to obtain the transition probability $P_i(E,b) = |a_i(+\infty)|^2$ or $|b_i(+\infty)|^2$. The differential cross section is defined in the Eikonal approximation to be:

$$\frac{d\sigma(\theta)}{d\Omega} = \left| i\mu v \int_0^\infty db\, b\, a_i(b,E)\, J_0(2\mu v b \sin\theta/2)\right|^2 \quad (5)$$

The total cross section can be calculated by using:

$$\sigma_i(E) = 2\pi \int_0^\infty db\, b\, P_i(E,b) \quad (6)$$

In the close-coupling calculation, the $He(1s^2;{}^1S)$, He(1s 2s; 1s), He(1s 2p; ^1p) and H(1s), H(2s), $H(2p_o)$, $H(2p_{\pm 1})$ states were used to represent the excitation and charge transfer channels.

Discussion

Figure 1 displays the angular differential cross sections for excitation of helium to its n=2 level by proton impact. The experimental data are taken from Kvale *et al.*[1] (1983). The Born approximation results[2] overestimate the differential cross section for all scattering angles reported and falls off much faster than the experimental measurements. This is not surprising because the large angle scattering is determined by the Coulomb interaction between the nuclei and this interaction does not yield any contribution in the first Born approximation.

The SSG and G2[2] represents single scattering Glauber and full Glauber approximations, respectively. The inclusion of the double scattering term in the Glauber approximation lowers the results by a factor of 2 at 25 keV. The two results become closer at higher energy. The VPSA (Vainstein-Presnyakov-Sobel'man approximation)[4] agrees fairly well at small scattering angles, but it fails as the scattering angle increases. This may be a consequence of the peaking approximation used.

The present close-coupling (CC) results are in reasonable accord with the experimental results of Kvale et al.[1] at scattering angles. An earlier one-center expansion calculation by Flannery and McCann[2] (not shown) is also in excellent agreement with experiment. However, this study clearly indicates that the inclusion of charge transfer channels at 25 keV is important. The neglect of the charge transfer channels in Ref. (2) should overestimate the cross section. Indeed, our results are about 15 $\sim$ 20% lower than theirs, although the magnitude and the shape of the cross sections are very similar.

REFERENCES

(1) T. J. Kvale, Ph.D. Thesis, Univ. of Missouri at Rolla (1984).

(2) M. R. Flannery and K. J. McCann, J. Phys. B 7, 1558 (1974).

(3) S. K. Sur, S. Datta and S. C. Mukherjee, Phys. Rev. A24, 2465 (1981).

(4) C. E. Theodosiou, Phys. Lett. A 83A, 254 (1981).

ACKNOWLEDGEMENTS

The research was supported by the Magnetic Fusion Energy Division of the U.S. Department of Energy. Useful discussions with T. J. Kvale, J. L. Peacher and R. E. Olson are also acknowledged.

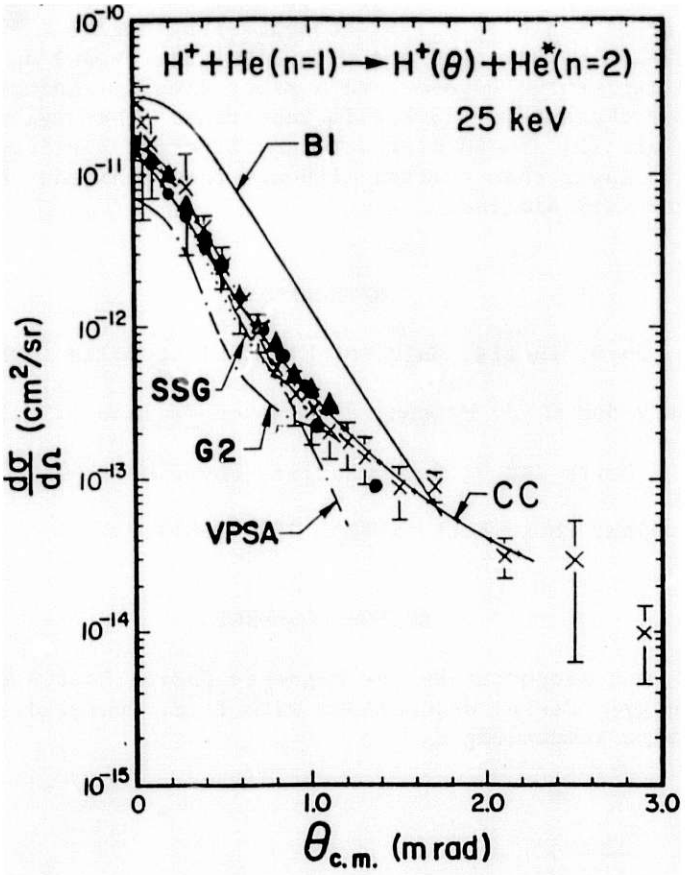
H+ + He(n=1) → H+(θ) + He*(n=2)
25 keV
BI
SSG
G2
CC
VPSA
dσ/dΩ (cm²/sr)
θc.m. (mrad)
10⁻¹⁰
10⁻¹¹
10⁻¹²
10⁻¹³
10⁻¹⁴
10⁻¹⁵
0
1.0
2.0
3.0

Figure 1.

THEORETICAL CROSS SECTIONS FOR INNER-SHELL VACANCY PRODUCTION BY HIGH-ENERGY ELECTRONS

James M. Peek

Sandia National Laboratories
Albuquerque, NM 87185

INTRODUCTION

The creation of inner-shell vacancies can play an important role in the transport of and energy deposition by fast incident particles. Most high-energy electron-transport models include this phenomenology. A large body of cross-section data is available for this purpose, but many gaps remain to be filled by interpolation or extrapolation methods. The published data become more sparse as the energy of the incident particle becomes relativistic and the nuclear charge of the target becomes large.

The use of relativistic Bethe-Born theory for inelastic electron scattering to augment the existing data for inner-shell vacancy production is described. The data required to implement this technique have been calculated with both a Hartree-Fock and a relativistic Hartree-Fock description used to define the target structure. The resulting cross sections are available for most elements and for most of their orbitals if the valence electrons are excluded. Comparisons of these data with existing experimental and theoretical inner-shell ionization information are summarized.

THEORY AND RESULTS

The Bethe-Born cross section for high-energy inelastic electron scattering can be written as

$$\sigma = 1.875 \cdot 10^{2}\ \beta^{-2} \left\{ S_i(-1) \left[\ell n[\beta^2/(1-\beta^2)] - \beta^2 \right] + C_i \right\} \text{ barn} \qquad (1)$$

where β is the collision speed divided by the speed of light. The dimensionless quantity $S_i(-1)$ is

$$S_i(-1) = \sum_j (\Delta E_{ij}/Ry)^{-1}\ f_{ij} \qquad (2)$$

where ΔE_{ij} is the excitation of the orbital i to the orbital j, f_{ij} is the associated dipole oscillator strength, and Ry is the Rydberg energy unit.

If Eq. (1) is to represent the removal of an electron from an inner shell, the sum in Eq. (2) is over all unoccupied electronic states of the target including the continuum. Techniques for evaluating this sum are described elsewhere[2,3] for the case of a target represented by a combination of orthogonal one-electron orbitals. Typical results for $S_i(-1)$ are shown in Fig. 1 for a 1s wave function generated by the Herman-Skillman (HS), the Hartree-Fock (HF), and the relativistic Hartree-Fock techniques. The HS and HF results are similar, as they should be, while the RHF data differ by increasing amounts as the target nuclear charge, Z, increases. This behavior is not unexpected for orbitals near the nucleus, but similar relativistic effects for higher-lying orbitals, not shown here, tend to be larger than expected.

The constant C_i must be specified to complete the definition of Eq. (1). The method used here is to equate Eq. (1) to the result from some other theory at a collision energy roughly 2-10 times the energy at which this cross section has its maximum value.

There are several sources for the low-energy cross section data, and one choice has been discussed elsewhere.[1] Equation (1) plus the cross-section data used to compute C_i define the cross section for all collision energies. This technique does not guarantee a prediction with a continuous first derivative, but a large number of comparisons[1] indicate that no unacceptable behavior in the energy dependence of the cross section is generated.

Reference 1 discusses the comparisons of cross sections generated by the present method with available experimental and theoretical subshell ionization data. In brief, these predictions are competitive with the best available for the ionization of the K, the L, and the averaged M shells, and a variety of targets. The main advantage of this technique is that it can provide a cross section for most interior subshells of any target at any collision energy without difficult or tedious interpolation or extrapolation of tables of existing data.

As implemented in the present study, the data storage requirements are modest and the computational times required to produce a cross section are small. The nature of this approach is such that more accurate low-energy data could be easily incorporated if they are available and are required for a particular application.

ACKNOWLEDGEMENT

This work was supported by the U.S. Department of Energy under Contract No. DE-AC04-76DP00789.

REFERENCES

1. J. M. PEEK and J. A. HALBLEIB, "Improved Atomic Data for Electron-Transport Predictions by the Codes TIGER and TIGERP: 1. Inner-Shell Ionization by Electron Collisions," Report Sand82-2887, Sandia National Laboratories (1983).

2. J. M. PEEK, Phys. Rev. A 26, 1030 (1982).

3. J. M. PEEK, L. C. PITCHFORD, AND E. J. SHIPSEY, Phys. Rev. to appear, (1983).

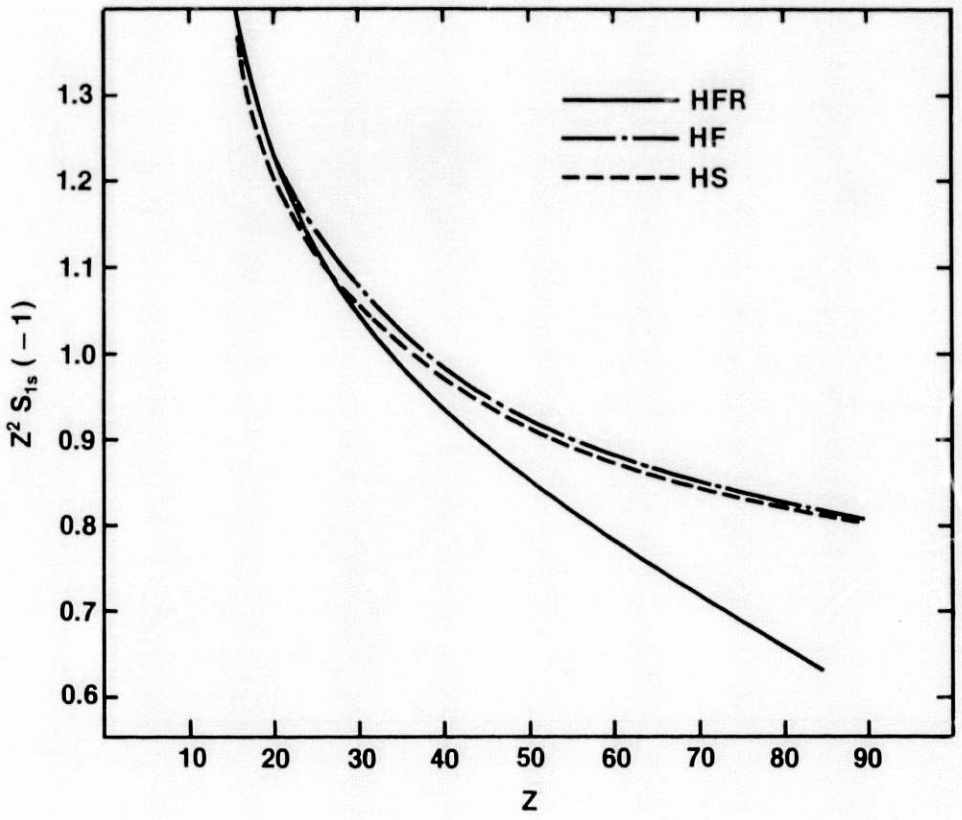

Fig. 1. The quantity defined by Eq. (2) multiplied by the nuclear charge squared of the target, Z^2, is shown as a function of Z. The dashed curve results from HS target wave functions, the broken curve from HF wave functions, and the solid curve from RHF wave functions.

COMMENT: Several presentations have included references to the role of inner-shell phenomena. I would like to bring the attention of this audience to my work, soon to be published, on the high-energy behavior of the cross sections for inner-shell vacancy production by fast electrons and protons. These results are suitable for use by large transport codes in that data for all elements are available, cross-section evaluation times are short, and computer storage requirements are modest. The expected relativistic effects for fast incident particles are displayed by these data while the influence of relativistic effects from the target's electronic structure is much larger that anticipated. (J. M. Peek, Sandia National Laboratories, Albuquerque, New Mexico - 87185)

DIPOLE OSCILLATOR STRENGTHS OBSERVED IN ELECTRON IMPACT

C.E. Brion
Department of Chemistry
University of British Columbia
Vancouver, B.C.
CANADA
V6T 1Y6

ABSTRACT

The measurement of absolute dipole oscillator strengths can be achieved by fast electron impact methods simulating photoabsorption, photoionisation, and photofragmentation. Measurements have been made in total and also partial channels for a variety of molecular targets inclusing H_2, CO, N_2, O_2,NO, HF, HCℓ, HBr, H_2O, NH_3, CH_4, N_2O, CO_2, COS, CS_2, and SF_6. The equivalent photon energy range is up to ~ 80eV for ionization and up to several hundred eV for absorption. A survey of all measurements made so far is given together with a complete bibliography.

INTRODUCTION

Dipole oscillator strengths (DOS) are to be found on that part of the Bethe surface[1], or generalised oscillator strength (GOS), df/dE (K), which corresponds to vanishingly small momentum transfer. As such, the DOS provides two items of information important to the more complete understanding of and the modeling of the particle and/or radiation induced decomposition of molecules. Firstly, the DOS provides a quantitative measure of the interaction of fast charged particles with matter in the appropriate kinematic range (negligible momentum transfer). Secondly, the DOS is identical to the optical oscillator strength (OOS) which gives the absolute probability for absorption of photons leading to processes of photoexcitation, photoionization, photodissociation, etc. Thus it may be said that the DOS is the common territory of fast electrons and photons. Furthermore, a knowledge of the absolute dipole oscillator strength provides an important reference point and possible means of putting other relative measurements, out on the Bethe surface and elsewhere, on to an absolute scale.

Although tuneable energy synchrotron radiation has become increasingly available in recent years for direct photoabsorption and photoionization experiments, gas phase work has been quite restricted in scope and such studies have often been limited by considerations of intensity, resolution, and spectral range mainly as a result of the properties of the dispersing monochromators. In particular absolute partial oscillator strengths (cross-sections) for photoionization are difficult to measure. The demand for this type of data has greatly increased because of the need to understand the dipole breakdown of molecules and also for the evaluation of new types of quantum calculation methods and continuum wave functions[2].

With the foregoing considerations in mind we started, in the early 1970's, at the University of British Columbia, to develop alternative new methods of measuring absolute oscillator strengths for photoabsorption and photoionization in both total and partial channels. All these new methods exploit the virtual photon field of a fast electron which induces a dipole field of equal intensity at all frequencies (energies) in the target species. The principles and underlying scattering theory have been reviewed in earlier publications[3-5] and only brief mention of these will be made here.

Much of the earlier work was done in collaboration with M.J. Van der Wiel and co-workers at the FOM Institute in Amsterdam. The methods provide a simple, inexpensive, laboratory-based alternative to the use of tuneable synchrotron radiation for quantitative gas phase molecular spectroscopy in the vacuum UV and soft X-ray regions.

In the limit of vanishingly small momentum transfer (achieved by using electrons of several kiloelectron volts energy and zero degree scattering angle) the Bethe-Born theory, as discussed by Lassettre[6] and Inokuti[1] relates the dipole (or optical) oscillator strength $(\frac{dfo}{dE})$ to the differential electron scattering cross-section $(\frac{d\sigma}{dE})$ according to the equation

$$\frac{dfo}{dE} = \frac{E}{2} \frac{ko}{kn} K^2 \frac{d\sigma}{dE} \qquad (1)$$

where E is the electron energy loss (analogous to the photon energy) and ko, kn, and K are the incident, scattered, and transfer momenta respectively. Thus dipole oscillator strengths may be obtained directly by simple kinematic conversion of the electron scattering intensities. The dipole oscillator strength is related to the cross section σ_{ph} for photoabsorption, photoionization, etc. by the equation

$$\frac{dfo}{dE} = \frac{mc^2}{\pi e^2} \sigma_{ph} \qquad (2)$$

In practice, of course, the scattering intensities are only determinable on a relative bases. However, unlike most photon continua the virtual photon field has equal intensity at all energy transfers (E) used[3,4], and thus the correct relative shapes of dipole oscillator strength spectra are obtained. It has now been repeatedly and convincingly shown that the wide range, relative photoabsorption spectrum thus obtained can readily be put on an absolute scale by sum rule normalization[3,4]. Specifically the TRK sum rule equates the total dipole oscillator strength to the number of electrons in the target species. In practice an effective shell separation exists for many molecules and the valence shell spectrum can be normalized to the number of valence electrons with a small correction for Pauli excluded transitions[7]. In this way absolute oscillator strengths with an accuracy better than 5% are obtained directly without making any absolute measurements. This is a very attractive feature of the electron impact simulation methods.

The application of the above ideas in conjunction with the use of electron energy loss spectroscopy (in some cases also with coincidence counting) has resulted in the measurement of a large number of dipole oscillator strengths for (1) Photoabsorption, by dipole (e,e) spectroscopy, (2) Partial photoionization to electronic states, by dipole (e,2e) spectroscopy (simulating tuneable energy photoelectron spectroscopy) and (3) Molecular and dissociative photoionization by dipole (e,e + ion) spectroscopy (simulating tuneable energy photoionization mass spectrometry). These methods have been fully discussed in earlier articles[3-5,8-11]. In addition the general basic theory of the dipole (e,2e) method has been investigated[12], while recently a more detailed and elegant theoretical treatment has been given by White[13].

The effectiveness and validity of these photon simulation experiments is clearly demonstrated by comparing with directly obtained photoabsorption and photoionization data in those cases where the direct optical studies have been made. Some examples are for photoabsorption of N_2O[14,15] and COS[16,17] as well as partial photoionization of H_2O[18,19] and COS[16,17] and the dissociative photoionization of O_2[20,21].

Using the dipole electron molecule technique optical oscillator strengths have been measured for a wide variety of photon induced processes for a large range of target molecules. These published results have now been incorporated into a generalized data compilation[22] to be discussed in a later part of the present article.

In the following sections recent advances in and the current status of the instrumentation are discussed together with some new possibilities promising increased resolution and sensitivity for dipole electron molecule experiments. Finally the data compilation is reviewed.

(a) Dipole (e,e) Spectrometers. Our existing high resoluton spectrometer[23] for valence and inner shell electronic excitation spectra is continuing to produce good results. However, it suffers from several disadvantages. Firstly since it is contained entirely within a single vacuum chamber it is rapidly contaminated by reactive gases, particularly by those that decompose on the hot tungsten cathode. This results in rapid deterioration of both sensitivity and resolution, and necessitates frequent tedious dismantling and cleaning procedures. In the case of inner shell spectra[23], small angle scattering must be employed to reduce the large non-spectral backgrounds that occur when the primary electron beam is allowed to enter the analyser. In order to overcome these operational difficulties and provide improved overall performance a new high resolution (e,e) spectrometer (SUPERSPEC) has been designed, built, and tested[5,24]. The design features and operation have been fully discussed in a recent publication[24]. The large hemispherical electron analysers (mean diameter 16 inches) and sophisticated electron optics ensure high sensitivity and high resolution at high impact energy while maintaining high analyser pass energies and reasonable lens ratios. The instrument functions well at zero degrees scattering angle with negligible non-spectral background for both valence and inner shell spectra. The spectrometer is presently being fitted with a microchannel-plate, position-sensitive detector which should result in further large improvements in performance. This detector is similar to that described by Hicks et al.[25], but uses fibre optics to couple directly the output of a phosphor screen to a photodiode array. The spectrometer is differentially pumped with separate sections for the gun, monochromator, collision chamber, and analyser regions. This permits study of reactive gases and eliminates almost all need for cleaning. Furthermore, neither the spectrometer tuning nor the absolute energy loss scale are affected by gas introduction or change of gas samples. The zero degree scattering angle will permit future measurements of dipole oscillator strengths for both valence and inner shell processes. The increased sensitivity and differential pumping make the instrument ideal for the study of absolute oscillator strengths for processes involving atoms, radicals and ions, as well as transient and reactive species present in fusion devices.

(b) Dipole (e,2e) Spectrometer. Full details of the design and operation of the existing magic angle coincidence spectrometer have been published earlier[8,16]. Future improvements are planned to increase both the sensitivity and resolution (at present 1.5 eV FWHM) of this instrument since both factors currently limit the range of possible studies. Sensitivity can be significantly improved by placing a microchannel plate position sensitive detector in the focal plane of the ejected (54°) analyser. Coincidence detection with positional information can be obtained by taking the fast timing signal off the exit face of the channel plate. Recently Cook et al.[26] have convincingly demonstrated the effectiveness of a similar position-sensitive coincidence system in a binary (e,2e) spectrometer. Following a recent suggestion by Cook[27] we are also exploring the possibility of obtaining high resolution (perhaps as good as 0.03eV) dipole (e,2e) spectra without any electron beam monochromation. This would be achieved by using the ideas put forward and experimentally demonstrated by Zscheile[28], who has shown how a thermal electron beam can be spatially dispersed into a parallel beam by an analyser without an exit slit. Electrons from this dispersed beam are then inelastically scattered off a target in the forward direction, analysed, and all electrons with the same energy loss, regardless of position, are focussed at a single point in the exit plane of the forward analyser. Now if a microchannel plate is put in the exit plane of the ejected electron analyser of the dipole (e,2e) spectrometer it would be possible to collect a range of energy losses simultaneously. The successful combined use of channel plates in both the ejected and the forward analyser together with the idea of Zscheile[28] offers the possibility of very significant gains in instrumental sensitivity and resolution in dipole electron-molecule coincidence experiments.

(c) Dipole (e,e + ion) Spectrometer. This instrument[9,10], originally built and operated by Van der Wiel et al. at the FOM Institute, Amsterdam, was moved in 1980 to

the University of British Columbia. It has since undergone a number of minor improvements and modifications[11]. Resolution and sensitivity could both be improved using the ideas discussed in the preceding section on the dipole (e,2e) spectrometer. However, on a relative basis the existing (e,e + ion) machine is already much more sensitive than the (e,2e) since the former collects all ions regardless of direction (and independent of the kinetic energy of fragmentation below 20eV), whereas the latter instrument is differential in that it only collects ejected electrons in a narrow cone about the magic angle of 54°. There is thus less need for improving sensitivity, particularly as present data rates are quite high in most cases.

RESULTS

Over the past decade the above techniques have been used to make dipole oscillator strength measurements for processes of photoabsorption, photoionization, and ionic photofragmentation in a wide variety of molecules including H_2, D_2, HD, CO, N_2, O_2, NO, HF, HCℓ, HBr, H_2O, NH_3, CH_4, N_2O, CO_2, COS, CS_2, and SF_6. In particular our detailed results[18] for H_2O, which are much more comprehensive than all the available, directly obtained, optical data, have already found wide application in the modelling and description of radiation induced decomposition processes and related topics (see other papers in the workshop). The measurements provide a detailed dipole breakdown pattern for the molecule in question. A typical set of more recent results[31] is shown for HCℓ in Figs. 1-7 below. Figure 1 shows the absolute photoabsorption oscillator strength of HCℓ, which has not been previously measured. The total oscillator strength is very small above 35eV and this results in poor statistics for the partial

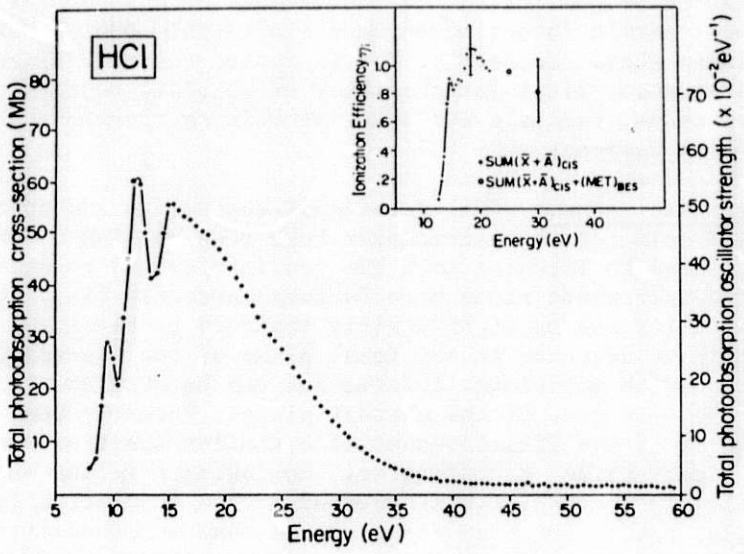

Figure 1

channel measurements at higher energies. Binding energy spectra shown in Fig. 2 are notable for the split ionic pole strength for 4σ ionization due to many-body effects. These latter effects for HCℓ have been studied in detail by binary (e,2e) spectroscopy[29] with all the structure above 20eV being assigned conclusively to the $(4\sigma)^{-1}$ process from a consideration of the measured electron momentum distributions. This behaviour represents a breakdown of simple MO theory in the case of ionization of the inner valence orbital and is indicative of extensive electron correlation effects. Figure 3 shows the partial oscillator strengths for photoionization of the three valence orbitals up to 40eV while in Fig. 4 the results for the lowest two states of $HC\ell^+$ are compared with the recent calculations by Faegri and Kelly[30]. In Figs. 5 and 6 are shown typical time-of-flight mass spectra and the partial oscillator strengths

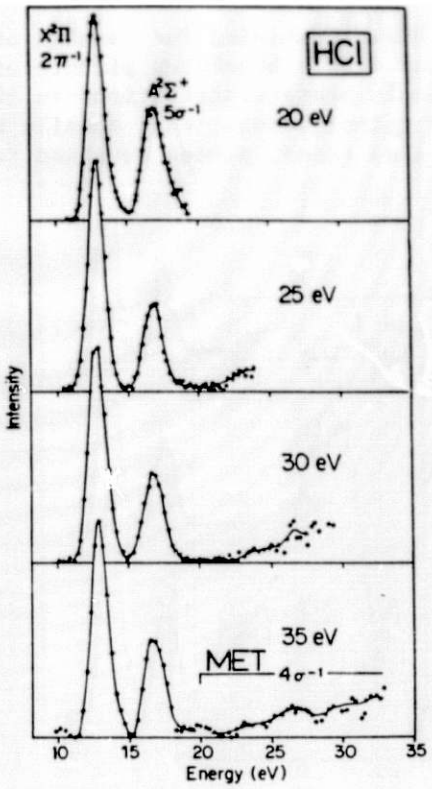

Figure 2

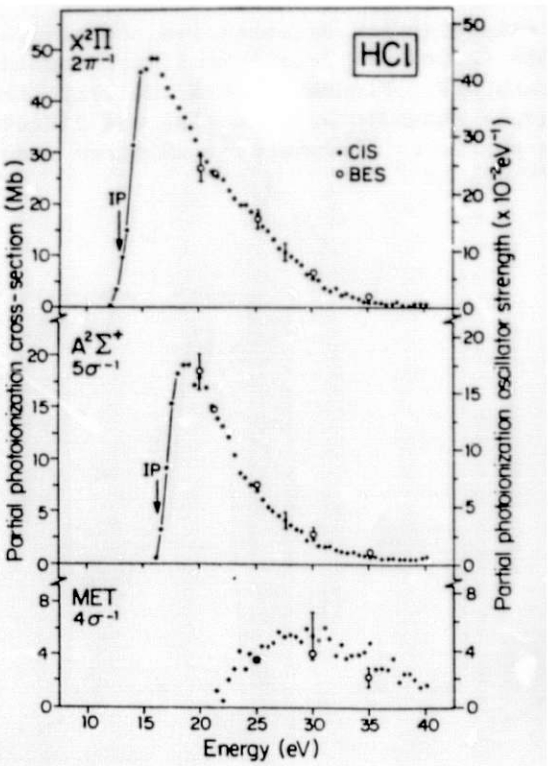

Figure 3

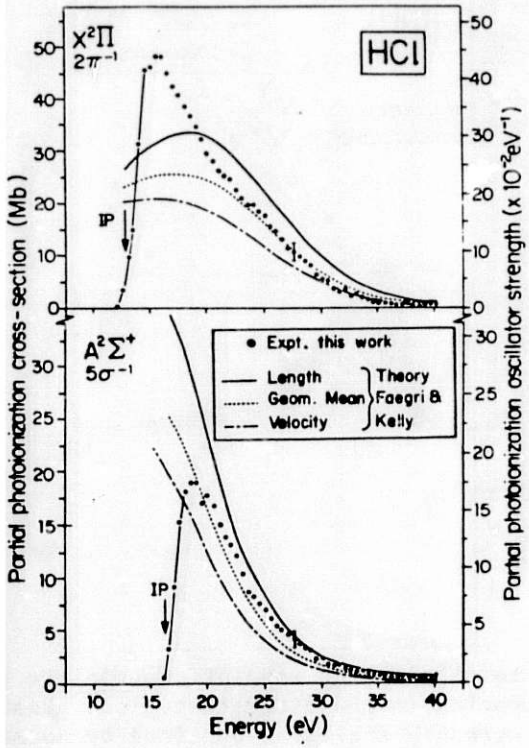

Figure 4

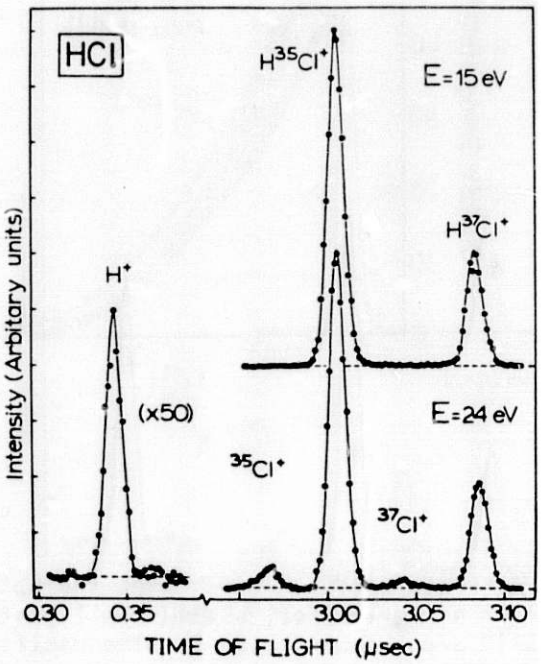

Figure 5

for molecular and dissociative photoionization of HCℓ. Combining the results of the dipole (e,2e) and (e,e + ion) experiments a detailed dipole breakdown picture of HCℓ is obtained. Figure 7 shows the respective electronic state contributions to the separate channels of molecular and dissociative photoionization. Full details have been published elsewhere[31]. Similar results have also recently been obtained for HBr[32] and NO[33].

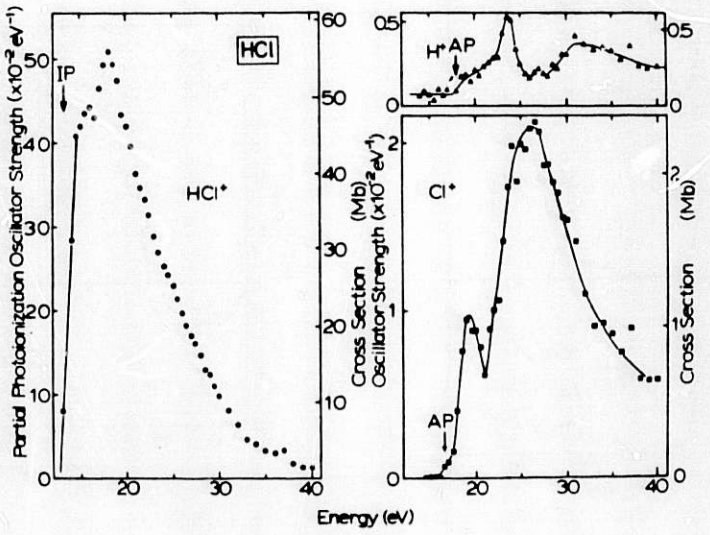

Figure 6

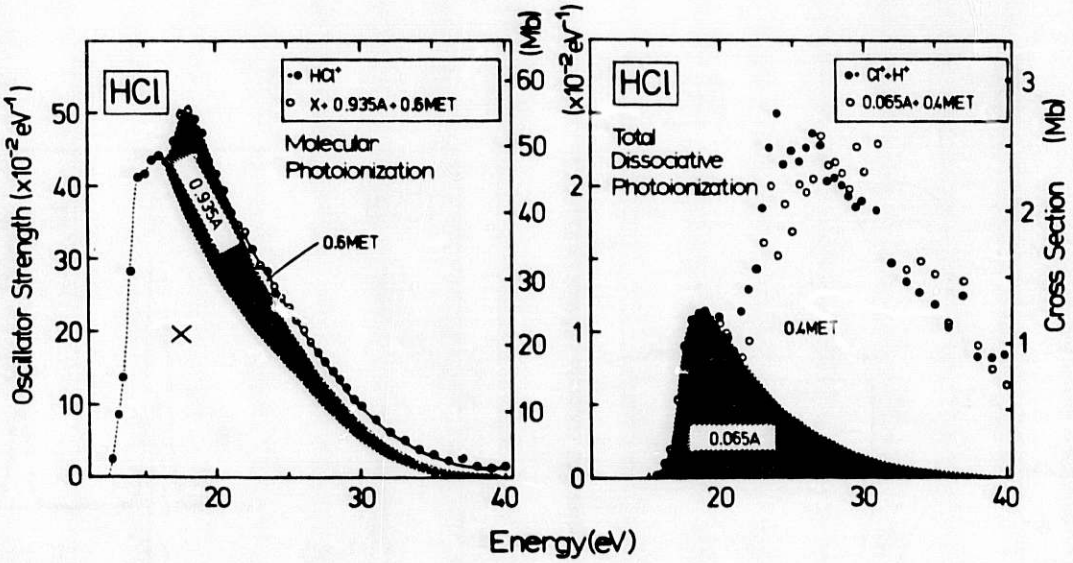

Figure 7.

A recent innovation has been the ability to obtain high resolution absolute oscillator strengths for valence shell photoabsorption in the discrete region. Results for HF[34] are shown in Fig. 8. . The oscillator strength scale was obtained by normalization on earlier low resolution dipole (e,e) spectra[35] in the smooth continuum region. The spectrum has been assigned [36] on the basis of detailed quantum calculations of final states as well as computed oscillator strengths.

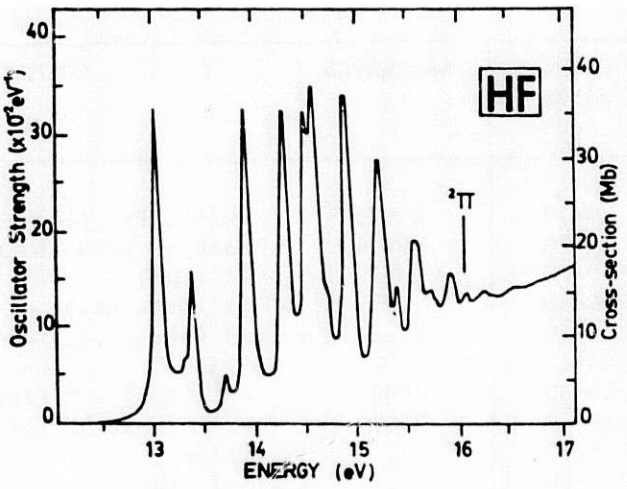

Figure 8

PUBLISHED OSCILLATOR STRENGTH DATA COMPILATION

In the past decade a large number of valence shell optical oscillator strength measurements have been made using the dipole electron molecule techniques discussed above. Absolute oscillator strength measurements of photoabsorption, photoionization and ionic fragmentation for H_2, CO, N_2, O_2, NO, HF, HCℓ, HBr, H_2O, NH_3, CH_4, N_2O, CO_2, CS_2, and SF_6 over a wide energy range have now been collected together and presented in standardized tables which are to be published[22]. A comprehensive data compilation and bibliography of dipole oscillator strengths measured by photon and electron impact is in preparation[36].

DATA SUMMARY AND BIBLIOGRAPHY OF PUBLISHED MEASUREMENTS OF OSCILLATOR STRENGTHS FROM DIPOLE ELECTRON-MOLECULE EXPERIMENTS

In the following tables the symbols have the meanings shown below.

ee	dipole (e,e) spectroscopy	(photoabsorption)
e2e	dipole (e,2e) spectroscopy	(photoionization, PES)
eei	dipole (e,e + ion) spectroscopy	(photoionization, PIMS)
eeiγ	dipole (e,e + ion + photon) spectroscopy	(photofluorescence)

PhAbs	photoabsorption data
PhI	photoionization data
BR	branching ratio data
(ion)	molecular and dissociative ionization data
(el.st.)	data for electronic states of ions

I. DIATOMICS

SPECIES	TYPE	ENERGY RANGE (eV)	REFERENCE	COMMENTS
H_2	eei	0-70	BWV76	PhAbs, PhI (ion), BR (ion)
HD	eei	0-70	BWV76	Some OS data shown
D_2	eei	0-70	BWV76	BR (ion)
		18-40	VV&79	PhI (el. st.)
HF	e2e	5-60	CTB81	BR (el. st.), PhI (el. st.)
		5-150		PhAbs
	eei	16-60	CB83	PhI (ion), BR (ion)
HCℓ	e2e	12-40	DI&83	BR (el. st.), PhI (el. st.)
		8-100		PhAbs
	eei	12-40		PhI (ion)
HBr	e2e	12-40	BC84	BR (el. st.), PhI (el. st.)
		8-100		PhAbs
CO	ee	40-500	KVV77	PhAbs, Carbon K edge detail
	e2e	18-50	HSB76	PhI (el. st.), BR (el. st.)
	eei	10-60	WVB76	PhI (ion), PhAbs
	eeiγ	10-60	BKV73	Photofluorescence
N_2	ee	40-600	KVV77	PhAbs, Nitrogen K edge detail
	e2e	18-50	HSB76	PhI (el. st.), BR (el. st.)
	eei	10-60	WVB76	PhI (ion), PhAbs
NO	e2e	18-60	BT81	PhAbs, BR (el. st.) PhI (el. st.)
O_2	e2e	5-300	BT&79	PhAbs
		5-75		PhI (el. st.), BR (el. st.)
	eei	5-75		PhI (ion)

II. TRIATOMICS

SPECIES	TYPE	ENERGY RANGE (eV)	REFERENCE	COMMENTS
H_2O	e2e	6-60	TB&78	PhAbs
		16-60		PhI (el. st.)
	eei	6-60		PhI (ion)
H_2S	e2e	5-80	BCT78	Binding energy spectra, BR (el. st.)
CO_2	e2e	20-60	BT78	PhAbs, PhI (el. st.), BR (el. st.)
	eei	8-75	HBV80	PhAbs, PhI (ion)
N_2O	e2e	20-60	BT78	PhAbs, PhI (el. st.), BR (el. st.)
	eei	8-75	HBV80	PhAbs, PhI(ion)
COS	ee	6-100	WLB81	PhAbs
	e2e	6-50		PhI (el. st.), BR (el. st.)
	eei	13-50	CH&82	PhI (ion)
CS_2	ee	5-40	CWB81	PhAbs
	e2e	5-40		PhI (el. st.), BR (el. st.)
	eei	13-40	CH&82	PhI (ion)

III. POLYATOMICS

SPECIES	TYPE	ENERGY RANGE (eV)	REFERENCE	COMMENTS
CH_4	e2e	8-90	BW&75	PhAbs
		10-35		PhI (el. st.)
		25-50	VS&76	PhI (el. st.)
	eei	14-80	BV75	PhI (ion) PhI (el. st.)
NH_3	e2e	15-50	BH&77	PhI (el. st.), BR (el. st.)
	eei	5-60	WVB77	PhAbs, PhI (ion)
SF_6	eei	160-230	HBV78	PhI (ion), S 2p ionization
		5-230		PhAbs
		5-63	HV79	PhAbs, PhI (ion)

IV. BIBLIOGRAPHY OF DIPOLE (e,e), (e,2e) AND (e,e + ion) PAPERS

BC84 C.E. Brion and F. Carnovale, to be published.

BCT78 C.E. Brion, J.P.D. Cook, and K.H. Tan; Chem. Phys. Lett. 59 (1978) 241-245. [H_2S, (e,2e)].

BH&77 C.E. Brion, A.Hamnett, G.R. Wight, and M.J. Van der Wiel; J. Electron Spectrosc. 12 (1977) 323-334. [NH_3, (e,2e)].

BKV73 C. Backx, M. Klewer, and M.J. Van der Wiel; Chem. Phys. Lett. 20 (1973) 100-103. [CO, (e,e + ion + γ)].

BT78 C.E. Brion and K.H. Tan; Chem. Phys. 34 (1978) 141-151. [N_2O and CO_2, (e,2e)].

BT81 C.E. Brion and K.H. Tan; J. Electron Spectrosc. 23 (1981) 1-11. [NO, (e,2e)].

BT&79 C.E. Brion, K.H. Tan, M.J. Van der Wiel, and Ph. E. Van der Leeuw; J. Electron Spectrosc. 17 (1979) 101-119. [O_2, (e,2e), (e,e + ion)].

BV75 C. Backx and M.J. Van der Wiel; J. Phys. B 8 (1975) 3020-3033. [CH_4, (e,e + ion)].

BWV76 C. Backx, G.R. Wight, and M.J. Van der Wiel; J. Phys. B 9 (1976) 315-331. [H_2, HD, D_2, (e,e + ion)].

BW&75 C. Backx, G.R. Wight, R.R. Tol, and M.J. Van der Wiel; J. Phys. B 8 (1975) 3007-3019. [CH_4, Total Threshold (e,2e), (e,e + ion)].

CB83 F. Carnovale and C.E. Brion; Chem. Phys. 74 (1983) 253-259. [HF, (e,2e)].

CH&82 F. Carnovale, A.P. Hitchcock, J.P.D. Cook, and C.E. Brion; Chem. Phys. 66 (1982) 249-259. [COS and CS_2, (e,e + ion)].

CTB81 F. Carnovale, R. Tseng, and C.E. Brion; J. Phys. B 14 (1981) 4771-4785. [HF (e,2e)].

CWB81 F. Carnovale, M.G. White, and C.E. Brion; J. Electron Spectrosc. 24 (1981) 63-76. [CS_2, (e,2e)].

DI&83 S. Daviel, Y. Iida, F. Carnovale, and C.E. Brion; Chem. Phys. 83 (1983) 391-406. [HCℓ, (e,2e), (e,e + ion).

HBV78 A.P. Hitchcock, C.E. Brion, and M.J. Van der Wiel; J. Phys. B 11 (1978) 3245-3261. [SF_6 (S 2p), (e,e + ion)].

HBV80 A.P. Hitchcock, C.E. Brion, and M.J. Van der Wiel; Chem. Phys. 45 (1980) 461-478. [N_2O and CO_2, (e,e + ion)].

HSB76 A. Hamnett, W. Stoll, and C.E. Brion; J. Electron Spectrosc. 8 (1976) 367-376. [CO and N_2, (e,2e)].

HV79 A.P. Hitchcock and M.J. Van der Wiel; J. Phys. B 12 (1979) 2153-2169. [SF_6, (e,e + ion)].

KVV77 R.B. Kay, Ph. E. Van der Leeuw, and M.J. Van der Wiel; J. Phys. B 10 (1977) 2513-2519. [N_2 and CO (K shell), (e,e)].

TB78 K.H. Tan and C.E. Brion; J. Electron Spectrosc. 13 (1978) 77-84. [Ar, (e,2e)].

TB&78 K.H. Tan, C.E. Brion, Ph. E. Van der Leeuw, and M.J. Van der Wiel; Chem. Phys. 29 (1978) 299-309. [H_2O, (e,2e), (e,e + ion)].

VS&76 M.J. Van der Wiel, W. Stoll, A. Hamnett, and C.E. Brion; Chem. Phys. Lett. 37 (1976) 240-242. [CH_4, (e,2e)].

VV&79 B. Van Wingerden, Ph. E. Van der Leeuw, F.J. de Heer, and M.J. Van der Wiel; J. Phys. B 12 (1979) 1559-1577. [D_2, H_2, (e,e + ion)].

WLB81 M.G. White, K.T. Leung, and C.E. Brion; J. Electron Spectrosc. 23 (1981) 127-145. [COS, (e,2e)].

WVB76 G.R. Wight, M.J. Van der Wiel, and C.E. Brion; J. Phys. B 9 (1976) 675-689. [N_2 and CO, (e,e + ion)].

WVB77 G.R. Wight, M.J. Van der Wiel, and C.E. Brion; J. Phys. B 10 (1977) 1863-1873. [NH_3, (e,e + ion)].

ACKNOWLEDGEMENTS

This work received financial support from the Natural Sciences and Engineering Research Council of Canada and also The Petroleum Research Fund administered by the American Chemical Society. I am indebted to Dr. J.P.D. Cook for suggestions and valuable discussions of ways to improve the performance of dipole (e,2e) and (e,e + ion) spectrometers. Special thanks go to Mr. J.P. Thomson for his careful and thorough work in assembling the data compilation and bibliography. Finally I would like to thank the numerous past and present co-workers at UBC and FOM who have skillfully participated in the measurement program.

REFERENCES

1. M. INOKUTI, Rev. Mod. Phys. 43, 297 (1971).
2. G.H.F. DIERCKSEN, W.P. KRAEMER, T.N. RESCIGNO, C.F. BENDER, B.V. MCKOY, S.R. LANGHOFF, and P.W. LANGHOFF, J. Chem. Phys. 76, 1043 (1982).
3. C.E. BRION and A. HAMNETT, in The Excited State in Chemical Physics, Part 2," Adv. Chem. Physics, 45, 1, (Ed. J.W. McGowan) John Wiley New York (1981).
4. C.E. BRION, in "Physics of Electronic and Atomic Collisions." Ed. S. Datz (North-Holland, 1982) page 579.
5. C.E. BRION, S. DAVIEL, R. SODHI, and A.P. HITCHCOCK, AIP Conference Proceedings No. 94 - X-Ray and Atomic Inner-Shell Physics (Ed. B. Crasemann), American Institute of Physics, (1982) page 429.
6. E.N. LASSETTRE, Rad. Research (Supp.) 1, 530 (1959).
7. J.A. WHEELER and J.A. BEARDEN, Phys. Rev. 46, 755 (1934).
8. C.E. BRION, A. HAMNETT, G.R. WIGHT and M.J. VAN DER WIEL, J. Electron Spectrosc. 12, 323 (1977).
9. C. BACKX and M.J. VAN DER WIEL, J. Phys. B. 8, 3020 (1975).
10. C. BACKX, G.R. WIGHT, R.R. TOL, and M.J. VAN DER WIEL, J. Phys. B. 8, 3007 (1975).
11. F. CARNOVALE and C.E. BRION, Chem. Physics 74, 253 (1983).
12. A. HAMNETT, W. STOLL, G. BRANTON, M.J. VAN DER WIEL, and C.E. BRION, J. Phys. B. 9, 945 (1976).
13. M.G. WHITE, Phys. Rev. A 26, 1907 (1982).
14. C.E. BRION and K.H. TAN, Chem. Physics 34, 141 (1978).
15. L.C. LEE, R.W. CARLSON, D.L. JUDGE, and M. OGAWA, J. Quant. Spectry. Rad. Transfer 13, 1023 (1973).
16. M.G. WHITE, K.T. LEUNG, and C.E. BRION, J. Electron Spectrosc. 23, 127 (1981).
17. T.A. CARLSON, M.O. KRAUSE, and F.A. GRIMM, J. Chem. Phys. 77, 1701 (1982).
18. K.H. TAN, C.E. BRION, PH.E. VAN ER LEEUW, and M.J. VAN DER WIEL, Chem. Physics 29, 299 (1978).
19. C.M. TRUESDALE, S. SOUTHWORTH. P.H. KOBRIN, D.W. LINDLE, G. THORNTON, and D.A. SHIRLEY, J. Chem. Phys. 76, 860 (1982).
20. C.E. BRION, K.H. TAN, M.J. VAN DER WIEL, and PH.E. VAN DER LEEUW, J. Electron Spectrosc. 17, 101 (1979).
21. J.A.R. SAMSON, G.H. RAYBORN, and P.N. PAREEK, J. Chem. Phys. 76, 393 (1982).
22. C.E. BRION and J.P. THOMSON, to be published in J. Electron Spectrosc., 1984.
23. A.P. HITCHCOCK and C.E. BRION, J. Electron Spectrosc. 13, 193 (1978).
24. S. DAVIEL, C.E. BRION, and A.P. HITCHCOCK, Rev. Sci. Instrum., to be published (1984).
25. P.J. HICKS, S. DAVIEL, B. WALLBANK, and J. COMER, J. Phys. E. Sci. Instrum. 13, 713 (1980).
26. J.P.D. COOK, I.E. McCARTHY, and E. WEIGOLD, to be published, J. Phys. B, (1984).
27. J.P.D. COOK, private communication.
28. H. ZSCHEILE, J.. Phys. E. Sci. Instrum. 15, 749 (1982).
29. C.E. BRION, S.T. HOOD, I.H. SUZUKI, E. WEIGOLD, and G.R.J. WILLIAMS, J. Electron Spectrosc. 21, 71-91 (1980).
30. K. FAEGRI, JR., and H.P. KELLY, Chem. Phys. Letters 85, 472 (1982).
31. S. DAVIEL, Y. IIDA, F. CARNOVALE, and C.E. BRION, Chem. Phys. 83, 391 (1984).
32. C.E. BRION, Y. IIDA, and F. CARNOVALE, to be published.
33. Y. IIDA, S. DAVIEL, F. CARNOVALE, and C.E. BRION, to be published.
34. A.P. HITCHCOCK, G.R.J. WILLIAMS, C.E. BRION, and P.W. LANGHOFF, Chem. Physics, to be published 1984.
35. F.C. CARNOVALE, R. TSENG, and C.E. BRION, J. Phys. B. 14, 4771 (1981).
36. J. GALLACHER, P.W. LANGHOFF, and C.E. BRION, to be published (in preparation at J.I.L.A. Data Center).

PARAMETERIZATION OF MOLECULAR PARTIAL OSCILLATOR STRENGTH DISTRIBUTIONS EMPLOYING A LEAST-SQUARES FIT TO A SPECIAL POLYNOMIAL

Michael A. Dillon

Argonne National Laboratory
Argonne, Illinois 60439

In a previous investigation[1] it was shown that an atomic oscillator strength distribution, f, can be represented by the polynomial fit,

$$f \simeq \sum_{n=0}^{n=N} A_n G^n \tag{1}$$

where

$$G = \frac{\varepsilon}{\varepsilon + I} . \tag{2}$$

In Eq. (2), I is the binding energy and ε is the ejected electron energy. Many applications of Eq. (1) to both experimental and theoretical data have demonstrated its general utility. The question arises as to whether the same procedure can be employed to fit molecular oscillator strength distributions. Certain considerations indicate the theoretical feasibility of this approach.

1. The variable G in Eqs. (1) and (2) arises from a demonstrated singularity in f at $\varepsilon = -I$ for all atoms where the initial and final states are represented by wave functions in the independent particle approximation. In the atomic case, this singularity is independent of the initial state angular momentum number and its existence depends only the asymptotic radial properties of the transition electron. This implies the presence of the same singularity in a molecular oscillator strength distribution which would then be independent of the initial state orbital symmetry.

2. Eq. (1) applies to atomic transitions where the continuum normalization constant is free of resonance features. This implies that Eq. (1) should be used to fit molecular oscillator strength distributions which are free of shape resonances.

It is possible to modify Eq. (1) by including a convergence factor which reflects large ε behavior. When data extending to large ε are available we could represent f by

$$f = F(G) \sum_{n=0}^{n=N} A'_n G^n \tag{4}$$

where

$$F = (1 - G)^{\rho} \to \varepsilon^{-\rho}, \text{ as } \varepsilon \to \infty. \tag{5}$$

The parameter ρ depends on the initial and final orbital angular momentum numbers. For example $\rho = 7/2$ for ionization from an s atomic orbital. The high energy limit of experimentally determined oscillator strengths is usually no more than a few times I so that the theoretical value of ρ is never approached. When experimental data extend to $\varepsilon \sim (2 - 5)$ times I it has been found empirically that $\rho = 2.5$ will enhance the convergence of Eq. (4). As a preliminary test, we have applied a least-squares fit of Eq. (4) to a few molecular f distributions from a compilation provided by C. E. Brion.[2] The partial ionizations selected were: $(1t_2)^{-1}$, $(2a_1)^{-1}$ (Methane) and $(1e)^{-1}$ (Ammonia). The data sets were chosen to run the gamut from large to small statistical scatter. In this preliminary report, we have adopted the procedure outlined in Fig. 1. First, the data points were interpolated to a one-hundred point mesh using a quadratic fitting spline. This was done in order to suppress oscillations in a possible large degree polynomial fit. This precaution was really unecessary in the present application since all least-squares fits were to polynomials of modest degree. In order to suppress instrumental and statistical fluctuations, the interpolated data were then smoothed using the optimal binomial filter proposed by Marchand and Marmet.[3] Although this procedure seemed to have little effect on the final results, it could still prove useful in the future. Least-squares fits of the prepared data to the polynomial in Eq. (4) [with Eq. (5) $\rho = 2.5$] are displayed in Figs. (2)-(4). The orbital binding energy employed was estimated by visual examination of the data. It is evident from the figures that the calculated points using Eq. (4) with fitting parameters A_n' fall within whatever reasonable error bars one might want to assign. Although these results are only preliminary, it is already evident that the data found in Brion's compilation can be compressed to one or two pages using the simple method outlined here. In addition, integrated f's are automatically obtained since

$$\int_0^\infty (1 - G)^{2.5}\, G^n\, d\varepsilon = I\, \frac{2^{n+1}\, n!}{(2n+3)!!}$$

in Eq. (4).

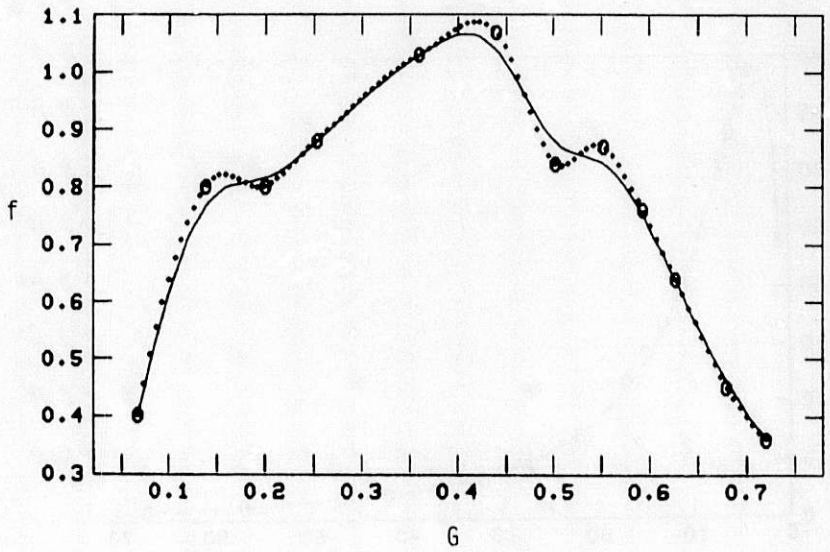

Fig. 1. Data preparation for $(2a_1)^{-1}$ ionization in methane.
o Data points
••• Quadratic interpolation
—— Interpolated points smoothed by a 25-point binomial filter

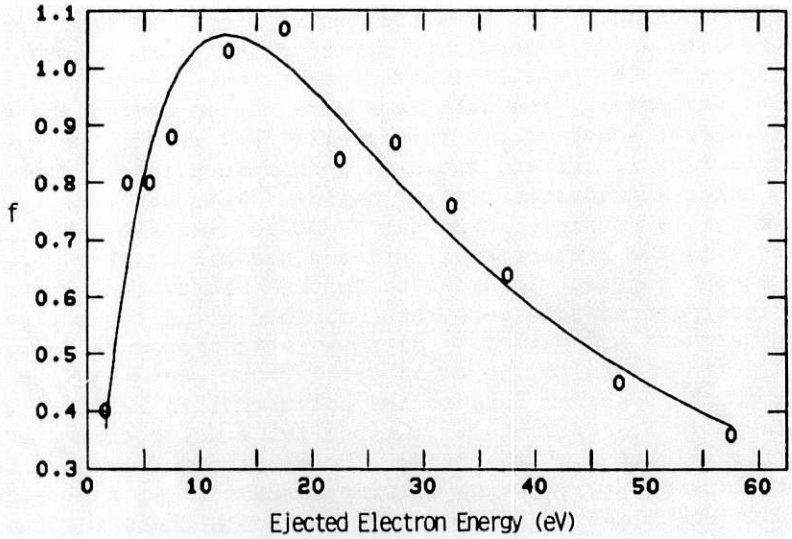

Fig. 2. Least-squares fit of the smoothed data in Fig. 1 to a second degree polynomial.

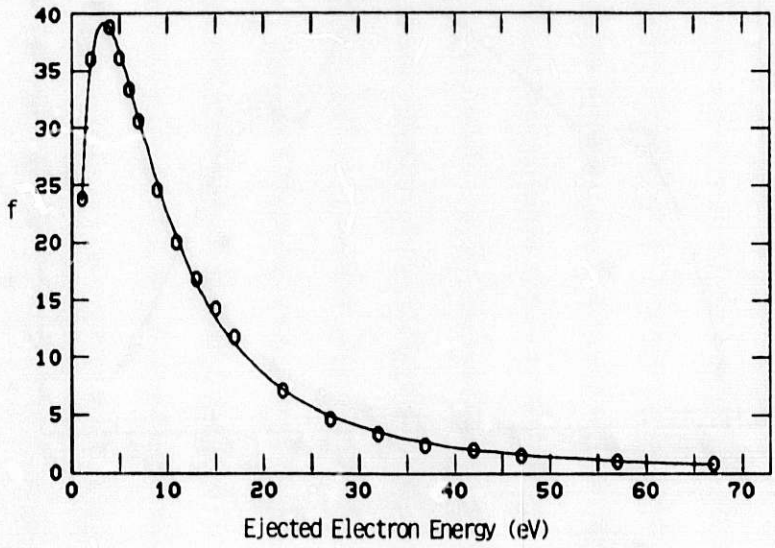

Fig. 3. Least-squares fit of the $(1t_2)^{-1}$ partial oscillator strength distribution in methane to a third degree polynomial.

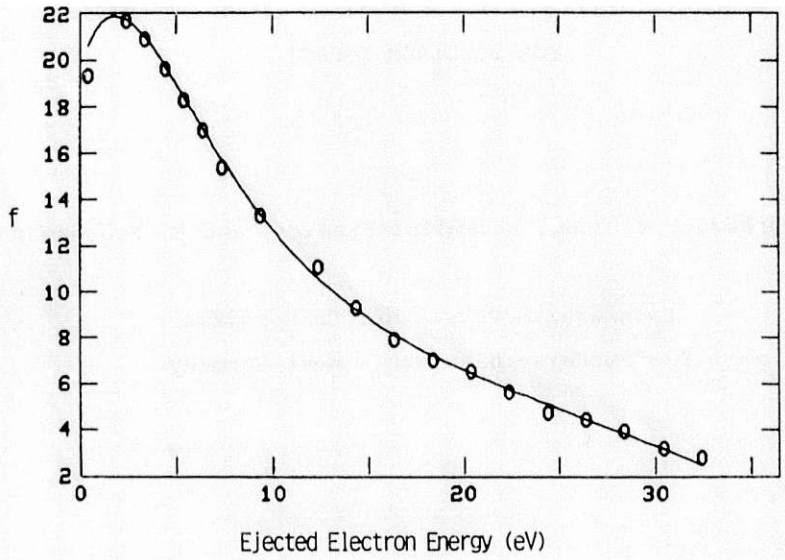

Fig. 4. Least-squares fit of the $(1e)^{-1}$ partial oscillator strength distribution in ammonia to a fourth degree polynomial.

REFERENCES

1. M. A. Dillon and M. Inokuti, J. Chem. Phys. 74, 6271 (1981).

2. C. E. Brion, see preceding contribution.

3. P. Marchand and L. Marmet, Rev. Sci. Instrum. 54, 1034 (1983).

ABSOLUTE DIFFERENTIAL IONIZATION CROSS SECTIONS FOR ELECTRON IMPACT

H. Ehrhardt, K. Jung, R. Müller-Fiedler, and P. Schlemmer

Fachbereich Physik der Universität
D-6750 Kaiserslautern, West Germany

ABSTRACT

Due to difficulties in the calculation and the measurement of differential electron impact ionization cross sections it is desirable to have highly reliable and low error experimental double and triple differential data for one standard target, to which in future normalization can be made. Only helium can serve as such a reference standard, since double ionization and simultaneous excitation and ionization is below 2% and therefore normalization to well-known photoionization oscillator strength data can be made. Absolute double differential cross sections for electron impact on helium are presented for incident energies E_o between 100 eV and 600 eV and ejection energies E_B between 2 and 20 eV. Absolute triple differential cross sections have been measured for E_o = 600 eV and E_B = 2,5 eV, 3,3 eV, 5,0 eV and 10 eV. Comparison with other experimental work is made and with the recommended differential cross sections for helium published by Y.-K. Kim (1983).

Qualitatively, the electron impact ionization process of atoms is quite well understood by now. If we assign E_o, E_A, E_B, $\vec{k}_o$, $\vec{k}_A$, $\vec{k}_B$ as the energies and momenta of the incoming (index o) electrons, the outgoing fast (index A) and slow (index B) electrons, IP the ionization potential and $q = |\vec{q}| = |\vec{k}_o - \vec{k}_A|$ the momentum transfer

during the collision, then it is well-known, that for large E_o (E_o > 5 IP) and small q (q << 1 a.u.) the electron impact ionization behaves similar as the photoionization and a rather simple first Born approximation is a good description. Another limiting collision model is found for large E_o and q >> 1 a.u., the so-called binary collision or electron-electron collision, in which the resulting ion is only a spectator. The ionization process is then similar to a (inelastic) billiard ball collision and even classical calculations give rather good descriptions.

On the other hand, the majority of ionizing collisions through electron impact occur (even for high E_o) in an intermediate range of momentum transfer (i.e. 0.5 < q < 2 a.u.). Here the theoretical description is very difficult and not yet in a satisfying state. It is therefore important to have good experimental data, especially of the differential cross sections

$$\frac{d\sigma}{dE} \quad , \quad \frac{d^2\sigma}{d\Omega\, dE} \quad \text{and} \quad \frac{d^3\sigma}{d\Omega_A\, d\Omega_B\, dE_B}$$

Such cross sections are also needed in applications such as radiation physics, gas discharges, and explosions with an accuracy of the order of 10% to 20%.

Experimentally also difficulties are to overcome, since the collision exit channel generally contains a fast electron scattered into a narrow cone around the direction of the primary electron beam and therefore the tail of this primary beam can easily disturb accurate measurements of the fast scattered electrons. The slow electrons, the majority of which have typically only few eV energy, can be partly masked by the background of migrating electrons from other gas and surface processes. Although a lot of differential electron impact ionization data have been published within the last decade (see Opal et al 1972, Rudd et al 1977, Shyn et al 1978, Oda 1975) there are still quite large discrepancies between the experimental results.

In this situation it is necessary to have measurements, which fulfill the following conditions:

i) For a given target atom the experimental cross section data should be of low error (typically 10% or lower) and as complete as possible, i.e. for a wide range of electron impact energies E_o all cross sections, total, single, double and triple differential, should be available and be used for consistency checks (Kim 1983)

ii) the range of momentum transfer q covered in the experiments must be representative for the majority of ionizing collisions, i.e. q_{min} < q < 1 or 2

a.u. and on the other hand, the experimentally detected lower limit of q should be very close to the optical limit in order to insure connection with reliable photoionization data (theoretical and experimental)

iii) the target must insure for all parameters E_o, E_A ... that only the simplest type of ionization process occurs, namely the direct (non-resonant), single ionization into the ground state of the ion. This condition holds only for atomic hydrogen and helium, all other targets have larger contributions from autoionization, simultaneous ionization and excitation and multiple ionization. In the case of helium these contributions are mostly up to approximately 2% for all E_o. Atomic hydrogen would have none of these disturbing processes and in addition has exactly known atomic eigenfunctions, but it is difficult to handle experimentally and therefore it cannot serve as a reference standard for normalization purposes.

In this paper, double and triple differential ionization cross sections are presented in the ranges

$$100 \text{ eV} < E_o < 600 \text{ eV}, \quad 0.3 \text{ a.u.} < q < 1 \text{ a.u.}$$

for the process

$$e^-(E_o) + He(1s^2) \rightarrow He^+(1s) + e^-(E_A) + e^-(E_B)$$

Connection is made to the optical limit $q \rightarrow 0$. The overall errors should be 15% or lower.

EXPERIMENTAL ARRANGEMENT

The apparatus used has been described earlier (Jung et al 1976). It is important to mention that both the gas beam and the electron beam are well defined (this has been measured independently, Müller-Fiedler et al 1984) and that the full interaction region is seen by both detector systems independent of their angular positions. This insures that no angular corrections have to be made in any angular dependence measurement.

Such cross sections with helium as a target gas have been measured for impact energies ranging from 30 eV to several keV and for many values of momentum transfer (Ehrhardt 1983 and references therein). Although this type of cross section may not be so important for applications as radiation physics, it is important for the test of theories, since it contains the most complete information on any individual collision process and the TDCS enables us to determine for which parameters the collision is close to the optical limit or to the binary limit. Typical TDCS's for the ejection of an s-electron are shown in figure 1 for E_o = 600 eV.

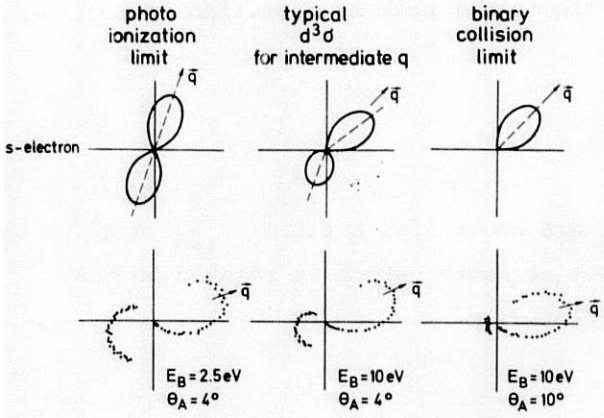

Fig. 1: Typical triple differential cross sections for the ejection of an atomic s-electron for E_o > 5 IP in polar diagrams. For lower E_o the recoil peak increases considerably. For clarity the upper row is shown schematically, the lower row represents experimental TDCS for E_o = 600 eV.

The left side diagram represents a situation close to photoionization, i.e. the ejected s-electron shows an angular dependence of a p-wave with its symmetry axis very close to the direction of momentum transfer $\vec{q}$. The right side represents a typical binary collision, in which the axis of the lobe is also in direction $\vec{q}$ and the width is due to the momentum distribution of the atomic electron before its ejection. Most collisions produce an angular distribution of the slow ejected electron similar to the figure in the middle. The binary peak and the recoil peak have no common axis and the intensities are quite different for both peaks.

The normalization of the TDCS can be made by extrapolation to the optical limit. For small q in first Born approximation it is

$$\frac{d^3\sigma}{d\Omega_A\, d\Omega_B\, dE_B} = \frac{4k_A\, k_B}{k_o\, q^4} \left| \varepsilon_o \vec{k}_B \left(\vec{q}\right) \right|^2 \qquad (1)$$

(Robb et al 1975) with the form factor

$$\varepsilon_{o\vec{k}_B}(\vec{q}) = \langle \psi_{\vec{k}_B} \mid \sum_j e^{i\vec{q}\vec{r}_j} \mid \phi_o \rangle = \sum_{n=1}^{\infty} A_n(\vec{k}_B, \theta)\, q^n \qquad (2)$$

The coefficients A_n are linear combinations of Legendre polynomials and θ is the angle between $\vec{q}$ and $\vec{k}_B$. If one considers only the intensity of $d^3\sigma$ in the direction of $\vec{q}$ of the binary peak, then $\theta = 0$ and equation (2) can be written as (Jung et al 1984)

$$d^3\sigma/\theta{=}0 \quad = \quad \frac{4k_A k_B}{k_o q^2} \quad (A_o + A_1 q + A_2 q^2 + \ldots)$$

Similarly one obtains for the intensity of the recoil peak in direction $-\vec{q}$, i.e. $\theta = \pi$

$$d^3\sigma/\theta{=}0 \quad = \quad \frac{4k_A k_B}{k_o q^2} \quad (A_o - A_1 q + A_2 q^2 - + \ldots)$$

The relative values of A_o, A_1, ..., A_5 are known from a fit of $\sum_{i=0}^{5} A_i q^i$ to the relative values of the generalized oscillator strength, which is related to the triple differential cross section by (Inokuti 1971)

$$\frac{df}{dE} = d^3\sigma \cdot q^2 \quad \frac{k_o}{4k_A} \quad \frac{(E_B + IP)}{R}$$

The extrapolation to $q \to 0$ and comparison with the dipole oscillator strength in absolute units taken from photoionization yields the coefficient A_o in absolute units and therefore also the other A_i and finally the TDCS. Figure 2 shows two examples of fitting the experimental data and extrapolating to $q \to 0$.

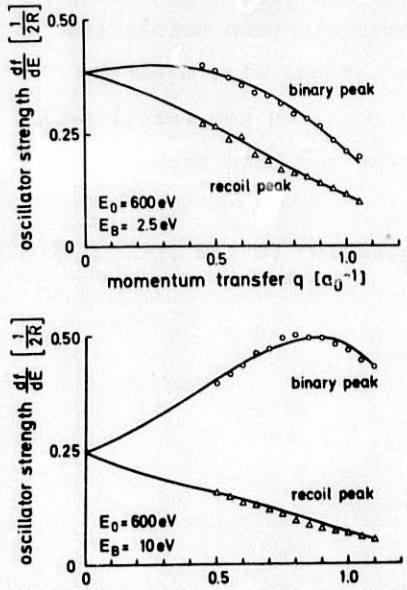

Fig. 2: Examples for the fit of the experimental data with a series $\sum_{i=0}^{5} A_i q^i$ (full curve) versus momentum transfer q and extrapolation to $q \to 0$. The extrapolation is needed for the connection of the TDCS to the known photoionization cross section in absolute units (for details see text).

The upper points represent the intensities of the binary peaks with varying momentum

transfer q, the lower points represent the recoil peak. Plotted are the measured count rates multiplied with the (from experiment) known kinematic factor $q^2 \frac{k_o}{2k_A}$ (E_B+IP). The full curves represent the fit with $\sum_{i=0}^{5} A_i q^i$. The extrapolation to q = 0 must give the same value for the upper and lower curve, since the binary peak and the recoil peak have the same intensity in forward and backward direction of a p-wave.

Figure 3 shows the TDCS in absolute units plotted versus momentum transfer for the binary peak (upper curve) and the recoil peak (lower curve) in the theoretically very difficult region 0.5 < q < 1.1 a.u. For the time being we have not yet made comparison with existing theories as such from Madison et al (1977), Bransden et al (1978), Byron et al (1980) and others. Clearly this has to be done next.

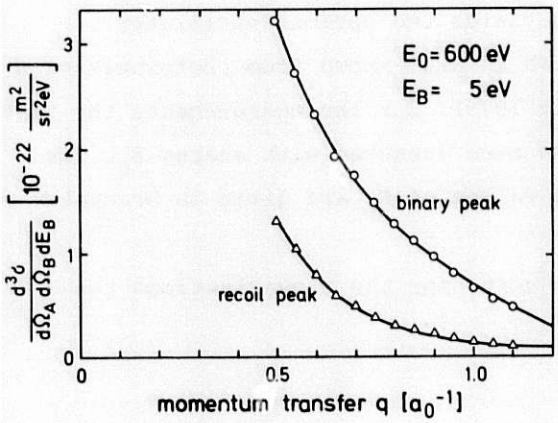

Fig. 3: The triple differential cross sections in absolute units for E_o = 600 eV and E_B = 5 eV. The full curve is only a connection of the experimental points. The intensities represent the count rates in direction of the momentum transfer $\vec{q}$ for the binary peak and the recoil peak.

DOUBLE DIFFERENTIAL CROSS SECTIONS (DDCS)

The DDCS's have been measured in the same apparatus without using the coincidence unit. The fast electrons are measured in collector A, the slow electrons in collector B. For each set of parameter E_o, E_A, θ_A resp. E_o, E_B, θ_B at least 10 000 counts have been collected and therefore the statistical errors are very low. Only angular dependences are measured, avoiding transmission errors in the electron optical systems due to energy changes.

Inokuti (1971) has shown that also the DDCS for the fast electrons is connected to the generalized oscillator strength df/dE

$$\frac{df}{dE} = \frac{1}{4}\sqrt{\frac{E_o}{E_A}}\,\frac{E}{R}\,q^2\,\frac{d^2\sigma}{d\Omega_A\,dE} \qquad (3)$$

where $E = E_o - E_A$ is the energy transfer to the helium atom and R the Rydberg

constant. If the right hand side of equation (3) is plotted in relative units versus ln q^2, then the extrapolation $q \to 0$ is a horizontal line which is equal to the dipole oscillator strength on the ordinate. This number is known within 2% in absolute units from photoionization experiments or calculations. Once this number is inserted on the y-axis all DDCS's of this plot are given in absolute units. The largest error of this procedure is the extrapolation to small q-values which is estimated to be 10% or lower. Figure 4 shows four examples of these plots.

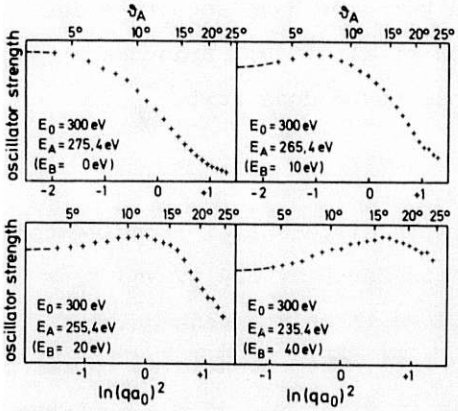

Fig. 4: Four examples of Fano plots for the extrapolation $q \to 0$ of the relative double differential cross section multiplied with a kinematic factor (see equation 3 of text). This extrapolation yields the optical oscillator strength, which is well-known from photoionization (see Berkowitz 1979). For the measurements the fast electrons have been detected with energy E_A. The corresponding values of E_B are given in brackets.

In order to obtain the DDCS's in absolute units for the slow electrons the following relation is used

$$\int \frac{d^2\sigma}{d\Omega_A\, dE_A}\, d\Omega_A = \frac{d\sigma}{dE_A} = \frac{d\sigma}{dE_B} = \int \frac{d^2\sigma}{d\Omega_B\, dE_B}\, d\Omega_B \qquad (4)$$

This relation is correct within 2% only for helium since in this case the contributions from double ionization and simultaneous excitation and single ionization are below 2% for all E_o.

Equation (4) implies that the DDCS for the fast electrons have to be extrapolated to $\theta_A = 0°$ and $\theta_A = 180°$. In the angular range from 4° to 0° one can safely use a curve shape (see equation 3)

$$d^2\sigma = \frac{C}{q^2}$$

since the cross sections are already described quite well by the 1. Born approximation. The constants C are derived from the measurements in the angular range $4° < \theta_A < 10°$.

For the extrapolation of $d^2\sigma/d\Omega_A\, dE_A$ to high angles θ_a the relation

$$d^2\sigma = a\, e^{-b\theta_A}$$

is used, since the DDCS must decrease very rapidly and contributions from angles θ_A, which have not been measured are below the percent limit. The errors due to the two extrapolations should be below 10%. The integration yields $d\sigma/dE_A$ in absolute units.

According to Kim (1983) the measured DDCS's for the slow secondary electrons can be fitted to a series of Legendre polynomials

$$\frac{d^2\sigma}{d\Omega_B\, dE_B} = \sum_{n=0}^{6} a_n P_n (\cos\theta_B) \qquad \text{for } E_B = \text{const}$$

The coefficients a_n are determined by

$$a_n = \frac{2n+1}{2} \int_{-1}^{+1} \frac{d^2\sigma}{d\Omega\, dE}(\theta)\; P_n(\cos\theta)\, d(\cos\theta)$$

To do the integration the measured DDCS must be extrapolated into the unobserved angular ranges

$$0 < \theta_B < 18° \qquad \text{and} \qquad 150° < \theta_B < 180°$$

Figure 5 shows four typical examples. These extrapolations can be done without introducing considerable errors since the parts of the integral tend to zero close to $\theta_A \to 0$ and $\theta_A \to 180°$.

The integration of $d^2\sigma$ for the slow electrons

$$\frac{d\sigma}{dE_B} = 2\pi \int \frac{d^2\sigma}{d\Omega_B\, dE_B}\, d(\cos\theta_B) = 4\pi\, a_o = \frac{d\sigma}{dE_A}$$

yields the coefficient a_o in absolute units since $\frac{d\sigma}{dE_A}$ is known absolutely. Since the ratios a_n/a_o are known from the relative measurements

$$\frac{d^2\sigma}{d\Omega_B\, dE_B} = a_o \sum_{n=0}^{6} \frac{a_n}{a_o} P_n(\cos\theta)$$

the DDCS is now on absolute scale.

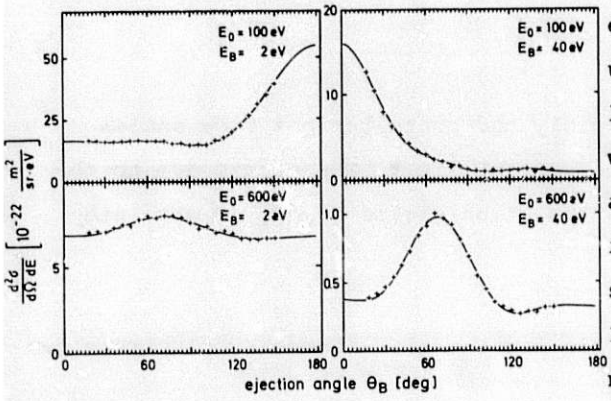

Fig. 5: Four typical examples for the extrapolation of the measured DDCS into the unobserved angular ranges below 18° and above 150°. The different curves exhibit structures, which are typical of DDCS's for different E_o and E_B: **a)** low E_o, low E_B: a large recoil peak in the TDCS produces strong backward scattering in the DDCS, **b)** E_B close to $(E_o - IP)/2$ (upper half, right side) resembles a mostly binary collision with strong forward peaking, **c)** large E_o and small E_B is for most collisions equivalent with small momentum transfer and therfore close to the optical limit. Binary peak and recoil peak have similar intensity. Integration over Ω_A yields a uniform distribution over θ_B in the DDCS, **d)** large E_o and large E_B is mostly a binary collision, the binary peak being close to ca. 60°.

A critical consideration of all errors in the whole procedure shows that the largest error derives from the low angle extrapolation $d^2\sigma_{fast} = C/q^2$, which is about 10% or lower. We estimate the overall error of our DDCS's for fast and slow electrons to be below 15%.

COMPARISON WITH OTHER DATA

In the literature exist electron impact ionization data on helium from measurements by Opal et al (1972), Oda (1975), Rudd et al (1977), Shyn et al (1979) and a few other authors. In addition, Kim has generated from these experimental cross sections so-called recommended DDCS by making consistency checks, renormalisations, comparison to generalized oscillator strength, etc. Figure 6 shows our data together with other experimental DDCS and the recommended DDCS of Kim.

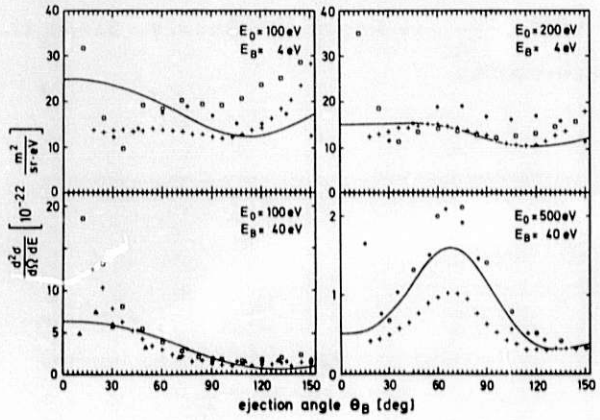

Fig. 6: Our DDSC's (+) in comparison to other measurements (squares: Shyn et al 1978, triangles: Rudd et al 1977, open cirlces: Opal et al 1972, full circles: Oda 1975) and to the recommended cross sections of Kim (1983, full line). For details see text.

Due to experimental errors Shyn's data are too high in forward direction and the DDCS of Opal et al are too low in forward and backward direction. Although Rudd uses a very different normalization procedure (absolute determination of the geometry of the interaction region, gas pressure etc.) his data agree quite well with our data within the error bars of both experiments. Kim's DDCS are generally good for high impact energies and low to intermediate energies of the ejected (slow) electrons. He underestimates the recoil peak (visible in the TDCS) for low E_o and low E_B and the binary peak for high E_o and high E_B.

A full set of our data will be published elsewhere (Müller-Fiedler et al 1984).

REFERENCES

Berkowitz J 1979 Photoabsorption, Photoionisation and Photoelectron Spectroscopy (Academic Press, New York)

Bransden BH, Smith JJ and Winters KH 1978 J. Phys. B: Atom. Molec. Phys. 11 3095-114

Byron FW, Jr., Joachain CJ and Piraux B 1980 J. Phys. B: Atom. Molec. Phys. 13 L673-6

Ehrhardt H 1983 Comments At. Mol. Phys. 13 115-25

Inokuti M 1971 Rev. Mod. Phys. 43 297-347

Jung K, Schubert E, Ehrhardt H and Paul DAL 1976 J. Phys. B: Atom. Molec. Phys. 9 75-87

Jung K, Müller-Fiedler R, Schlemmer P and Ehrhardt H 1984 to be published

Kim Y-K 1983 Phys. Rev. A28 656-66

Madison DH, Calhoun RV and Shelton WN 1977 Phys. Rev. A 16 552-62

Müller-Fiedler R, Jung K, Ehrhardt H and Kim Y-K 1984 to be published

Oda N 1975 Radiat. Res. 64 80-95

Opal CB, Beaty EC and Peterson WK 1972 At. Data 4 209-467

Robb WD, Rountree SP and Burnett T 1975 Phys. Rev. A 11 1193-99

Shyn TW and Sharp WE 1979 Phys. Rev. A 19 557-67

Rudd ME and DuBois RD 1977 Phys. Rev. A 16 26-32

MEASUREMENTS OF SECONDARY ELECTRON CROSS SECTIONS BY THE PULSED ELECTRON BEAM TIME-OF-FLIGHT METHOD. I. MOLECULAR NITROGEN

R. R. Goruganthu, W. G. Wilson, and R. A. Bonham

Department of Chemistry
Indiana University
Bloomington, Indiana 47405

ABSTRACT

The secondary electron cross sections for gaseous molecular nitrogen are reported at ejection angles of 30, 45, 60, 75, 90, 105, 120, 135 and 150°, for the energy range 1.5 eV to 20 eV and incident electron energy of 1 keV. The pulsed electron beam time-of-flight method was employed. The results were placed on an absolute scale by normalization to the elastic scattering. They were compared, where possible, with those reported by Opal, Beaty, and Peterson (OBP). The agreement is somewhat better when the OBP data are divided by $0.53 + 0.47 \sin\theta$ as suggested by Rudd and DuBois. Fits of our data by Legendre-polynomial expansions are used to estimate the low-energy portion of the cross-section, $d\sigma/dE$. This work suggests that existing experimental cross sections for secondary electron ejection as a function of angle and ejected energy may be no better known than ±40%, especially in the low energy region.

A new pulsed electron beam time-of-flight apparatus designed for measuring secondary electron cross sections has recently been placed into operation. We wish to report here our first results obtained for molecular nitrogen at an incident electron energy of 1 keV for a range of ejection angles and energies.

The apparatus consists of a pulsed electron beam source[1] with time-of-flight detection[1] of scattered or ejected electrons. In Fig. 1, a schematic view of the instrument is shown. Provision is made for double pulsing the incident beam although this was not used in the present experiment. That is, provided the electron beam energy is less than about 20 eV, a pulse formed at the first skimmer may be swept across a second skimmer to produce a more monoenergetic source. The pulse is incident upon a gas-jet target, and scattered or ejected electrons are detected by two microchannel plate (MCP) detectors, one 43.8 cm and the other 52.2 cm from the scattering center. One of the detectors can be used to scan the angular range from 20° to 160°, while the other can be used to measure the scattering at 2° on either side of the forward direction. The acceptance angles of these detectors are 1.5° and 0.1°, respectively. For the present study, angles of 30, 45, 60, 75, 90, 105, 120, 135, and 150° were employed. In this study a timing resolution of about 1.5 nanoseconds was used. This translates into an energy resolution of 125 eV at 1000-eV kinetic energy and 0.125 eV at 10 eV. Data were collected in a pulse-height analyzer using a sample grid of 1.6 nsec/channel. In order to place the data from different angles on the same relative scale, data were collected at 90° then at the angle under consideration and then back to 90°. The count totals, integrated over

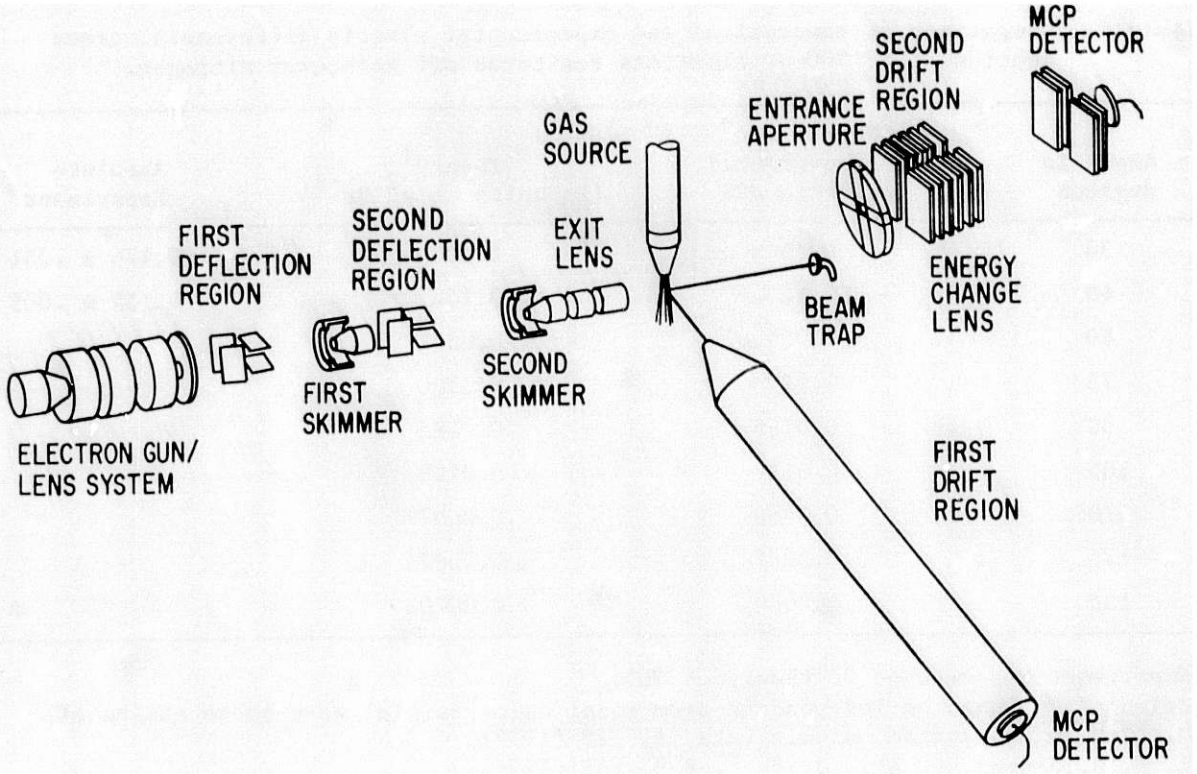

Fig. 1. Schematic view of the pulsed electron beam time-of-flight apparatus.

all energies, for each of the angles were then used to establish a normalization scheme for the data. As a final check, the elastic-scattering itensity was matched to theory and absolute experimental measurement.[2] The theory was based on the independent-atom model[3] using the atomic partial-wave scattering amplitudes due to Fink and Ingram.[4] The results, given in Table 1, agree with the shape given by theory to better than 15%. The theory agrees with the results of Jansen et al., from 23° to 54°, the range of the experimental data, to within the experimental uncertainties (~6%). Hence, the simple theory seems to be adequate for 1000-eV incident electrons and was used to normalize our data to an absolute scale at 90°. This was done because our 125-eV resolution in the elastic line cannot rule out small contributions from inelastic scattering at small scattering angles thus making it desirable to match at larger scattering angles. We believe that the excellent agreement between theory and our experiment, shown in Table 1, confirms the accuracy of our procedure for placing the secondary electron spectra on the same relative scale. This procedure should also place the secondary electron data on the same absolute scale except for two things. The first is that the relative detector efficiency is not the same for 1-eV and 1000-eV electrons. In Fig. 2 we show the detector efficiency as a function of the incident electron kinetic energy. The detector, however, is operated with a high-transmission wire mesh just in front of it in order to accelerate all electrons with a bias voltage of 200 eV. This guarantees that the lowest-energy electrons are detected with maximum efficiency but high-energy electrons will be detected with slightly lower efficiency. Unfortunately, the wire mesh (copper ~91% transmittancy) contributes secondary electrons, which modify the detector efficiency as shown in Fig. 3. We have chosen to use an efficiency correction of unity and to attach an uncertainty to our absolute scale of ±20%. The reason for doing this is that the scale for 1-eV electrons relative to 1-keV electrons should be 10% lower than the elastic scale but 10% higher with the grid correction. Because it is difficult to pin down the exact role of the grid-scattered secondaries we take an efficiency of 1 with a correspond-

Table 1. Comparison of theoretical and experimental elastic differential cross sections for 1000-eV electrons scattered off molecular nitrogen.

Angle in degrees	Normalized* experimental elastic DCS	Theory† (in units of a_0^2 Sr^{-1})	Absolute Experiment‡
30	0.56	0.504	0.474 ± .031
45	0.16	0.144	0.135 ± .009
60	0.054	0.0541	
75	0.029	0.0300	
90	0.0185	0.0185	
105	0.011	0.0129	
120	0.0086	0.00977	
135	0.0086	0.00824	
150	0.0080	0.00709	

*Experiment was matched to theory at 90°.
†Calculation based on independent atom model using partial wave phase shifts of M. Fink and J. Ingram, Atomic Data, 4, 129 (1972).
‡R. H. J. Jansen, et al., J. Phys. B 9, 185 (1976).

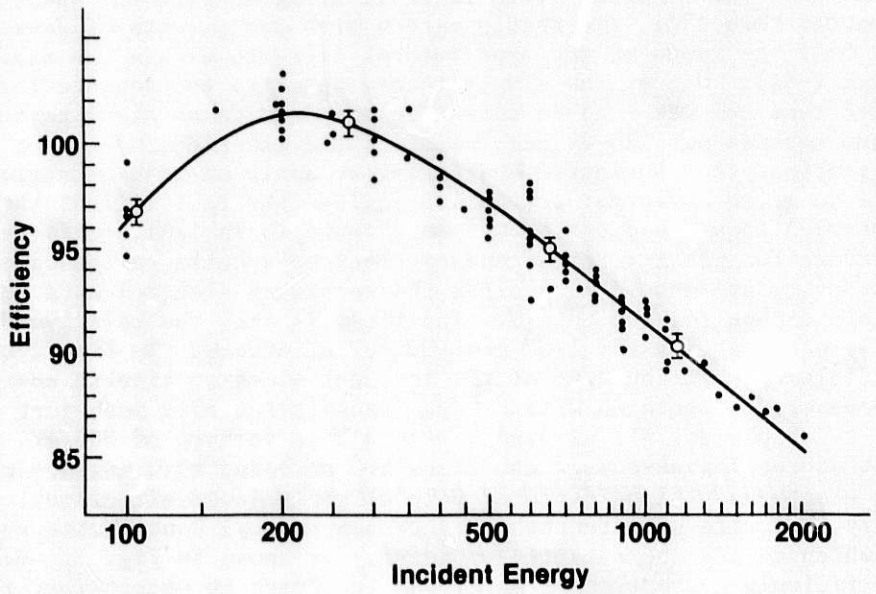

Fig. 2. Relative detector efficiency as a function of incident energy with no correction for grid-produced secondaries.

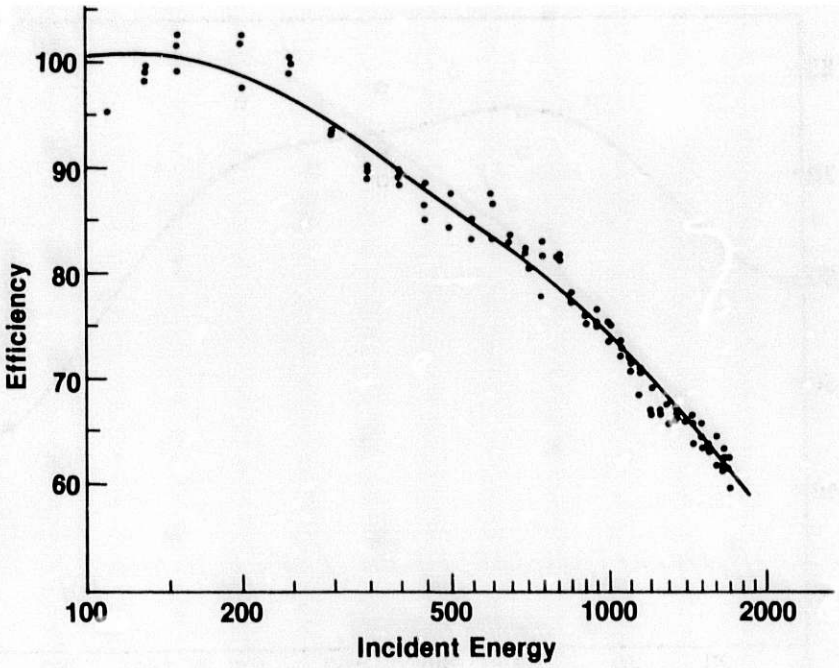

Fig. 3. Relative detector efficiency as a function of incident electron energy including grid-produced secondaries.

ing increase in the uncertainties. In future work, we plan to coat the grid with a conducting carbon film, which should reduce the grid scattering by at least a factor of 5. The second problem is the attenuation of secondary electrons by the background gas. The chamber pressure during data collection was about 4×10^{-5} Torr. This leads to an angle-independent absorption correction less than 10% for all energies except for the region around the 2.5-eV nitrogen resonance, where the correction may be as large as 20%. A third possible source of systematic uncertainty would be the loss of transmission for low-energy electrons due to stray fields. Magnetic shielding reduced the residual magnetic field to below 1 m Gauss. With regard to this source of error, whether it is electric or magnetic, our values must lie below the true result. Because the absorption effect also produces a lower bound, it seems unlikely that our uncorrected results could lie above the true cross section at low ejected energies. The present results are corrected only for the absorption effects and a small constant background.

The results are shown in Figs. 4-12 where our angle data for the energies 1.5, 2.0, 3.0, 4.0, 6.0, 8.0, 10.1, 14.7, and 18.6 are displayed. The first four figures display results which have not been previously reported. For 6.0 eV and above the Opal, Beaty, and Peterson[5] (OBP) results are displayed. The OBP results have been presented in two ways: the first as originally given by the authors and represented on the figures by triangles, and the second by the original data values divided by $0.53 + 0.47 \sin\theta$, as suggested by Rudd and DuBois,[6] and represented by squares. In general, our results agree well with the OBP results in the vicinity of 90°. Cumulative error in these angle dependent double differential cross-sections for ejected energies between 1 and 20 eV is estimated to be ~20%.

In all our figures, the solid line represents a fit of our data for the double differential cross section (DDCS) by an expansion in terms of Legendre polynomials of the form

$$\frac{d^2\sigma}{d\Omega dE} = \sum_{n=0}^{4} a_n(E) P_n(\cos\theta). \qquad (1)$$

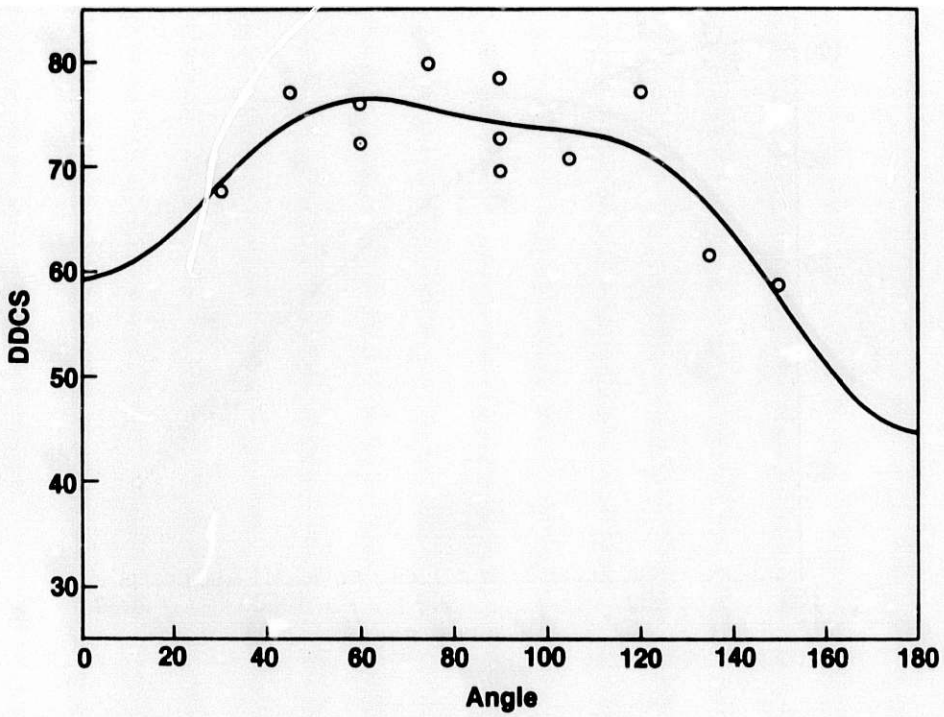

Fig. 4. Absolute double differential cross section (DDCS) for secondary emission from N_2 in units of 10^{-20} cm^2/eV-Sr for an incident energy of 1000 eV and ejected energy of 1.5 eV as a function of ejection angle in degrees. The solid line is the fit of the data points, indicated by circles by Eq. (1).

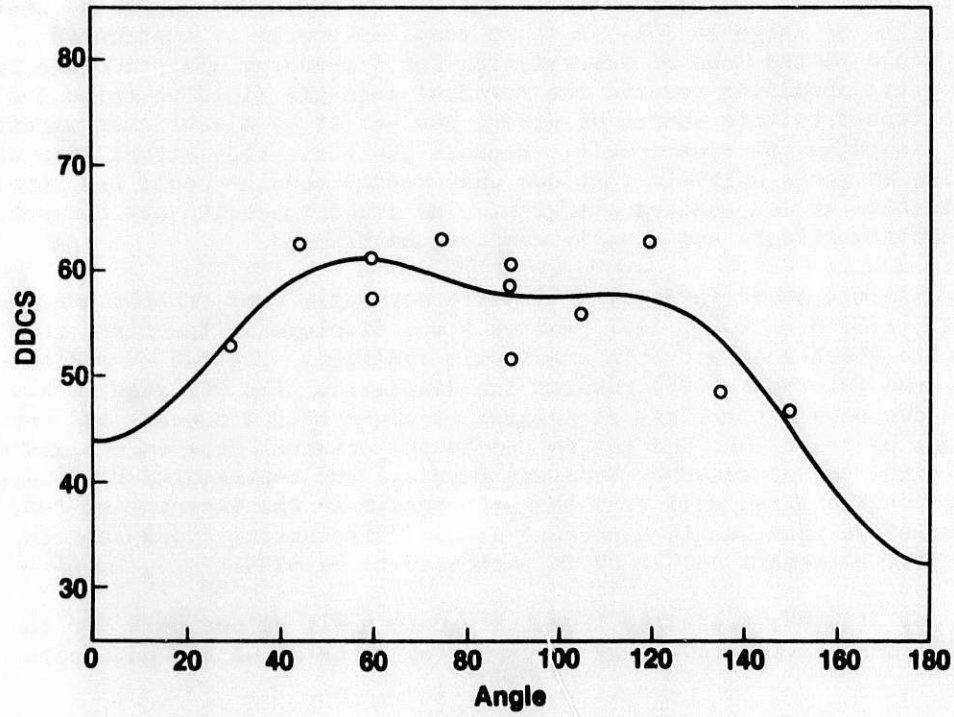

Fig. 5. Absolute DDCS for N_2 for 2.0-eV electrons. See Fig. 4 caption for further details.

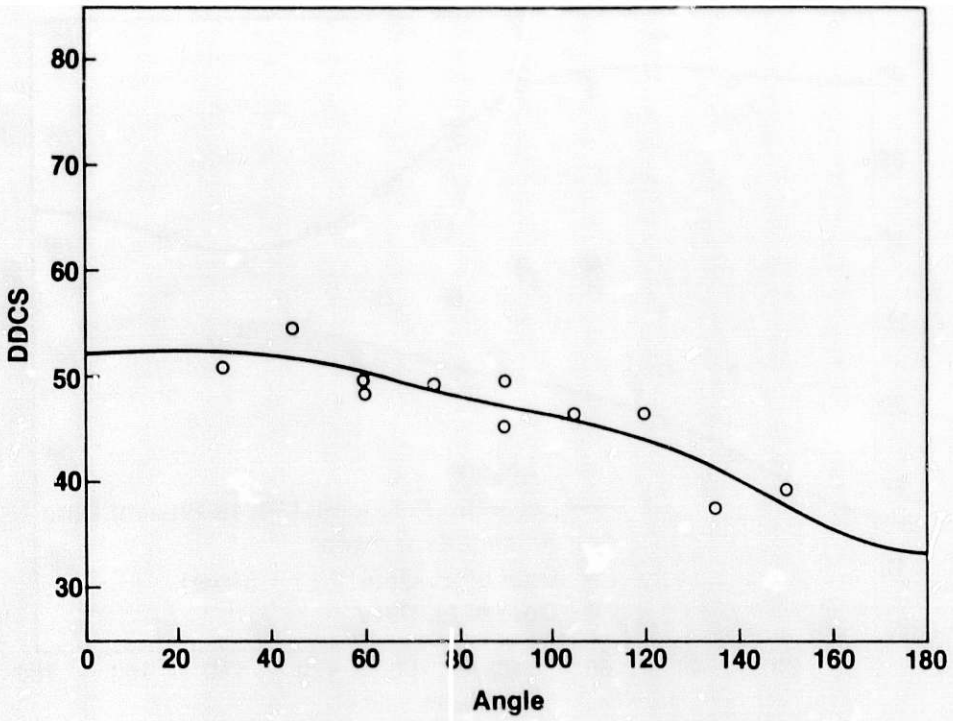

Fig. 6. Absolute DDCS for N_2 for 3.0-eV electrons. See Fig. 4 caption for further details.

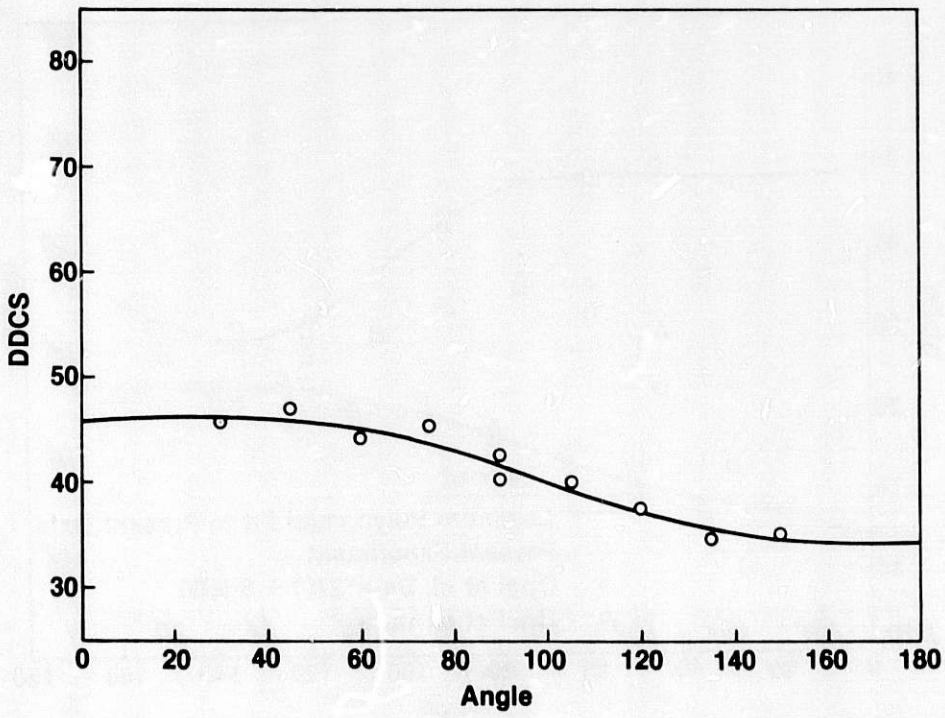

Fig. 7. Absolute DDCS for N_2 for 4.0-eV electrons. See Fig. 4 caption for further details.

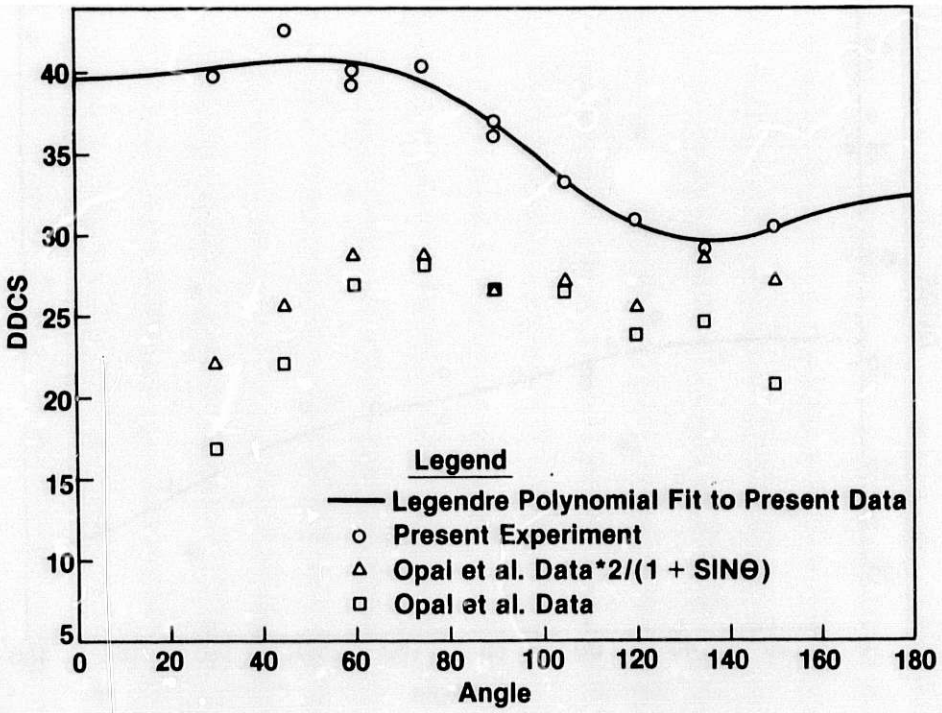

Fig. 8. Absolute DDCS for N_2 for 6-eV ejected energy. The triangles denote the original data of Ref. 5 and the squares denote the Ref. 5 data divided by 0.57 + 0.43 sinθ. See Fig. 4 caption for further details.

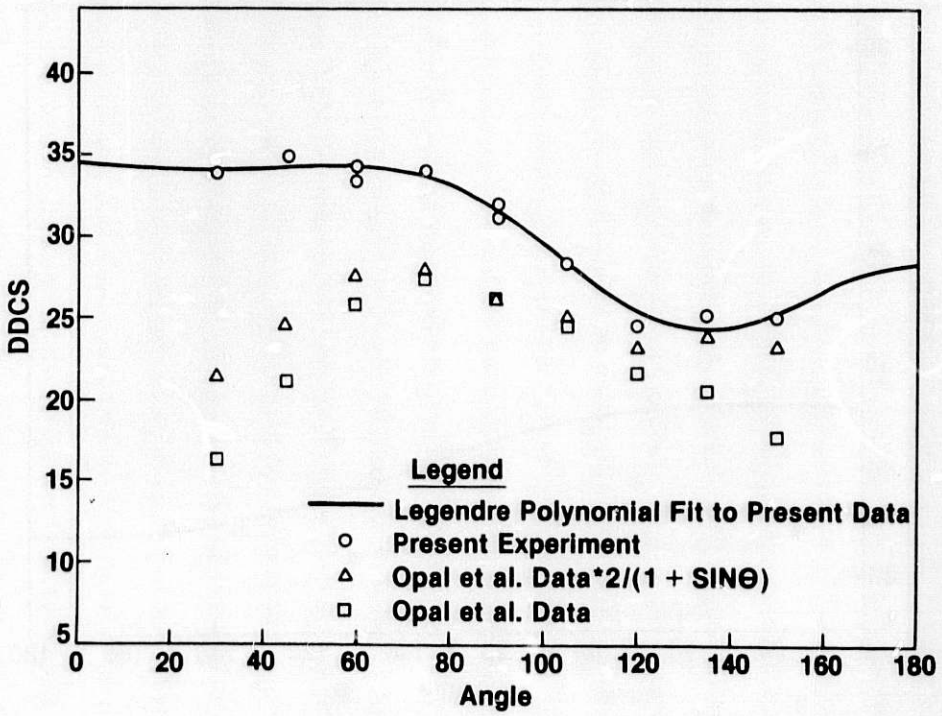

Fig. 9. Absolute DDCS for N_2 for 8.0-eV ejected energy. See Fig. 8 caption for details.

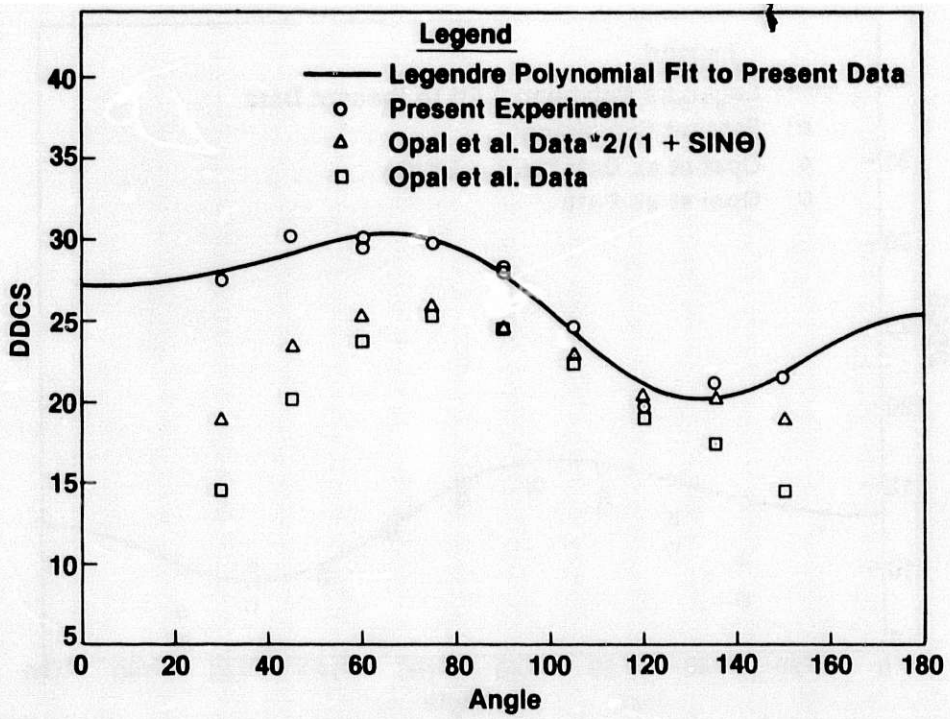

Fig. 10. Absolute DDCS for N_2 for 10.1-eV ejected energy. See Fig. 8 caption for details.

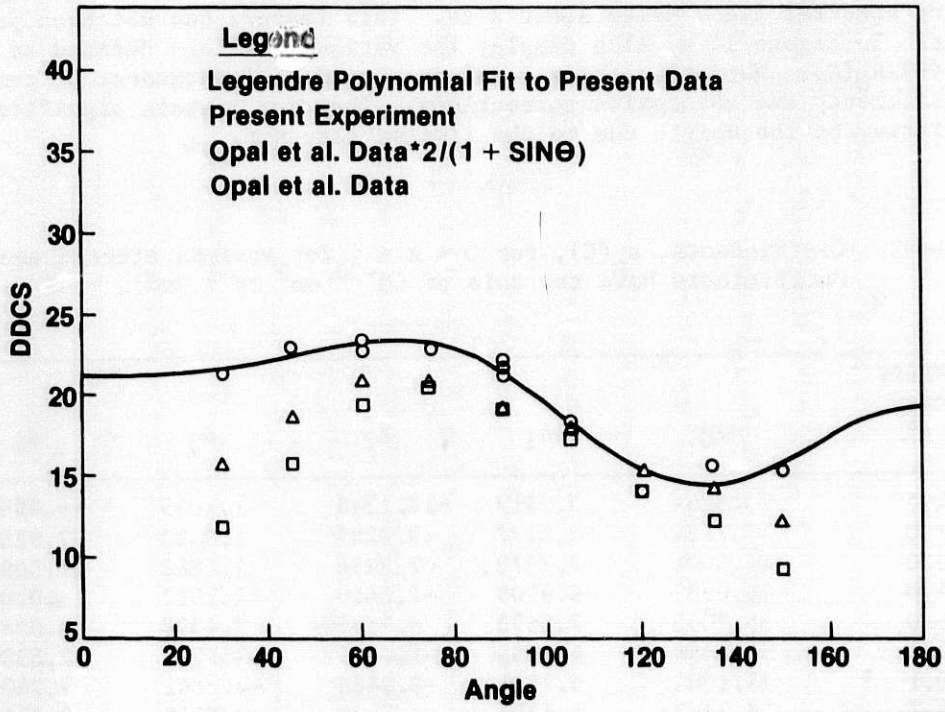

Fig. 11. Absolute DDCS for N_2 for 14.7-eV ejected energy. See Fig. 8 caption for details.

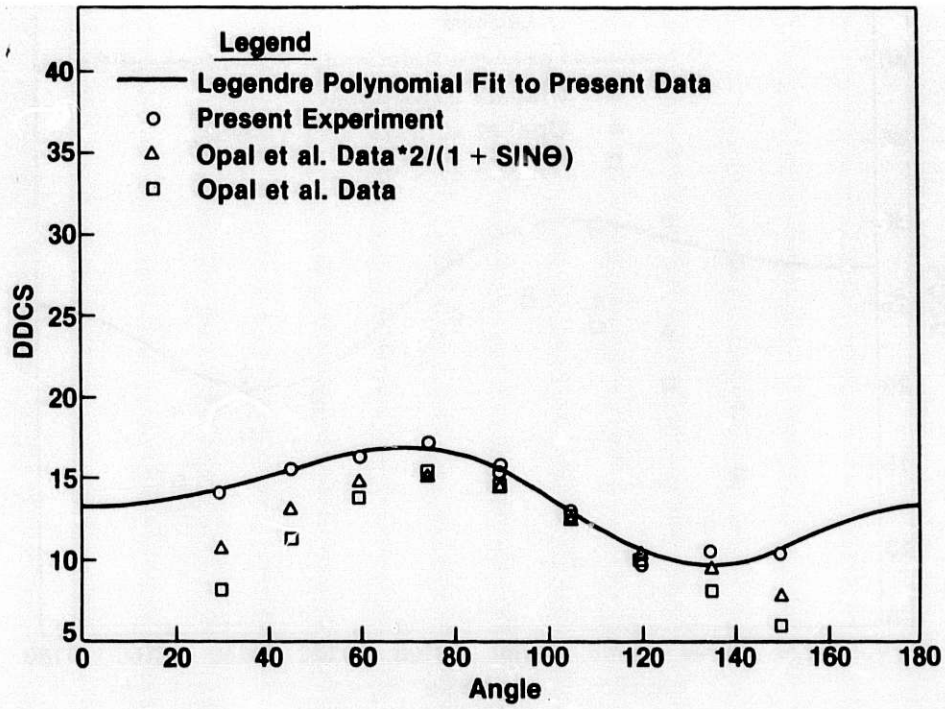

Fig. 12. Absolute DDCS for N_2 for 18.6-eV ejected energy. See Fig. 8 caption for details.

The energy-dependent coefficients are given in Table 2. The cross section $d\sigma/dE$ is then given by $4\pi\ a_0(E)$, which is shown in Fig. 13. Note the strong increase in $d\sigma/dE$ as the energy decreases. This is probably due to the onset of strong autoionizing spectral lines below about 2 eV. This feature has not been previously pointed out. In Figure 14 we also display the various β values defined as $\beta_n(E) = a_n(E)/a_0(E)$. Note that these β values should be independent of the relative detector efficiency and absorption corrections. They may contain significant errors from the fitting to the points due to the limited data set.

Table 2. Coefficients, $a_n(E)$, for $0 \leq n \leq 4$ for various ejected energies. Coefficients have the unis of 10^{-20} cm^2 eV^{-1} Sr^{-1}.

Ejected energy in eV	a_0	a_1	a_2	a_3	a_4
1.5	70.5264	5.9917	-12.1314	1.2659	-6.4293
2.0	55.7124	4.6777	-9.8285	1.0593	-7.9267
3.0	46.6001	7.7573	-2.3294	1.6863	-1.5093
4.0	41.0933	6.9909	-1.0420	-1.1912	.0788
6.0	35.9065	7.0693	-.9695	-3.4398	1.0948
8.0	30.3858	6.1851	-1.0323	-3.1297	2.0385
10.1	26.1004	5.2406	-2.0486	-4.3841	2.2405
14.7	19.7960	4.6254	-1.7888	-3.7349	2.2367
18.6	13.7242	3.3229	-2.1921	-3.3186	1.6950

In addition to the work reported above we have investigated the use of the symmetry properties of Eq. (1) as a means for determining errors in the choice of the zero angle. We calculated the DDCS for electron-impact ionization of helium in the Born approximation for an impact energy of 2000 eV, for an ejection energy of 2 eV. These compared very well with those of Kingston and Bell,[7] and were employed with various levels of random errors added to investigate the effect of the uncertainty in the zero angle. Fits against the even function (+) and odd function (-) of the form

$$\frac{d^2\sigma}{d\Omega dE}(\theta + \Delta) \pm \frac{d^2\sigma}{d\Omega dE}(\pi - \theta + \Delta), \qquad (2)$$

where Δ is an assumed error in choice of zero angle, indicated that for typical levels of uncertainty (1 - 10%) the value of Δ necessary to reliably indicate that an error in the zero angle had been made were in excess of 1°. Because our maximum uncertainty in determining the zero angle is ±0.2°, such a test will not prove useful. Our exercise has shown, however, that low-energy secondary cross sections (<2 eV) are not particularly sensitive to zero-angle shifts in our apparatus.

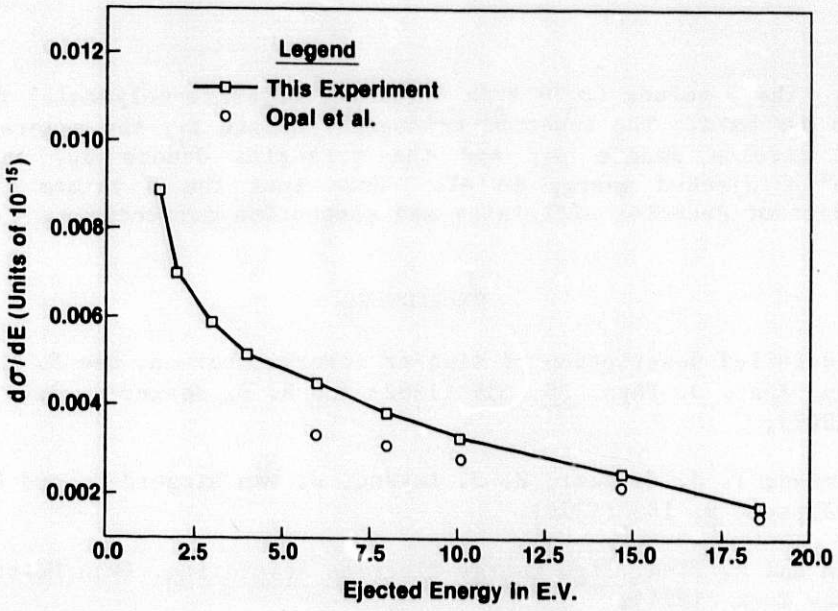

Fig. 13. The absolute singly differential cross section, $d\sigma/dE$, in units of 10^{-15} cm^2/eV. The circles indicate the result of Ref. 5 and the squares our results. Note the peaking at low energy probably due to the strong autoionizing lines in the low energy N_2 spectrum.

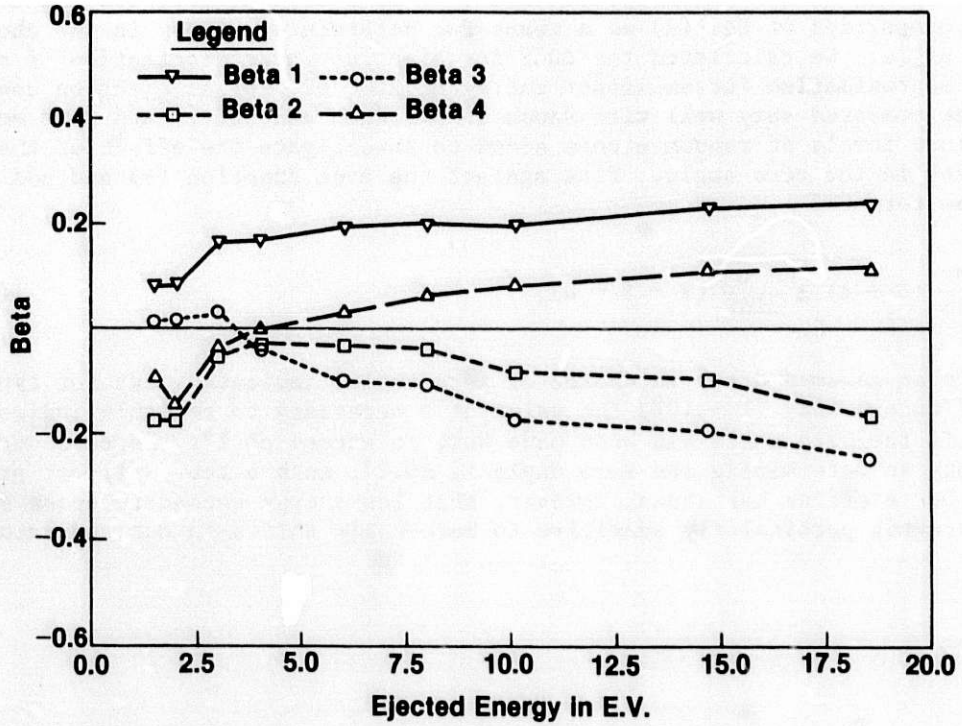

Fig. 14. The β values ($\beta_n = a_n/a_o$) for the Legendre-polynomial fits [Eq. (1)] to our data. The inverted triangles denote β_1, the squares denote β_2, the circles denote β_3, and the triangles denote β_4, each as a function of ejected energy in eV. Note that the β values should be independent of detector efficiency and absorption corrections.

REFERENCES

1. For a more detailed description of similar instrumentation, see R. K. Jones and R. A. Bonham, Aust. J. Phys. 35, 559 (1982) and R. E. Kennerly, Rev. Sci. Instr. 48, 1682 (1977).

2. R. H. J. Jansen, F. J. de Heer, H. J. Luyken, B. van Wingerden, and H. J. Blaauw, J. Phys. B 9, 185 (1976).

3. R. A. Bonham and M. Fink, High Energy Electron Scattering, (Van Nostrand-Reinhold, New York, 1974).

4. M. Fink and J. Ingram, Atomic Data 4, 129 (1972).

5. C. B. Opal, E. C. Beaty, and W. K. Peterson, Atomic Data, 4, 209 (1972).

6. M. E. Rudd and R. D. DuBois, Phys. Rev. A 16, 26 (1977).

7. K. L. Bell and A. E. Kingston, J. Phys. B 8, 2666 (1975).

CROSS SECTIONS FOR ELECTRON IMPACT EXCITATION OF MOLECULES

S. Trajmar

California Institute of Technology
Jet Propulsion Laboratory
Pasadena, CA 91109

ABSTRACT

The discussion in this chapter is restricted to elastic scattering, rotational, vibrational, and electronic excitation and total scattering cross sections in electron molecule collisions. Experimental data on differential, integral and momentum transfer cross sections are surveyed and short remarks are made on experimental techniques and theoretical approaches used for generating cross section data.

INTRODUCTION

Research activities related to electron-molecule collision studies have greatly increased during the past two decades. However, most of these activities produced only qualitative information and our knowledge of cross section data for various collision processes is still very meager. The practical difficulties in measuring cross sections are associated with the establishment of the absolute scale (conversion of the measured scattering intensities to absolute cross sections) and with the time and work requirements for collecting and analyzing large amount of data with high accuracy. Fortunately, considerable progress was made in recent years in experimental techniques and one could expect that accurate (~10-15%) cross sections will be measured for a large variety of processes for a number of molecules in the coming years. On the theoretical side, it has been demonstrated that first order perturbation type scattering calculations are not reliable. Recent efforts at the distorted wave level show good qualitative agreement with experimental differential cross sections but further improvements are required for quantitative agreement.

DEFINITION OF CROSS SECTIONS

The differential cross section (DCS) for scattering process n at electron impact energy (E_o) is written as

$$[DCS_n(\theta)]_{E_o} = \left[\overline{\frac{d\sigma_n(\Omega)}{d\Omega}}\right]_{E_o} \qquad (1)$$

Here Ω stands for the scattering spherical polar (θ) and azimuthal (ϕ) angles. The left hand side of Eqn. (1) represents the experimentally measured DCS. We want to indicate here that this experimental DCS is the actual differential cross section averaged over the instrumental energy and angular resolution and includes all experimentally indistinguishable processes (hyperfine and magnetic sublevels, various target and spin orientations, unresolved rotational structure etc.). In almost all cases the ϕ dependence of the DCS can be disregarded. It is very important in using

and comparing cross section data that the averaging processes involved in obtaining the DCS be clearly specified.

Integration of the DCS over all solid angles yield the corresponding integral, $\sigma_n(E_o)$ and momentum transfer, $\sigma_n^M(E)$ cross sections:

$$\sigma_n(E_o) = 2\pi \int_o^\pi [DCS_n(\theta)]_{E_o} \sin\theta \, d\theta \tag{2}$$

$$\sigma_n^M(E_o) = 2\pi \int_o^\pi [DCS_n(\theta)]_{E_o} \left[1 - \frac{k_f}{k_i} \cos\theta\right] \sin\theta \, d\theta \tag{3}$$

The final cross section that is of interest to us here is the total electron scattering cross section:

$$\sigma_{TOT}(E_o) = \sum_n \sigma_n(E_o) \tag{4}$$

CROSS SECTION MEASUREMENT TECHNIQUES AND DATA

1. Total Electron Scattering Cross Sections

There are three widely utilized methods for determining $\sigma_{TOT}(E_o)$:

a. Electron transmission measurements
b. Electron transmission measurements with time-of-flight analysis
c. Recoil measurements

In addition, some total cross sections have been generated by indirect methods (ion cyclotron resonance, line shape vs. pressure).

The transmission and transmission with time-of-flight methods have been extensively used in recent years for determining highly accurate (~1-3%) total scattering cross sections ranging from impact energies of 20 meV to 2,000 eV for a number of molecular species. Table I summarizes the total cross section data available since 1970. For a more detailed discussion see Refs. 1 and 2 and for numerical data see Ref. 3. Recoil measurements were made on alkali halide molecules. The difficulty with this method lies in the detection of neutral molecular species.

2. Integral Cross Sections

Integral cross sections could be obtained by measuring the electron scattering signal associated with a given process over all angles. Although some efforts in this direction were made, practically all integral electron scattering cross sections, in the area with which we are concerned here, have been obtained from DCS measurements. The available integral cross section data will be reviewed below under differential cross sections.

One can also deduce electron impact excitation integral cross sections from measuring the optical radiation induced by the electron impact excitation. This topic will be covered elsewhere in this report by McConkey.

For more detailed discussions and data on integral cross sections see Refs. 1-4.

Table I. Summary of Recent (since 1970) Total Cross Section Data

Molecule	Energy Range (eV)	Molecule	Energy Range (eV)
H_2	0.02-2,000	H_2O	0-10
N_2	0.25-1,600	CO_2	0.07-700
CO	0.3-8	N_2O	0.5-10
O_2	100-1,600	SO_2	0-10
NO	100-1,600	H_2S	0-10
Li_2	0.5-10	OCS	1-8
Na_2	0.5-50	CH_4	0.5-100
K_2	0.5-50	SF_6	0.036-100
KI	0.81-15.7	C_2H_2	0.3-5
CsF	0.69-6.81	CCl_4, CCl_3F_1	
CsCl	0.47-15.7	CCl_2F_2, $CClF_3$, CF_4	0.5-100

3. Differential Cross Sections

Differential (in angle) scattering cross sections (DCS's) represent information one level more detailed than integral cross sections. This type of data is needed for modeling of electron energy degradation processes for cases in which the angular dependence of the scattering process is explicitly considered, for stringent testing of theoretical models, and for obtaining momentum transfer cross sections. Integral cross sections obtained by direct integration of differential cross sections are free from many of the deficiencies encountered in measurement of the integral cross section (e.g., cascade effects) but are subject to some errors due to the need for extrapolation of the measured data beyond the experimentally accessible regions (to 0° and 180° scattering angles).

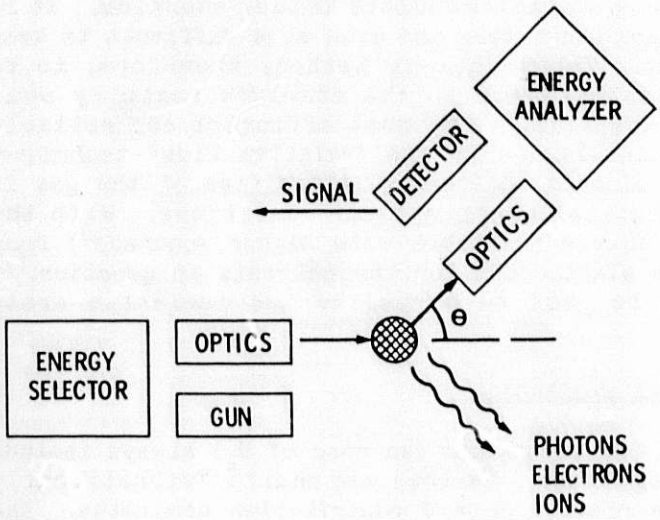

Fig. 1. Schematic diagram for differential scattering cross section measurements.

The first step in obtaining DCS's is to generate the energy-loss spectra at various scattering angles and impact energies. The experimental arrangement is schematically shown in Fig. 1. An energy selected, well collimated electron beam of desired kinetic energy is produced and focused on the target molecules. The target is either a beam or a static gas. Electrons scattered into a small solid angle at a given scattering angle with respect to the incoming electron beam are energy analyzed and detected as a function of energy loss. A typical energy-loss spectrum generated this way is shown in Fig. 2. The location of the spectral features characterizes the energy-level scheme of the target and the scattering intensities are related to the corresponding DCS's. A large numer of studies have been carried out leading to energy-loss spectra e.g. for the purpose of identifying optically forbidden excitations. However, only in much fewer cases have the energy loss spectra been converted to absolute cross sections.

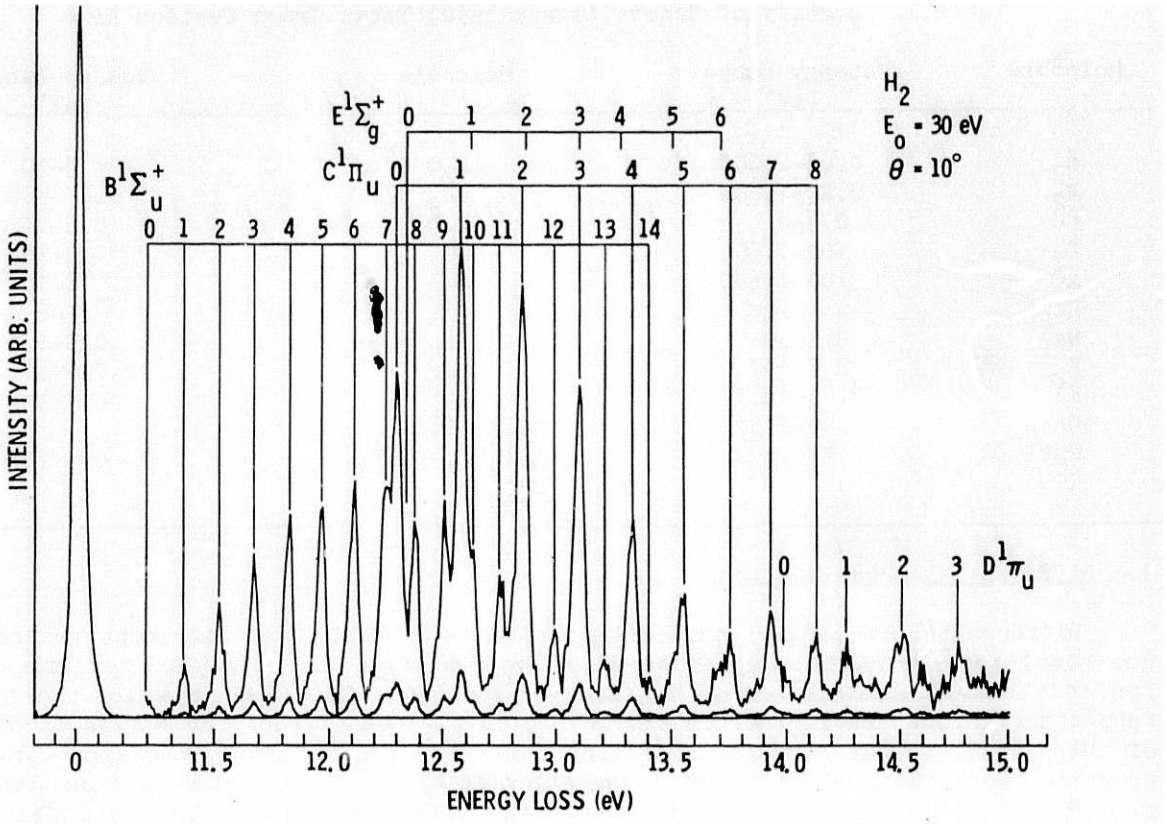

Fig. 2. Electron-impact energy-loss spectrum for H_2.

The straight forward approach to obtain DCS by experimentally determining all parameters which relate the measured electron scattering intensity to the corresponding DCS is not feasible at low and intermediate impact energies. It is very difficult to measure these parameters accurately and even more difficult to keep them constant during the measurement. The practical method, therefore, is to generate relative DCS's and then normalize them to the absolute scale by some procedure. (See Refs. 1, 4 and 5 for details.) The most efficient and reliable method of normalization for gaseous molecules is by the "relative flow" technique. In this aproach one measures relative elastic scattering intensities of the gas in question with respect to He under "identical experimental" conditions. With the knowledge of the He elastic DCS's (which are available with higher accuracy[6]) from the intensity ratios one can obtain the elastic DCS for the molecule in question.[1,7] The elastic cross sections then can be used to normalize the inelastic cross sections.

a. Elastic Scattering and Rotational Excitation

Elastic cross section data, with a few exceptions (in case of H_2) always include elastic and rotational excitation together. In this composite "vibrationally elastic" cross section usually the true elastic $\Delta J = 0$ contribution dominates. The exceptions are high angle scattering where $\Delta J = 2$ type transitions and highly polar molecules where the $\Delta J = \pm 1$ dipole process dominate.

Figure 3 displays the incident electron energy dependence of the measured integral vibrationally elastic scattering cross section for a variety of molecules, ranging from H_2 to SF_6. The purpose of this figure is to illustrate the substantial variation, in both the magnitude and electron energy dependence of the integral cross sections.

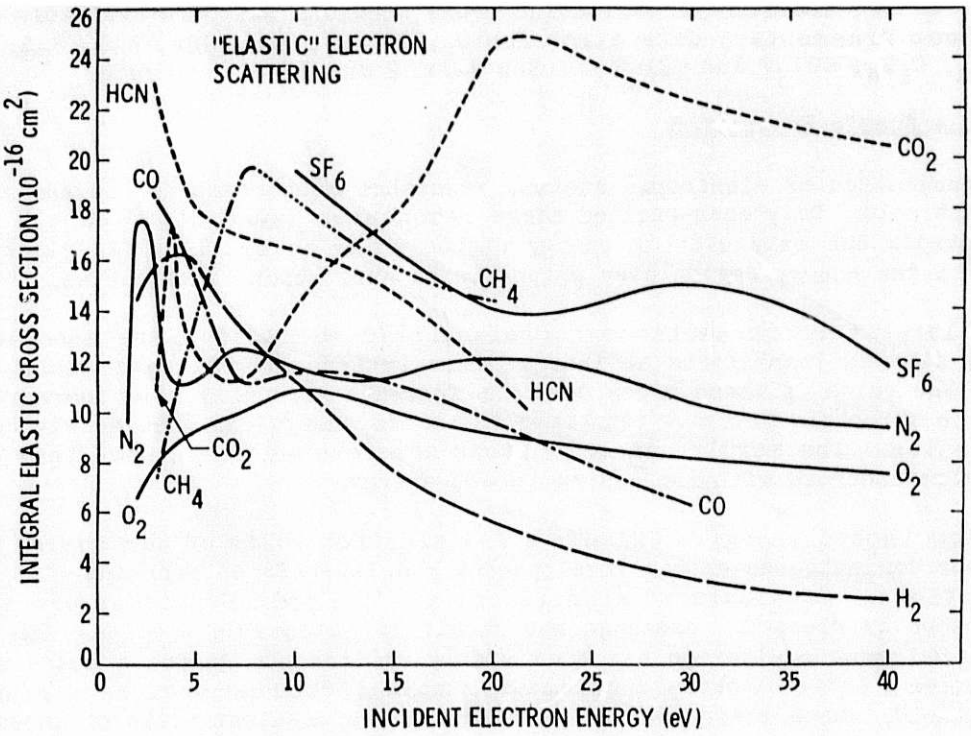

Fig. 3. Integral elastic scattering cross sections for a variety of molecules.

A reasonably complete set of differential and integral elastic cross sections is available for H_2 and N_2 at impact energies ranging from about 0.1 to 1,000 eV. Fragmentary data are available for O_2, CO, NO, HF, HCl, HBr, LiF, KI, CsF, C_3Cl, H_2O, H_2S, HCN, CO_2, N_2O, SO_2, NH_3, As_4, CH_4, C_2H_2, C_2H_4, C_2H_6, C_3H_8, CCl_2F_2, CCl_3F, CCl_4, SF_6 and UF_6. (See Refs. 3 and 4.)

Pure rotational excitation cross sections have been measured for H_2 and obtained by unfolding techniques for N_2, CO and H_2O but only over very limited angular and energy ranges. (See Refs. 3 and 4.)

b. Vibrational Excitation

Electrons are quite effective in producing vibrational excitation, particularly at low impact energies, by interacting with the molcular electron distribution which is coupled with the nuclear vibrational motion. Especially effective are the resonance mechanisms for vibrational excitation which involve temporary electron capture. The increased electromagnetic interaction causes an efficient distortion of the molecular charge distribution and this distortion leads to efficient energy transfer into vibrational excitation. (At low energies typical cross sections are 10^{-16} cm^2.) Resonance processes can also lead to excitation of high vibrational levels. The behavior of the vibrational excitation cross section in the resonance region depends critically on the lifetime and the symmetry of the negative ion state.

The direct electron-impact vibrational excitation of molecular vibration, especially at high impact energies, tends to approximate the $\Delta v = 1$ selection rule. These direct-excitation cross sections are of the order of 10^{-18} cm^2 and change smoothly with impact energy and are usually forward peaked. Excitation to overtone or combination bands decrease by about an order of magnitude with increasing vibrational quantum numbers. The angular behavior of the cross sections depends on the relative importance of short- and long-range interaction terms and is usually similar for the fundamental and overtone bands.

Most of the vibrational excitation cross sections that are available are for H_2 and N_2. Some fragmentary data exist for O_2, CO, HF, HCl, HBr, H_2O, H_2S, CO_2, SO_2, CH_4, C_2H_4, C_2D_4, CCl_3F and CCl_2F_2. (See Refs. 2 and 3.)

c. Electronic Excitation

In excitation of electronic states, resonance mechanisms do not apear to play a signficiant role. Only core-excited shape resonances cause signficantly increased cross sections but only over an energy region which is small (a few electron volts) compared to the energy region over which direct excitation is effective.

The largest cross sections for electronic excitation are associated with optically allowed transitions at intermediate impact energies (and small scattering angles). The value of these cross sections increase gradually with increasing impact energy from threshold to about ten times threshold energy and then slowly decrease at high energies. The angular distributions are forward peaked and this character becomes more enhanced with increasing impact energy.

At low impact energies (within a few electron volts of threshold) forbidden transitions dominate the energy loss spectra and, therefore, represent the important cross sections. Particularly significant are the spin-forbidden processes that readily occur by electron exchange and result in metastable species. This property of electron-impact excitation has been widely utilized to generate metastable atoms and molecules. Integral cross sections for spin-forbidden processes rise steeply near threshold, reach their peak value within a few electron volts of threshold, and then decrease sharply with increasing energy. The DCS's associated with these processes are nearly isotropic, reflecting the short-range nature of the spin exchange reaction.

No simple characteristics can be identified for symmetry-forbidden excitations. The integral cross sections for these processes are usually smaller than for optically allowed excitations, reach their peak value at lower impact energies, and their DCS's show a large variety of behavior. There is, however, a very unique character associated with parity-unfavored transitions ($\Sigma^+ \leftrightarrow \Sigma^-$) the DCS's for these excitations go to zero at 0° and 180° scattering angles.

In practically all of the measurements carried out so far, the initial states for electron scattering processes have been the ground electronic and vibrational state of the molecule. Only for excitation from the O_2 ($a^1\Delta_g$) metastable state are some fragmentary cross section data available. The major difficulty here is the generation of a sufficient number of excited species for collision studies; it is hoped that with the application of lasers, this situation will improve.

The only reasonably complete coverage of electronic state excitation cross sections is for N_2. Some fragmentary data are available for H_2, O_2, SO_2 and CH_4. (See Refs. 2 and 3.)

MOMENTUM TRANSFER CROSS SECTIONS

Elastic momentum transfer cross sections at low energies (below a few eV) are commonly and most accurately determined by the electron swarm technique. Beam/beam experiments which yield both elastic and inelastic momentum transfer cross sections are mandatory at higher energies. The swarm and the beam/beam measurements cover complementary energy ranges and it is important to compare the cross section data obtained by these two methods in the overlapping energy range. We would like to point out that in modeling inelastic momentum transfer is usually neglected. However, in many cases inelastic momentum transfer cross sections are significant and may be comparable to elastic momentum transfer cross sections.

For recent discussion and compilations of momentum transfer cross section data

see Refs. 3, 4, 8-10.

COMPARISON OF EXPERIMENTAL AND CALCULATED CROSS SECTIONS

The comparison of experimental data with theoretical calculations provides information about the validity of various approximations and allows some insight into the physics of the scattering process.

The type of questions one should ask about the physics of the scattering processes are:

1. What is the role of nuclear motion in the scattering process? Under what conditions can we take the nuclei fixed? (Adiabatic Nuclei Approximation)

2. Is it necessary to solve the complete LF-CC (Laboratory Frame-Close Coupled) or BF-CC (Body Frame-Close Coupled) equations or does the DW (Distorted Wave), Glauber or Born Approximation suffice?

3. What is the relative importance of the various parts of the interaction potential; such as static, exchange, polarization, and absorption terms?

The general conclusions from these comparisons are: 1. The treatment of the nuclear motion by different methods yields the same results (with the same potentials). 2. Born and various first order theories underestimate the cross sections especially at high scattering angles. (CC and DW models give qualitatively good agreement with experiment.) 3. Exchange and polarization effects have to be included in the interaction potential to get even qualitatively correct results. 4. Further improvement in theoretical methods are required before quantitative agreement between experiment and theory can be achieved. For more details see Refs. 4 and 11.

ACKNOWLEDGEMENT

This work was supported by the National Aeronautics and Space Administration, Contract No. NAS7-100.

REFERENCES

1. S. Trajmar and D. F. Register, "Experimental Techniques for Cross Section Measurements" in Electron-Molecule Collisions, eds. K. Takayanagi and I. Shimamura, Plenum Press, in print.

2. S. Trajmar and D. C. Cartwright, "Excitation of Molecules by Electron Impact", Chapter II in Electron-Molecule Interactions and Their Applications, ed. L. G. Christophorou, Academic Press, in print.

3. S. Trajmar, D. F. Register and A. Chutjian, "Electron Scattering by Molecules. II. Experimental Methods and Data", Physics Reports 97, 219-356 (1983).

4. G. Csanak, D. C. Cartwright, S. K. Srivastava and S. Trajmar, "Elastic Scattering of Electrons by Molecules", Chapter I in Electron-Molecule Interactions and Their Applications, ed. L. G. Christophorou, Academic Press, in print.

5. R. T. Brinkmann and S. Trajmar, J. Phys. E: Sci. Instrum. 14, 245-255 (1981).

6. D. F. Register, S. Trajmar and S. K. Srivastava, Phys. Rev. A21, 1134-1151 (1980).

7. S. K. Srivastava, A. Chutjian and S. Trajmar, J. Chem. Phys. 63, 2659-2665 (1975).

8. Y. Itikawa, Momentum Transfer Cross Sections for Electron Collisions on Atoms and Molecules and their Application to Effective Collision Frequencies, Argonne National Laboratory Report, ANL-77939, April, 1972; Atomic Data and Nuclear Data Tables 14, 1-10 (1974); ibid 21, 69-775 (1978).

9. M. Hayashi, Recommended Values of Transport Cross Sections for Elastic Collision and Total Collision Cross Section for Electrons in Atomic and Molecular Gases, Report IPPJ-AM-19, Inst. Plasma Phys., Nagoya Univ., Japan, November 1981.

10. J. W. Gallagher, E. C. Beaty, J. Dutton and L. C. Pitchford, "A Compilation of Electron Swarm Data in Electro Negative Gases", JILA Report No. 22, Aug. 1, 1982 and J. Phys. Chem. Ref. Data 12, 109-152 (1983).

11. N. F. Lane, Rev. Mod. Phys. 52, 29-119 (1980).

OPTICAL EXCITATION CROSS-SECTIONS FOR ELECTRON COLLISIONS WITH ATOMS AND MOLECULES

J. W. McConkey

California Institute of Technology, Jet Propulsion Laboratory
Pasadena, CA 91109
and
Physics Department, University of Windsor
Windsor, Ontario N9B 3P4, Canada

ABSTRACT

A brief review of the status of absolute electron-impact excitation cross-section measurements for atoms and molecules is presented. Some of the reasons for the wide discrepancies which exist in the published data are discussed. Tables are presented of recent publications in the field which are not included in the J.I.L.A. compilations. A tabular compilation of the existing data for e-impact on H_2O is also given and discussed. Some recent experiments of particular interest to the development of the theory of electron-molecule excitation are mentioned.

INTRODUCTION

Absolute cross-sections involving collisions of electrons with atoms and molecules are essential input data for any modelling of the interaction of radiation with matter. These cross sections need to be known over a wide energy range covering the energy spectrum of secondary electrons resulting from the interaction of high energy primary radiation of various types with matter. Of particular importance is the detailed behavior of the cross-sections at energies below 100 eV. The present paper considers optical excitation cross-sections. A number of reviews of this subject have been presented over the years. Heddle [1] and Heddle and Keesing [2] have discussed the measurement of optical excitation-functions and mentioned many of the problems which are encountered. They did not, however, attempt to review the existing measurements. More recently Heddle [3] has updated his earlier work concentrating on recent developments in the field but again does not attempt to review the measurements. Robin et al. [4] have presented a review of electron-molecule excitation looking at the subject more from the point of view of using the technique as a spectroscopic tool useful in chemical analysis. They do not present any absolute cross section data but provide a useful listing of the large number of organic molecules that have been studied in this way. Trajmar et al. [7] have very recently reviewed the field of electron-molecule scattering and note, but do not discuss a limited amount of optical excitation information available for a few molecules, particularly the diatomics H_2, N_2 and CO. The only quantitative reivew seems to be the old 1968 discussion of Moiseiwitch and Smith [5] which considered only atomic excitation-functions. There is a distinct need for an up-to-date critical review of absolute optical excitation-function measurements for both atoms and molecules. It is gratifying to know that such a review is under consideration at the present time [6].

For someone wishing to find out what information is available on a particular atom or molecule a good starting point would be the J.I.L.A. or Oak Ridge bibliographic compilations. For example, the J.I.L.A. publications [8] provide a

listing of absolute excitation data listed by atom or molecule and cover material published up until 1980. Direct and dissociative excitation of molecules are listed separately. This present paper attempts to add references to work published in the 1980's. No attempt is made to include a listing of earlier work except in a few cases of special interest as discussed later.

DIFFICULTIES OF ABSOLUTE EXCITATION FUNCTION MEASUREMENTS

The difficulty of making accurate absolute optical emission cross-section measurements becomes apparent when one observes the wide spread of data reported for the same emission by different experimenters in different (and sometimes even the same!) laboratories. Although many of the precuations which have to be taken with this type of measurement are well known and were spelled out clearly in the early review articles [1,2,5], it is clear that systemtic errors are still plaguing the field. Clearly any publication which hopes to be taken seriously must clearly outline the precautions taken, the experimental parameters used and the secondary checks carried out, in addition to providing a realistic and detailed estimate of the errors involved in the experiment.

In an effort to bring some order into the chaos, Van Zyl et al. [9] set out to do a "bench-mark" experiment which would serve as a standard for other experimenters. They chose the n^1S-2^1P transitions of helium where there should be relative freedom from experimental problems involving radiation polarization, radiation trapping and excitation transfer. In addition since branching ratios and cascade contributions are well known in He they were able to convert their measured line emission cross-sections to level cross-sections with a high degree of confidence.

Although these cross-sections should be ones which could be measured with greatest confidence Van Zyl et al. point out that previous measurements of these cross-sections often differed by up to a factor of three. It is very probable that some of this problem can be attributed to gas target impurity problems; a small N_2 background in the collision chamber could lead to large overestimates of the cross-sections since the N_2 optical cross-sections are often very much larger than the He ones. The rest of the differences are probably due to difficulties involved in the basic experimental techniques of absolute radiometry, target density determination and electron beam handling and measurement. Van Zyl et al. consider these problems in great detail and go to a lot of trouble to assess possible uncertainties in the measured parameters. They estimate that their emission cross-sections at 500 eV incident energy are accurate to 3.5%. These represent the most accurately measured cross-sections in the literature. Prospective experimenters would do well to study this paper in detail as it highlights the often subtle pitfalls which can be encountered in this type of work. For example they demonstrate clearly the need not only to use a monochromator to isolate the emission under study but also to use an appropriate filter to take care of light scattering and other effects within the monochromator which would show up when a standard continuum source was being used for absolute radiometry.

Most emissions are not as straightforward as the n^1S-2^1P transitions of He where many of the usual source effects are either absent or can be taken account of quantitatively. Collisional transfer of excitation is often a problem which can effect either the population or loss rates appropriate to a particular level or both. This effect is illustrated dramatically in Fig. 1 which shows how the He 4^3D apparent excitation cross-section varies with pressure. Note how the effect varies with incident electron energy. Resonance radiation trapping effects also show up on plots of emission intensity versus pressure. Thus a clear demonstration that a low enough pressure has been used to avoid such effects, or that an extrapolation to zero pressure has been made, is of paramount importance. Linearity of intensity-beam current plots should also be demonstrated particularly if high currents are being used. Robin et al. [4] stress the importance of this in dissociative excitation to

decide whether or not the excitation is a single-step mechanism.

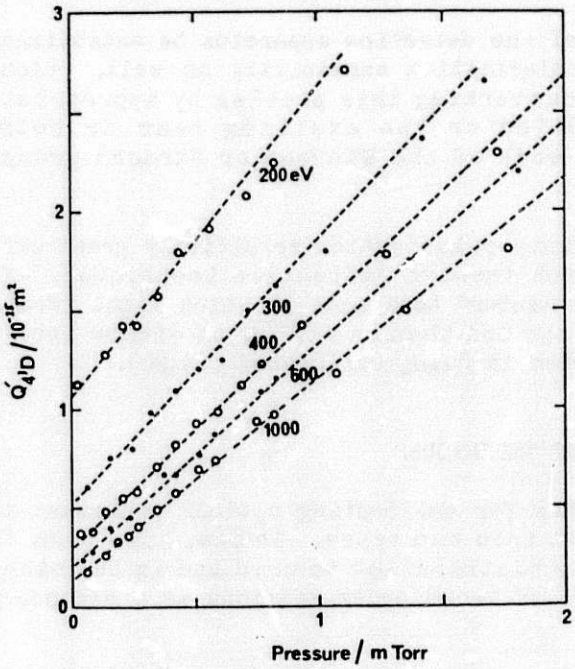

Fig. 1. Effect of pressure on the apparent cross-section for He (4^3D) excitation for several values of incident electron energy, [10].

Another factor which has profoundly influenced the shapes of the cross-sections presented in the literature has been the presence of secondary electrons in the beam of much lower energy than the primary ones. These could arise from collisions of electrons with beam defining apertures, could be especially significant in magnetically collimated beams, and have greatest effect in the measurement of cross- sections which are sharply peaked at low energy (i.e. excitation involving electron exchange). It seems that it was not until the mid-1970's that these problems were well enough taken care of in even He, the simplest species to handle experimentally [11,12].

Various factors can result in a change of effective source size. If the radiating state has a long lifetime then the excited species could drift out of the field of view of the detecting optics thus leading to measured cross-sections which would be too low. Systems such as the Lyman-Birge-Hopfield bands of N_2 which have a lifetime of more than 100 μS would be ones which require special care to accomodate this effect. As the incident electron energy is reduced towards threshold, space charge effects tend to become more significant leading to a "blowing-up" of the electron beam diameter and thus the interaction volume.

It is in the threshold region that other problems too become most significant and thus it is usually the near threshold region of the excitation function which is least accurately known. Apart from the obvious problem that light intensities, and thus statistical accuracy of signals, are reduced, one also has to exercise care with the energy calibration of the incident electron beam. The energy resolution of the electron beam is also most important in this region as it is here that resonance effects are most significant. Finally the polarization of the radiation is usually at a maximum at threshold and so problems associated with the angular anisotropy of the light from the source are most severe in this region.

If a crossed-beam rather than a static gas target is used, and often this is a necessity because of the nature of the species being excited, a new set of problems related to beam overlap and density determination are introduced. In such cases some form of internal calibration is often employed in which comparison is made with the emission from a reference species whose cross-sections are well known. Source geometry effects are automatically taken care of in this way and the relative densities of the species are determined by some form of relative flow technique [13,14].

Problems can arise of course not only from the source of the radiation but also from the instrumentation which detects that radiation. Even assuming that reliable techniques are available to establish the relative sensitivity of the detecting monochromator, the work of the FOM group [15] shows that even with modern holographic gratings, sharp variations in sensitivity over small wavelength regions can occur. This necessitates a large number of calibration points over the wavelength range of interest. Often these are not readily available and so interpolation between widely

separated points has often occurred.

Not only must the absolute sensitivity of the detection apparatus be established as a function of wavelength, but also its polarization sensitivity as well. Clout and Heddle [16] have discussed ways of circumventing this problem by appropriate orientation of either the detection optics or the exciting beam or both. Illustrations of this can be found in the work of the Windsor or Utrecht groups [17,18].

Since each reflection can introduce some polarization sensitivity great care must be taken with calibration methods which involve reflection techniques. An example here is the so-called "double monochromator" technique in which light from a source passes through a primary monochromator and then is reflected either into a detector or into the second monochromator which is being calibrated [19,20].

OPTICAL CALIBRATION TECHNIQUES

A summary of the commonly used techniques for calibrating optical equipment is shown in Fig. 2. It is evident that they fall into two types. In one, some form of standard source of known spectral intensity distribution is used and in the other some form of internal calibration, making use of known cross-sections as a secondary standard, is involved.

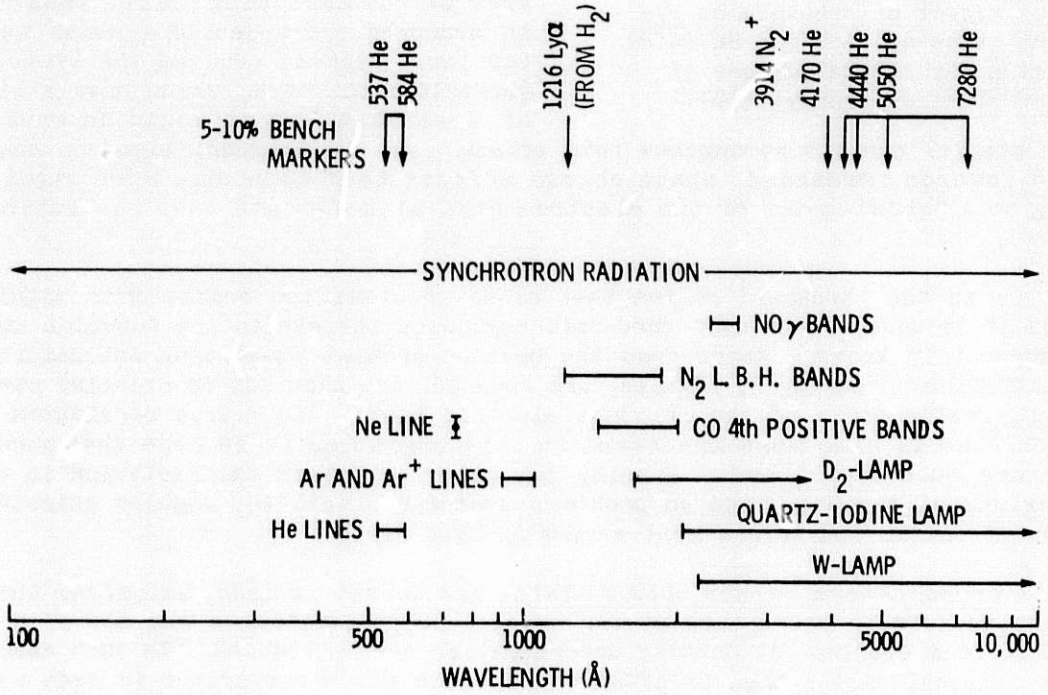

Fig. 2. Optical calibration techniques

The double-monochromator technique already mentioned is an example of the former type and must be used cautiously as discussed. In principle the use of synchrotron radiation seems very attractive as it should be possible to accurately predict its intensity distribution over a very wide spectral range. The radiation, however, is strongly polarized and thus the polarization sensitivity of any optics being used must be known accurately. Other problems have been discussed by McPherson et al. [21]. This source should be very important in the VUV spectra region. Currently it is planned to use this source to provide an absolute calibration for a wide range of

Ar excitation cross sections between 50 and 110 nm. In the visible and near UV various sources are available which trace their calibration back to N.B.S. or another National Standards facility. In addition, Van Zyl et al. [9] used a copper-point blackbody standard source and supply details of its construction.

Assuming that the optical oscillator strength of a transition is accurately known and that cascade effects can be neglected then a Bethe-Born normalization procedure [17,22] can be used to put emission cross-sections on an absolute scale. Because the accuracy of this procedure depends on the accuracy of the optical oscillator strengths this technique has been limited to the lower members of the rare gas series. The molecular branching ratio technique [23,24,25] provides a very attractive and widely used method of obtaining a relative spectral response over a limited wavelength interval. The most widely used band systems are indicated on Fig. 2 (see also discussion in Ref. 15).

In addition to the bench-mark cross-sections provided by Van Zyl et al., Fig. 2 indicates that there are a few others which are generally accepted as being known to a precision of 5-10% at 100 eV incidence energy. These are the He (n^1P-1^1S) resonance lines [17,18], H (Lyman α, 2p-1s) following dissociative excitation of H_2 [26] and N_2^+ (B-X (0,0) band) [27]. These references include references to earlier work.

DISCUSSION OF DATA

Since about 1960 when this field experienced a renaissance there has been steady activity over the succeeding years. Technical developments, such as the development of commercial phase-sensitive detectors in the early 1960's or the advent of channel electron-multipliers which paved the way for the extensive VUV measurements of the 1970's, have had a significant impact on the field. Other factors which have influenced output has been the requirements of the scientific community, e.g. the need for data on stratospheric species in the mid-1970s or the need for data on planetary atmospheric species stimulated by the Voyager flights of the 1980's. The I.C.P.E.A.C. international conference series has also stimulated a significant amount of effort.

Fairly extensive atomic data have been available since the 1960's on the rare gases and the alkalis. The 1970's saw some data emerging on the alkaline earths, some of the other metals, and also some data on C, N and O though in these latter cases the data are still very fragmentary. References to these works can be obtained from the J.I.L.A. compilations [8]. In the 1980's considerable progress has been made in pushing the available data on atoms towards the species occupying more central positions in the periodic table. It is noteworthy that most of this effort has occurred in the Soviet Union and has stemmed from developments in the manufacture and monitoring of atomic beams of these fairly exotic species. Table I indicates the species studied and gives other relevant details of these recent works.

In the molecular area absolute data are available for 11 diatomics H_2, HD, D_2, N_2, CO, NO, O_2, CN, HF, HCl and HBr. A heavy emphasis has occurred for H_2, N_2, CO and O_2. Most of this work can be traced through the tables in Ref. [7]. Recent data are given in Table II. Data are available for 10 triatomic species, CO_2, SO_2, N_2O, CS_2, H_2O, D_2O, H_2S, $HgBr_2$, HgI_2 and $HgCl_2$. In view of the interest in H_2O the available data are given in Table III and are discussed in some detail below. For larger molecules the available information is even more fragmentary with only NH_3 and CH_4 receiving much attention. Fig. 3 taken from Orient and Srivastava [28], shows the excitation of Lyα from CH_4 and illustrates clearly that there is a very wide spread in existing data, all from relatively recent experiments. This highlights again, the difficulty of these experiments and also the need for additional input

Table 1. Recent Publications in Electron-Atom Excitation

Target Species	Excited Species	Energy Range (eV)	Wavelength Range (nm)	Reference
He	He		visible	Arqueros [34]
He	$He(4^1S,5^1S,4^3S,4^3P)$	T-400	visible	Shaw [35]
Li	Li^+, Li^{++}	T-1000	Soft X-Ray	Zhminyak [[36]
Be^+	Be^+ (2p)	T-740	313.1	Taylor [37]
B	B, B^+	T-200	190-400	Kuchenev [38]
Na	Na^+	T-200	250-510	Smirnov [39]
Na	Na(nS,nP,nD,nF)	T-150	254-1140	Phelps [40]
Mg	Mg (L shell)		10-40	Vukstich [41]
Si	Si	T-200	199-290	Kolosov [42]
K	K^{++}	T-200	250-350	Smirnov [47]
Ca	$Ca(4\ ^3P_{0,1,2})$	T-20	657	Dobryshin [43]
Ca,Sr,Ba	Ca^{++},Sr^{++},Ba^{++}	T-300	40-74	Aleksakhin [44]
Ca^+	$Ca^+(5s^2\ ^2D_{5/2}$, $5p\ ^2P_{3/2})$	T-13	214-441	Hane [45]
Ca	$Ca(3p^6$ subshell)	T-300	40-100	Ugrin [46]
V	V	T-250	300-600	Melnikov [48]
V	V	T-200	367-573	Krasavin [49]
Cr	Cr	T-200	200-600	Melnikov [50]
Cr	Cr^+	T-200	260-290	Melnikov [51]
Mn	$Mn(n^6P^o)$	T-200	200-630	Melnikov [52]
Mn	$Mn(n^8S,n^8D,z^8P^o)$	T-200	250-550	Melnikov [53]
Mn	Mn^+	T-200	200-630	Melnikov [54]
Fe^+	Fe^+	T-250	217-295	Kolosov [55]
Cu	Cu	T-200	219-465	Krasavin [56]
Cu	Cu	T-300	223-510	Alexsakhin [57]
Zn	Zn, Zn^+	T-150	468-748	Bogdanova [58]
Zn^+	$Zn^+(4p^2P,5s^2S)$	T-790	202-256	Rogers [59]
Ga^+	$Ga^+(4^1P)$	T-400	141	Stephani [60]
Ge	Ge	T-200	190-600	Kolosov [61]
Rb^+	Rb^{++}	T-200	360-600	Smirnov [62]
Rb^+,Cs^+	Rb^{++}, Cs^{++}		Soft X-Ray	Zapesochnyi [63]
Rb^+	Rb^+			Imre [64]
Mo	Mo, Mo^+	T-200	200-400	Bogdanova [65]
Ag	Ag	T-250	200-500	Krasavin [66]
Ag	Ag^+	T-250	206-293	Krasavin [67]
Cd^+	Cd^+	T-20	219-325	Hane [68]
Cd	$Cd^+(5p,5s^2,6s,5d)$	T-200	214-442	Goto [69]
Cd^+	$Cd^+(5s^2,5p)$	T-20	214-442	Hane [70]
Cs^+	Cs^{++}	T-200	240-290	Smirnov [71]
Au	Au	T-300	242-479	Shafranosh [72]
Hg	$Hg(6^1P_1)$	7.5-14	185	McLucas [73]
Bi	Bi	T-50	220-600	Shafranosh [74]
Sm	$Sm(6s6p,5d6s^2)$	T-100	436-566	Mityereva [75]
Sm	Sm	T-300	370-600	Shimon [76]
Yb	Yb, Yb^+	T-300	220-770	Shimon [77]

into the field to try to remove some of the systemtic differences which still seem to divide different laboratories. In the meantime error estimates have clearly to be treated with some caution. Table II lists the data which has been measured since about 1979, and which is not mentioned in [8].

A considerable amount of excitation data is available for e-impact on H_2O. This is summarized in Table III which gives the species studied, (in all cases reported, dissociation of the molecule occurred), the energy and wavelength ranges covered and

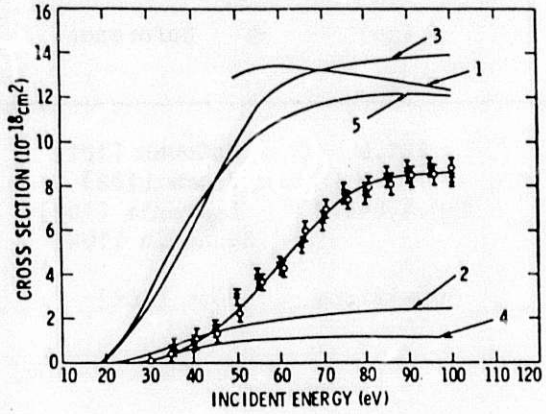

Fig. 3. Emission cross-sections for Lyα radiation from CH_4. For details see Orient and Srivastava [28].

the estimated accuracy of the measurements if this is given. As can be seen, H, O, O^+ and OH emissions have been measured with major emphasis on H(2p). Mohlmann et al. [111] compare the magnitudes of the cross-sections for Lyman α production at 100 eV and show that it takes a factor of 4 to cover the data from different groups. The most recent measurements differ by a factor of two which is strange since both groups trace their normalization procedure to the same original source! Rather wide discrepancies (up to a factor of 2) exist in the data on the Balmer radiation also. At 300 eV measurements of OH radiation differ by a factor of 2.7. At lower energies where an additional measurement exists the disagreement is even larger. Little agreement is evident in the shape of the cross-section either below 100 eV. Clearly there is a need for additional careful measurements to tidy up this situation.

Table 2. Recent Publications in Electron-Molecule Excitation

Target Species	Excited Species	Energy Range (eV)	Wavelength Range (nm)	Reference
H_2,D_2	H, D	T-2000		de Heer [78]
H_2,D_2,T_2	H_2,D_2,T_2,H,D,T	T-2000		de Heer [79]
H_2	$H_2(d^3\Pi_u)$	T-100	600	Bogdanova [80]
H_2	$H_2(B^1\Sigma_u^+, C^1\Pi_u)$	T-400	100-185	Ajello [81]
H_2	H_2(B,B',B'',C,D,D')	T-350	70-170	Ajello [82]
H_2,D_2	H_2,D_2(B,C) H,D(2p)	T-500	115-170	Becker [83]
N_2	$N_2(b^1\Pi_u)$	T-500	89-135	Zipf [84]
N_2,CO	N_2, CO^+	T-500	200-650	Arqueros [85]
N_2	N	T-300	415-1060	Filippelli [86]
N_2	$N_2^+(B^2\Sigma_u^+, A^2\Pi_u)$	T-400	300-850	Skubenich [87]
N_2	$N_2^+(B^2\Sigma_u^+)$	T-200	391	Bogdanova [88]
N_2,O_2	$N_2(C^1\Sigma_u)$,N^+,O,O^+	T-300	50-120	Morgan [89]
N_2	$N_2^+(B^2\Sigma_u^+)$ $N_2(C^3\Pi)$	T-400	337-480	Shaw [90]
CO	$CO^+(B^2\Sigma, A^2\Pi)$	T-500	200-650	Arqueros [91]
CO	$CO^+(B^2\Sigma, A^2\Pi)$	T-500	200-650	Arqueros [92]
CO	$CO^+(B^2\Sigma, A^2\Pi)$	T-400	210-780	Skubenich [93]
CO,CO_2	$CO(a^3\Pi)$	T-20	225-260	Erdman [94]
H_2O	$OH(A^2\Sigma^+)$	T-100	280-330	Becker [95]
D_2O	$OH(A^2\Sigma^+)$	T-1000	300-330	Becker [96]
CS_2	CS_2^+,CS,C,S,S^+,S^{++}	T-125	110-510	Ajello [97]
SO_2	O,O^+,O^{++},S^+,S^{++}	T-500	45-110	Becker [98]
NH_3	N_2^+(B), H(np)	T-200	390-650	Bogdanova [99]
CH_4	H(3p)		650	Fujita [100]

COMPARISON WITH THEORY AND RECENT DEVELOPMENTS

No attempt has been made to compare experiment and theory. In general, the level of agreement particularly at low energy is rather poor except perhaps for the simpler atomic species. For additional details the reader is referred to one of the

Table 3. Summary of Optical Excitation-Function Measurements in H_2O

Species Excited	Impact Energy (eV)	Quoted Accuracy	λ (nm)	Reference
H(2p)	T-200	Factor x 2	121.6	McGowan [101]
H(2p,3p,4p,5p,6p)	50-6000	20-45%	121.6	Vroom [102]
O($3s\ ^3S^o$, $3p\ ^3P$)	35-850	$\lesssim$45%	130.4,844.7	Lawrence [103]
OH($A^2\Sigma^+$)	T-60			Sushanin [104]
O (various) O^+(various) H(n = 2-7)	100	Unclear	500-121.6	Bőse [105]
H(n = 3) OH($A^2\Sigma^+$)	T-400	50%		Tsurubuchi [106]
H(2p) O($3s\ ^3S^o$)	T-250	13%	121.6-130.4	Morgan [107]
OH $A^2\Sigma^+$ H(n = 3-6) O($3p\ ^5P$) O($3p\ ^3P$)	T-1000	20%	280-844.7	Beenakker [108]
H(3s)	300	-	656.3	Tsurubuchi [109]
H(3s,3p,3d)	1000-2000	-	656.3	Mohlmann [110]
H(2p)	20-2000	-	121.6	Mohlmann [111]
H(n = 3-11)	T-2000	12-20%	400-656.3	Mohlmann [112]

recent reviews on this topic [29]. Individual papers give detailed comparison with theory when any is available.

One development in the last decade which has resulted in considerable fine tuning of the theory has been the carrying out of many electron-photon coincidence experiments [30]. Providing, as they do, the most basic possible information about the excitation process, they enable comparisons with theory to be made at the most fundamental level. So far these have been almost entirely concerned with atomic excitation but just recently some preliminary data for diatomic molecules have appeared [31,32]. As these data become more specific they will provide molecular theoreticians with a proving ground for their theories similar to what is currently available in the atomic case.

A parallel and related experimental development has been the introduction of supersonic-beam gas targets into electron-molecule excitation experiments. Already it has been demonstrated [33] using this device that at electron energies below 100 eV, significant deviations from dipole excitation routes occur. The supersonic-nozzle jet cools the target molecules into one or a very limited number of rotational levels. This greatly simplifies the excitation scheme. Experiments are currently under way at Windsor and J.P.L. to combine these two technologies and obtain electron-photon coincidence data following excitation from and to very specific rotational levels in molecules.

ACKNOWLEDGEMENTS

The writing and publication of this paper was supported by the Jet Propulsion Laboratory, California Institute of Technology, under contract with the National Aeronautics and Space Administration. The author gratefully acknowledges the hospitality of the Jet Propulsion Laboratory and the award of an NRC Senior Research Associateship. He also acknowledges financial support from the National Science and Engineering Research Council of Canada.

REFERENCES

1. D. W. O. Heddle, "The Measurement of Optical Excitation Functions" in Methods of Expt. Phys., L. Marton, Ed. 7a, 43 (1968).

2. D. W. O. Heddle and R. G. W. Keesing, Adv. At. Mol. Phys. 4, 267 (1968).

3. D. W. O. Heddle, Adv. At. Mol. Phys. 15, 381 (1979).

4. M. L. Robin, G. K. Schweitzer and E. L. Wehry, App. Spect. Rev. 17, 165 (1981).

5. B. L. Moiseiwitsch and S. J. Smith, Rev. Mod. Phys. 40, 238 (1968).

6. J. W. Gallagher, J.I.L.A. Data Centre, Private Communication (1983).

7. S. Trajmar, D. F. Register and A. Chutjian, Physics Reps. 97, 219 (1983).

8. L. J. Kieffer, N.B.S. Special Pub. #426 (1976) and subsequent supplements.

9. B. Van Zyl, G. H. Dunn, G. Chamberlain and D. W. O. Heddle, Phys. Rev. A. 22, 1916 (1980).

10. A. F. J. van Raan and J. van Eck, J. Phys. B. 7, 2003 (1974).

11. A. F. J. van Raan, P. G. Moll and J. van Eck, J. Phys. B. 7, 950 (1974).

12. J. G. Showalter and R. B. Kay, Phys. Rev. A 11, 1899 (1975).

13. S. K. Srivastava, A. Chutjian and S. Trajmar, J. Chem. Phys. 63, 2659 (1975).

14. K. Becker, W. van Wijngaarden and J. W. McConkey, Planet Sp. Sci. 31, 197 (1983).

15. H. A. van Sprang, H. H. Brongersma and F. J. de Heer, Chem. Phys. Lett. 65, 55 (1979).

16. P. N. Clout and D. W. O. Heddle, J. Opt. Soc. Amer. 59, 715 (1969).

17. F. G. Donaldson, M. A. Hender and J. W. McConkey, J. Phys. B. 5, 1192 (1972).

18. W. B. Westerveld, H. G. M. Heideman and J. van Eck, J. Phys. B. 12, 115 (1979).

19. J. E. Mentall and H. D. Morgan, Phys. Rev. A. 14, 954 (1976).

20. J. M. Ajello et al., Phys. Rev. A, In press (1984).

21. A. McPherson et al., Abst. 13th ICPEAC, Berlin (Ed. J. Eichler et al.), 125 (1983).

22. Y. K. Kim and M. Inokuti, Phys. Rev. 175, 176 (1968).

23. J. W. McConkey, J. Opt. Soc. Amer. 59, 110 (1969).

24. J. F. M. Aarts and F. J. de Heer, J. Opt. Soc. Amer. 58, 1666 (1968).

25. M. J. Mumma, J.I.L.A. Info Centre Rep. 12 (1972).

26. M. J. Mumma and E. C. Zipf, J. Chem. Phys. 55, 1661 (1971).

27. W. L. Borst and E. C. Zipf, Phys. Rev. A. 1, 834 (1970).

28. O. Orient and S. K. Srivastava, Chem. Phys. 54, 183 (1981).

29. B. Buckley, Phys. Reps. 97, (1983).

30. K. Blum and H. Kleinpoppen, Phys. Reps. 52, 203 (1979).

31. K. Becker, H. W. Dassen and J. W. McConkey, J. Phys. B. 16, L177 (1983).

32. K. Becker, H. W. Dassen and J. W. McConkey, J. Phys. B. 17, In press (1984).

33. S. P. Hernandez, P. J. Dagdigian and J. P. Doering, J. Chem. Phys. 77, 6021 (1982).

34. F. Arqueros, J. Campos, An. Fis. Ser. B (Spain) 77, 133-42 (1981).

35. M. Shaw and Y. J. Campos, An. Fis. Ser. A (Spain) 78, 180-7 (1982).

36. Y. V. Zhminyak, V. S. Vukstich, I. P. Zapesochnyi, Ukr. Fiz Zh (USSR) 27, 1578-80 (1982).

37. P. O. Taylor, R. A. Phaneuf, G. H. Dunn, Phys. Rev. A 22, 435-44 (1980).

38. A. N. Kuchenev, Y. M. Smirnov, Opt. & Spect. (USA) 51, 176-77 (1981).

39. Y. M. Smirnov and M. B. Shapochkin, J. App. Spect. (USA) 34, 491-4 (1981).

40. J. O. Phelps, C. C. Lin, Phys. Rev. A 24, 1299-326 (1981).

41. V. A. Vukstich, Y. V. Zhmenyak, E. N. Postoi, I. P. Zapesochnyi, Ukr. Fiz Zh (USSR) 25, 2008 (1980).

42. P. A. Kolosov, A. Y. Krasavin, Y. M. Smirnov, Sov. Astron. (USA) 25, 690-2 (1981).

43. V. E. Dobryshin, V. I. Rakhovskii, V. M. Shustryakov, Opt. & Spect. (USA) 52, 364-6 (1982).

44. I. S. Aleksakhin, E. E. Bogachev, I. P. Zapesochnyi, S. Y. Ugrin, Opt. & Spect. 51, 426-9 (1981).

45. K. Hane, T. Goto, S. Hattori, J. Phys. D 15, L47-9 (1982).

46. S. Y. Ugrin, J. App. Spect. (USA) 29, 868-70 (1978).

47. Y. M. Smirnov, M. B. Shapochkin, Opt. & Spect. (USA) 51, 242-4 (1981).

48. V. V. Melnikov, Y. M. Smirnov, Opt. & Spect. (USA) 53, 15-18 (1982).

49. A. Y. Krasavin, A. N. Kuchenev, Y. M. Smirnov, J. App. Spect. (USA) 36, 575-80 (1982).

50. V. V. Melnikov and Y. M.. Smirnov, Opt. & Spect. (USA) 52, 362-3 (1982).

51. V. V. Melnikov and Y. M. Smirnov, Opt. & Spect. (USA) 50, 325-6 (1981).

52. V. V. Melnikov, Y. M. Smirnov, and Y. Sharonov, Opt. & Spect. (USA) 50, 357-60 (1981).

53. V. V. Melnikov, Y. M. Smirnov, Y. D. Sharonov, Opt. & Spect. (USA) 51, 423-5 (1981).

54. V. V. Melnikov, Y. M. Smirnov, Y. D. Sharonov, Opt. & Spect. (USA) 52, 329 (1982).

55. P. A. Kolosov and Y. M. Smirnov, Sov. Astron. (USA) 26, 304-5 (1982).

56. A. Y. Krasavin, A. N. Kuchenev, Y. M. Smirnov, J. App. Spect. (USA) 36, 631-5 (1982).

57. I. S. Alexsakhin et al., J. App. Spect. (USA) 30, 158-61 (1979).

58. I. P. Bogdanova, S. V. Ryazantseva, V. E. Yakhontova, Opt. & Spect. (USA) 51, 244-6 (1981).

59. W. T. Rogers, G. H. Dunn, J. Ostgaard Olsen, M. Reading, G. Stephani, Phys. Rev. A 25, 681-41 (1982).

60. G. Stephani, R. Camilloni, G. H. Dunn, W. T. Rogers, Phys. Rev. A 25, 2996-3002 (1982).

61. P. A. Kolosov, Y. M. Smirnov, Opt. & Spect. (USA) 53, 243-5 (1982).

62. Y. M. Smirnov and M. B. Shapochkin, Opt. & Spect. (USA) 47, 131-2 (1979).

63. A. I. Zapesochnyi, A. I. Imre and I. S. Aleksakhin, Jetp. Lett. (USA) (1980).

64. A. I. Imre, A. I. Zapesochnyi, V. M. Tsil'o and M. V. Rishko, Ukr. Fiz. Zh (USSR) 25, 1561-3 (1980).

65. S. N. Bogdanov, A. Y. Bodylev, A. N. Kuchenev, Y. M. Smirnov, J. App. Spect. (USA) 37, 989-92 (1982).

66. A. Y. Krasavin, A. N. Kuchenev, Y. M. Smirnov, Opt. & Spect. (USA) 54, 11-13 (1983).

67. A. Y. Krasavin, A. N. Kuchenev, Y. M. Smirnov, J. App. Spect. (USA) 36, 373-7 (1982).

68. K. Hane, T. Goto, S. Hattori, J. Phys. B. 16, 629-37 (1983).

69. T. Goto, K. Hane, M. Okuda, S. Hattori, Phys. Rev. A 27, 1844-50 (1983).

70. K. Hane, T. Goto, S. Hattori, Phys. Rev. A 27, 124-31 (1983).

71. Y. M. Smirnov and M. B. Shapochkin, Opt. & Spect. (USA) 47, 448-9 (1979).

72. I. I. Shafranosh, T. A. Shishova, I. S. Aleksakin, Opt. & Spect. (USA) 50, 210-11 (1981).

73. C. W. McLucas, H. J. E. Wehr, W. R. MacGillivray, M. C. Standage, J. Phys. B. 15, 1883 (1982).

74. I. I. Shafronosh, V. P. Starodub, T. A. Shishova, I. S. Aleksakhin, Opt. & Spect. (USA) 50, 360-2 (1981).

75. A. A. Mityereva, Opt. & Spect. (USA) 49, 556-7 (1980).

76. L. L. Shimon, N. V. Golovchak and I. I. Garga, Opt. & Spect. (USA) 51, 19-21 (1981).

77. L. L. Shimon, N. V. Golovchak, I. I. Garga, I. V. Kurta, Opt. & Spect. (USA) 50, 571-5 (1981).

78. F. J. de Heer, H. A. van Sprang, G. R. Mohlmann, J. Chim. Phys. and Phys. Chim. Biol. 77, 773-7 (1980).

79. F. J. de Heer, Phys. Scr. (Sweden) 23, 170-8 (1981).

80. I. P. Bogdanova et al., Opt. & Spect. (USA) 50, 63-5 (1981).

81. J. M. Ajello, S. K. Srivastava and Y. L. Yung, Phys. Rev. A 25, 2485 (1982).

82. J. M. Ajello, D. Shemansky, T. L. Kwok and Y. L. Yung, Phys. Rev. A, (1984), In press.

83. K. Becker and J. W. McConkey, Can. J. Phys. (1984), In press.

84. E. Zipf and Gorman, J. Chem. Phys. 73, 813-9 (1980).

85. F. Arqueros, J. Campos, An. Fis. Ser. B (Spain) 77, 133 (1981).

86. A. R. Filippelli, P. A. Sharpton, and C. C. Lin, J. Chem. Phys. 76, 3597-606 (1982).

87. V. V. Skubenich and I. P. Zapesochnyi, Geomag. & Aeron. (USA) 21, 355-60 (1981).

88. I. P. Bogdanova, G. V. Efremova, V. I. Yakovleva, Opt. & Spect. (USA) 52, 563-4 (1982).

89. H. D. Morgan and J. E. Mentall, J. Chem. Phys. 78, 1747 (1983).

90. M. Shaw and J. Campos, J. Quant. Spect. Rad. Trans. 30, 73-6 (1983).

91. F. Arqueros and J. Campos, J. Phys. B 14, 2159-61 (1981).

92. F. Arqueros and J. Camoos, Physica B & C 112, 131-7 (1982).

93. V. V. Skubenich, Geomag. & Aeron. (USA) 21, 632-6 (1981).

94. W. P. Erdman and E. C. Zipf, Planet Spa. Sci. 31, 317-21 (1983).

95. K. Becker and G. Schulz, Chem. Phys. Lett. 73, 102-5 (1980).

96. K. Becker and G. Schulz, Can. J. Phys. 60, 1168-75 (1982).

97. J. M. Ajello and S. K. Srivastava, J. Chem. Phys. 75, 4454 (1981).

98. K. Becker, W. van Wijngaarden and J. W. McConkey, Planet Spa. Sci. 31, 197-206 (1983).

99. I. P. Bogdanova, G. V. Efremova, V. I. Yakovleva, Opt. & Spect. 52, 582-3 (1982).

100. I. Fujita, K. Fukui, K. Kuwata, Z. Phys. Chem. (Wiesbaden) 127, 55-60 (1981).

101. J. W. McGowan, J. F. Williams and D. A. Vroom, Chem. Phys. Lett. 3, 614 (1969).

102. D. A. Vroom and F. J. de Heer, J. Chem. Phys. 50, 1883 (1969).

103. G. M. Lawrence, Phys. Rev. A 2, 397 (1970).

104. I. V. Sushanin and S. M. Kishko, Opt. & Spect. 30, 315 (1971).

105. N. Bose and W. Sroka, Z. Naturforsch 28a, 22 (1973).

106. S. Tsurubuchi, T. Iwai and T. Horie, J. Phys. Soc. Japan 36, 537 (1974).

107. H. D. Morgan and J. E. Mentall, J. Chem. Phys. 60, 4734 (1974).

108. C. I. M. Beenakker, F. J. de Heer, H. B. Krop and G. R. Mohlmann, Chem. Phys. 6, 445 (1974).

109. G. R. Mohlmann, S. Tsurubuchi and F. J. de Heer, Chem. Phys.18, 145 (1976).

110. S. Tsurubuchi, G. R. Mohlmann and F. J. de Heer, Chem. Phys. Lett. 48, 477 (1977).

111. G. R. Mohlmann,, K. H. Shima and F. J. de Heer, Chem. Phys. 28, 331 (1978).

112. G. R. Mohlmann and F. J. de Heer, Chem. Phys. 40, 157 (1979).

MEASUREMENT OF ABSOLUTE EXCITATION CROSS SECTIONS NEAR THRESHOLD

David Spence and Michael A. Dillon

Argonne National Laboratory
Argonne, IL 60439

Though many electron impact excitation cross sections have been measured with fair degrees of accuracy, often to several hundred eV above threshold, cross section measurements within the first 10 or 20 eV above threshold, (often the most important energy region for modeling calculations[1] and particularly so for modeling of low energy plasmas) are particularly difficult to make with any degree of accuracy using conventional techniques.[2] Though one can to some extent guess the functional shape of a cross section in this energy region, this is not a particularly desirable procedure. For example, while optically forbidden triplet states often have a maximum cross section near threshold due to charge exchange processes, optically allowed states tend to increase monotonically from threshold. However, the actual magnitude of cross sections are often governed by the presence of negative ion resonances lying energetically just below or above the threshold for excitation.[3,4]

Recently, we have employed a modified version of the so-called "trapped electron method" to measure for the first time the total (with respect to angle) individual excitation functions of the ^3S, ^1S, ^3P and ^1P states of He to about 4 or 5 eV above their respective thresholds with high resolution. We note here that similar measurements have been by Brongersma et al.[5] for the ^3S and ^1S states, but as we have pointed out in previous reports[6,7] the mode of data acquisition by these authors leads to non-unique excitation functions.

Specifically, Brongersma et al.[5] operated their apparatus in the "constant energy loss" mode which yields an excitation function as a function of incident energy. We operate our similar apparatus in the "constant residual energy" mode[6,7] which yields a spectrum of energy loss peaks at a chosen energy above threshold. The areas of the energy loss peaks are then measured[7] to yield a relative cross section at the chosen energy above threshold. Thus, each of our energy loss spectra yield one point on several excitation functions. This mode, though much more tedious than the "fixed energy loss mode," yields excitation functions free of several experimental systematic errors.[6,7]

An example of the excitation functions we have obtained in He are shown in Fig. 1, where we compare our results with two ab-initio theoretical cross sections obtained by Fon et a.[3] and by Oberoi and Nesbet.[4] We have normalized our data at the first peak of the ^3S cross section to 6.2×10^{-18} cm^2, the value recently obtained experimentally by Johnston and Burrow.[8] Theoretical values obtained by Fon et al.[2] and Oberoi and Nesbet[3] are 6.1×10^{-18} and 5.6×10^{-18} cm^2 respectively, and we have normalized these values also to 6.2×10^{-18} cm^2 for easier comparison of the data. Our data are the first obtained with sufficient resolution and statistics to provide meaningful comparison with theory, and serve to illustrate differences between these theories. For example, the calculation of Fon et al.[2] using an R-matrix approach becomes increasingly inaccurate above about 22.5 eV because of the increasing density of states which are not included in the calculation, whereas the

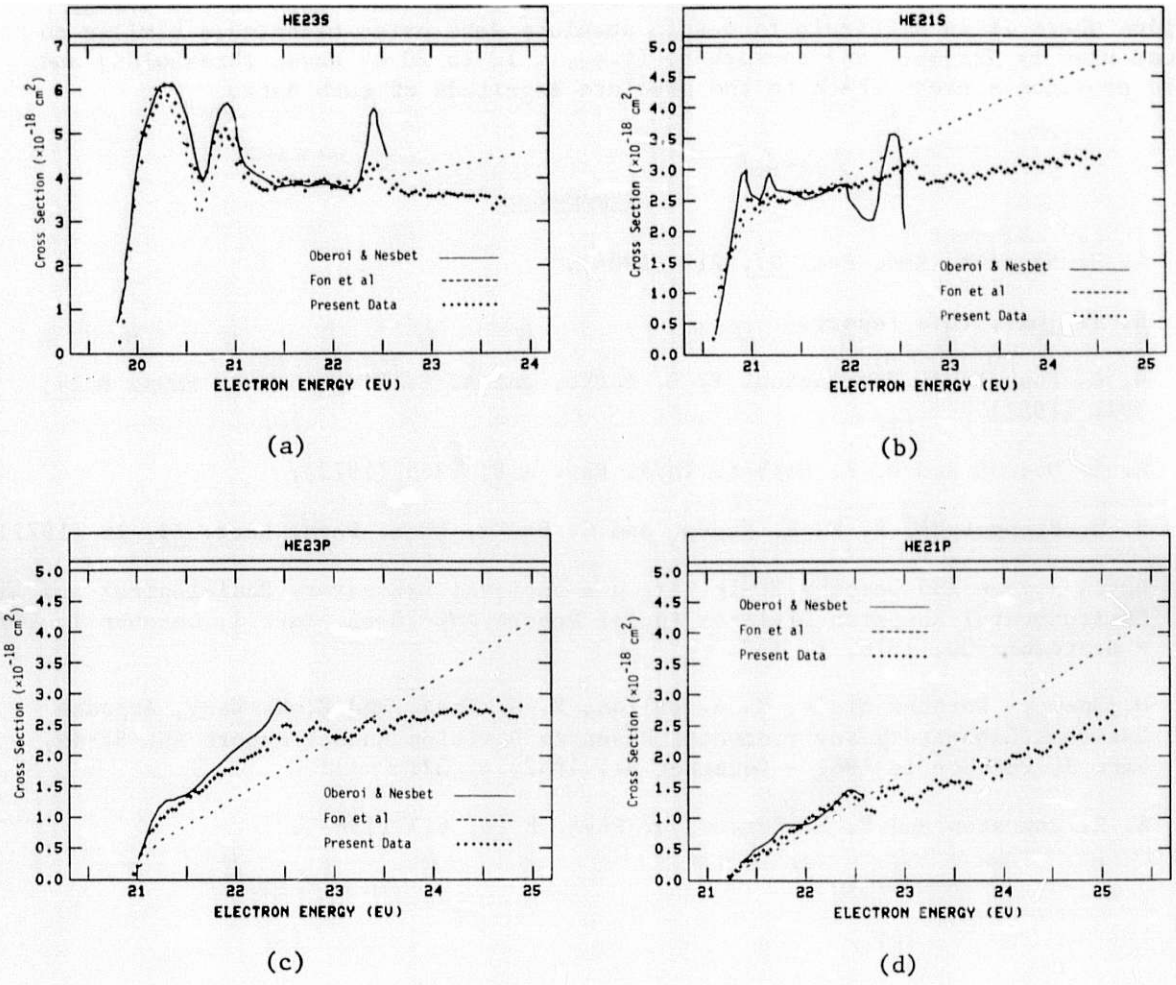

Fig. 1. Total cross sections compared with results of Oberoi and Nesbet[4] and Fon et al.[3] for: (a) He 2^3S; (b) He $2\ ^1S$; (c) He 2^3P; and (d) He 2^1P.

resonance contributions to the cross sections in the variational calculation of Oberoi and Nesbet[3] at about 21 eV and 22.5 eV appear to be somewhat overestimated.

One should note that there is only <u>one</u> normalization point in these four cross sections, i.e., at the peak of the ^3S cross section. The four curves are <u>not</u> individually normalized. As such, the close agreement between experiment and both theories must be considered to be very good.

With increased instrumental resolution obtained by incorporating improvements suggested by Johnston and Burrow,[8] we expect to make cross section measurements to about 10 eV above threshold (this time on an <u>absolute</u> basis by measuring directly all the required experimental parameters). This should be feasible in all those atoms and molecules in which the electronic states are sufficiently well separated for us to resolve experimentally. Such targets include most diatomic and many triatomic molecules of interest to modeling calculations.

The absolute cross sections we obtain in this way thus fill in the energy region where it is difficult to obtain absolute data using techniques similar to those used by Trajmar[2] and co-workers (i.e., < 10 to 20 eV above thresholds) and also provides a cross check to the absolute magnitude of such data.

REFERENCES

1. L. V. Spencer, Rad. Res. 97, 219 (1984).

2. S. Trajmar, this report.

3. W. C. Fon, K. A. Berrington, P. G. Burke, and A. E. Kingston, J. Phys. B 14, 2921 (1981).

4. R. S. Oberoi and R. K. Nesbet, Phys. Rev. A 8, 2969 (1973).

5. H. H. Brongersma, F. W. E. Knoop, and C. Backx, Chem. Phys. Lett. 13, 16 (1972).

6. David Spence and Dorothy Stuit, Argonne National Laboratory Radiological and Environmental Research Division Annual Report ANL-78-63, Part I, October 1, 1977 - September 30, 1978, p. 133.

7. D. Spence, Dorothy Stuit, M. A. Dillon, R.-G. Wang, and Z.-W. Wang, Argonne National Laboratory Environmental Research Division Annual Report ANL-82-65, Part I, October 1, 1981 - December 31, 1982, p. 37.

8. A. R. Johnston and P. D. Burrow, J. Phys. B 16, 613 (1983).

CROSS SECTIONS FOR COLLISIONS OF SUBEXCITATION ELECTRONS WITH MOLECULES

Yukikazu Itikawa

Institute of Space and Astronautical Science
Komaba, Meguroku, Tokyo 153, Japan

ABSTRACT

A short review is given on the present knowledge about the collision processes of subexcitation electrons (i.e., electrons whose energy is below the threshold of the first electronically excited state) with molecules. The processes considered are: vibrational and rotational excitations and elastic scattering. As an example, stopping cross sections for those processes (and electronic excitation and ionization, for comparison) are shown graphically for N_2 and H_2O.

INTRODUCTION

When energetic electrons are injected into a molecular gas, they quickly lose their energy through electronic excitation and ionization of the molecules. However, once after their energy falls below the first electronic excitation potential, their rate of energy loss drops. When electrons have the energy less than the threshold of the first excited state, they are called subexcitation electrons.

The subexcitation electrons spend a relatively long time before they get thermalized. A slowing-down time of an electron can be defined by

$$t_s = \int_{E_0}^{E} \frac{dE}{dE/dt} \quad . \tag{1}$$

The quantity t_s denotes the time spent by the electron during the slowing-down of its energy from E_0 to E. The rate of energy-loss, dE/dt, of the electron is given by

$$\frac{dE}{dt} = - NvS(E) \quad . \tag{2}$$

Here N is the number density of the molecule and v is the electron velocity. S(E) is the stopping cross section defined by

$$S(E) = \sum_j (\Delta E)_j \, Q_j(E) \quad , \tag{3}$$

where Q_j is the cross section for the process j and $(\Delta E)_j$ is the energy-loss of the electron due to the process. Thus the slowing-down time can be calculated by

$$t_s = N^{-1} \int_E^{E_0} \frac{dE}{vS(E)} \quad . \qquad (4)$$

Here the continuos slowing down of the electron has been assumed.

Usually the stopping cross section is very small when $E < E_1$ (E_1 being the threshold of the first electronically excited state). Correspondingly the rate of slowing down decreases very much and the subexcitation electron stays for a long time in the region of $E < E_1$. Sometimes resonant excitations occur in this region. In that case the electron quickly goes through the resonance region, but the overall slowing-down time is not much changed.

The energy of the subexcitation electron is too low to induce electronic-excitation or ionization. The energy, however, is very high with regard to the thermal level. In this sense, the subexcitation electron is 'hot' or 'suprathermal'.

Collision processes involving the subexcitation electrons are:

(i) elastic scattering
(ii) rotational excitation
(iii) vibrational excitation
(iv) attachment

The attachment process is rather special, since it usually occurs in particular molecules and in a particular region of collision energies. It will not be mentioned in this paper.

VIBRATIONAL EXCITATION

On the vibrational excitation, especially on the experimental aspect of the process, Trajmar and his collegues have recently published two review articles.[1,2] They listed the molecular species for which any experimental data are available. Those molecules are H_2, N_2, O_2, CO, HF, HBr, HCl, H_2O, H_2S, CO_2, SO_2, CH_4, CCl_3F, and CCl_2F_2. Most of the numerical data for those molecules are reproduced in one of the papers.[1] As clearly stated in those reviews, the cross section data are very fragmentary. Most of the data have been obtained only over a very limited range of electron energy or in the form of the differential cross section at a few points of scattering angles.

The remarkable feature of the vibrational cross section is its resonant structure.[3] In the resonant region, the cross section is enhanced very much. The magnitude of the vibrational cross section is normally less than 10^{-17} cm^2, but at the resonance energy, it becomes larger by one or two orders of magnitude. It should be noted, however, that the absolute value of the peak cross section sometimes uncertain. For instance, in the case of nitrogen, Schulz said in his review article, "The absolute values shown here may be too low by a factor of up to two".[3] This problem of uncertainty has not been clearly solved yet.

Another interesting thing is the threshold behavior. In 1976 Rohr and Linder[4] found a sharp peak at the threshold of the vibrational cross sections of some molecules (e.g., HCl, HBr, HF). Very recently Ehrhardt and his collegues[5] have studied the threshold cross sections in detail and pointed out the role of the virtual-state process in the threshold structure. It is very difficult to measure

the threshold cross section by beam method. Instead swarm analysis has been often applied to get information about the threshold valu. The reliability of the resulting cross section, however, is not definitely known. For example, in the case of CO, there has been a factor of two discrepancy between the threshold values of the vibrational cross sections (v=0 - 1) obtained by beam and swarm methods.[6] The most recent beam measurement by Ehrhardt and others[5] confirms the old beam-data.

ROTATIONAL EXCITATION

Charge distribution of a molecule is not spherical. Molecules have a permanent dipole, quadrupole, or other multipole moment. Through this anisotropy of charge distribution, rotational excitation can be induced easily by electron collisions. In some cases the rotational cross section is expected to be very large. In particular, a theory shows that the rotational cross section for polar molecules becomes as large as 10^{-14} to 10^{-12} cm^2 at lower electron energies.[7] The rotational cross section for nonpolar molecule is around 10^{-17}-10^{-16} cm^2

The interval of the rotational energy levels is very small. Except for H_2, the level spacing is a few meV or less. This makes it very difficult to measure state-to-state cross sections by beam method. It is also difficult to do any elaborate calculation by a coupled-equation method. Furthermore, a wide range of rotational states are populated by the molecule, unless the temperature is extremely low. An analysis of experimental data, if any, should be very complicated.

Inspite of these difficulties, there are several attempts to derive rotational cross sections from experimental energy-loss spectra. Recently Jung and others[8] have made an analysis of line shape of the electron energy-loss spectra using the high-J approximation. They obtained differential cross sections for the rotational transitions with specific ΔJ for N_2, CO and H_2O. Their cross sections are a sort of averaged cross sections over the rotational states populated by the target molecules. As for the magnitude of the rotational cross section, Jung et al. reached the following conclusion. For N_2, cross sections for $|\Delta J| = 2$ and 4 are as large as 4×10^{-16} cm^2 in the resonance region (E ≅ 2.3 eV), but they are still much less than the purely-elastic one ($\Delta J = 0$). In the non-resonant region, the rotational cross sections ($|\Delta J| = 2$ being dominant) are less than 10^{-18} cm^2. The case of CO has a similar situation at the resonance (E ≅ 2 eV). The transitions with $|\Delta J| = 1$ and 3 also occur in CO. A weak dipole of CO gives rise to a fairly large rotational ($|\Delta J| = 1$) cross section even below the resonance region. For water molecules, the rotational cross section is larger than the purely-elastic one. The absolute magnitude of the rotational cross section is around 10^{-16} cm^2 over the electron energies considered (0.5-6 eV).

Assuming that the rotational transition is caused mainly through an electric multipole moment of the molecule, one can easily obtain a rough estimate of the rotational cross section by a theory. An accurate calculation, however, needs detailed information about the electron-molecule interaction and has to take into account the coupling among a number of rotational states. Although there have been many attempts, no calculation has been confirmed to be reliable to give a rotational cross section for a wide range of electron energy.[9]

For instance, a lot of calculations have been done for N_2 around the resonance peak at 2.3 eV. Below this region, there is only one calculation by Geltman and Takayanagi. From a comparison with recent calculations at higher energies,[10] their cross sections seems less reliable. Jain and Thompson[11] have recently made an elaborate calculation for H_2O. They compared their cross sections with the measured ones of Jung et al.[8] As stated before, those experimental data are the cross sections averaged over a number of rotational states. On the other hand the theoretical values are the cross sections for the excitation from the

ground rotational state. The comparison between the experiment and the theory only indicates a qualitative agreement. They showed further that the Born calculation is very good in this case. In the case of polar molecule, therefore, rotational cross sections can be calculated fairly well by using the Born method, as has been indicated before.[7]

ELASTIC SCATTERING

Elastic scattering contributes not much to the energy loss of the electrons. It mainly contributes to the change of the direction of the electron velocity. The efficiency of the changing the electron momentum is determined by the so-called momentum-transfer cross section. It is defined by

$$Q_m(E) = 2\pi \int_0^{\pi} (1 - \cos\theta)\, q(\theta) \sin\theta \, d\theta \quad , \tag{5}$$

where θ is the scattering angle and $q(\theta)$ is the differential cross section for elastic scattering. The mean energy-loss of the electron in the elastic collision can be given also by the momentum-transfer cross section:

$$(\Delta E)_{elastic} = \frac{2m_e}{M} E \frac{Q_m(E)}{Q_{elastic}(E)} \quad . \tag{6}$$

Here m_e is the electron mass and M is the mass of the molecule. Thus the effective stopping cross section for elastic scattering can be defined by

$$S_{elastic}(E) = \frac{2m_e}{M} E\, Q_m(E) \quad . \tag{7}$$

Due to the small factor of the mass ratio, this quantity is usually very small.

The data on the momentum-transfer cross section have been surveyed and compiled by Itikawa[12,13] and more recently by Hayashi.[14] They have determined recommended values of Q_m for a number of atoms and molecules. In general, Q_m for lower energy region are determined from swarm analysis and for higher energy region they are obtained by an integration of the elastic differential cross sections measured by beam method.

As has been mentioned in the last section, it is very difficult to experimentally resolve individual rotational transition. Almost all of the elastic cross sections measured by beam method, therefore, include rotational cross sections. In other words they are the vibrationally-elastic cross sections defined by

$$'Q_{elastic}' = \sum_{J_i} g(J_i) \sum_{J_f} Q(J_i \rightarrow J_f) \quad . \tag{8}$$

Here $g(J_i)$ is the initial population of the rotational states of the target molecules. The right side of eq(8) can be expressed as

$$'Q_{elastic}' = \sum_{J_i} g(J_i)\, Q(J_i \rightarrow J_i) + \sum_{J_i} g(J_i) \sum_{\substack{J_f \\ (\neq J_i)}} Q(J_i \rightarrow J_f) \; . \qquad (9)$$

The first sum represents the purely-elastic cross section averaged over the rotational population. Only when the relation

$$Q(\Delta J=0) \gg Q(\Delta J \neq 0) \qquad (10)$$

holds, the measured values give the true elastic cross sections. In many instances, this is the case. In the case of polar molecules, however, the rotational cross section often exceeds the purely-elastic one (see, for example, the case of H_2O[8]). Care should be taken, therefore, about how to apply those data to practical problems.

CONCLUDING REMARKS

Finally to get some idea about the effectiveness of each process, two examples of stopping cross sections are shown Figs. 1 and 2.

Fig. 1 shows the case of nitrogen molecules. A very large resonant peak is seen around 2.3 eV. Here the vibrational excitation has the largest effect. Also in the region from the vibrational-threshold to about 1 eV, the vibrational process seems most effective for the electron energy loss. Unfortunately, however, only a crude information from swarm analysis is available there. Below the vibrational threshold (0.28 eV), rotational transitions dominate. As has been mentioned before, no reliable calculation exists for rotational excitations in this region.

The second example is water molecule (Fig. 2). In this case rotational excitation is very important. For H_2O, a simple perturbation theory can be used to obtain rotational cross sections. Vibrational excitation is effective around the threshold and in the region of 5-10 eV. Because of the dominance of rotational excitation, it is difficult to make a good estimate of the purely-elastic cross section. If the elastic cross section is assumed to have the same magnitude as the rotational one, the effective stopping cross section for the elastic scattering can be calculated as indicated in Fig. 2. This should give an upper limit to the contribution of elastic scattering to the electron energy loss.

As a conclusion, many fragmentary information is now available on the cross sections for the collisions of subexcitation electrons with molecules. Based on this information a semiquantitative picture can be drawn about the collision processes. The absolute magnitude of the most cross sections, however, is still accompanied by a large uncertainty. Furthermore a very limited number of molecular species have been investigated in detail so far. More quantitative studies will be needed for a wide range of electron energies and for a wide range of molecular species.

ACKNOWLEDGEMENT

The author would like to thank Profs. K. Takayanagi, M. Hayashi, H. Tanaka, and Dr. K. Onda who provided valuable information during the preparation of this report.

REFERENCES

1. S. Trajmar, D. F. Register and A. Chutjian, Phys. Rept. 97, 219 (1983).

2. S. Trajmar and D. C. Cartwright, in Electron-Molecule Interactions and their Applications, ed. by L. G. Christophorou (Academic Press, to be published) Chapt.2.

3. G. J. Schulz, in Principles of Laser Plasmas, ed. by G. Bekefi (Wiley, 1976) p.33.

4. K. Rohr and F. Linder, J. Phys. B 9, 2521 (1976).

5. H. Ehrhardt, this Workshop.

6. J. E. Land, J. Appl. Phys. 49, 5716 (1978).

7. Y. Itikawa, Phys. Rept. 46, 117 (1978).

8. K. Jung, Th. Antoni, R. Müller, K.-H. Kochem and H. Ehrhardt, J. Phys. B 15, 3535 (1982).

9. For a review of theory, see N. F. Lane, Rev. Mod. Phys. 52, 29 (1980).

10. K. Takayanagi, in Electron-Molecule Collisions and Photoionization Processes, ed. by V. McKoy et al. (Verlag Chemie International Inc., 1983) p.133.

11. A. Jain and D. G. Thompson, J. Phys. B 16, 3077 (1983).

12. Y. Itikawa, Atomic Data Nucl. Data Tables 14, 1 (1974).

13. Y. Itikawa, Atomic Data Nucl. Data Tables 21, 69 (1978).

14. M. Hayashi, Rept. IPPJ-AM-19, Inst. Plasma Phys., Nagoya Univ. (1981).

15. H. Tanaka, T. Yamamoto and T. Okada, J. Phys. B 14, 2081 (1981).

16. A. G. Engelhardt, A. V. Phelps and C. G. Risk, Phys. Rev. 135, A1566 (1964).

17. I. Shimamura, Phys. Rev. A 23, 3350 (1981). The stopping cross sections in this paper are incorrect due to the error in the unit of the original cross sections used.

18. N. Chandra and A. Temkin, Phys. Rev. A 14, 507 (1976).

19. A. E. S. Green, J. J. Olivero and R. W. Stagat, in Proc. of Biophysical Aspects of Radiation Quality Symposium (Int. Atomic Energy Agency, 1971) p.79.

20. G. Seng and F. Linder, J. Phys. B 9, 2539 (1976).

21. Y. Itikawa, J. Phys. Soc. Jpn. 32, 217 (1972).

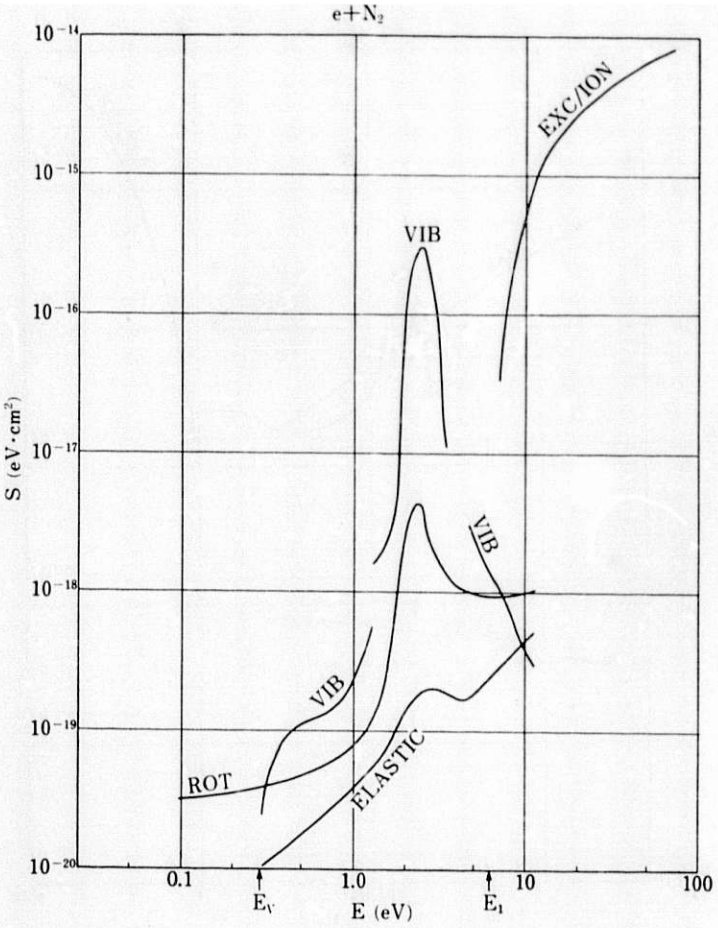

Fig. 1. Stopping cross sections for electron collisions with N_2. Contribution of electronic excitation and ionization has been calculated by K. Takayanagi (private communication) based on various experimental data on the relevant cross sections. For vibrational excitation, the beam cross sections are employed for the resonance region[3] and above.[15] The threshold values are from swarm analysis.[16] Stopping cross sections for rotational transitions has been evaluated by Shimamura's method[17] with the theoretical cross sections.[18] Contribution of elastic scattering is calculated with the use of eq(7) and the values of Q_m recommended by Hayashi.[14]

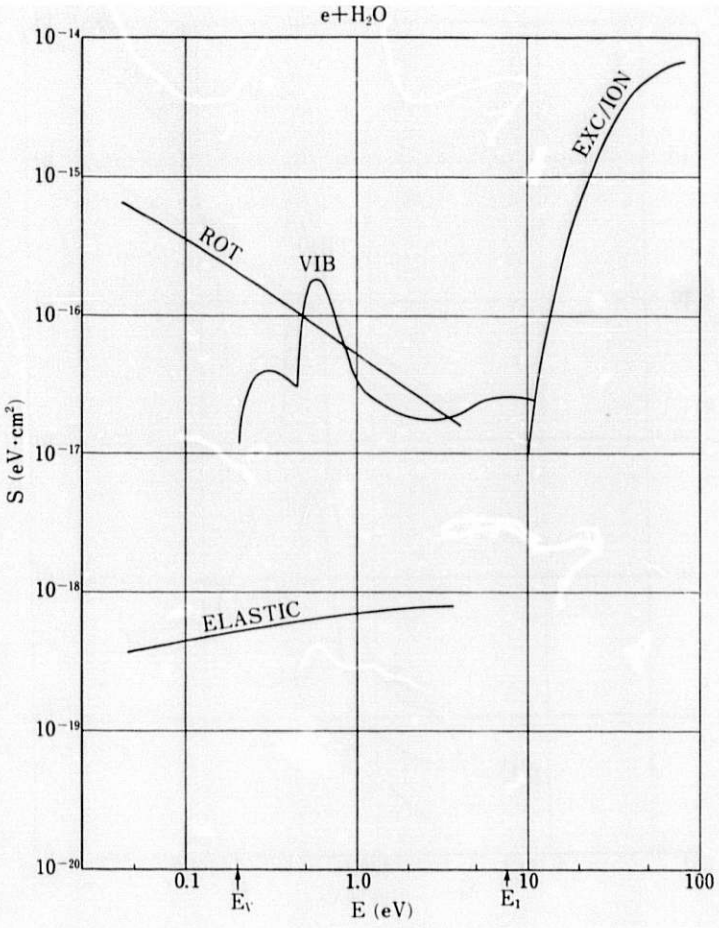

Fig. 2. Stopping cross sections for electron collisions with H_2O. Contribution of electronic excitation and ionization has been taken from the estimate by Green et al.[19] The vibrational cross section is based on the beam measurement by Seng and Linder.[20] The rotational stopping cross section has been calculated with the use of the Born cross section for $0_0 \rightarrow 1_0$.[21] The contribution of elastic scattering indicates its upper limit (see text).

ACTIVITIES OF THE JILA ATOMIC COLLISIONS CROSS SECTIONS DATA CENTER

Jean W. Gallagher

Joint Institute for Laboratory Astrophysics, National Bureau of Standards
and University of Colorado, Boulder, CO 80309

ABSTRACT

The JILA Atomic Collisions Cross Sections Data Center compiles, critically evaluates, and reviews cross sections and rates for low energy (<100 keV) collisions of electrons, photons, and heavy particles with atoms, ions, and simple molecules. Reports are prepared which provide easily accessible recommended data with error limits, list the fundamental literature related to specific topics, identify regions where data are missing, and point out inconsistencies in existing data. The general methodology used in producing evaluated compilations is described. Recently completed projects and work in progress are reported.

The goals of the JILA Atomic Collisions Cross Section Data Center are to compile, critically evaluate and review cross sections and rates describing processes which occur when electrons, photons, or heavy particles collide with atoms, ions and simple molecules. Processes of interest include collisional excitation and relaxation, charge exchange, ionization, recombination, dissociation, and elastic scattering. This work is intended to summarize and organize the output of research in atomic and molecular physics and chemical physics for the use of both scientists who produce these data and those who apply it in such areas as energy research, astrophysics, aeronomy, and gaseous discharges. The Data Center produces reports on selected topics which present recommended data with uncertainty estimates and include listings of the fundamental related literature. These reports point out inconsistencies in existing data and identify regions where no data are available.

Due to the immense quantity of material involved, the Data Center cannot be comprehensive in all aspects of the defined subject area. To be effective, we must isolate specific, limited subjects and concentrate on these. In this context, the following steps are invoked to produce Data Center reports:

1. Subjects are identified for data compilation and evaluation. Within the defined range of subjects, these should be of broad fundamental scientific interest or have significant applications and also be mature enough so that interpretation of the results is not speculative.

2. Collaborators are identified who have expertise in the selected field and who are able to devote the required time to participate in the evaluation of the data. Ideally, participation by both an experimentalist and a theoretician is sought. Such individuals may be drawn from JILA's permanent and visiting scientific staff or invited as short-term visitors to the Data Center.

3. A further consideration of the subject is made to clearly establish limitations on the material to be treated. These may include a selection of incident or

target particles, boundaries on the energy range, or a restriction on the form in which the data have been reported.

4. Sources of pertinent data are identified from the scientific literature. Bibliographies, reports, and prior review articles as well as computer searches of Physics Abstracts and Chemical Abstracts are utilized for this step. Frequently, an appeal is made to prominent workers in the field for listings of associated publications. Copies of all publications are obtained, assigned a unique Data Center citation number, and stored in the Data Center microfiche library. Lists of these references, sorted alphabetically by first author, by citation number, or by year of publication, are prepared.

5. Each source is reviewed to identify numerical data suitable to the project. Data presented in figures are digitized and stored in individual data files or records with the following indexing information: bibliographic source, incident particle, target particle (with electronic and vibrational state), process, products (final state of target or new particles), method (experimental or theoretical), identity of dependent and independent variables, identity of associated parameters and their values. Tabular data are stored in the same fashion. Sorted indices of these files are made. Hard copies of all records are retained for detailed inspection.

Standard graphics techniques are used to prepare comparative figures of data from various sources which describe the same process. These figures provide a fundamental tool to be used in the review of the data in that they display the range of variables over which data are available and compare data from different sources; e.g., they may compare measurements made by different laboratories or compare values arrived at by experimental and theoretical methods.

6. In some cases, an attempt is made to describe the data in an analytic form for which parameters must be determined and goodness-of-fit tested. Programs appropriate to the specific problem are developed and implemented.

7. The expert collaborator works with the Data Center staff to determine criteria for evaluation of the data. These may take different forms depending on the subject treated. Criteria for theoretical data could be whether wave functions used in the calculation accurately predict known energy levels and whether aproximations are properly applied; i.e., in energy regions where they are valid. For measured data, a list is made of experimental circumstances contributing errors. The accuracy of various methods of normalization is considered. A frequently suitable evaluation criterion is whether the data display well-known asymptotic behavior. Where possible, consistency checks are identified.

8. Various procedures are applied to evaluate the data. Each research report is studied to determine how well the criteria described in #7 were met. The authors' own uncertainty estimates are considered, and a judgement is made as to whether or not these are realistic. Consistency checks may be applied, especially in cases where this was not done in the original research. Data from various sources are compared using the figures described in #5. With this information, a judgement is made on the reliability of each data set and an evaluation rating is assigned. Occasionally the data are manipulated by renormalization or averaging over an energy distribution.

9. A report which lists the sources and characteristics of the data, describes the criteria and findings of the evaluation, and presents the most reliable data in graphical and/or tabular form is prepared. The emphasis in the presentation may vary depending on the planned disposition of the report.

The following articles have recently been completed by the Data Center in collaboration with scientists in various fields:

1. "Rate Coefficients for Vibrational Energy Transfer Involving the Hydrogen Halides," S. R. Leone, J. Phys. Chem. Ref. Data 11, 953 (1982).

2. "An Annotated Compilation and Appraisal of Electron Swarm Data in Electronegative Gases," J. W. Gallagher, E. C. Beaty, J. Dutton, L. C. Pitchford, J. Phys. Chem. Ref. Data 12, 109 (1983).

3. "Angular and Energy Distribution of Secondary Electrons from Helium. Slow Electrons Ejected by Electron Impact," Y.-K. Kim, Phys. Rev. A 28, 656 (1983).

4. "Evaluated Theoretical Cross Section Data for Charge Exchange of Multiply Charged Ions with Atoms," R. K. Janev, B. H. Bransden, J. W. Gallagher.
"I. Hydrogen Atom-Fully Stripped Ion Systems," J. Phys. Chem. Ref. Data 12, xxx (1983).
"II. Hydrogen Atom-Partially Stripped Ion Systems," J. Phys. Chem. Ref. Data 12, xxx (1983).
"III. Non-Hydrogenic Target Atoms," (submitted J. Phys. Chem. Ref. Data).

5. "Rate Data for Inelastic Collision Processes in the Diatomic Halogen Molecules," J. I. Steinfeld, in press, J. Phys. Chem. Ref. Data.

6. "Scaling Laws for Inelastic Collision Processes in Diatomic Halogens," J. I. Steinfeld and Patricia Ruttenberg, JILA Data Center Report #23 (1983).

Work is in progress on several other evaluated compilations and reviews:

1. "Electron Production in Proton Collisions: Total Cross Sections," M. E. Rudd, Y.-K. Kim, D. Madison, and J. W. Gallagher.

2. "Cross Sections for Photoionization of Molecular Targets. Theory and Experiment," P. W. Langhoff, C. E. Brion, and J. W. Gallagher.

3. "An Evaluated Compilation of Data on Charge Transfer of Hydrogen Ions and Atoms in Metal Vapors," T. J. Morgan, A. S. Schlachter, R. E. Olson, and J. W. Gallagher.

4. "Atomic Data for Electron-Impact Excitation of Ions," J. W. Gallagher and A. K. Pradhan.

Work planned for the near future includes a review of electron impact excitation cross sections for atomic targets.

ORNL'S CONTROLLED FUSION ATOMIC DATA CENTER

C. F. Barnett and D. C. Gregory

Oak Ridge National Laboratory
Oak Ridge, Tennessee 37831, U.S.A.

ABSTRACT

The Data Center maintains a detailed bibliography of atomic data measurements and calculations for processes of interest to the fusion community. One hundred nineteen journals are regularly searched for papers of interest, including back issues to 1950. Entries are categorized by author, process, reactants, energy range, and theory/experiment. Complete bibliographies have been published since 1978 and a computerized data retrieval system is available. In addition, an updated and extended multi-volume critical compilation of cross sections (the ORNL Redbooks) is under way.

In 1959 an effort was initiated by the Thermonuclear Research Division of the Oak Ridge National Laboratory to identify, compile, evaluate, and publish those atomic and molecular collision cross sections relevant to controlled fusion research. Two years later a collection of graphical, numerical, and bibliographical data was published as an ORNL report, ORNL-3113. This compilation, along with the revisions over the past two decades, has become known to researchers in the fusion energy community as "The Redbook."

In 1965 a formal agreement was made between the Technical Information Division of the Atomic Energy Commission and the Office of Standard Reference Data at the National Bureau of Standards to jointly sponsor and fund an information center at Oak Ridge to be known as the "Atomic and Molecular Processes Information Center." The joint funding was continued until 1970 at which time the funding and administration was assumed by the Energy Research and Development Administration (now the Department of Energy) with a name change to Controlled Fusion Atomic Data Center (CFADC).

The total field of atomic and molecular collision processes is enormous so that it has been necessary for us to restrict the scope of our activities in favor of performing a thorough and critical job in a useful region. Since the beginning we have tried to avoid the vast field of collisions encountered in organic chemistry by restricting our coverage to molecules having less than 5 or 6 atoms per molecule. This broad scope was further restricted in 1982 to H_2, H_3, HeH, N_2, O_2, CO, CO_2, OH, H_2O, CH, CH_2, CH_3, and CH_4 molecules and their ions. Major categories that are currently used in classifying the bibliographical input are listed in Table I while the subcategories of electron-particle interactions are tabulated in Table II. The entries in each table should be self-explanatory except for "C. Particle Penetration in Macroscopic Matter." In this category emphasis is placed on energy loss, stopping power, range, multiple scattering, and charge and excited state populations when electrons, ions, or neutral particles pass through gases or solids. These reactions are

Table I. Major Categories Used in Classifying the Controlled Fusion Atomic Data Center's Bibliographical Input

A.	Heavy Particle - Heavy Particle Interactions
B.	Interactions of Atomic Particles with Electromagnetic Fields
C.	Particle Penetration in Macroscopic Matter (ions, neutrals, and electrons)
D.	Particle Interactions with Solid Surfaces
E.	Electron-Particle Interactions
F.	Photon Collisions with Heavy Particles and Electrons ($h\nu < 100$ keV)
G.	Data Compilations
H.	Reviews and Books
I.	Bibliographies

Table II. Subcategories for Electron-Particle Interactions

A.	General	H.	Collisional Line Broadening
B.	Elastic Collisions	I.	Negative Ion Formation
C.	Excitation	J.	Free-free Transitions (bremsstrahlung)
D.	Dissociation	K.	Electron Detachment from Negative Ions
E.	Ionization	L.	Fluorescence
F.	Recombination (electron-ion)	M.	Angular Scattering
G.	Collisional De-excitation	N.	Momentum Transfer

characterized by multiple collisions. Another major category, Transport Phenomena and Average Properties in Gases, was discontinued in 1982. These processes included drift velocities, diffusion, scattering and energy loss parameters, ionization coefficients, and attachment coefficients and are of marginal interest to fusion research. Discontinued categories and reactants are available, of course, in the bibliographies tabulated before those search criteria were dropped.

The functions of the data center are to: (1) store and retrieve bibliographical and evaluated data; (2) evaluate published data and publish results in form of data compilations and review articles; (3) publish bibliographies of refereed, published papers; (4) perform literature and data searches upon reasonable requests; and (5) in the course of review and evaluation to point out lacunae in the data, so as to provide guidance to future research. To carry out these functions, our in-house group of atomic physicists spend up to 20% of their time in literature search, data evaluation and compiling data. Of tremendous value is the use of university teachers who specialize in atomic physics. At the present we have five university staff members under subcontract who search the literature and prepare reviews.

During the past 20 years, research emphases have changed, new journals started (and some discontinued), and computer techniques have become more sophisticated. All of these have contributed to changes in the way we search, input bibliographical data, store, and retrieve data. Literature searches are available from 1950 up to the present. References prior to 1978 are stored off-line on a computer tape with retrieval being done manually. Papers appearing since 1977 are on-line with instant retrieval using the collision process (subcategory) and reactants. Before 1982, the number of papers cited in the bibliography averaged 2670 per year. With the reduced scope in 1982 (119 journals were searched for 82 subcategories), the number of entries decreased to 1685 in that year, greatly reducing our workload with practically no information of principal interest to the fusion community lost.

The storage of evaluated numerical data has always been a philosophical problem. In the past we have taken the viewpoint that data is more useful to researchers if they have the data readily available for look-up, much like a telephone book. With increased cost of publications, the complexity of plasma modeling calculations, and the availability of computer links, we have decided to store the numerical data base on ORNL's IBM computers and at the Fusion Energy Computer facilities at Livermore for easy computer access by the technical community.

All bibliographical entries are currently stored on computers and are available as a hard-copy computer printout. A bibliography for the years 1978-81 has been published as ORNL reports ORNL-5921/V1 and ORNL-5921/V2. Future plans include the publication of yearly bibliographies, with the 1982 bibliography due to appear in May 1984. The 1983 edition will be published in collaboration with the Research Information Center, Institute of Plasma Physics, Nagoya University, Nagoya, Japan. This collaboration has already resulted in the publication of a report, "Recommended Data on Excitation of Carbon and Oxygen Ions by Electron Collisions." "Best" experimental and theoretical cross sections an[illegible]s for Maxwellian distributions were compiled for electron collisional excitati[illegible] C^{+}-C^{5+} and O^{+}-O^{7+} ions. This report, IPPJ-AM-27, as well as the ORNL reports [illegible] previously, are available from CFADC upon request.

The last revision of our "Redbook" series appeared in 1977. Presently, the compilations are undergoing extensive revisions. Volumes 1 and 2 (ORNL-5206 and ORNL-5207) are being revised to include recent data and to include reaction rate coefficients. Volume 3 of the new series will cover particle interactions with solid surfaces. Two new volumes will be added in the future: work has begun on a compilation of C and O ions with heavy particles and electrons, and a later volume will be added on the interaction of Fe ions with electrons, ions, and neutrals.

Over the years our work has indicated that the compiling of bibliographical and numerical data can consume an infinite amount of time and funds. The ORNL Controlled Fusion Atomic Data Center has concentrated on those areas in which we have the greatest expertise. Using this approach the data center has made a definite contribution to fusion research by pointing out the atomic data needs in the fusion program. In addition data have been provided that are used in the cooling, heating, transport, loss, diagnostics, and modeling of high temperature plasmas.

ACKNOWLEDGMENTS

The operation of a data evaluation and compilation activity is a group or team activity. Thus, many people are involved in our final output. The present ORNL in-house staff consists of C. F. Barnett, D. C. Gregory, H. T. Hunter, A. M. Howald, C. C. Havener, M. I. Kirkpatrick, F. W. Meyer, and R. A. Phaneuf. University professors or others under subcontract include H. B. Gilbody, Queen's University; E. W. McDaniel, Georgia Tech; R. H. McKnight, National Bureau of Standards; T. J. Morgan, Wesleyan University; and E. W. Thomas, Georgia Tech. D. H. Crandall, now in the Office of Fusion Energy, Department of Energy, made significant contributions to the data center's activity while director of the center from 1980 through 1983 and as a staff member 1973-83.

The work of the data center is supported by the Office of Fusion Energy of the U.S. Department of Energy under contract No. W-7405-eng-26 with the Union Carbide Corporation.

APPENDIX 1.

LIST OF PARTICIPANTS

Professor J. N. Bardsley
Dept. of Phys. & Astronomy
University of Pittsburgh
Pittsburgh, PA 15260

Dr. Martin J. Berger
Center for Radiation Research
National Bureau of Standards
Washington, DC 20234

Dr. Joseph Berkowitz
Physics Division
Argonne National Laboratory
Argonne, IL 60439

Dr. Mohammed A. Bolorizadeh
Department of Physics & Astronomy
University of Nebraska
Lincoln, NE 68588-0111

Professor R. A. Bonham
Department of Chemistry
Indiana University
Bloomington, Indiana 47401

Dr. D. J. Brenner
Radiological Research Lab
630 W. 168th St.
College of Physicians & Surgeons
Columbia University
New York, NY 10032

Professor C. E. Brion
Dept. of Chemistry
The University of British Columbia
2075 Wesbrook Place, Vancouver
British Columbia, CANADA V6T 1W5

Dr. K.-T. Cheng
Physics Division
Argonne National Laboratory
Argonne, IL 60439

Dr. Charles W. Clark
Atomic and Plasma Radiation Div.
National Bureau of Standards
Washington, DC 20234

Dr. David Crandall
ER 542, Germantown
U.S. Department of Energy
Washington, DC 20545

Dr. J. L. Dehmer
Environmental Research Division
Argonne National Laboratory
Argonne, Illinois 60439

Dr. P. M. Dehmer
Environmental Research Division
Argonne National Laboratory
Argonne, Illinois 60439

Dr. Michael A. Dillon
Environmental Research Division
Argonne National Laboratory
Argonne, Illinois 60439

Dr. Eugenia Eggarter
Dep. de Fisica
Univ. Nacional de San Luis
Chacabuco y Pedernera
5700 San Luis, Argentina

Professor H. Ehrhardt
Fachbereich Physik
Universität Kaiserslautern
D-6750 Kaiserslautern
West Germany

Professor U. Fano
James Franck Institute
5640 Ellis Avenue
Chicago, IL 60637

Dr. K. P. Funabashi
Radiation Laboratory
University of Notre Dame
Notre Dame, Indiana 46556

Dr. Jean W. Gallagher
Joint Institute for Laboratory
Astrophysics
Campus Box 440
University of Colorado
Boulder, Colorado 80309

Dr. D. C. Gregory
Oak Ridge National Laboratory
Oak Ridge, Tennessee 37830

Professor Y. Hatano
Dept. of Chemistry
Tokyo Institute of Technology
Meguro-ku, Tokyo 152
JAPAN

Dr. Keh-Ning Huang
Institute of Atomic & Mol. Sciences
Academia Sinica, P.O. Box 23-166
Taipei, Taiwan, Republic of China

Dr. Russell H. Huebner
Office of the Director
Argonne National Laboratory
Argonne, IL 60439

Dr. Mitio Inokuti
Environmental Research Division
Argonne National Laboratory
Argonne, IL 60439

Professor Yukikazu Itikawa
Institute of Space and
Astronautical Science
Komaba, Meguro-ku
Tokyo 153, Japan

Professor R. E. Johnson
University of Virginia
Dept. of Nuclear Eng. & Eng. Physics
Charlottesville, VA 22901

Dr. Robert Katz
Department of Physics & Astronomy
University of Nebraska
Lincoln, Nebraska 68588

Dr. Yong-Ki Kim
National Bureau of Standards
Building 221
Washington, DC 20234

Dr. M. Kimura
Department of Physics
University of Missouri at Rolla
Rolla, Missouri 65401

Professor Edwin N. Lassettre
Mellon Institute of the
Carnegie-Mellon University
4400 Fifth Avenue
Pittsburgh, Pennsylvania 15213

Dr. Maryvonne LeDourneuf
James Franck Institute
5640 Ellis Avenue
University of Chicago
Chicago, IL 60637

Dr. K.-T. Lu
Graduate School
Academia Sinica
P.O. Box 3908
Beijing, People's Republic of China

Professor Steven T. Manson
Dept. of Physics & Astronomy
Georgia State University
University Plaza
Atlanta, Georgia 30303

Dr. J. W. McConkey
Jet Propulsion Laboratory, 183-601
California Institute of Technology
4800 Oak Grove Drive
Pasadena, CA 91103

Dr. John H. Miller
Pacific Northwest Laboratory
Richland, WA 99352

Professor Nunir Nayfeh
Physics Department
University of Illinois
Champaign, IL 61801

Dr. Antonio Pagnamenta
Environmental Research Division
Argonne National Laboratory
Argonne, IL 60439

Dr. H. G. Paretzke, Institut für
Strahlenschutz, Gesellschaft für
Strahlen- und Umweltforschung mbH
Ingolstädter Landstrasse 1
D-8042 Neuherberg, West Germany

Dr. James M. Peek
Organization 1231
Sandia National Laboratories
Albuquerque, New Mexico 87185

Dr. P. Plenkiewicz
Université de Sherbrooke
Médecine Nucléaire & Radiobiologie
3001, 12e Avenue Nord, Sherbrooke
P.Q. Canada J1H 5N4

Dr. Stephen T. Pratt
Environmental Research Division
Argonne National Laboratory
Argonne, IL 60439

Professor M. Eugene Rudd
Department of Physics & Astronomy
University of Nebraska
Lincoln, Nebraska 68588

Dr. T. W. Shyn
Space Physics Laboratory
University of Michigan
Ann Arbor, Michigan 48109

Dr. David Spence
Environmental Research Division
Argonne National Laboratory
Argonne, IL 60439

Dr. S. C. Sung
P.O. Box 289
Loma Linda, California 45409

Professor C. E. Theodosiou
Dept. of Physics
University of Toledo
Toledo, Ohio 43606

Dr. L. H. Toburen
Pacific Northwest Laboratory
Richland, WA 99352

Dr. S. Trajmar
California Institute of Technology
Jet Propulsion Laboratory, 183-601
4800 Oak Grove Drive
Pasadena, California 91103

Dr. Ren-guang Wang
Department of Physics
Chengdu University of Science & Technology, Chengdu
People's Republic of China

Dr. Zhi-wen Wang
Institute of Atomic and Molecular Physics
Jilin University, Changchun
People's Republic of China

Dr. W. E. Wilson
Pacific Northwest Laboratory
Richland, WA 99352

Dr. M. A. Zaider
Radiological Research Lab.
630 W. 168th St.
College of Physicians & Surgeons
Columbia University
New York, NY 10032

APPENDIX 2.

PROGRAM OF THE WORKSHOP ON ELECTRONIC AND IONIC COLLISION CROSS SECTIONS NEEDED IN THE MODELING OF RADIATION INTERACTIONS WITH MATTER

Argonne National Laboratory
December 6-8, 1983

Tuesday, December 6

Workshop Opening
Alan Schriesheim, Senior Deputy Director,
Argonne National Laboratory

Session I (Mitio Inokuti, Chairman)
Introduction
M. Inokuti (Argonne National Laboratory)

Discussion of Electron Cross Sections for Transport Calculations
Martin J. Berger (National Bureau of Standards)

Cross Sections Needed for Investigations Into Track Phenomena and Monte-Carlo Calculations
H. G. Paretzke (Gesellschaft für Strahlen- und Umweltforschung München)

Cross Sections Used in Proton-Track Simulations
W. E. Wilson, L. H. Toburen, J. H. Miller, and R. DuBois (Pacific Northwest Laboratory)

Session II (D. Spence, Chairman)
Absolute Differential Ionization Cross Sections for Electron Impact
H. Ehrhardt, K. Jung, R. Müller-Fiedler, and P. Schlemmer (Universität Kaiserslautern)

Ion and Electron Impact Ionization Cross Sections
M. Eugene Rudd (University of Nebraska)

Measurements of Secondary-Electron Cross Sections by the Pulsed Electron Beam Time-of-Flight Method. I. Molecular Nitrogen
R. R. Goruganthu, W. G. Wilson, and R. A. Bonham (Indiana University)

Wednesday, December 7

Session III (L. H. Toburen, Chairman)
Remarks on the Theory of Slow Electron Collisions and of Condensed Matter Effects
U. Fano (University of Chicago)

Electron Ejection Cross Sections in Electron and Ion Impact Ionization: Ab Initio and Semiempirical Calculations
Steven T. Manson (Georgia State University) and John H. Miller (Pacific Northwest Laboratory)

The Transport of Low-Energy Electrons in Water and Some Physico-Chemical Implications
D. J. Brenner and M. Zaider (Columbia University)

Electron Collision Cross Sections and Radiation Chemistry
Y. Hatano (Tokyo Institute of Technology)

Session IV (Michael A. Dillon, Chairman)

Cross Sections for Electron Impact Excitation of Molecules
S. Trajmar (Jet Propulsion Laboratory)

Optical Excitation Cross-Sections for Electron Collisions with Atoms and Molecules
J. W. McConkey (Jet Propulsion Laboratory and University of Windsor)

Dipole Oscillator Strengths Observed in Electron Impact
C. E. Brion (University of British Columbia)

Measurement of Absolute Excitation Cross Sections Near Threshold
David Spence and Michael A. Dillon (Argonne National Laboratory)

Thursday, December 8

Session V (Russell H. Huebner, Chairman)

Activities of the JILA Atomic Collisions Cross Sections Data Center
Jean W. Gallagher (Joint Institute for Laboratory Astrophysics, Colorado)

ORNL's Controlled Fusion Atomic Data Center
C. F. Barnett and D. C. Gregory (Oak Ridge National Laboratory)

Cross Sections for Collisions of Subexcitation Electrons with Molecules
Yukikazu Itikawa (Institute of Space and Astronautical Science, Tokyo)

Cross Section Needs in the Study of Gas Discharges
J. N. Bardsley (University of Pittsburgh)

Cross Sections Relevant to Sputtering & Desorption of Condensed Gases by Ions and Electrons
R. E. Johnson (University of Virginia)

Session VI

General discussion led by Yong-Ki Kim (National Bureau of Standards)

Distribution for ANL-84-28

Internal:

A. Schriesheim
K. L. Kliewer
H. Drucker
P. F. Gustafson
A. J. Dvorak
M. Inokuti (70)
J. D. DePue
Participants (10)
ANL Patent Dept.
ANL Contract File
ANL Libraries (2)
TIS Files (6)

External:

DOE-TIC, for distribution per UC-34A and UC-4 (244)
Manager, Chicago Operations Office, DOE
Environmental Research Division Review Committee:
A. K. Blackadar, Pennsylvania State U.
B. M. Hannon, U. of Illinois
D. W. Moeller, Harvard School of Public Health
R. A. Reck, General Motors Research Labs.
R. E. Wildung, Battelle Pacific Northwest Labs.
Participants (41)
P. Ausloos, National Bureau of Standards
P. D. Burrow, U. of Nebraska
R. J. Celotta, National Bureau of Standards
L. G. Christophorou, Oak Ridge National Lab.
R. N. Compton, Oak Ridge National Lab.
D. Dill, Boston U.
D. A. Douthat, U. of Alaska/Anchorage
G. H. Dunn, U. of Colorado
M. Fink, U. of Texas
G. Freeman, U. of Alberta
W. R. Garrett, Oak Ridge National Lab.
A. E. Green, U. of Florida
M. E. Gress, Office of Basic Energy Sciences, USDOE
M. Hayashi, Nagoya Inst. of Technology
R. Holroyd, Brookhaven National Lab.
Y. Hsu, U. of Missouri/Rolla
R. J. Kandel, Office of Basic Energy Sciences, USDOE
W. E. Kauppila, Wayne State U.
C. C. Lin, U. of Wisconsin/Madison
S. Lipsky, U. of Minnesota
D. H. Madison, Drake U.
J. Magee, Lawrence Berkeley National Lab.
J. Wm. McGowan, Jr., U. of Western Ontario
W. J. Meath, U. of Western Ontario
G. Meisels, U. of Nebraska
A. Mozumder, U. Notre Dame
C. Naleway, American Dental Assoc., Chicago
D. W. Norcross, U. of Colorado
Notre Dame, U. of, Radiation Lab.
Wm. R. Ott, National Bureau of Standards
D. Penn, National Bureau of Standards
L. C. Pitchford, Sandia National Labs.
R. H. Pratt, U. of Pittsburgh
R. H. Ritchie, Oak Ridge National Lab.
L. Sanche, U. of Sherbrooke
R. H. Schuler, U. Notre Dame
H. Schwarz, Brookhaven National Lab.

K. Takayanagi, Institute of Space & Astronautical Science
J. K. Thomas, U. Notre Dame
J. E. Turner, Oak Ridge National Lab.
H. F. Wellenstein, Brandeis U.
H. F. Winters, IBM, San Jose
R. W. Wood, Office of Energy Research, USDOE
H. A. Wright, Oak Ridge National Lab.